The molecular composition and localization of Dystrophin-Associated Protein Complexes (DPCs) and ε-sarcoglycan in mammalian brain.

A Thesis Submitted for the Degree of
Doctor of Philosophy in the University of London

June 2012

Parolaro Nathalie

Department of Neuroscience,
School of Biological Sciences,
Royal Holloway, University of London.

Declaration

The work presented in this thesis was carried out mainly at the Department of Neuroscience, School of Biological Sciences, at Royal Holloway College and partially at the Department of Pharmacology, at the University of Oxford. Except where acknowledgement is made, all the work presented in this thesis is my own and has not been submitted for any other degree in this or any other University or Institute.

Parolaro Nathalie

-Abstract-

The molecular composition and localization of Dystrophin-Associated Protein Complexes (DPCs) and ε-sarcoglycan in mammalian brain.

Duchenne muscular dystrophies (DMD) arise from mutations in the DMD gene. In the brain, the DMD gene product, dystrophin, localizes at the post-synaptic density (PSD) of inhibitory GABAergic neurons (Brunig *et al*, 2002). PSDs are specialised cytoskeletal structures that underlie and are attached to the post-synaptic membrane. In PSDs of the brain, dystrophin is part of a multi-protein complex, namely the dystrophin-associated protein complex (DPC) found exclusively at GABAergic synapses. Recent studies have identified a novel alternatively spliced dystrophin product in the brain, referred to as delta dystrophin, whose molecular associations and functions are unknown. In this thesis I have investigated whether delta dystrophin may form novel DPC complexes at GABAergic synapses of the brain. Results suggest that in the brain, delta dystrophins exhibit different regional and subcellular distributions when compared to classical dystrophins and do not co-localise with any of the PSD markers or DPC components tested. Rather, delta dystrophins fully co-localise with β3-tubulin, a component of the microtubule (MT) cytoskeleton. These studies suggest, that unlike classical dystrophin, delta dystrophin is likely to form novel delta DPC complexes outside rather than within the GABAergic synapse, and therefore may have a different molecular composition and function compared to classical dystrophin-containing DPC complexes. Therefore, delta dystrophin co-localisation with the MT network may provide a potential novel route by which cognitive pathology in DMD patients may be initiated.

ε-sarcoglycan, is a well-established DPC component in smooth muscle. However, the present studies suggest that it may not be a component of classical and delta dystrophin-containing DPC complexes at GABAergic synapses and microtubule structures, respectively. Its membrane localization suggests ε-sarcoglycan is likely to be part of novel, yet unidentified complexes in the brain. However, attempts to raise high affinity antisera that could be used to purify and characterize ε-sarcoglycan complexes were unsuccessful.

Acknowledgements

The studies described in this thesis were mainly supported by the Biotechnology and Biological Sciences Research Council (BBSRC) and Royal Holloway University of London.

My first and most important thank you is for my first supervisor, Professor Philip Beesley, he has given me this very important opportunity to do a PhD in such an important project. He has provided professional guidance, vast knowledge and expertise in this project, and has never stopped believing in me. I would also like to thank my second supervisor, Professor Pavlos Alifragis, who arrived at a very critical point of my project, and has been important not only for discussions on various stand-stills of my project, but together with his beautiful wife Dina, have given me a lot of moral support. I would also like to thank my advisor from the Pharmacological Department of the University of Oxford, Professor Derek J Blake, for the long and productive conversations on the project and for supplying a number of vectors and in-house antibodies that proved fundamental for this thesis. A big thank you to Christopher T Esapa, a post-doc working in the Derek J Blake lab, for the time and great help he has given me. I would also like to thank my advisors Mark Crompton and Chris Rider for their support. There are a number of people in my lab I also would like to thank. First of all, Michaela Kraus, a post-doc that has guided me in the first two years of my PhD. I would also like to thank Rosemary Mummery, the lab technician, who meticulously introduced me to various equipments and experiments. Ivan, my Italian friend from Napoli (who always thinks about Italian food!!!), always made himself available when I needed his help for my project. Takis, the Greek with the belly (it's muscle, he says!), has been a good listener and gave me a number of precious advices. Claire and Molly, thank you for all the help you gave me during my PhD. People from lab 302a and 302b, thank you all.

Michelle and Jason, thank you for always being there for me. Francesca V, Francesca B., Chiara M., Ramona, Stella, Lynn, Doug, and Sophia, thank you for the fun times. I would like to thank everyone that I have not already mentioned above!

Special dedication

I would like to thank my parents Irene and Roberto for their constant support during my PhD, in what I believe to be the biggest challenge I have yet had to deal with.

I would like to thank Luca for his constant support and wonderful person he is.

I would like to send a big thank you to my grandmother Emma, and to the memory of my grandparents Ida, Angelo and Piero, who would also have been very proud to see my achievements.

Glossary of Abbreviations

AA	amino acid
α-DG	α-dystroglycan
Amp	Ampicillin
AO	antisense oligonucleotides
B	brain
β-DG	β-dystroglycan
BH	Brain Homogenate
bla	ampicillin resistance gene
BL21(DE3)	an all purpose strain of competent cells for high-level protein expression and easy induction
BLAST	Basic Local Alignment Search Tool
BMD	Becker Muscular Dystrophy
C	cerebellum
Ca^{+}	calcium
CA1	Cornus Ammonis area 1
cDp	classical dystrophin
cDp427	427kDa classical dystrophin
cDp140	140kDa classical dystrophin
cDp116	116kDa classical dystrophin
cDp71	71kDa classical dystrophin
Cexon 78	classical exon 78
CH	calponin homology domain
CHO	Chinese Hamster Ovary
CNS	Central Nervous System
Cos	acronym, derived from the cells being **C**V-1 (simian) in **O**rigin, and carrying the **S**V40 genetic material
Cos-7	a form of Cos cell line
Cre-loxP	**c**auses **re**combination-**lo**cus of **X**-over **P**1
Cs	cell soluble
CT	C-terminus
Cys	cysteine
DB	dystrobrevin
DBS	Deep Brain Stimulation
dDp	delta dystrophin
dDp427	427kDa delta dystrophin
dDp140	140kDa delta dystrophin
dDp116	116kDa delta dystrophin
dDp71	71kDa delta dystrophin
Dexon 78	delta exon 78
div	days in vitro
DMD	Duchenne Muscular Dystrophy
DMEM	Dulbeccos modified eagles media
DMSO	dimethyl sulphoxide
DYT11-MDS	Myoclonus Dystonia Syndrome due to a mutation of the SGCE gene
DNA	Deoxyribonucleic acid
DPC	Dystrophin Associated Protein Complex
E. coli	*Escherichia coli*
EF hand	helix-loop-helix structural domain

EGFP	enhanced green fluorescent protein
ER	endoplasmic reticulum
ERK	extracellular-signal-regulated kinase
ERS	even-related synchronization
F	forebrain
F1 origin	f1 origin of replication
F-actin	filamentous polymers of actin
G	general
$GABA_A R$	γ-aminobutyric acid receptor
GAD65	glutamic acid decarboxylase 65
Gp	glycoprotein
Gpi	Globus pallidus internus
Grb2	growth factor receptor-bound protein 2
H	hinge
H1 and H2	helical leucine-heptad motifs
HBS	HEPES buffered saline
HFS	high frequency stimulation
His-tag	Histidine-tag
HS	horse serum
IgG	Immunoglobulin G
IP	Immunoprecipitate
IPTG	Isopropyl β-D-1-thiogalactopyranoside
IQ	Intelligence quotient
Kif5A	kinesin heavy chain isoform 5A
lac 1	lac repressor
Leu	leucine
LGMD	limb-girdle muscular dystrophy
LM	light membrane
LNS	**l**aminin, **n**eurexin, **s**ex-hormone-binding protein domain
LTD	long-term depression
LTP	long-term potentiation
M	muscle
μ	micro
mAb	Monoclonal Antibody
ng	nanogram
nm	nanometer
M	marker
MAP2	microtubule-associated protein
MCS	multiple cloning site
mdx	a strain of mouse used as a disease model for human muscular dystrophy
MEK2	mitogen-activated protein kinase kinase
Mc	microsomes
mRNA	messenger RNA
Mt	mitochondria
MT	microtubule
My	myelin
N	n-octyl-pyranoside
nNOS	neuronal nitric oxide synthase
NMDA R	*N*-methyl *D*-aspartate receptor
Np65, 55	neuroplastin 65, 55

OMIM	Online Mendelian Inheritance in Man
np	neuroplastin
ORF	Open Reading Frame
Ori	Origins of Replication
P	Purkinje
P2	Pellet 2
PAGE	Polyacrylamide gel electrophoresis
PBS	phosphate buffered saline
PDZ	**p**ost synaptic density protein, **D**rosophila disc large tumor suppressor, **z**onula occludens-1 protein
PEG 6000	polyethylene glycol
pEGFP-N3 vector, expression vector that can be transfected into mammalian cells	
pET32b vector, a bacterial plasmid designed to enable quick production of a desired protein	
PFA	paraformaldehyde
PH	pleckstrin homology domain
pH	potential of hydrogen, a measure of the acidity or basicity of an aqueous solution
Phal	rhodamine-phalloidin
PI	protease inhibitors
PSD	Post-Synaptic Density
R	retinal
R(1-23)	rod domain
rEK	recombinant enterokinase
RIPA buffer	radioimmunoprecipitation assay buffer
RNA	ribonucleic acid
RNase	ribonuclease A
S	Schwann cells
SDS	sodium dodecyl sulphate
Ser	serine
sg	sarcoglycan
SGCE	ε-sarcoglycan gene
SM	synaptic membrane
Synapto	synaptophysin
S-tag	15 amino acid long peptide (S-peptide) derived from the N-terminus of RNase A
STD	short-term depression
STP	short-term potentiation
SU	syntrophin unique domain
Syn	syntrophin
T	Triton X-100
TCA cycle	tricarboxylic acid cycle
Thr	threonine
TM	transmembrane
TMS	transcranial magnetic stimulation
TrxA	thioredoxin 1
Trp	tryptophan
Vr3	variable region 3
Wt	Wild type
WW domain	a protein domain with two highly conserved tryptophans that binds proline-rich peptide motifs
ZZ	(zinc-binding)-type zinc domain

Table of contents

Title page…..…….....…….1
Declaration…….....2
Abstract…….....3
Acknowledgements…….....4
Special dedication……....5
Glossary of abbreviations…….....6
List of contents..…….…….9
List of figures…….....13
List of tables……...…….....15
Chapter 1:..……...16
1.0 ***Part 1***……..……....16
1.1 The DPC complex in the Brain…..…….....…..……17
1.1.1 Introduction and major aims……...17
1.1.2 Molecular genetics of the DMD gene and encoded proteins….....20
1.1.3 Localization and developmental expression of dystrophins ……...24
1.1.4 Structure of classical and delta dystrophin…….…….....27
1.1.5 DMD gene mutations…….…….....29
1.1.6 A naturally occurring mutation in mice to study the function of dystrophin in brain: the mdx mouse.....33
1.1.7 Protein interactions of the DMD gene product: the DPC complex.....41
1.1.8 The functions of the DPC complex in brain……....47
1.1.9 *Summary*……...…….....52

1.2 ***Part 2***…….……...……....53
1.3 ε-sarcoglycan and the DPC complex in the Brain……..……..54
1.3.1 Introduction and major aims……...……...……..54
1.3.2 Molecular genetics of the ε-sarcoglycan gene and encoded protein……..…...……..56
1.3.3 Localization and developmental expression of ε-sarcoglycan.....60
1.3.4 Protein structure of 47kDa and 49kDa ε-sarcoglycan isoforms..…63
1.3.5 ε-sarcoglycan mutations lead to Myoclonus Dystonia Syndrome (MDS)……..……....64
1.3.6 Proteins interacting with ε-sarcoglycan……..….....67
1.3.7 The function of ε-sarcoglycan in the brain……...……..……69
1.3.8 *Summary*……...……...…….....73
Chapter 2:....…….……74
2.0 Materials and Methods..……...……...……..……....74
2.1 Reagents and equipment…….……...…….....75
2.1.1 General Reagents……..…….....75
2.1.2 Chemicals……...…….....75
2.1.3 Biological kits and systems…..…….……..75
2.1.4 Markers and enzymes……..…….…….....75

2.1.5 Media, buffers and solutions…..…….....75
2.1.6 Equipment and suppliers……..…….....76
2.1.7 Reagents and Equipment for specific protocols…..…….....76
2.1.8 Antibodies used in Western blotting and Immunocytochemistry detection analysis……..76
2.2 Isolation of subcellular fractions and protein detection……..77
2.2.1 Protease inhibitors……...…….....77
2.2.2 Preparation of subcellular fractions from rat forebrain or cerebellum…...77
2.2.3 Preparation of PSD in rat Forebrain/Cerebellum by the Gurd *et al* (1982) method……..80
2.2.4 Preparation of PSD in Forebrain by the Carlin *et al* (1980) method…..….80
2.2.5 Protein determination by the Folin-Lowry method……81
2.2.6 Sample preparation for SDS-gel analysis……..…….....82
2.2.7 SDS-polyacrylamide gel electrophoresis……..…….....82
2.2.8 Coomassie Blue staining for protein-detection in polyacrylamide gels….83
2.2.9 Western blotting……...…….....83
2.2.10 Ponceau S staining for protein-detection on Western blotted nitrocellulose…….…….....83
2.2.11 Development of Western blots: Enhanced chemiluminescence (ECL) detection system…….....…….....83
2.3 Isolation and detection of ε-sarcoglycan binding partners…….....85
2.3.1 Preparation of solubilised ε-sarcoglycan and binding partners from forebrain-derived light membrane..…….....85
2.3.2 Cross-linking of anti-ε-sarcoglycan antibody to Dynabeads Protein G….85
2.3.3 Immunoprecipitation of ε-sarcoglycan binding partners……..……86
2.4 Cell culture of cortical neurons…….....87
2.4.1 Preparing the coverslips…….....87
2.4.2 Preparation of cortical neurons from E18 prenatal rats…….....87
2.4.3 Preparation of DNA……...88
2.4.4 Transfection of cortical neurons with pEGFP-N3Cexon78 and pEGFP-N3Dexon78 vectors…….....88
2.4.5 PFA-Fixation (for cDp, dDp, ε-sg, MAP2, MANDAG, $GABA_AR$, GAD65, β3-tubulin and synaptophysin antibodies) of mature cortical neurons…….....89
2.4.6 Methanol-Fixation (for dDp, PSD95 and NR1 antibodies) of mature cortical neurons…….....89
2.4.7 Viewing fixed neurons under the microscope……89
2.5 Antibody production…….....90
2.5.1 Endofree Maxiprep Plasmid Kit for amplification of the epitope-containing DNA…….....90
2.5.2 Analysis of DNA by sequencing……91
2.5.3 Spectrophotometric determination of DNA……...91
2.5.4 Preparation of Lysogeny broth (LB) agar ampicillin plates……..….91
2.5.5 Transformation protocol of *E. coli* with pET32b ε-sarcoglycan peptide...92
2.5.6 Induction of target protein using IPTG on a large scale……92

2.5.7 Preparation of cleared BL21(DE3) lysates under denaturing conditions for purification of the target protein……...93
2.5.8 Batch purification of 6xHis-tagged proteins from BL21(DE3) cells under denaturing conditions…….....93
2.5.9 Selection and preparation of Dialysis Membrane…….....94
2.5.10 Dialysis of ε-sarcoglycan peptide…….…….....94
2.5.11 Concentrating the purified ε-sarcoglycan peptide…….…….....94
2.5.12 Recombinant Enterokinase (rEK) treatment on the 33kDa ε-sarcoglycan peptide…….…95
2.5.13 Isolation of the ε-sarcoglycan peptide from the S-tag-containing peptide…….……95
2.5.14 Bradford Protein Assay (for protein and antibody)…..……..…...96
2.5.15 Lyophilisation…….……..……96
2.5.16 Antibody production…….…….....97
2.6 Isolation of anti-ε-sarcoglycan antibody from immunised Rabbit serum……...98
2.6.1 Cross-linking of ε-sarcoglycan peptide to the AminoLink Column….....98
2.6.2 Affinity purification of anti-ε-sarcoglycan antibody from immunised Rabbit serum……...…….....99
Chapter 3……..…….....100
3.0 Classical and delta dystrophin isoforms are differently localized in brain and hence likely to form different DPC complexes……..……..100
3.1 Introduction……...100
3.2 Results……...103
3.2.1 BLAST database search…….....103
3.2.2 Isolation of brain subcellular fractions……...…….….105
3.2.3 Classical and delta dystrophin are differently distributed in the forebrain…….114
3.2.4 Classical and delta dystrophin are differently distributed in the cerebellum…….…….……..121
3.2.5 Dystrophin is an integral PSD protein of the forebrain…...….....126
3.3 Discussion…….....130
3.3.1 Classical and delta dystrophin exhibit different regional and subcellular distribution in forebrain and cerebellum, hence they are likely to form different DPC complexes…….…….....130
3.4 Conclusion……..……...136
Chapter 4:...……...138
4.0 Delta dystrophin does not replace classical dystrophin at GABAergic synapses to form novel delta dystrophin-containing DPC complexes…….…….....138
4.1 Introduction…….…….....138
4.2 Results…….…….....140
4.2.1 Comparison of delta dystrophin with PSD-95 …….…….....140
4.2.2 Comparison of delta dystrophin with NMDA R …….……...……..142
4.2.3 Comparison of delta dystrophin with $GABA_A$ R …….144
4.2.4 Comparison of delta dystrophin with GAD 65…….....146
4.2.5 Comparison of delta dystrophin with synaptophysin …….....148

4.2.6 Comparison of delta dystrophin with β-dystroglycan ……..……...151
4.2.7 Comparison of delta dystrophin with classical dystrophin ..…….....153
4.2.8 Comparison of delta dystrophin with rhodamine-phalloidin……..…....155
4.2.9 Delta dystrophin and MAP2 exhibit substantial co-localization…….....157
4.2.10 Delta dystrophin co-localizes with β3-tubulin……..…….....159
4.2.11 Recombinant Cexon78 EGFP and Dexon78 EGFP sequences are unable to traffick differently in the cell……..…….....162
4.3 Discussion…….....166
4.3.1 Delta dystrophin does not replace classical dystrophin at GABAergic synapses to form novel delta dystrophin-containing DPC complexes....166
4.4 Conclusion…….……..……..171
Chapter 5:..…...……..……173
5.0 ***Part 2***……...……..….....173
5.1 ε-sarcoglycan is likely to form novel complexes in the brain that are not related to dystrophin protein complexes…….....…….....174
5.2 Introduction…….....174
5.3 Results…….....177
5.3.1 Isolation of forebrain and cerebellum subcellular fractions…….....177
5.3.2 ε-sarcoglycan is a membrane-associated protein of the forebrain, and only present in low levels in PSDs...…….....178
5.3.3 ε-sarcoglycan is a membrane-associated protein of the cerebellum, and only present in low levels in PSDs……..……..….....182
5.3.4 ε-sarcoglycan, classical and delta dystrophin are differently distributed in cortical neurons, suggesting ε-sarcoglycan is unlikely to be a component of classical and delta dystrophin-containing DPC complexes in cortical neurons……..187
5.3.5 The low levels of classical dystrophin isoforms imunoprecipitated by ε-sarcoglycan suggest ε-sarcoglycan is unlikely to associate with classical dystrophin-containing DPC complexes in the forebrain ……...……191
5.3.6 Anti-ε-sarcoglycan antibody production for the characterization of ε-sarcoglycan binding partners……..……..….....199
5.4 Discussion……..……..….....214
5.4.1 ε-sarcoglycan is likely to form novel complexes in the brain that are not related to dystrophin protein complexes ……..……..….....214
5.6 Conclusion……...……..221
Chapter 6:..…….....….....222
6.1 Conclusions……..…….....222
6.1.1 Part 1…….....222
6.1.2 Part 2…….....224
6.2 Future Work…….....225
6.2.1 Part 1……...225
6.2.2 Part 2……228
References:……..230
List of Appendices:…….….....259

Appendix I General Molecular Biology Reagents..……..…260
Appendix II Media, solutions and reagents for cell culture…….....265
Appendix III Antibodies……..…….....266

List of figures

Chapter 1:

Part 1

Figure 1.1.2.1: Domain structure of classical full-length and shorter dystrophin isoforms……...……..……..…....22
Figure 1.1.2.2: Domain structure of classical and delta dystrophin……...…….....23
Figure 1.1.7.1: The established molecular organization of the DPC complex in neurons……..…...42
Figure 1.1.7.2: Domain structure of α and β-dystroglycan……..44
Figure 1.1.7.3: Domain structure of β-dystrobrevin…….....45
Figure 1.1.7.4: Domain structure of syntrophin isoforms……...……..46

Part 2

Figure 1.3.2: ε-sarcoglycan protein structure and relative exonic composition……..58

Chapter 2:

Figure 2.2.2: Subcellular fractions prepared by the Cotman *et al* (1971) method…...79

Chapter 3:

Figure 3.2.2.1: SDS PAGE separation of forebrain subcellular fractions……..106
Figure 3.2.2.2: Western Blot of forebrain subcellular fractions immunodeveloped with anti-neuroplastin antibody (Gp65)…...…….....109
Figure 3.2.2.3: Western Blot of forebrain synaptic fractions immunodeveloped with anti-neuroplastin antibody (Gp65). PSDs were isolated by the Triton X-100 (T) or n-octyl glucopyranoside methods……...110
Figure 3.2.2.4: Western blot of forebrain subcellular fractions immunodeveloped with anti-Gp50 antibody. PSDs were prepared by the n-octyl glucopyranoside method…….…….…….....111
Figure 3.2.2.5: Western blot of forebrain subcellular fractions immunodeveloped with anti-PSD95 antibody. The PSD fraction was prepared by the Triton X-100 (T) method ……...……..113
Figure 3.2.3.1: SDS PAGE separation of forebrain subcellular fractions, together with PSDs isolated by either the Triton X-100 detergent method or the n-octyl glucopyranoside method…….....116

Figure 3.2.3.2: Western blot of forebrain subcellular fractions immunodeveloped with anti-β-dystrobrevin antibody…….……117
Figure 3.2.3.3: Western blot of forebrain subcellular fractions immunodeveloped with anti-classical dystrophin antibody…….....118
Figure 3.2.3.4: Western blot of forebrain subcellular fractions immunodeveloped with anti-delta dystrophin antibody…….....120
Figure 3.2.4.1: Western blot of forebrain and cerebellar subcellular fractions immunodeveloped with anti-classical dystrophin antibody….....124
Figure 3.2.4.2: Western blot of forebrain and cerebellar subcellular fractions immunodeveloped with anti-delta dystrophin antibody…….....125
Figure 3.2.5.1: Western blot of forebrain subcellular fractions including PSDs prepared using the Triton X-100 or n-octyl glucopyranoside method and immunodeveloped with anti-delta dystrophin antibody…….....128
Figure 3.2.5.2: Western blot of forebrain subcellular fractions including PSDs prepared using the Triton X-100 or n-octyl glucopyranoside method and immunodeveloped with anti-classical dystrophin antibody…….....129

Chapter 4:

Figure 4.2.1: comparison of delta dystrophin with PSD-95…….…….....141
Figure 4.2.2: comparison of delta dystrophin with NMDA R…….……..……..143
Figure 4.2.3: comparison of delta dystrophin with $GABA_A$ R…….……..…….....145
Figure 4.2.4: comparison of delta dystrophin with GAD 65…….…….....147
Figure 4.2.5: comparison of delta dystrophin with synaptophysin……..……..150
Figure 4.2.6: comparison of delta dystrophin with β-dystroglycan……..…….....152
Figure 4.2.7: comparison of delta dystrophin with classical dystrophin…..…….…..154
Figure 4.2.8: comparison of delta dystrophin with rhodamine-phalloidin……..…....156
Figure 4.2.9: delta dystrophin exhibits substantial co-localization with MAP2….....158
Figure 4.2.10: delta dystrophin co-localizes with β3-tubulin…..…….....161
Figure 4.2.11.1: pEGFP-N3 vectors containing cDNAs of classical or delta exon 78 fused with enhanced green fluorescent protein (EGFP)…..164
Figure 4.12.11.2: Dexon78 and Cexon78 exhibit a similar subcellular distribution in neurons…….....……..…….165

Chapter 5:

Figure 5.3.2: Western blot of forebrain subcellular fractions immunodeveloped with anti-ε-sarcoglycan antibody……..……181
Figure 5.3.3: Western blot of forebrain and cerebellar subcellular fractions immunodeveloped with anti ε-sarcoglycan antibody……..…….186
Figure 5.3.4: ε-sarcoglycan does not co-localize with classical dystrophin…..……189
Figure 5.3.5.1: Western blot containing anti-ε-sarcoglycan immunoprecipitated proteins of the forebrain, immunodeveloped with

anti-ε-sarcoglycan antibody……..……...193
Figure 5.3.5.2: Western Blot from figure 4 stripped with Glycine pH 2.5, and subsequently immunodeveloped with anti-rabbit secondary antibody……....195
Figure 5.3.5.3: Western blot containing anti-ε-sarcoglycan immunoprecipitated proteins of the forebrain, immunodeveloped with anti-classical dystrophin antibody……..……....198
Figure 5.3.6.1: A pET32b vector designed for cloning and high-level expression of peptide sequences. ε-sarcoglycan peptide has been inserted in the Multiple Cloning Site (MCS)…….……....….....201
Figure 5.3.6.2: SDS PAGE separation of BL21 (DE3) cells transformed with the pET32b ε-sarcoglycan peptide and treated with IPTG…….....202
Figure 5.3.6.3: Western Blot of IPTG induced BL21 (DE3) cells immunodeveloped with anti-His antibody…….……..……..203
Figure 5.3.6.4: SDS PAGE separation of ε-sarcoglycan peptides isolated using a Nickel Column……..……..……...205
Figure 5.3.6.5: Western blot of purified 33kDa ε-sarcoglycan peptides immunodeveloped with anti-His antibody….……...….206
Figure 5.3.6.6: SDS PAGE separation of 18kDa tag and a 14kDa ε-sarcoglycan peptide obtained by recombinant Enterokinase (rEK) digestion of the 33kDa ε-sarcoglycan peptide……..……..….....208
Figure 5.3.6.7: SDS PAGE separation of the purified 14kDa ε-sarcoglycan peptide…….209
Figure 5.3.6.8: Western blot containing a forebrain homogenate preparation, and an aliquot of pure 33kDa ε-sarcoglycan peptide, immunodeveloped with the new anti-ε-sarcoglycan antibody……..212
Figure 5.3.6.9: Western blot containing a forebrain homogenate preparation, and an aliquot of pure 33kDa ε-sarcoglycan peptide, immunodeveloped with the last aliquot of anti-ε-sarcoglycan antibody provided by our Oxford collaborators…….213

List of Tables

Chapter 3:

Table 3.2.1: classical and delta exon 78 contain no putative conserved domain…….……...……...……104

Chapter 5:

Table 5.3.6: Spectrophotometer reading used to identify the elution containing the new anti-ε-sarcoglycan antibody……..…….....211

Chapter1:

1.0 Part 1

1.1 The DPC complex in the Brain

1.1.1 Introduction and major aims

Duchenne Muscular Dystrophy (DMD) is a recessive, fatal, X-linked disorder discovered by French physician Duchenne de Boulogne (Duchenne *et al*, 1860), whilst he was examining the motion and verbal skills of a seven year old boy (reviewed by Blake *et al*, 2000). It was only by 1987 that Koenig *et al*, through a technique known as positional cloning approach, isolated and characterized the gene responsible for DMD, and named it the DMD gene (Koenig *et al*, 1987; Koenig *et al*, 1988). The protein product of the DMD gene, named dystrophin, was identified by Hoffman *et al* (1987). The name of the DMD gene product, whose mutation gives rise to DMD, was chosen to reflect the effects the muscle undergoes in DMD patients. In brief, when a DMD muscle carries out a simple movement, the muscle tears and only at the early stages of the disease can the muscle repair the damages caused. With time, the muscle is no longer able to rescue all the damage being continuously created, degenerates and thus the disease starts to take over. It is this muscle wasting that suggested the DMD protein product to be named dystrophin, in latin, meaning muscle wasting. Muscle dystrophin is a very large protein, precisely 427kDa.

DMD involves a complex pathophysiology that is not easily explained by the loss of the protein dystrophin, the primary defect in DMD (Wehling-Henricks *et al*, 2009). This is because dystrophin (427kDa) in the muscle is part of a multiprotein complex called the Dystrophin Associated Protein Complex (DPC), which in turn binds to a series of additional proteins, many of which have already been identified, that together lead to DMD. One well established function of the DPC complex is to maintain the integrity of the muscle tissue by linking the intracellular parts of the cell to the exterior of neighboring cells and the extracellular matrix. In other words, when a healthy individual utilizes his/her own muscle, the muscle remains intact, thanks to these functional inter-linking mechanisms between neighboring cells of the muscle tissue. A mutation of the DMD gene disrupts the dystrophin protein, which in turn breaks the linking mechanism normally exhibited by the DPC complex, thus generating DMD in the muscle whenever the muscle is being

utilised. At birth, these boys appear clinically normal, but the continuing muscle tearing as a consequence of a mutated DMD gene generates neuromuscular wasting which becomes clinically evident by the age of five. As they grow older, the muscle progressively weakens such that by the age of twelve they are confined to a wheel chair. It is the weakening and hence failure of diaphragm and cardiac muscles that eventually leads to death of most patients by their early twenties (Benson *et al,* 1996; Blake *et al,* 1999; reviewed in Blake *et al,* 2002).

The muscle is not the only organ to be affected in these individuals, the brain, the focus of this thesis, is also affected. Cognitive defects were first identified as a feature of the pathology of DMD in 1868 (Duchenne *et al*, 1868; Allen *et al*, 1960, Marsh *et al*, 1974). When numerous DMD individuals faced simple language skills (IQ) tests, it became evident that DMD boys have IQs that are about one standard deviation below normal, and more than 30% of DMD boys score in the mentally retarded range (Karagan *et al,* 1979; Emery *et al,* 1993; Deng *et al,* 2009), encountering poor language skills as well as other cognitive impairments (Lidov *et al,* 1996). There is now a sufficient body of evidence to show that cognitive impairment in one third of these patients is a consequence of the mutation of the DMD gene (reviewed in Blake *et al,* 2002). The route by which mental impairments in DMD patients originates appears to have high similarity to that in the muscle, as several groups (Brunig *et* al, 2002, Culligan *et al,* 2002) including our collaborators (Blake *et al,* 1999) have revealed the existence of DPC complexes in the brain, which are of similar although not identical composition to the muscle DPC complex. However, the neurological aspects of DMD are still not well understood.

The DMD gene product in brain, which in this thesis I will refer to as classical full-length dystrophin, is a 427kDa protein. Unlike the muscle, the brain contains a variety of shorter classical dystrophin isoforms that arise from highly regulated promoters located along the DMD gene. These shorter classical dystrophin isoforms are also known to form additional DPC complexes in the brain (Blake *et al,* 1999), however, to date only DPC complexes containing the classical full-length dystrophin have been identified at the synapse of neurons (Blake *et al,* 1999; Culligan *et al,* 2002; Blake et al 2009). Studies have shown that mice lacking the full-length protein only, whilst shorter classical dystrophin isoforms continue to be expressed in

the brain, can lead to mental impairments that are very similar to the brain dysfunctions observed in DMD patients (Kim *et al*, 1992). This is a crucial finding as it demonstrates that classical full-length dystrophin plays a major role in the brain abnormalities observed in DMD patients. On the basis of these studies, in this thesis I present a new and potentially very important protein. It is the alternatively spliced form of classical full-length dystrophin protein. I named this novel protein delta full-length dystrophin. Very little is known about this protein, but given its high homology to classical full-length dystrophin, and the crucial importance classical full-length dystrophin is known to have on the brain (see section on the mdx mouse), I determined (chapter 3 & 4) whether delta full-length dystrophin can replace classical full-length dystrophin to form novel and yet unidentified delta DPC complexes in the brain. This would help better understand the molecular dynamics underlying DMD brains, and increase our understanding on the molecular complexity and functional roles of DPCs in the rat brain.

1.1.2 Molecular genetics of the DMD gene and encoded proteins

I begin by describing the molecular genetics of the DMD gene (figure 1.1.2.1). The DMD gene is the largest gene found in human beings, it comprises of nearly 0.1% (2.5 Mb of genomic DNA) of the entire genome (Koenig *et al*, 1987; Anderson *et al*, 2002) and it is found within chromosome Xp21.2 (Koenig *et al*, 1987; Muntoni *et al*, 2003). This gene is very complex, and comprises of 85 exons including seven unique exons (figure 1.1.2.1) linked to the independent tissue-specific promoters, generating at least three full-length and four shorter dystrophin isoforms (Muntoni *et al*, 2003; Sadoulet-Puccio *et al*, 1996). Three independently regulated promoters (namely B, M and P) are found within a 400kb genomic interval (Mehler *et al*, 2000), these encode full-length dystrophin for muscle (Dp427m), brain (Dp427b) and Purkinje cells (Dp427p) (reviewed in Blake *et al*, 2002; Muntoni *et al*, 2003). Each transcribed product consists of a unique first promoter, followed by a common set of 78 exons that generate a 427kDa protein product (Torelli *et al*, 1999; Spence *et al*, 2004). Four internal promoters independently regulate the expression of shorter dystrophin proteins. The four shorter dystrophin isoforms each contain a unique 5'-exon, but contain a C-terminal domain that is identical to that of full-length dystrophin. Each of these promoters (figure 1.1.2.1) uses a unique first exon that splices into exons 30, 45, 56, and 63, respectively, to generate shorter dystrophin products whose names are given based on their molecular weight, i.e 260kDa (Dp260), 140kDa (Dp140), 116kDa (Dp116) and 71kDa (Dp71), respectively.

In addition to these isoforms, the dystrophin gene generates an even greater number of isoforms by using an alternative poly(A)-addition site, localized in intron 70 of the dystrophin gene, and also by alternative splicing that occurs at the 3'-end of the dystrophin gene (Feener *et al*, 1989; Kudoh *et al*, 2005). This thesis strictly focuses on two dystrophin isoforms only, the classical full-length dystrophin and the delta full-length dystrophin (figure 1.1.2.2). In other words, the DMD gene is transcribed into pre-mRNA, and if the cell machinery decides to keep classical exon 78, a classical full-length dystrophin protein is obtained (figure 1.1.2.2A). On the other hand, if the pre-mRNA of dystrophin undergoes alternative splicing of classical

exon 78 (Cexon78) at the C-terminus, and replaces it by a longer and unique sequence I name delta exon 78 (Dexon78) (figure 1.1.2.2B), a delta full-length dystrophin product is produced. This alternative splicing is known as mutually exclusive alternative splicing. That is, the two exons are never present together in the dystrophin protein, if classical exon 78 is present, delta exon 78 is not, and vice versa. Hence the two proteins can be easily distinguished from one another using an antibody that strictly targets one of the two exons only.

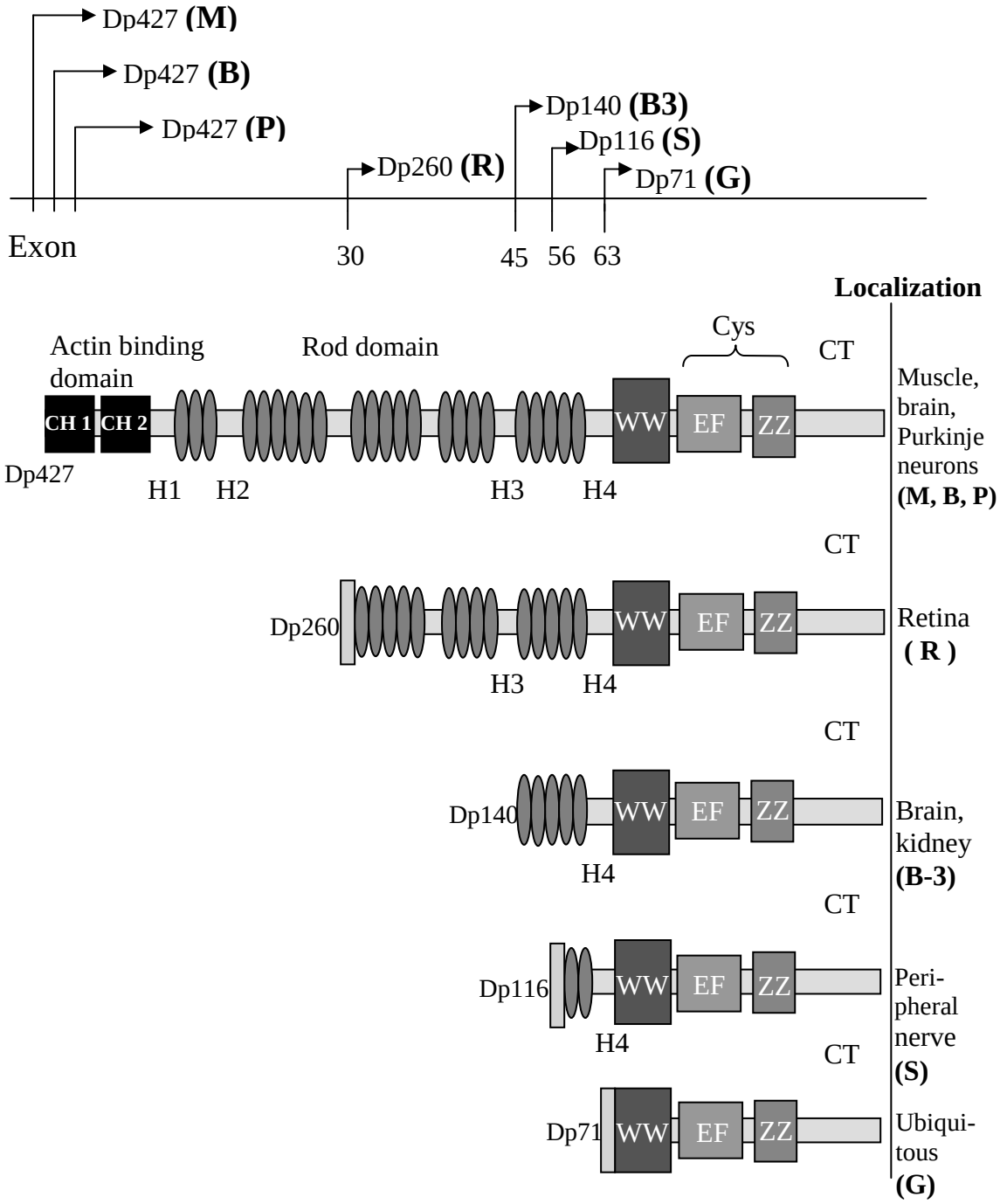

Figure 1.1.2.1: Domain structure of classical full-length and shorter dystrophin isoforms. The figure shows the domain structure of classical dystrophin isoforms. There are 7 tissue-specific promoters along the DMD gene. The dystrophin proteins are named according to their molecular weight, hence Dp427 (427kDa protein), Dp260, Dp140, Dp116, and Dp71. The promoters are referred to as M-promoter (Muscle), B-promoter (Brain), P-promoter (Purkinje), R-promoter (Retinal), Brain-3 promoter (Brain & kidney), S-promoter (Schwann cells) and G-promoter (General). CH, calponin homology domain; H1 & H2, hinge regions; WW, tryptophan-containing domain; EF, EF hand domain; Cys, cysteine-rich region; ZZ, zinc finger domain; CT, C-terminal domain. This figure is adapted from Blake *et al* (2000).

A: Classical Dystrophin (cDp427)

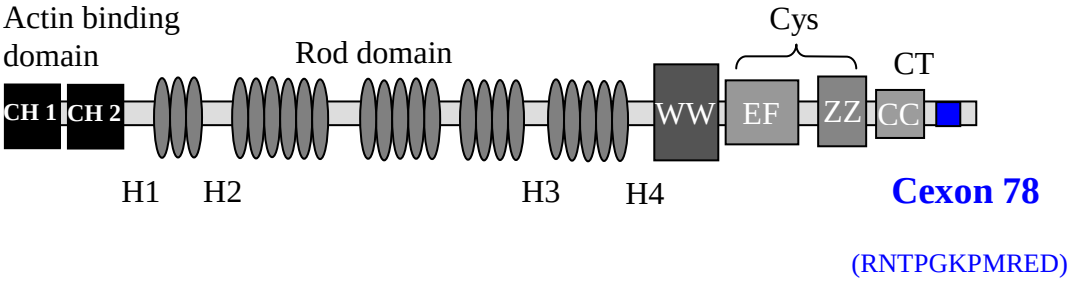

B: Delta Dystrophin (dDp427)

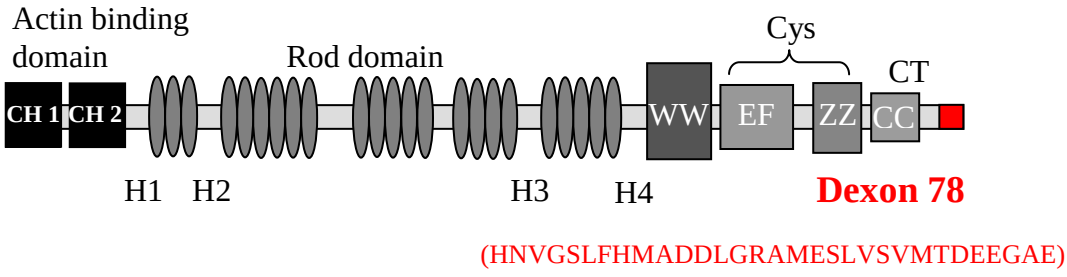

Figure 1.1.2.2: Domain structure of classical and delta dystrophin.

The figure shows the domain structure of classical and delta full-length dystrophin, both have a similar molecular weight close to 427kDa. They comprise of an N-terminal domain, a rod domain, WW domain, cysteine-rich domain (2 EF hands and 1 ZZ domain) and a C-terminal (CT) domain. An unknown domain region separates the coiled-coil domain from the C-terminal site where alternative splicing can occur. Cexon 78 and Dexon78, represented by the blue and red box respectively, are the exonic sequences that distinguish classical full-length dystrophin from delta full-length dystrophin. Delta full-length dystrophin arises via alternative splicing, whereas classical full-length dystrophin is taken as a conventional isoform. In brackets is the amino acid sequence of Cexon78 (blue) and Dexon78 (red), respectively. Delta dystrophin is 20 amino acids longer than classical dystrophin. This figure is adapted from Blake *et al* (2000).

1.1.3 Localization and developmental expression of dystrophins

As highlighted in the preceding section, dystrophin in the brain exists as various isoforms of differing molecular weights. Seven separate promoters at the DMD gene locus code for alternate transcripts that exhibit nervous system developmental, regional and cell type specificity (figure 1.1.2.1). There are three separate full-length dystrophin transcripts whose protein products are restricted to distinct sites. Dp427m (muscle dystrophin) is expressed predominantly in skeletal, cardiac, and smooth muscles, and also at very low concentrations, in brain astrocytes and vascular endothelial cells (Mehler *et al,* 2000). Dp427b (brain dystrophin) is an isoform expressed in the forebrain, precisely within hippocampal and cortical neurons (Nudel *et al,* 1989; Mehler *et al,* 2000). Dp427p (Purkinje dystrophin) is expressed in fetal cerebral cortex and in mature cerebellar Purkinje cells and skeletal muscle (Torelli *et al,* 1999; Mehler *et al,* 2000; Spence *et al,* 2004). Immunofluorescent studies on adult mice have demonstrated that the dystrophin isoforms localize within proximal somadendritic regions, notably in cerebral cortex, hippocampus and cerebellum (Gorecki *et al,* 1992; Lidov *et al,* 1993). According to immunoblotting studies, only the full-length dystrophin isoform localizes in neurons (Lidov *et al,* 1990; Kim *et al,* 1993; Blake *et al,* 1999), whereas the shorter isoforms localize in glial cells (Blake *et al,* 1999).

The brain contains additional shorter dystrophin transcripts whose cell, tissue and developmental transcription are also highly controlled. Dp260 is present in the retina, precisely at the synapse between retinal photoreceptor and on bipolar cells (reviewed in Mehler *et al,* 2000). Dp140 is expressed in the brain and kidney and various other parts of the CNS, such as the astroglial processes throughout the neuropil during development, on leptomeningeal surfaces and along penetrating blood vessels, ensheathing the olfactory nerve and in the neurohypophysis (Lidov *et al,* 1990; Lidov *et al,* 1995; Lidov *et al,* 1996). Dp116 is expressed in the late human fetal brain and in the postnatal diencephalon (caudate/putamen). Dp116 is also expressed in the peripheral nerve. Dp71 is ubiquitously expressed in the brain (Lederfein *et al,* 1992; Austin *et al,* 1995). Dp71 is found in early embryonic stem cells, in areas of

mesenchymal-epithelial interactions, in embryonic midbrain and hindbrain (reviewed in Mehler *et al*, 2000). It is also present in perinatal brain correlated with stages of terminal neural differentiation, and preferentially in early embryonic forebrain. Dp71 expression continues from embryonic stages until adult life, specifically in the cerebral cortex, granule neurons of the dentate gyrus of the hippocampus, olfactory bulb, pituitary and retina (reviewed in Mehler *et al*, 2000). Dp71 is also present in neocortical regions associated with continuing neurogenesis and synaptic plasticity (reviewed in Mehler *et al*, 2000). At a subcellular level, Dp71 transcripts are present in association with synaptic vesicles, microsomes and mitochondria (reviewed in Mehler *et al*, 2000).

Dystrophins play important roles in brain neural development. Truncated dystrophin isoforms are known to be present in the developing neural tube prior to the onset of neurogenesis and the start of regional patterning (reviewed in Mehler *et al*, 2000). They are also located in selected areas of the embryonic and postnatal neuraxis, suggesting dystrophin isoforms may be involved in the regulation of neurogenesis, neuronal migration and cellular differentiation during development (reviewed in Mehler *et al*, 2000). Separate studies suggest full-length dystrophin is only detectable at week 12 of gestation, reaching peak at week 15 and then remaining stable, thus full-length dystrophin is most probably involved in stabilization of specific neuronal structures, rather than participation in neuronal network formation (Spence *et al*, 2004). Thus existing synaptic connections are maintained and excessive remodeling prevented (Brunig *et al*, 2002; Fritchy *et al*, 2003). However, there is still no clear understanding on the function of dystrophin during development. Furthermore, given that the brain contains classical and well as delta dystrophin isoforms, it would be interesting to separately investigate their localization and expression time points during brain neural development, such that their involvement in brain development can be studied and compared in more detail.

Once all the neural networks are formed and have reached a state of maturity, classical full-length dystrophin, but no shorter isoforms, is enriched in the PSD fraction (Blake *et al*, 1999; Brunig *et al*, 2002). What is more, Brunig *et al* (2002) show classical dystrophin exclusively localizes at the PSD of inhibitory (GABAergic) synapses in mature hippocampal neurons. Together, these studies suggest classical full-

length dystrophin modulates the functions of the inhibitory synapse apparatus. Immunochemical analyses using adult mouse brain confirm the localization of classical dystrophins at post-synaptic densities (PSDs) not only in hippocampus, but also in the cerebral cortex, cerebellum, and olfactory bulb, with highest regional expression of dystrophin being in the cerebellum (Kim *et al*, 1992; Lidov *et al*, 1993). The PSD is a proteinaceous structure found at the post-synapse of neurons and is important for receiving many signals from the presynaptic nerve ending and converting them to the appropriate responses in the postsynaptic neuron. Given its localization at the PSD, classical full-length dystrophin may be implicated in modulating synaptic terminal integrity, plasticity as well as cellular signal integration. PSD localization of classical full-length dystrophin at these brain regions also suggests that it is implicated in cognitive functions, motor coordination, olfactory information processing, and altered synaptic plasticity, respectively (Kim *et al*, 1992). In fact, mutation of classical full-length dystrophin in brain, whilst shorter classical dystrophin isoforms continue to be expressed, leads to mental impairments that are very similar to the brain dysfunction observed in DMD patients (Kim *et al*, 1992). This clearly suggests that classical full-length dystrophin exhibits a very important role in the brain. It is therefore one of the foci of my thesis to compare the cellular and subcellular distribution of classical full-length dystrophin with a novel and potentially important delta full-length dystrophin (figure 1.1.2.2), to determine whether it too may contribute to the brain dysfunctions in DMD patients.

1.1.4 Structure of classical and delta dystrophin

Koenig *et al* (1988) carried out a number of structural studies and sequence analyses that highlight five different structural domains (figure 1.1.2.1 & 1.1.2.2) present in the DMD gene product. Given that classical and delta exon 78 are not included and do not interfere with these structural domains, I confidently suggest that these structural domains apply to both classical full-length dystrophin as well as delta full-length dystrophin. The proteins contain an N-terminal domain, a rod domain, WW domain, ZZ-type domain and a coil-coiled C-terminal domain. At the N-terminus of both dystrophin proteins there exist two calponin homology domains (CH1 and CH2) altogether encoding three actin-binding sites (ABS1-3), thus allowing dystrophin to associate with actin (Winder *et al*, 1997; Norwood *et al*, 2000). CH is a superfamily of actin-binding domains found in both cytoskeletal and signal transduction proteins, which cross-link actin filaments into bundles and networks. Pairs of CH domains are also said to confer binding to microtubules and α-helical peptide motifs (Slep *et al*, 2007, Sjoblom *et al*, 2008), however, this binding ability has yet to be investigated in dystrophin proteins. An unknown domain region separates the CH domain from the rod domain, made of 23 spectrin-like α-helical repeats. The rod domain (R1-23) enables the protein to be flexible, such that homo- and hetero-oligomeric parings can take place. The two subdomains R1-3 and R4-19 interacts with lipids and F-actin, while the distal sub-domain R20-23 does not exhibit any interaction (Legardinier *et al*, 2009). R16 and 17 in classical full-length dystrophin anchor nNOS to the membrane (Lai *et al*, 2009). An unknown domain region separates the rod domain from the WW domain, a short 32 amino acid sequence which folds as a stable, triple stranded beta-sheet. The name of the WW domain derives from the presence of two signature tryptophan (Trp,W) residues. The WW domain of dystrophin binds to proteins with proline rich domains (for example, the cytoplasmic proline rich C-terminal domain, XPPY motif, of β-dystroglycan) (Einbond *et al*, 1996), and it is frequently associated with other domains typical for proteins in signal transduction processes, such as γ1-syntrophin (Culligan *et al*, 2002). An unknown domain separates the WW domain from the ZZ (zinc-binding)-type zinc domain. The ZZ domain is able to bind two zinc atoms, and contains finger-like protrusions that make tandem contacts with their target molecule, thought to function in protein-protein interactions.

The coding significance of classical exon 78 and delta exon 78, for classical and delta dystrophin proteins respectively, is not known. Both exons encode two completely different sequences to one another (figure 1.1.2.2). In chapter 3 & 4 I have investigated the significance of these exons. I have determined whether they are homologous to any already established functional domains recently published on the database. What is more, I have tested whether this C-terminal difference affected the subcellular distribution and function of classical full-length dystrophin when compared to delta full-length dystrophin.

Shorter classical and delta dystrophin isoforms are identical to the classical and delta full-length dystrophin isoforms, but lack parts of the N-terminus domain, as shown in figure 1.1.2.1..

1.1.5 DMD gene mutations

The DMD gene has a high mutation rate, 1 x 10^{-4} genes per generation (Amalfitano *et al*, 1997), that occurs at a frequency of about 1 in 3,500 new born males (Emery *et al*, 1993). Duchenne Muscular Dystrophy (DMD) and Becker Muscular Dystrophy (BMD) are two disease phenotypes that originate by mutation of the DMD gene. As a result, the brain and other organs are affected. Approximately one third of all new cases result from a spontaneous mutation (Barbujani *et al,* 1990; Anderson *et al,* 2002; Nowak *et al,* 2004) of the DMD gene, these are mostly due to very small deletions and point mutations that lead to premature stop codons (reviewed in Blake *et al,* 2002). Hundreds of independent mutations can be found (reviewed in Blake *et al,* 2002) which include frame-shift (due to insertion), deletion or point mutations (www.dmd.com). Spontaneous mutations seem to lead to the expression of very unstable protein products, which may explain the very low amounts of the protein that can be detected (reviewed in Blake *et al*, 2002).

Depending on the type of DMD gene mutation, a more severe (DMD) or less severe (BMD) phenotype is obtained. The most common type of mutation in the DMD gene is an intragenic deletion. In fact these account for 65% of dystrophin mutations, whose consequences can induce either the DMD or the milder BMD phenotype. Less frequent mutations are gene duplications that account for only 5-15% of the cases of dystrophin mutations. There are two 'hot spots' where large deletions often take place, and these are found to cluster in exons 45-53 (which remove part of the dystrophin rod domain), and exons 2-20 (which remove some or all of dystrophin actin-binding domain, and part of its rod domain) causing the DMD phenotype (reviewed in Blake *et al,* 2002). Outside of these 'hot spots' however, there have been only a few cases, whereby gross deletions do not shift the normal open reading frame, and smaller but functional truncated dystrophin proteins are produced, leading to the milder BMD form (reviewed in Blake *et al,* 2002; reviewed in Muntoni *et al,* 2003).

The "reading frame hypothesis" represents 90% of DMD gene mutations observed to date, and is commonly used both as a diagnostic confirmation of dystrophinopathies and for the differentiation of DMD and BMD (reviewed in Muntoni

et al, 2003). In DMD, deletion and duplications have been observed which disrupt the reading frame (frame-shift, also known as out of frame), resulting in unstable RNA that eventually leads to the production of nearly undetectable concentrations of truncated proteins, hence leading to the more severe dystrophy named DMD (reviewed in Muntoni *et al*, 2003). In BMD, mutations have been observed which maintain the reading frame (in-frame), generally resulting in abnormal but partly functional dystrophin, hence leading to the less severe dystrophy named BMD (reviewed in Muntoni *et al*, 2003). There is no relation between the size of the deletion and the resultant clinical disease, as shown in a BMD patient that possessed a large deletion that involve nearly 50% of the gene (England *et al*, 1990). On the contrary, deletion of exon 44 only, was found in a patient with DMD. Generally, the outcome on the severity of the disease is manifested by the in-frame or out-of-frame nature of the mutation, rather than the size of the deletion (reviewed in Muntoni *et al*, 2003). When studying the effects that mutations have on the dystrophin protein, Legardinier *et al* (2009) and Singh *et al* (2010) showed that mutations alter the stability and folding processes of the protein, leading to a decrease in the net functional dystrophin concentration. These mechanisms shed light as to how mutations trigger muscular dystrophy.

There are exceptions to "the reading frame hypothesis", however, where frame-shift mutations yield a BMD phenotype rather than the expected DMD phenotype (reviewed in Muntoni *et al*, 2003). These mutations can either be a result of deletions or duplications in the 5' end of the DMD gene (exons 3-7; 5-7; 3-6) or further downstream (exons 51, 49-50, 47-52, 44 or 45). If these children have no family history of such a disease, diagnosis of the severity of the disease with a purely molecular genetic approach (for example, forward genetics) may be difficult in these patients. In fact, only some will develop DMD or BMD (reviewed in Muntoni *et al*, 2003). It is not clear why, it may be down to the efficiency in exon skipping, creating in-frame deletions which lead to the production of functional dystrophin. Therefore, the best method to diagnose whether the disease necessarily develops or not, would be to carry out a muscle biopsy in this patient in order to verify whether dystrophin is produced or not. Only at this point can the severity of the disease be predicted (reviewed in Muntoni *et al*, 2003). Exon skipping events, whereby the cellular machinery is encouraged to "skip over" specific exons, are limited to a few fibers and are routinely found in the dystrophin deficient mdx mice and in about 50% of children

with DMD. The induction of exon skipping (by using small pieces of DNA called antisense oligonucleotides (AO) in order to mask the exon that needs to be skipped) is currently being investigated for gene therapy by several researchers, in the hope that it will provide a possible therapeutic strategy in the future for patients with DMD (reviewed in Muntoni *et al*, 2003; Wilton *et al*, 2008).

A second exception to "the reading frame hypothesis" involves the diagnosis of in-frame mutations that yield DMD rather than then the expected BMD phenotype. Normally the disease phenotype is related to the ability to produce dystrophin. But this is not always the case. There are exceptions whereby the disease phenotype is dictated by the location of the mutation along the gene. For instance, in-frame deletions of the rod domain generally seem to cause BMD, as long as the amino and carboxy-termini of dystrophin are maintained. On the other hand, when the 5' ABS domain has an in-frame deletion of say, exons 3-13, this is usually associated with DMD. Disruption of the ABS domain, severely affects the ability of the dystrophin protein to link the cytoskeleton of the cell with neighboring cells, via the DPC complex. Thus it would resemble a situation where no dystrophin protein is expressed (reviewed in Muntoni *et al*, 2003).

As highlighted earlier, the brain and the muscle exhibit differences in the severity of the disease. One of the causes is due to the different physiological stresses they are faced with. Secondly, the differences between the brain and the muscle is further accentuated by the location of the mutation along the gene. In the muscle, mutations at the 5'-end of the dystrophin protein disrupt the ABS domain of full-length dystrophin, the only dystrophin expressed in the muscle, thus blocking the intercellular linkage of neighboring cells leading to muscle wasting. The situation in the brain is completely the opposite. In fact, mutations in the 5'-end of the dystrophin protein reduce the severity of the mental impairment in brain (reviewed in Muntoni *et al*, 2003). This is because mutations found at the 5'-end only affect the full-length dystrophin isoforms, but the brain also contains shorter dystrophin isoforms that lack the exon containing the mutation of full-length dystrophin, hence leaving intact the transcription and function of all remaining shorter isoforms, and hence the DPC-like complexes they are found in brain are able to function as normal. Consistent with this, DMD patients that possess 5' mutations have been diagnosed with just a mild form of

cognitive impairment. On the other hand, DMD patients found to have mutations in proximity to the 3'-end of dystrophin gene, causes a disruption of all classical dystrophin isoforms in the brain, and as a consequence, these DMD patients have been diagnosed with more severe cognitive impairment (reviewed in Muntoni *et al,* 2003). The availability of a greater number of dystrophin isoforms in the brain may partly explain why the mental disorders in DMD patients are less severe than the outcomes in the muscle.

DMD patients display a range of cognitive deficits including memory impairments, and these have been attributed to a lack of dystrophin in brain structures involved in cognitive functions, such as the hippocampus and neocortex (Anderson *et al,* 2002). Classical dystrophin is a major candidate protein considered to participate in cognitive deficits of DMD, but with the discovery of several shorter C-terminal isoforms of the full-length protein, the complexity of studies directed at understanding the molecular and cellular bases of the cognitive impairment in brains of DMD has increased in complexity. It is believed that the absence of classical full-length (427kDa) brain dystrophin affects cognitive function to a variable extent, although most patients exhibit some degree of memory deficits (Hinton *et al,* 2000), whereas mutations also affecting the shorter forms of dystrophin lead to more severe cerebral dysfunction (Moizard *et al,* 1998). However, the nature, magnitude and biological support of the cognitive deficits involving classical full-length dystrophin still remain unclear, and it is still just partly addressed by studies in the dystrophin-deficient mouse (see the subsequent section), a genetic model of DMD commonly named the mdx mouse (Anderson *et al,* 2002; Vaillend *et al,* 2002; Vaillend *et al,* 2004). This mouse model shows that total deficiency of full-length dystrophin alone, leads to abnormal brain responses recorded via a number of electrophysiological studies. It is important to note that in the brain of mdx mice, all remaining shorter dystrophin isoforms remain intact, as the mutation is not in the sequence containing shorter dystrophin isoforms. Hence the brain malfunctions in mdx mice is exerted and can therefore be attributed to the full-length dystrophin alone, rather than the truncated isoforms. In this thesis, I therefore focus on full-length dystrophin protein only.

1.1.6 A naturally occurring mutation in mice to study the function of dystrophin in brain: the mdx mouse

Studies on dystrophin CNS function have benefited from the mdx mouse, a naturally occurring animal model for DMD that has been available for over 20 years (Allamand *et al*, 2000). Mdx mice arise via a naturally occurring point mutation in exon 23 of the DMD gene that creates a premature stop codon. The pathological dystrophin transcripts lack the normal N-terminus and therefore are unable to attach to the plasma membrane and are degraded in the cytoplasm, leading to total deficiency of full-length dystrophin protein in muscle (Vainzof *et al*, 2008). This total deficiency of full-length dystrophin protein is also observed in the brain of these mdx mice (Muntoni *et al*, 1991). On the other hand, the brain contains additional shorter dystrophin isoforms whose expression remains intact in these mdx mice models (Sicinski *et al*, 1989). At the early stages of life, mdx mice show no obvious muscle weakness and their lifespan is not grossly reduced unlike human DMD, however simple in vivo tests have confirmed that mdx mice do resemble DMD, but exhibit such resemblance at later times relative to the life span in humans DMD. The reasons for these differences between humans and mice are not known. The accessibility of the mdx mice model has meant that more invasive biochemical measurements have been possible in order to study the function of dystrophin, to screen for strategies to treat the disease, and also to test the treatments on these mice (Allamand *et al*, 2000).

The major clinical issue in DMD is the skeletal muscle pathology, however there is now a sufficient body of data to appreciate that the brain functions of these patients are impaired (Anderson *et al*, 2002). Cognitive defects are non-progressive in these brains (Emery *et al*, 1993), and have been linked to the absence of classical full-length dystrophin that is otherwise expressed in cerebral structures involved in cognitive functions, such as the hippocampus and neocortex (Lidov *et al*, 1996). The functional importance of classical full-length dystrophin in the brain has been reported in numerous studies in mdx mice. The mdx mutant shows morphological alterations of pyramidal neurons (Sbriccoli *et al*, 1995), specific learning and memory deficits (Muntoni *et al*, 1991, Vaillend *et al*, 1995; Vaillend *et al*, 1998), facilitated synaptic plasticities (Vaillend *et al*, 2002), altered neuronal calcium homeostasis (Hopf

et al, 1992), and enhanced sensitivity of CA1 hippocampal neurons to hypoxia (Mehler *et al*, 1992).

The mdx mouse is not the only mouse model created to represent DMD, but it is the most commonly used mouse model to study the brain and muscle. Only briefly, a number of mdx strains will be described. The mdx^{2cv} mouse model contains a point mutation in the splice acceptor sequence of intron 42 that abolishes the expression of Dp427 and Dp260 only, whilst the remaining shorter dystrophin isoforms continue to be expressed (Im *et al*, 1996). The mdx^{3cv} mouse model contains a mutant splice acceptor site in intron 65 that abolishes the expression of all dystrophins (Sesay *et al*, 1996; Im *et al*, 1996; Vaillend *et al*, 1998). The mdx^{4cv} mouse model contains a point mutation in exon 53 that abolishes the expression of Dp427, Dp260 and Dp140, thus allowing only the expression of Dp116 and Dp71 isoforms (Im *et al*, 1996). The mdx^{5cv} mouse model contains a 53bp deletion in exon 10 generating a premature stop-codon that impedes the expression of Dp427, whilst the remaining shorter dystrophin isoforms continue to be expressed (Im *et al*, 1996). The mdx^{5cv} mice have been reported to display essentially the same muscle pathology as mdx mice, with additional phenotypes observed (Im *et al*, 1996).

Recently, and most importantly, a DMD-null mouse model has been produced via a 2.4Mb deletion of dystrophin gene (the entire DMD gene) through the use of Cre-loxP recombination system (Kudoh *et al*, 2005). The DMD-null mouse model is important as it is the only mouse model where there is absolutely no expression of the dystrophin protein or isoforms. In contrast, a range of reversion frequencies has been reported in the various mdx strain mouse models listed above (Danko *et al*, 1992). Given that the production of multiple dystrophin isoforms through alternative splicing or exon skipping is totally prevented in the DMD-null mouse, these new mutants will provide an improved model system for functional studies of dystrophin and its isoforms. With this recombination system, it is possible to specifically inactivate the expression of specific isoforms in the brain, and study their individual functions. Regardless the availability of different DMD mouse models, the mdx alone remains the most widely used mouse model to study the neurodegenerative and muscle disease in DMD (Allamand *et al*, 2000; Durbeej *et al*, 2002; Collins *et al*, 2003). This is because the phenotypic discrepancies between all the mouse strains

currently available have not been explained clearly, furthermore, they all show similar phenotype and little advantage over the original mdx model (Allamand *et al*, 2000; Durbeej *et al*, 2002; Collins *et al*, 2003).

Through the availability of the mdx mouse brains, there is histological evidence connecting cognitive impairment with the lack of classical full-length dystrophin in the brain. First of all, the cell packaging of the mdx mouse is varied when compared to control mice. For example, some mdx brains have been found to have a higher cell packing density than controls, whereas other mdx brains contained a lower cell density than controls (Anderson *et al*, 2002). What is more, these brains often exhibit neuronal loss, gliosis, neurofibrillary tangles, Purkinje cell loss, dendritic abnormalities, disordered architecture, astrocytosis and perinuclear vacuolation (Anderson *et al*, 2002). The Red nucleus, a structure in the restral (anterior) midbrain involved in motor coordination, revealed significantly lower cell counts in mdx animals when compared to controls (Carretta *et al*, 2001). Sbriccioli *et al* (1995) demonstrated a reduced number of cortico-spinal neurons in the major motor pathway of the cortico-spinal (CS) system when compared to controls, suggesting an involvement of the CNS in DMD (Sbriccioli *et al*, 1995; Carretta *et al*, 2001; Carretta *et al*, 2003; Carretta *et al*, 2004; Venoux *et al*, 2008). In analogy to mdx mice, in DMD brains examined pathologically, there is evidence of disordered cortical architecture, predominantly in frontotemporal regions, altered neuronal migration, and abnormal neuronal orientation with attenuated terminal dendritic arborizations (Mehler *et al*, 2000). Variable decreased cortical excitation is also a feature in patients with DMD (Mehler *et al*, 2000).

Muntoni *et al* (1991) was the first to report cognitive deficit in the mdx mice following mass training in the water maze, and noticed a reduced memory of the passive avoidance response in mdx mice when compared to controls. Vaillend *et al* (1998) also found that following massed training in the water maze, mdx mice are not impaired in task acquisition, procedural memory, behavioral exploration of a novel object, nor the encoding of a new experience or short-term memory for objects (Sesay *et al*, 1996, Vaillend *et al*. 1998). However, the consolidation or expression of long-term recognition memory and long-term spatial memory was impaired in mdx mice, whilst their acquisition abilities remained unaffected (Vaillend *et al*, 1995; Vaillend *et*

al, 2004). The impairments described above are very similar to the brain dysfunctions observed in DMD patients (Kim *et al*, 1992).

To identify the cellular mechanisms that may underlie the deficits in DMD brains, a number of electrophysiological studies have been carried out in the brains of mdx mice. Although no single region of the brain is solely responsible for the formulation or recall of memories, numerous observations implicate the hippocampus (Deng *et al*, 2009). For example, a human patient who received a bilateral hippocampectomy lost all ability to remember recent events, although long-distant memories and higher, abstract cognitive skills remained intact (Scoville *et al*, 1957). Similarly, rodents with hippocampal lesions show impaired memory (Morris *et al*, 1982). Together, these observations indicate that the hippocampus may be a site in the central nervous system in which functional defects result from the loss of full-length dystrophin (Deng *et al*, 2009), and is therefore used by electrophysiologists to study the altered functions of mdx brains.

Electrophysiological studies show that although basal synaptic transmission in mdx mice is similar to that observed in wild type (wt) (Vaillend *et al*, 2002), dystrophin deficiency in CA1 hippocampal neurons facilitates the induction of short-term potentiation (STP) and depression (STD), early long-term potentiation (LTP) and depression (LTD) of glutamatergic neurotransmission in mdx mice (Vaillend *et al*, 1998; Vaillend *et al*, 1999; Vaillend *et al*, 2002; Vaillend *et al*, 2004; Kueh *et al*, 2008). These forms of synaptic plasticity in CA1 hippocampal neurons are known to be via the NMDA receptor of glutamatergic synapses (Vaillend *et al*, 2002). The enhanced NMDA receptor-mediated synaptic plasticity in mdx mice may be due to a reduced GABAergic neurotransmission due to dystrophin deficiency (Vaillend *et al*, 2002). In fact, Knuesel et al (1999) found classical full-length dystrophin co-localizes with $GABA_A$ receptors clusters at inhibitory synapses in wild type (wt) mice. The author (Knuesel *et al*, 1999) reports a 50% decrease in the number of $GABA_A$ receptor clusters in the hippocampus of mdx mice, which may reduce GABAergic neurotransmission, thus increasing the capacity of NMDA receptor to be activated. This is possible because Vaillend *et al* (2002) showed that by application of a $GABA_A$ receptor antagonist bicuculline, both mdx and wt respond with the same magnitude of potentiation. Hence, the abnormal organization of $GABA_A$ receptor clusters is involved

in facilitating synaptic activities, and may do so by reducing GABAergic neurotransmission (Vaillend *et al*, 2002; Vaillend *et al*, 2004; Kueh *et al*, 2008), leading to the various facilitated forms of plasticity observed in mdx mice. Vaillend *et al* (2002) further showed that it is the reduced Mg^{2+} ion block in NMDA receptors of mdx that enhances the NMDA receptor mediated synaptic plasticity in mdx mice. This is because when they reduced the Mg^{2+} ion concentration in the bath, the facilitated induction in mdx was blocked and became similar to wild type. All in all, the lack of classical full-length dystrophin disrupts the $GABA_A$ receptor cluster size, which may reduce inhibitory neurotransmission. Thus, although the mechanism is not known, it may modulate the voltage-dependent block of NMDA receptor by Mg^{2+}, hence, facilitating synaptic activities in mdx mice (Vaillend *et al*, 2002).

The absence of dystrophin may have important consequences in cellular signal integration, in addition to the already stated membrane integrity, ion channel physiology, and structural reorganization of the synapse (Mehler *et al*, 2000). This too may underlie some of the behavioural problems and cognitive impairment reported in DMD (Kueh *et al*, 2008). DMD and mdx exhibit an 80% loss of an enzyme named nitric oxide synthase (NOS) because dystrophin deficiency leads to a secondary loss of a specific form of NOS in muscle, named nNOS (neuronal NOS) (Brenman *et al*, 1995; Chang *et al*, 1996; Deng *et al*, 2009). Interestingly, the concentration of nNOS in the brain is not affected in mdx mice (Deng *et al*, 2009). The consequences for a loss in NOS activity are numerous. NOS activity produces NO, and the muscle-derived NO is not only used by the muscle but it is also delivered elsewhere via the systemic circulation for use by other organs, such as the brain. The brain produces its own NO but also makes use of systemic NO, and NO is said to normalize cell proliferation and neuronal differentiation in the dendate gyrus (DG) of the hippocampus (Deng *et al*, 2009). In fact, muscle-derived NO regulates adult neurogenesis in the brain and loss of muscle nNOS has been shown to abnormally increase cell number and cell density in DG (Deng *et al*, 2009). Therefore, loss of muscle-derived NO in mdx mice may underlie the cognitive defects in the CNS of DMD patients (Deng *et al*, 2009). Dystrophin is therefore important for preventing the loss of nNOS in muscle.

Through the availability of mdx, Wehding-Henricks *et al* (2009) showed that there is a reduction in the glycolytic metabolism and an increased

fatigability in dystrophin muscle. They propose that loss of nNOS may underlie the defects in glycolytic metabolism observed in mdx mice. This is because their studies demonstrate that mdx mice containing nNOS transgene, the glycolytic metabolism is enhanced and the endurance of mdx mice increased. What is more, they demonstrate that nNOS can modulate the glycolytic pathway by directly interacting with a rate-limiting enzyme of the glycolytic pathway, named phosphofructokinase (PFK). They also show that PFK activity is increased upon binding to nNOS transgene. They conclude that a loss of positive allosteric interaction between nNOS and PFK may partly underlie the defects in glycolytic metabolism observed in mdx muscle. Dystrophin is therefore somehow important in promoting such interaction between nNOS and PFK.

The metabolic profile in mdx is easily distinguishable from wild type (wt). In mdx brain, a number of metabolic processes are affected, and these include β-oxidation, the TCA cycle, phosphocreatine/ATP cycle, lipid metabolism and osmoregulation (Griffin *et al*, 2001). Mdx mice have also been shown to be more sensitive to brief periods of severe hypoxia compared to wt, as synaptic transmission in the CA1 region of mdx mice is markedly more sensitive to hypoxia-induced damage compared to wild type. This suggests dystrophin plays an important role in protecting neurons from hypoxia-induced damage (Mehler *et al*, 1992), but the precise mechanism is yet to be established. It is being suggested that the altered response to hypoxia may also be influenced by the reported reduced $GABA_A$ receptor clustering in mdx mice (Knuesel *et al*, 1999), as $GABA_A$ receptor activation has been shown to exacerbate oxygen deprivation-induced neuronal injury (Muir *et al*, 1996). What is more, mdx neurons have increased intracellular calcium when compared to wt (Hopf *et al*, 1992), due to a calcium-specific regulatory defect in granule neurons. Changes in neuronal calcium homeostasis could have profound implications for the proper elaboration of a number of integral cellular functions, including excitability, associativity, neurotransmitter release, synaptic plasticity, gene transcription and the graded regulation of neuronal firing patterns (Mehler *et al*, 2000). A compartmentalized elevation of calcium could have a consequence of activating proteolytic enzymes and or apoptotic pathways (Burdi *et al*, 2009). Altogether, all

these mechanisms are likely to participate in generating the mental impairments observed in DMD patients, due to the absence of functional dystrophin.

As therapeutic approaches to DMD are being developed, mutant animals represent good models in which they can be tested (Allamand *et al*, 2000). It is the ease with which the murine genome can be manipulated that has made it particularly useful in testing functional hypotheses. Early transgenic experiments, using full-length as well as mini-dystrophin constructs, have demonstrated that expression of 20% of the dystrophin protein is sufficient to prevent the development of muscle pathology in mdx mice, thus generating great hope for a treatment for DMD (Allamand *et al*, 2000). Proteosome inhibitors as a therapy for DMD has been tested in mdx mice and results emphasise the effectiveness of the pharmacological approach as a potential treatment for DMD (Bonuccelli *et al*, 2007).

The mdx mouse is the most effective model for characterizing the structural and functional properties of dystrophin and therapeutic interventions (Chamberlain *et al*, 2007). The study of animal models for genetic diseases, in spite of the existence of differences in some phenotypes, can provide important clues to the understanding of the pathogenesis of these disorders and are also very valuable for testing strategies for therapeutic approaches (Vainzof *et al*, 2008). For clinical trials, it is being suggested to move one step forward from the mdx mouse, and use the canine golden retriever MD model, as it represents a more clinically similar model of DMD due to the animals larger size and significant muscle weakness (Vainzof *et al*, 2008).

In conclusion, studies carried out on mdx mice have demonstrated that brain full-length dystrophin performs diverse developmental and mature cellular functions. In the mature state these cellular functions are limited to a highly restricted subset of anatomically distributed neuronal subpopulations. These particular populations may mediate the specific cognitive functions and subsystems that are impaired in patients with DMD. There is contradicting evidence on the function of full-length dystrophin during development. Some say (Mehler *et al*, 2000) that full-length dystrophin may be involved in neuronal migration, cellular maturation and synaptogenesis during neural development (Mehler *et al*, 2000), whereas other researchers (Tretter *et al*, 2008) suggest that full-length dystrophin is unlikely to induce

synaptogenesis. It is being suggested that dystrophin may orchestrate the dynamic organization of neuronal microdomains by regulation of the orientation, spatial array and complement of multiple cellular proteins (Mehler *et al*, 2000). It is important to note that the mdx mutation of full-length dystrophin in the brain leads to the abolition of classical full-length dystrophin, as well as delta full-length dystrophin. It is therefore important to establish the functions of delta full-length protein. As previously stated, one of the major aims of this thesis was to study the molecular associations and subcellular localization of delta full-length dystrophin to determine its potential involvement in the pathology of DMD.

1.1.7 Protein interactions of the DMD gene product: the DPC complex

Through a series of co-immunoprecipitation, yeast two-hybrid interactions and co-localization studies, classical full-length dystrophin has been found to interact with a range of proteins, which in analogy to the muscle, make up the DPC complex in the brain (figure 1.1.7.1). The brain contains a variety of DPC-like complexes whose composition varies according to the cell-type it is found in and the dystrophin isoform it associates with (Blake *et al*, 1999; Culligan *et al*, 2002; Graf *et al*, 2004; Blake *et al*, 2009; Pilgram *et al*, 2009; Waite *et al*, 2009). In this thesis, only the DPC complex containing the classical full-length dystrophin is described and investigated. In the brain, the DPC complexes containing classical full-length dystrophin are exclusively localized at PSD structures of inhibitory synapses (Brunig *et al*, 2002) whereas DPC complexes containing the shorter dystrophin isoforms are said to localize in glial cells (Blake *et al*, 1999; Culligan *et al*, 2002; Graf *et al*, 2004; Blake *et al*, 2009; Pilgram *et al*, 2009). DPC complexes containing classical full-length dystrophin comprise of: a transmembrane and extracellular domain (α, β-dystroglycan), a cytoplasmic complex (classical full-length dystrophin, syntrophin-(α1, γ1, γ2), β-dystrobrevin and neuronal nitric oxide (nNOS)) and an extracellular domain (figure 1.1.7.1). While some say (Blake *et al*, 2009; Pilgram *et al*, 2009) that α-neurexin is the extracellular component that links to the DPC, others state that only β1-neurexin, rather than α-neurexin, is present at inhibitory synapses and associates with the DPC (Culligan *et al*, 2002; Graf *et al*, 2004). Classical dystrophin is always found associated with the DPC complex only, and it never appears to be on its own (Brunig *et al*, 2002), therefore, based on studies on mdx mice, this implicates the entire DPC complex, and not just classical full-length dystrophin, to participate in brain impairments found in DMD brains.

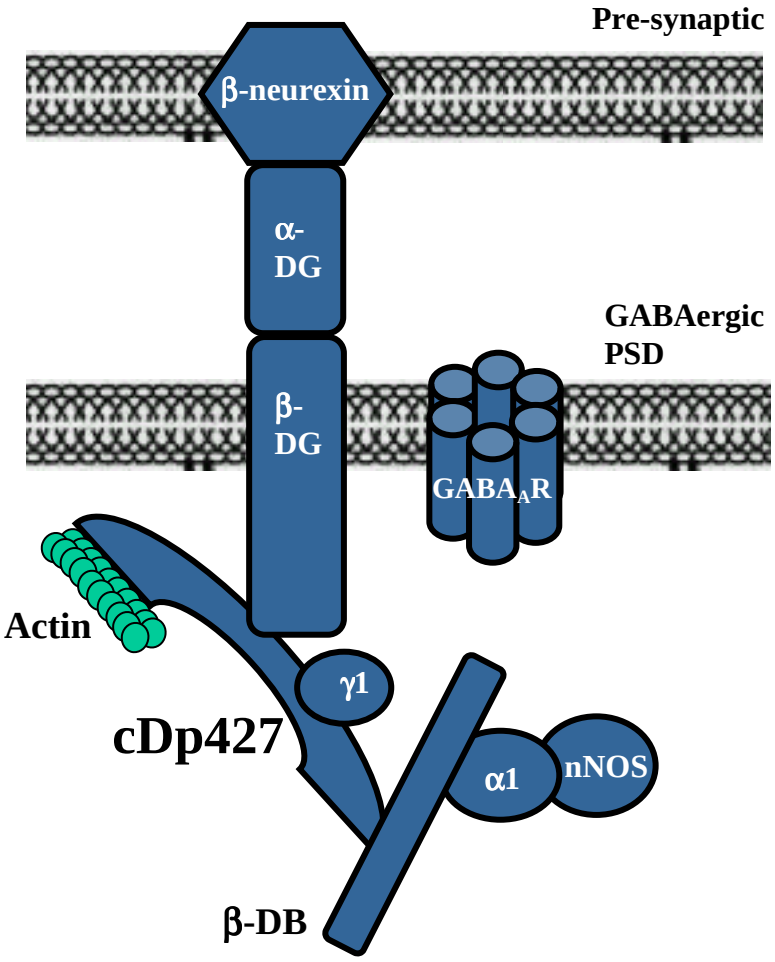

Figure 1.1.7.1: The established molecular organization of the DPC complex in neurons.

This figure shows the suggested model for the DPC complex present at PSDs of GABAergic synapses. Post-synaptic density (PSD), β-Neurexin (β-NX), α-dystroglycan (α-DG), β-dystroglycan (β-DG), syntrophin (α1 and γ1), Neuronal nitric oxide synthase (nNOS), β-dystrobrevin (β-DB), classical full-length dystrophin (cDp427), $GABA_A$ receptor ($GABA_AR$). For the purpose of clarity, only a subset of syntrophin isoforms has been added. This figure is adapted from Culligan *et al* (2002), Pilgram *et al* (2009) and Waite *et al* (2009).

The molecular interactions between the DPC components are as follows. The extracellularly exposed side of α-DG (the N-terminus) binds with high affinity (figures 1.1.7.1 & 1.1.7.2) to pre-synaptic β1-neurexins (LNS domain) (Graf et al, 2004), and the latter associates with post-synaptic neurologin 2 (Clarris *et al*, 2002; Graf *et al*, 2004). The C-terminal domain of α-DG (figure 1.1.7.2) forms non-covalent contacts with the N-terminus ectodomain of β-DG (Sciandra *et al*, 2001). β-DG has a transmembrane domain, hence it anchors the entire DPC complex into the postsynaptic membrane of GABAergic synapses (figures 1.1.7.1 & 1.1.7.2). The intracellular domain of β-DG contains a 15 amino acid C-terminus WW domain (Hnia *et al*, 2007) that binds to the WW-domain of classical dystrophin (Cavaldesi *et al*, 1999; Huang *et al*, 2000). The EF hand and the ZZ-type-zinc finger domains (figure 1.1.2.2) in the classical dystrophin protein stabilize and strengthen this interaction (reviewed in Blake *et al*, 2002). Classical dystrophin utilises the CH domain to enable a tight interaction with actin, such that the protein and the entire DPC complex is anchored to the cytoskeleton that underlies the membrane of neurons (figure 1.1.7.1). The coiled coil region of β-dystrobrevin (figure 1.1.7.3) is required to associate with the coiled coil region of classical dystrophin (Peters *et al*, 1997). Classical dystrophin has an unknown domain that separates the ZZ-type domain from the coiled-coil region, found at the C-terminus of dystrophin, and is made of two heptad repeats of leucine that make up helical coils (reviewed in Blake *et al*, 2002) with which it can bind to syntrophins (figure 1.1.7.4). R16 and 17 in classical full-length dystrophin anchor nNOS to the membrane (Lai *et al*, 2009) whereas β-dystrobrevin contains two syntrophin binding domains within the ZZ domain, which enables its interaction with the PH2 and SU domains of syntrophin (Blake *et al*, 2002; Blake *et al*, 2009) (figure 1.1.7.4). The syntrophins utilize their PDZ domain to interact with the PDZ domain of nNOS (Brenman *et al*, 1995; Albrecht *et al*, 2002).

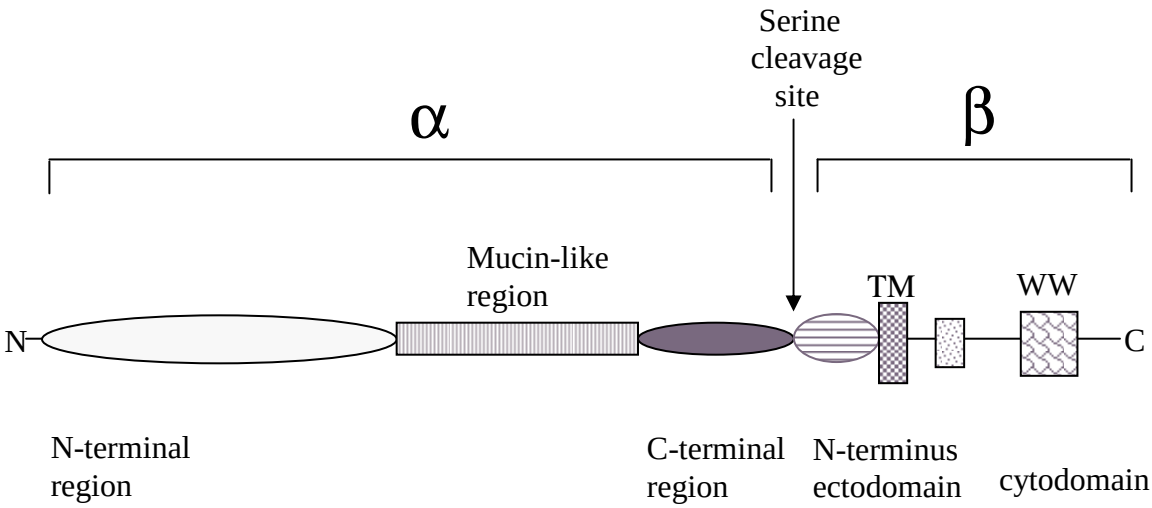

Figure 1.1.7.2: Domain structure of α and β-dystroglycan.

The figure shows the domain structure of α and β-dystroglycan. The two proteins initially arise as a single dystroglycan product followed by a post-translational cleavage site (serine), generating two dystroglycan products: α and β-dystroglycan. The N-terminal (residues 35-315) globular domain of α-dystroglycan is utilised for binding to the LNS domain of pre-synaptic β1-Neurexin. The mucin-like region separates the N-terminus from the C-terminus of the α-dystroglycan protein. The C-terminal (residues 485-651) globular domain of α-dystroglycan forms non-covalent contacts with the N-terminus ectodomain of β-dystroglycan. The transmembrane domain (TM) of β-dystroglycan anchors the entire dystroglycan complex to the membrane, whereas the WW domain of β-dystroglycan binds to the WW domain of classical dystrophin. This figure is adapted from Zaccaria *et al* (2001) and Hnia *et al* (2007).

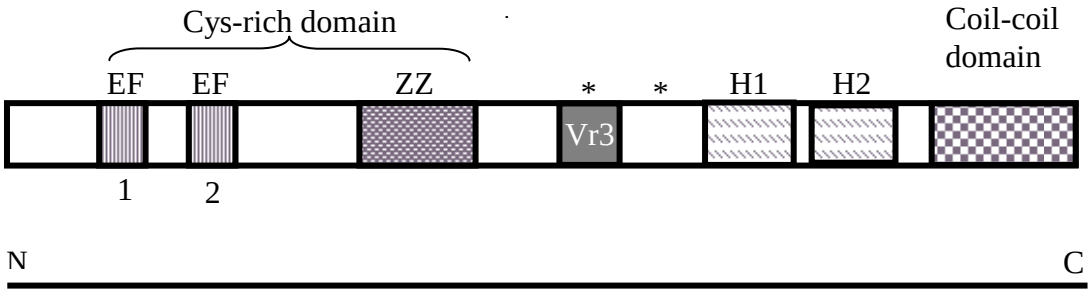

Figure 1.1.7.3: Domain structure of β-dystrobrevin.

The figure shows the domain structure of β-dystrobrevin. Two EF hands and one ZZ domain comprise the cysteine-rich domain. The EF hands domain contains hairpins of α-helices that can bind Ca^{2+}, while the ZZ domain, a putative zinc finger, may function as a calmodulin-binding site. The carboxy-terminal domain comprises of a α-helical region and two sets of helical leucine-heptad motifs (H1 and H2). The α-helical region contains two syntrophin binding sites (asterisks), one of which is within the vr3 (alternatively spliced variable region 3) region. The two helical leucine-heptad motifs (H1 & 2) are predicted to combine to form the coiled-coil region, which binds to the coiled-coil region located on dystrophin. This figure is adapted from Newey *et al* (2000), Albrecht *et al* (2002).

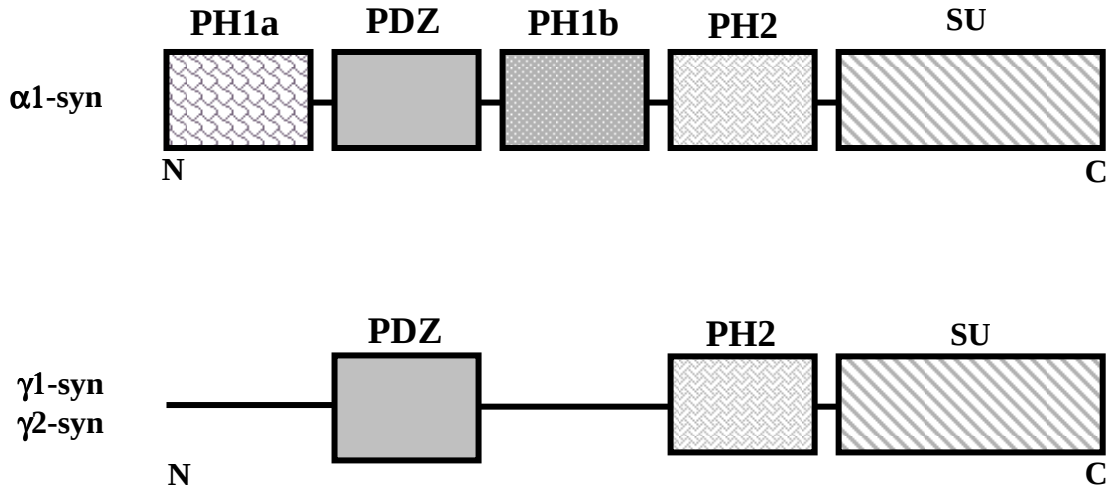

Figure 1.1.7.4: **Domain structure of syntrophin isoforms.**

The figure shows the domain structure of syntrophin isoforms. Syntrophins are molecular adapter proteins found at the cytoplasmic side of the peripheral membrane. They contain at least one plekstrin homology (PH) domain utilized to bind phosphoinositol 4,5-phosphate. The PDZ domain is utilized to interact with other PDZ-containing proteins, such as signaling molecule nNOS (Brenman *et al*, 1995). Syntrophin utilizes PH2 and the syntrophin unique (SU) domain to associate with the ZZ domain of β-dystrobrevin (Blake *et al*, 2002; Blake *et al*, 2009), and utilizes these same domains to associate with dystrophin (Piluso *et al*, 2000, Chen *et al*, 2006; Blake *et al*, 2009). The SU domain is slightly different in each syntrophin isoform and this ensures each syntrophin isoform to have different specificities to the protein it associates with. The figure is adapted from Albrecht *et al* (2002).

1.1.8 The functions of the DPC complex in brain

DPC complexes containing classical full-length dystrophin localize at PSD structures of GABAergic synapses and are said to be important for cell-cell adhesion. Such adhesion is provided by the dystroglycan (DG) complex (figure 1.1.7.2), the core component of the DPC complex of the PSD, as it is capable of associating with the pre-synaptic nerve ending, hence linking neighboring cells to one another (Ervasti *et al*, 1993; Moore *et al*, 2010). Precisely, dystroglycan associates with the pre-synaptic protein neurexin, and concominantly associates with the post-synaptic protein dystrophin, which in turn binds to actin. Altogether these DPC components provide cell-cell adhesion, by linking the intracellular actin-binding dystrophin protein to the extracellular pre-synaptic β1-neurexin of a neighboring cell. There is definite evidence that disruption of dystroglycan expression in brain impairs neuronal adhesion at some sites (Moore *et al*, 2002; Satz *et al*, 2010). In fact, Cre-inducible conditional mutation in the dystroglycan gene of mouse neuronal cultures showed that the knock-out of the dystroglycan gene eliminated the entire DPC complex from GABAergic synapses (Luscher *et al*, 2004), and impaired neuronal adhesion at these synapses (Moore *et al*, 2002).

The DPC is also important for post-synaptic differentiation (Clarris *et al*, 2002; Graf *et al*, 2004), based on the association between the pre-synaptic protein β1-neurexin and post-synaptic neurologin-2, which initiates the clustering of post-synaptic $GABA_A$ receptors at inhibitory synapses. Upon the formation of $GABA_A$ receptor clusters, the DPC complex prevents disassembling, or shifting of $GABA_A$ receptors around the synapse. Hence the DPC complex is also important for stabilizing the newly formed $GABA_A$ receptor clusters. Maintaining the stability of $GABA_A$ receptor clusters is important, as these are then able to respond to a major inhibitory neurotransmitter named GABA, which translates into inhibitory synaptic responses (Clarris *et al*, 2002; Graf *et al*, 2004). In DMD patients, the DPC complex is unable to stabilize $GABA_A$ receptors (Knuesel *et al*, 1999), therefore the $GABA_A$ receptor clusters disassemble, the inhibitory responses of the neuron become altered, this may in part underlie the mental impairments exhibited in these patients. Hence, the DPC complex may participate in mental impairments of DMD patients.

The DPC complex may participate in memory formation. In fact, mice that have dystroglycan selectively deleted in the brain only, but whose expression continues and is unaltered outside the brain, showed that defects in the dystroglycan gene, a core component of the DPC complex, is central to the pathogenesis of structural and functional brain abnormalities (Moore *et al*, 2002; Satz *et al*, 2010). High frequency stimulation (HFS) induced in hippocampal neurons of mice brains lacking dystroglycan, induced only a short-term potentiation (STP) rather than the expected long-term potentiation (LTP) as obtained in control mice (Moore *et al*, 2002). This suggests dystroglycan is required for HSF-induced LTP at CA3-CA1 synapses in the hippocampus (Moore *et al*, 2002). Satz *et al* (2010) studied in more detail the functions of dystroglycan in the brain, and provided genetic evidence that dystroglycan functions in the adult and developing CNS are cell-type specific. In fact, when Satz *et al* (2010) selectively deleted dystroglycan expression from neurons only, whilst dystroglycan expression in glial cells was allowed to continue, he found that the cytoarchitecture of these mice appeared normal. Satz *et al* (2010) therefore suggested that loss of dystroglycan expression in glial cells is the primary mechanism responsible for the abnormal cytoarchitecture of the cerebral cortex observed in dystroglycan null mouse brain. Hence, dystroglycan in glial cells, but not in neuronal cells, is involved in generating the normal cytoarchitecture of the cerebral cortex. What is more, Satz *et al* (2010) was also able to demonstrate that deletion of dystroglycan expression in neurons blunted hippocampal LTP, indicating that in neurons, dystroglycan is involved in synaptic activity. Given that dystroglycan is part of the DPC complex in neurons and glial cells (Blake *et al*, 1999; Brunig *et al*, 2002), these results suggest that the structural and functional brain abnormalities in DMD may be a consequence of DPC-like complexes in astrocyte cells in addition to the DPC complex found at the PSD of neuronal synapses.

The precise mechanisms by which β-dystroglycan may lead to brain pathogenesis is unknown. Studies in Cos-7 cells have shown that β-dystroglycan associates with signaling molecules such as ERK, MEK2 (Spence *et al*, 2004) and Grb2 (Russo *et al*, 2000; Spence *et al*, 2004), thus β-dystroglycan appears to be implicated in more than one signaling pathway. This would therefore also implicate the DPC complex in signaling cascade events. The precise role of dystroglycan in the transduction and modulation of various signaling cascades is not yet clear. In muscle

cells it has been established that dystroglycan and integrin are both able to bind to the extracellular matrix laminin component, and they are said to have opposing roles in laminin-mediated extracellular signal-regulated kinase activation (Ferletta *et al*, 2003). In other words, upon β-dystroglycan association with laminin, the former is then able to target MEK to membrane ruffles rather than to focal adhesions, consistent with the ability of dystroglycan to suppress the activation of MEK and ERK in response to integrin engagement (Ferletta *et al*, 2003). In these muscle cells, dystroglycan may therefore simply sequester MEK away from the rest of the MAP kinase cascade, preventing the efficient phosphorylation of ERK by MEK. Whether or not dystroglycan exhibits the same role in neurons, still needs to be established. However these experiments shed light to novel functions that dystroglycan may have in neurons as well. MAP kinases mediate specific cellular responses, including morphogenesis, cell death and stress responses. Dystroglycan, via its association to laminin may be important in participating in the regulation of these signaling responses in the brain.

In addition to classical full-length dystrophin and the dystroglycan complex, β-dystrobrevin and syntrophin (α, γ1, γ2) are also components of the core DPC that are expressed in the PSD of neurons in the brain. β-dystrobrevin (figure 1.1.7.3) is a 71kDa dystrophin-related protein cytosolic component of the DPC complex in the PSD, and it is suggested to participate in the transportation of some DPC components to specific sites of the cell (Macioce *et al*, 2003). The suggested transporting abilities of β-dystrobrevin came from a yeast two-hybrid experiment, which identified KIF5A as a binding partner of β-dystrobrevin. Kif5A is a neuronal member of the Kif5 family of proteins that consists of heavy chains of conventional kinesin, and is known for its role in transport of proteins along neuronal processes. The C-terminal region of Kif5A binds to β-dystrobrevin via the heavy-chain-mediated kinesin interaction (Macioce *et al*, 2003). There are separate studies that support the transportation capabilities of β-dystrobrevin, as studies show β-dystrobrevin translocates from the neuronal membrane and back to the nucleus. It lacks a nuclear localization signal and instead possesses a ZZ-domain, a feature typical of nuclear proteins. This nucleus to membrane translocation mechanism has also been described as important not just for transportation capabilities, but it also reflects a number of proteins that are involved in the acquisition of long-term memory (LTP) (Blake *et al*,

1999). β-dystrobrevin associates with classical dystrophin in the DPC complex, it is therefore possible that classical dystrophin is transported via the KIF5A-kinesin-β-dystrobrevin complex (Ceccarini *et al*, 2005). The route and mechanism by which β-dystrobrevin may transport some or perhaps all DPC components still needs to be established.

β-dystrobrevin binds directly to classical full-length dystrophin through reciprocal coiled-coil interactions (Peters *et al*, 1997; Beesley *et al*, 1999; Albrecht *et al*, 2002). In addition, β-dystrobrevin and classical full-length dystrophin bind to the syntrophin protein family (figure 1.1.7.4). In the brain, there exist 3 syntrophin isoforms (α1, γ1, γ2) of approximately 57-60 kDa (Piluso *et al*, 2000). Each syntrophin has a characteristic domain organization in mammalian brain (figure 1.1.7.4). Two pleckstrin homology (PH1 and 2) domains and one PDZ domain are present, with the first PH domain split into two regions (PH1a and PH1b) by the PDZ domain and its flanking regions. Syntrophin utilizes PH2 and the SU (syntrophin unique) domain to associate with the ZZ domain of β-dystrobrevin (Blake *et al*, 2002; Waite *et al*, 2009), PH2 and SU domains are also used to associate with dystrophin (Piluso *et al*, 2000; Chen *et al*, 2006; Waite *et al*, 2009). However, in the majority of studies reporting these syntrophin-dependent interactions, the effect on the DPC has not been explored. Even so, a number of functions have been attributed to syntrophin based on its cytosolic binding partners. Syntrophins, like many PDZ-domain-containing proteins, have been shown to play a key role in targeting, anchoring and stabilizing proteins to the cell membrane, leading to a cascade of cellular events that would otherwise be unable to occur. Syntrophins may therefore implicate the DPC complex in aggregating and stabilizing protein complexes at the PSD.

Syntrophins have been shown to associate with neuronal nitric oxide (nNOS) via reciprocal PDZ domains (Brenman *et al*, 1995; Brenman e*t al*, 1996), anchoring nNOS to specialized cellular domains in the PSD (Thomas *et al*, 1998; Sander *et al*, 2000). Neuronal NO synthase (nNOS), the enzyme that consistently produces NO in brain (Southan *et al*, 1996; Deng *et al*, 2009), is a component of the DPC complex (Yoshida *et al*, 1994) and contributes to transmission from one neuron to another (Deng *et al*, 2009). In addition to syntrophins, other proteins bearing a PDZ

domain can interact directly with the PDZ domain of nNOS (Brenman *et al*, 1996), thus influencing the subcellular distribution and activity of the enzyme (Sander *et al*, 2000; Thomas *et al*, 1998). nNOS modulates physiological functions such as learning and memory, neurogenesis and is involved in a number of diseases (Hindley *et al*, 1997; Cheng *et al*, 2003; Parcker *et al*, 2003; Moreno-Lopez *et al*, 2004). The DPC is involved in regulatory mechanisms that control nNOS expression (Deng *et al*, 2009), in fact, loss of dystrophin from the DPC complex leads to decreased NO levels in dystrophic neurons (Deng *et al*, 2009). This in turn leads to alterations in synaptic plasticity normally mediated by NO (Deng *et al*, 2009). In conclusion, the DPC complex is important for affecting the subcellular distribution and function of nNOS, and therefore the DPC complex indirectly modulates physiological functions such as learning, memory, neurogenesis and more (Hindley *et al*, 1997; Cheng *et al*, 2003; Parcker *et al*, 2003; Moreno-Lopez *et al*, 2004).

NO plays an important role during development (Deng *et al*, 2009). In fetal brains, nNOS concentration is significantly higher than in adults, suggesting an important role of NO during neuronal development (Moukhles *et al*, 2001). It has been demonstrated that NO may be involved in the regulation of process outgrowth and remodeling and may be capable of changing the morphology of growth cone (Moukhles *et al*, 2001). Thus lower amounts of NO in developing brains of dystrophic neurons may lead to altered neuron maturation and to the establishment of abnormal connections by developing neurons. Although syntrophin and dystrophin, and therefore the DPC complex, can together modulate the functions of nNOS, the cell has established a mechanism that can block such interaction (Moukhles *et al*, 2001). This is achieved by splicing-out exons 71-74 found within dystrophin, which removes the syntrophin-binding site, hence blocking the interaction between dystrophin and syntrophin, and any downstream signaling normally carried out by the syntrophin protein (Mehler *et al*, 2000). Thus the DPC can modulate the function of nNOS as well as syntrophin in neurons.

1.1.9 Summary

It is evident that the functions of the DPC complex in brain neurons containing full-length dystrophin are important for development, appropriate cell targeting, stability of the synapse as well as of $GABA_A$ receptors, and for bringing in proximity various signaling proteins which would otherwise be mislocalized and therefore unable to carry out their functions. Immunoprecipitation experiments and immunocytochemistry identify classical full-length dystrophin to always associate with the DPC in the PSD of the brain, and to exclusively localize at inhibitory synapses. There is no knowledge on the cellular localization and function of delta full-length dystrophin. Studies on mdx mice however, reflect the function of classical as well as delta full-length dystrophin in these mice, as both proteins originate from the same gene and are absent in the mdx mouse. To date, mental impairments have been attributed to the absence of full-length dystrophin protein only. With the recent discovery of delta full-length dystrophin (Blake *et al*, 1999), it is now becoming evident that delta full-length dystrophin, in collaboration with classical full-length dystrophin, may also contribute to the mental impairments observed in these mice. Therefore, one major aim of this thesis was to determine whether delta full-length dystrophin may replace classical full-length dystrophin in the formation of novel delta DPC complexes at the PSD of inhibitory synapses, hence participating in brain alterations found in the mdx mouse. As described earlier, classical and delta dystrophin only differ by a single exon, therefore, unless this change affects delta dystrophin's localization, function or structure, it is highly likely that the latter replaces classical full-length dystrophin to yield novel DPC-like complexes in PSDs of inhibitory synapses in the brain.

1.2 Part 2:

1.3 ε-sarcoglycan and the DPC complex in the Brain

1.3.1 Introduction and major aims

Recently, a protein that is known to associate with the DPC complex in the muscle has also been identified in the brain, but its association with the DPC complex in the brain remains to be established. This protein is known as ε-sarcoglycan. ε-sarcoglycan is a member of the sarcoglycan protein family (Chan *et al*, 2005), composed of α, β, γ, δ, and ζ-sarcoglycan (Fanin *et al*, 1997; Wheeler *et al*, 2002), each encoded by a separate gene. Most members of the sarcoglycan family, including ε-sarcoglycan, have been shown to contribute to the formation of the dystrophin-associated protein complex (DPC) in muscle (Liu *et al*, 1999; Durbeej *et al*, 1999; Straub *et al*, 1999; Imamura *et al*, 2000), which serves to link the extracellular matrix to the cytoskeleton of the cell (Holt *et al*, 1998). Unlike other sarcoglycan family members, which are largely or exclusively restricted to muscle, ε-sarcoglycan is highly expressed in many tissues including brain (Roberds *et al*, 1994; Noguchi *et al*, 1995; Zimprich *et al*, 2001; Xiao *et al*, 2003), therefore in chapter 5 I determine whether ε-sarcoglycan may associate with DPC-like complexes in the brain, in analogy to the muscle, or whether it is part of separate molecular complexes. Antisera against ε-sarcoglycan were raised in order to further purify and characterize ε-sarcoglycan complexes. The aim of the second part of this thesis was to increase the knowledge on the molecular complexity and functional roles of ε-sarcoglycan in rat brain.

The cellular function of ε-sarcoglycan remains unknown. Unlike other sarcoglycans whereby recessive mutations result in various types of limb-girdle muscular dystrophies (LGMDS), mutations of the ε-sarcoglycan protein are not associated with muscular dystrophy, instead it leads to a different disorder known as Myoclonus Dystonia (MDS), a syndrome of neurological origin (Estrada *et al*, 2006; Hjermind *et al*, 2008). MDS is a non-degenerative neurological disorder (Grabowski *et al*, 2003) principally characterized by myoclonic jerks and dystonia (Asmus et *al*, 2002; Chan *et al*, 2005; Tai *et al*, 2009) but also exhibits mild psychiatric symptoms (Tai *et al*, 2009; Chan *et al*, 2005; Asmus *et al*, 2002). The study of the cellular

localization and molecular associations of ε-sarcoglycan in mammalian brain is therefore important for the identification of molecular partners, candidate neuronal groups and circuits through which ε-sarcoglycan mutations lead to the dystonic and specific psychiatric symptom complex associated with MDS.

1.3.2 Molecular genetics of the ε-sarcoglycan gene and encoded protein

The ε-sarcoglycan gene (SGCE; OMIM: 604149) has been identified only relatively recently by an electronic database searching for sequences homologous to α-sarcoglycan (Ettinger *et al*, 1997; McNally et *al*, 1998; Kobayashi *et al*, 2003). It is being suggested that both genes may have originated from a common ancestor by gene duplication (Ozawa *et al*, 2005), given their high similarity in gene structure. The human gene for ε-sarcoglycan consists of 12 exons (figure 1.3.2) corresponding to 71kb of genomic DNA in human chromosome region 7q21.3 (McNally *et al*, 1998; Grabowski *et al*, 2003), whilst the murine gene for ε-sarcoglycan maps to mouse chromosome 6 (McNally *et al*, 1998). A potential promoter region upstream of the initiation codon facilitates the transcription of the SGCE gene into a major 1.7 kb mRNA product (www.dMDS.nl/), subsequently translated into a 47kDa glycosylated protein in a variety of tissues, including the brain.

According to studies carried out in the mouse, the brain is the only tissue where the mRNA product derived from the SGCE gene is alternatively spliced to yield more than one ε-sarcoglycan isoform, whilst all other tissues tested only express the conventional 47kDa protein (Nishiyama *et al*, 2004). There are however, inconsistencies as to the number of ε-sarcoglycan protein isoforms detected in brain. Ettinger *et al* (1997) identified a total of three ε-sarcoglycan protein isoforms in the mouse brain, with molecular weights 45kDa, ~47kDa and ~48kDa. However, later publications by different research groups (Nishiyama *et al*, 2004; Chan *et al*, 2005; Esapa et *al*, 2007) consistently detected only two ε-sarcoglycan isoforms (figure 1.3.2A) that correspond to approximately 47 kDa and 49kDa proteins in mouse whole brain. The third isoform is never visible in their western blots, and these authors (Nishiyama *et al*, 2004; Chan *et al*, 2005; Esapa *et al*, 2007) do not justify the inability to identify the third alternatively spliced isoform that has been previously reported by Ettinger *et al* in 1997. Only Yokoi *et al* (2005) proposed a third alternatively spliced ε-sarcoglycan mRNA (type 3 isoform), however they do not verify whether the type 3 mRNA isoform is also translated into a protein. More studies are clearly required to

verify the number of isoforms expressed in the brain, at the protein level. In chapter 5 I present the number of ε-sarcoglycan isoforms I have identified in rat adult brains.

Nishiyama *et al* (2004) searched for variations in the alternatively spliced ε-sarcoglycan transcripts, to determine the exonic sequences that distinguish the 47kDa protein from the 49kDa protein (figure 1.3.2B). They found that alternative splicing occurs at the C-terminus. More precisely, when alternative splicing removes exon 11b only, whilst exon 8 is kept, the 47kDa ε-sarcoglycan isoform is obtained (figure 1.3.2B). Whereas when alternative splicing removes exon 8 only, and maintains exon 11b, the 49kDa ε-sarcoglycan isoform is obtained (figure 1.3.2B). Both ε-sarcoglycan isoforms, therefore, clearly differ in their alternatively spliced C-terminal end (figure 1.3.2), whilst they exhibit identical N-terminal ends. Yokoi *et al* (2005) describes the novel potential alternative splice mRNA variant (type 3 isoform) having a new exon named 11c, from which two subtypes of clones encoding type 3 C-terminal mRNA sequences have been isolated. These either contain or lack exon 8, similar to what has been reported for the 47kDa and 49kDa isoforms by Nishiyama *et al* (2004). Again, these potential mRNA variants described by Yokoi *et al* (2005) remain to be confirmed at the protein level, and therefore have not been included in figure 1.3.2.

A. Protein domains of mouse brain 47kDa and 49kDa ε-sarcoglycan isoforms, respectively.

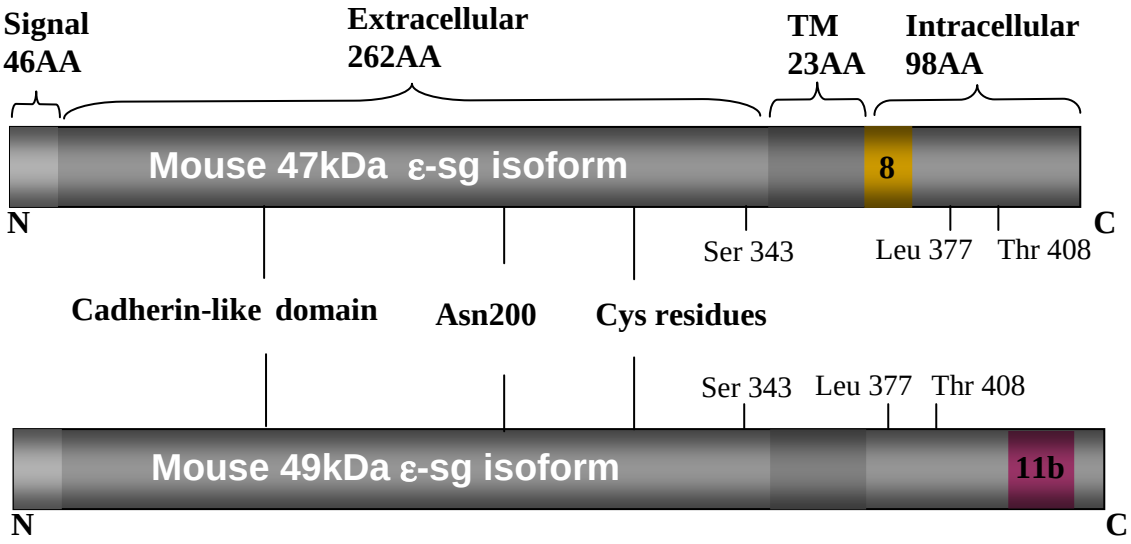

B. Exonic composition of mouse brain 47kDa and 49kDa ε-sarcoglycan isoforms, respectively.

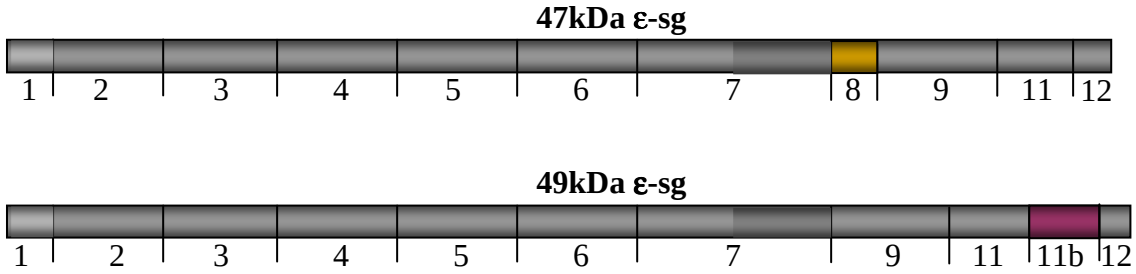

Figure 1.3.2: ε-sarcoglycan protein structure and relative exonic composition

A. This figure shows the domain structure of two ε-sarcoglycan isoforms expressed in the brain, 47kDa and 49kDa, respectively. Both isoforms contain a 46 amino acid (AA) N-terminus signal sequence, followed by a 262 AA extracellular domain. The 262 AA domain contains a cadherin and calcium-binding domain and the potential N-glycosylation site on the asparagines (Asn) 200. The 262 AA domain also contains four cysteine residues (Cys235, Cys248, Cys258 and Cys271), which enable the protein to form intramolecular S-S interactions. Adjacent to this domain is a 23AA transmembrane domain, and a 98 AA intracellular domain (www.dmd.nl/; Ettinger *et al*, 1997). The 98 AA cytoplasmic domain differs between the two isoforms, as highlighted by the yellow and red boxes.

B. This figure shows the exonic composition of the two ε-sarcoglycan isoforms expressed in the brain. The 47kDa protein contains exon 8 (yellow) whilst it lacks exon 11b (red), whereas the cytoplasmic domain of the 49kDa protein isoform contains exon 11b (red) whilst it lacks exon 8 (yellow). These differences suggest that the two isoforms bind different partners. Both murine isoforms contain three consensus sites for phosphorylation at their cytoplasmic domains; Ser343, Thr377 and Thr408 (www.dmd.nl/; Nishiyama *et al*, 2004). Exon 10 of the SGCE gene has not been found in the mouse genome database (Nishiyama *et al*, 2004), hence it is not included in the figure. This figure is adapted from Ettinger *et al* (1997) and Nishiyama *et al* (2004).

1.3.3 Localization and developmental expression of ε-sarcoglycan

The precise expression pattern of ε-sarcoglycan in the human CNS has not been studied (Kinugawa *et al*, 2009). On a wider scale, western blot analyses demonstrate that ε-sarcoglycan is widely distributed in the body. In fact, its expression has been detected in whole brain homogenate samples as well as in whole heart samples, striated muscle, smooth muscle, vascular smooth muscle, kidney, liver, spleen, testis, sciatic nerve, capillary blood vessels, Schwann cells in peripheral nerves, and lung samples (alveoli and bronchioles) (Mahloudji *et al*, 1967; Ettinger *et al*, 1997; Imamura *et al*, 2000; Hack *et al*, 2000; Xiao *et al*, 2003; Nishiyama *et al*, 2004). The highest level of expression of ε-sarcoglycan appears to be within the heart and lung (Ettinger *et al*, 1998; McNally *et al*, 1998; Xiao *et al*, 2003; Nishiyama *et al*, 2004), although its expression in the brain is also abundant.

Mouse brain slices containing various brain regions have been used to study ε-sarcoglycan distribution at the protein and mRNA levels by methods such as immunohistochemistry and fluorescence in situ hybridization (FISH), respectively. Results suggest that both mRNA and protein levels of ε-sarcoglycan exhibit a "distinct and inhomogeneous distribution" in many brains structures, but only a subset of cells in these brain structures have been found to contain ε-sarcoglycan both at the mRNA and protein level (Chan *et al*, 2005). The protein has been detected in neurons within pons, cerebral cortex, hippocampal formation, neocortex, olfactory bulb, cerebellar cortex, cerebellar Purkinje cell layer, in midbrain monoaminergic cell groups, brainstem nuclei, basal ganglia and spinal cord (Xiao *et al*, 2003; Nishiyama *et al*, 2004; Chan *et al*, 2005; Kinugawa *et al*, 2009). Different neuronal groups express different levels of the protein (Chan *et al*, 2005). In fact, the highest level of expression was found in the "mitral cells of the olfactory bulb, Purkinje cells of the cerebellum and in monoaminergic cell groups of the brainstem and hypothalamus" (Chan *et al*, 2005). This is followed by slightly lower levels of ε-sarcoglycan expressed in dopaminergic (DAergic) neurons, serotoninergic (5-HTergic) neurons and in noradrenergic (NAergic) neurons (Chan *et al*, 2005). In the hippocampal formation, there are moderate levels of the ε-sarcoglycan protein. It is also found in moderate

levels in several hypothalamic nuclei, the amygdala, and the molecular cell layer of the cerebellum (Chan *et al*, 2005). Low expression level of the protein has been detected within the neocortex, globus pallidus and thalamic nuclei (Chan *et al*, 2005).

ε-sarcoglycan is anchored at the plasma membrane of neuronal bodies and processes in the CNS, and is found within intracellular inclusions and the Golgi apparatus (Nishiyama *et al*, 2004;Chan *et al*, 2005; Esapa *et al*, 2007; Kinugawa *et al*, 2009). According to western blot analysis by Nishiyama *et al* (2004) using various subcellular fractions of mouse whole brain, ε-sarcoglycan appears to be predominantly extrasynaptic rather than at PSD structures (Nishiyama *et al*, 2004), because both ε-sarcoglycan isoforms enrich in the membrane fraction but neither isoform is enriched in the PSD fraction of total mouse brain homogenates, although their results highlight it certainly exists within the PSD (Nishiyama *et al*, 2004). These studies also demonstrate that the two ε-sarcoglycan isoforms (47kDa and 49kDa) differentially localize within the synaptosomal membranes isolated and attribute these differences to the structural differences of the two isoforms found at their alternatively spliced cytoplasmic domains (figure 1.3.2B).

To date, there is no immunocytochemical data singularly describing the localization of the 47kDa isoform or the 49kDa ε-sarcoglycan isoform in the brain, because no antibody reacting to just the 47kDa or the 49kDa isoforms is currently available (Nishiyama *et al*, 2004). Nishiyama *et al* (2004) carried out an immunocytochemical study using an in-house antibody generated against the whole cytoplasmic region of ε-sarcoglycan, therefore unable to distinguish the 47kDa isoform from the 49kDa isoform, and shows that ε-sarcoglycan isoforms (47kDa and/or 47kDa isoforms) are not only expressed in neurons, but they are also expressed in astrocytes and capillary endothelial cells (Nishiyama *et al*, 2004). They further determined, via a western blot analysis, the expression of ε-sarcoglycan isoforms in an astrocyte-rich fraction. Only the 47kDa ε-sarcoglycan isoform, but not the 49kDa isoform, is closely associated with astrocytic cells. It would be interesting to obtain antibodies that can distinguish the two isoforms, enabling a detailed immunocytochemical study that can be carried out to study which isoform is expressed in which cell (neurons and/or astrocytes) and subcellular structures of the brain. It would also be interesting to

investigate whether the known DPC components found in astrocytic cells, such as the astrocyte-specific cDp140 dystrophin isoform (Blake *et al*, 1999; Waite *et al*, 2009), may associate with the 47kDa ε-sarcoglycan isoform.

The developmental expression pattern of ε-sarcoglycan in the brain remains to be established. Instead, developmental studies carried out outside the brain highlight ε-sarcoglycan is a widely expressed protein, what is more, its developmental expression patterns and time-points have been shown to clearly differ from other sarcoglycan family members. Developmental studies using an immunohistochemical approach on mouse embryos have detected ε-sarcoglycan protein expression as early as embryonic day 8.5 (E8.5), whereas other sarcoglycan family members are absent (Straub *et al*, 1999; Xiao *et al*, 2003). At E12, ε-sarcoglycan is found in myoblasts, myotubes, cardiac myocytes, surrounding lung, bronchi and vascular endothelium (Straub *et al*, 1999; Xiao *et al*, 2003), whereas, other sarcoglycan family members are absent. By E15, ε-sarcoglycan is abundant in smooth muscle of lungs, in the smooth muscle of the bronchi, skeletal myotubes and cardiac myocytes, and other tissues from a variety of endodermal and ectodermal lineages (Straub *et al*, 1999), whilst other sarcoglycans are largely restricted to skeletal and cardiac muscle (Straub *et al*, 1999). In adult mouse, ε-sarcoglycan is expressed in smooth muscle cells of gastrointestinal tract, bladder, lung and uterus (Straub *et al*, 1999), whereas some sarcoglycan family members are absent (Straub *et al*, 1999). In skeletal muscle of adult mouse, ε-sarcoglycan expression dramatically declines, whilst the expression of other sarcoglycan family members is high in the adult stage. In contrast, smooth muscle cells continue to express ε-sarcoglycan protein at high levels in adult mice (Xiao *et al*, 2003). These are only a few examples to highlight the developmental profile and time-points of ε-sarcoglycan, which clearly differ and precede that of other sarcoglycans. Early expression of ε-sarcoglycan during development suggests it may participate in the development of the organs it is found in.

1.3.4 Protein structure of 47kDa and 49kDa ε-sarcoglycan isoforms

47kDa and 49kDa ε-sarcoglycan isoforms are considered type I transmembrane glycoproteins (Singer *et al*, 1990), because they are glycosylated proteins that transpass the membrane only once, with the N-terminal portion of the polypeptide exposed to the exterior of the cell and the C-terminal portion exposed to the interior of the cell, a typical feature of this class of proteins (Singer *et al*, 1990). Both isoforms share an identical N-terminal domain (figure 1.3.2) that is found at the extracellular interface of the cell. The N-terminal domain is composed of a 46 amino acid hydrophobic signal sequence (McNally *et al*, 1998), and a large 262 amino acid extracellular domain (amino acid 47-316). Within the 262 amino acid domain, there exists a cadherin-like domain (Dickens *et al*, 2002), one conserved site for asparagine-linked N-glycosylation (Asn 200) (McNally *et al*, 1998) and four conserved cysteine residues (Cys235, Cys248, Cys258 and Cys271) (Nishiyama *et al*, 2004; www.dmd.nl). Adjacent to the extracellular domain is a stretch of 23 amino acids that constitute the hydrophobic transmembrane (TM) region (aa317-339) that enables either isoform to transpass the membrane of the cell once. This TM region is also identical in the two isoforms. Adjacent to the TM is the 98 amino acid cytoplasmic domain (aa339-437), whereby the two isoforms exhibit differences in their exonic composition (figure 1.3.2), giving rise to two well distinguished isoforms of 47kDa and 49kDa. The functional significance of the exons (exon 8 and exon 11b) that distinguish the two isoforms from one another has yet to be established. The cytoplasmic domain of both isoforms contains three phosphorylation consensus sites at Ser 343 (next to TM region exon 7), Leu 377 and Thr408 (exon 9, cytosolic domain) (Nishiyama *et al*, 2004; Ettinger *et al*, 1997).

1.3.5 ε-sarcoglycan mutations lead to MDS

Myoclonus-dystonia syndrome (MDS, *DYT11*) is caused by a non-degenerative neurological disorder (Grabowski *et al*, 2003; Estrada *et al*, 2006; Hjermind *et al*, 2008) that generates myoclonic jerks and dystonia (Asmus *et al*, 2002; Chan *et al*, 2005; Tai et al 2009). In some cases, mild psychiatric symptoms are also a feature of this syndrome (Asmus *et al*, 2002; Chan *et al*, 2005; Tai *et al*, 2009). MDS can either be inherited in an autosomal dominant manner (Zimprich *et al*, 2001) or may occur sporadically, such as birth-related or other physical trauma or infection (Valente *et al*, 2003; Hedrich *et al*, 2004; Schüle *et al*, 2004). The disease becomes apparent during the first or second decade of life (Gerrits *et al*, 2009). Myoclonus is usually the main and most disabling feature in MDS patients, by predominantly affecting the upper limbs and axial muscles and is alcohol responsive (Kinugawa *et al*, 2009). Dystonia is also a feature of the disease, but it is in a much milder form and often manifests as cervical dystonia or writer's cramp (Kinugawa *et al*, 2009). The symptoms presented by MDS patients are not related to age or sex (Kinugawa *et al*, 2009).

Myoclonus Dystonia Syndrome is considered to be genetically heterogeneous (Kock *et al*, 2004) because some MDS patients have been diagnosed with allelic heterogeneity, whilst other MDS patients have been diagnosed with locus heterogeneity (Asmus *et al*, 2002). Allelic heterogeneity has been observed within the SGCE gene, a major culprit gene in MDS patients (Kinugawa *et al*, 2009; Grabowski *et al*, 2003; Zimprich *et al*, 2001; Klein *et al*, 2002). This is because various families having the MDS phenotype do not exhibit the same mutation within the SGCE gene, instead, many families differ in the region of mutation within the SGCE gene (Asmus *et al*, 2002; Grabowski *et al*, 2003). MDS also exhibits locus heterogeneity because the SGCE gene is not the only gene whose mutation has been linked to MDS. In fact, other loci have been found to yield the MDS phenotype, and these patients do not exhibit mutations within the SGCE gene. One example is the DYT15 gene (OMIM number; 607488), located in chromosome region 18p11, whose mutation gives rise to an MDS phenotype identical to that of patients with mutations in the SGCE gene (Grimes *et al*, 2002). In these patients, no mutation in the SGCE gene was detected. In a separate study, Asmus *et al* (2005) also found that 30% of familial cases exhibiting MDS had no mutation in the SGCE gene, suggesting that mutation of a different locus may also

give rise to MDS. Valente *et al* (2003) describes 16 patients with either sporadic or familial MDS, with no mutations in the SGCE gene identified. It is clear from these studies that a lot more work is required to characterize the causes of MDS. The mutations in the genes that lead to MDS vary from a nonsense mutation, missense mutation, deletion, insertion, duplication, or splicing mutations (Kinugawa *et al*, 2009).

Pedigree analysis shows reduced penetrance of the phenotype upon maternal inheritance of the mutated SGCE allele, which is a consequence of maternal imprinting (Grabowski *et al*, 2003). In the brain, the CpG island containing the promoter region of the maternal SGCE allele, together with the first exon of the SGCE gene, is completely methylated (Muller *et al*, 2002; Grabrowski *et al*, 2003). This leads to silencing of the maternal allele and consequently the transcription of the ε-sarcoglycan gene from the maternal allele is prevented, whilst the paternal allele is always expressed (Asmus *et al*, 2006; Tezenas du Montcel *et al*, 2005). In other words, when the paternal SGCE allele is in the wild-type state, whilst the maternal SGCE allele is mutated, the individual is healthy because the paternal allele yields the native ε-sarcoglycan protein. However, when the paternal SGCE allele is mutated, whilst the maternal SGCE allele is in the wild-type state, the individual will exhibit the MDS syndrome because the maternal wild-type SGCE allele cannot be transcribed and translated due to methylation.

The molecular mechanisms through which the detected mutations may contribute to MDS remain to be established (Klein *et al*, 2002). One possible route has only recently been suggested after comparing the subcellular localization of wild-type ε-sarcoglycan with several mutated ε-sarcoglycan proteins. The mutated proteins each carried a single mutation that has been previously reported in MDS patients (Esapa *et al*, 2007). According to their studies, these mutations lead to misfolding of the proteins and block their trafficking to the plasma membrane where the protein normally resides (Esapa *et al*, 2007). Therefore, impaired trafficking may be one of many mechanisms that contribute to the initiation of the disease. Separate studies also suggest high levels of expression of ε-sarcoglycan protein in wild-type monoaminergic midbrain neurons, thus mutation of the SGCE leading to the reduction of ε-sarcoglycan activity at the membrane of these neurons may provide a potential neurochemical explanation of both

movement disorders and psychiatric symptoms observed in MDS patients (Chan *et al*, 2005).

Pharmacological treatments such as clonazepam and valproate are currently available to treat the disease (Kurtis *et al*, 2010), and ethanol has been demonstrated to often ameliorate the symptoms (Cif *et al*, 2004). However, when MDS patients become refractory to pharmacological treatments, Deep brain stimulation (DBS) seems to be the only cure (Cif *et al*, 2004). DBS induces bilateral electrical stimulation of the Gpi (globus pallidus internus), an effective and safe treatment for MDS, which suppresses abnormal movements and improves quality of life (Cif *et al*, 2004; Kurtis *et al*, 2010). This amelioration has been recognized in the long term as an efficient therapeutic strategy for MDS patients who are not necessarily immune to pharmacological treatments, as well as for patients who are immune to pharmacological treatments (Cif *et al*, 2004).

1.3.6 Proteins interacting with ε-sarcoglycan

In the brain, the molecular associations of ε-sarcoglycan are not known. ε-sarcoglycan is part of a sarcoglycan family, composed of α, β, γ, δ and ζ-sarcoglycan. Outside of the brain, the sarcoglycans are known to associate with one another to form a tetrameric sarcoglycan complex that frequently (Ervasti *et al*, 1990; Yoshida *et al*, 1990; Ozawa *et al*, 1998), but not always (Durbeej *et al*, 1999; Fort *et al*, 2005), associates with DPC-like complexes in various types of tissues. The α, β, γ, δ-sarcoglycan complex is restricted to skeletal muscle and associates with the DPC complex therein (Ervasti *et al*, 1990; Yoshida *et al*, 1990; Ettinger *et al*, 1997; Ozawa *et al*, 1998; Liu *et al*, 1999; Durbeej *et al*, 2000; Imamura *et al*, 2000). The ε, β, γ, δ-sarcoglycan complex exists in both skeletal muscle (Liu *et al*, 1999) and smooth muscle (Straub *et al*, 1999; Imamura *et al*, 2000). In the smooth muscle, the ε ,β ,γ ,δ-sarcoglycan complex associates with the DPC complex (Straub *et al*, 1999; Lapidos *et al*, 2004; Imamura *et al*, 2005; Shiga *et al*, 2006), and this is also true in skeletal muscle (Lapidos *et* al, 2004; Imamura *et al*, 2005). In the Schwann cell outermost membrane, a sarcoglycan complex composed of ε, β, δ, ζ sarcoglycans associates with dystroglycan and a Schwann cell-specific dystrophin isoform (Dp116) (Imamura *et al*, 2000; Cai *et al*, 2007). In the lung, a sarcoglycan complex containing ε-sarcoglycan is found associated with DPC components (Durbeej *et al*, 1999). Separate studies have transfected the various sarcoglycan components into Chinese Hamster Ovary cells (CHO), in order to determine the molecular combinations of sarcoglycan complexes that may form. Their results show four different and potential sarcoglycan complexes that may also form *in vivo*, and these include: 1.α, β, ζ, δ-sarcoglycan, 2.α, β, γ, δ-sarcoglycan, 3.ε, β, ζ, δ-sarcoglycan and 4.ε, β, γ, δ-sarcoglycan, all of which have been shown to associate with the DPC complex (Shiga *et al*, 2006) in the plasma membrane of CHO cells. No studies have yet been carried out to determine whether any of these sarcoglycan complexes exist in the brain and whether any of these associate with the DPC complex in the brain.

According to various publications studying sarcoglycans and their expression in the brain, it appears that if a sarcoglycan complex exists in neurons, it will differ significantly from the complex found in muscle. In fact, γ-sarcoglycan is

absent in brain (Bönnemann *et al*, 1995; Lim *et al*, 1995; Nigro *et al*, 1996; Hack *et al*, 2000; Noguchi *et al*, 2000) whereas δ-sarcoglycan and ζ-sarcoglycan are both expressed in the brain at the mRNA level (Shiga *et al*, 2006), although their translation into a protein has yet to be confirmed. Only ε and β-sarcoglycan have been detected in the brain at the protein level (Wheeler *et al*, 2002; Shiga *et al*, 2006). According to studies by Shiga *et al* (2006), all four sarcoglycan components (ε,β,ζ and δ-sarcoglycan) that have to date been detected either at the mRNA or protein level in the brain, have been shown to complex together in CHO cells, suggesting that a similar complex may also form in the brain.

1.3.7 The function of ε-sarcoglycan in the brain

The function of ε-sarcoglycan in the brain remains largely unknown (Chan *et al*, 2005; Tai *et al*, 2009; Kinugawa *et al*, 2009), however an important role for ε-sarcoglycan in the brain is defined by the appearance of the myoclonus dystonia syndrome (MDS) when the SGCE gene is mutated (Xiao *et al*, 2003). Biochemical fraction studies of rat/mouse forebrain highlight that ε-sarcoglycan is present in synaptic membranes, raising the possibility that ε-sarcoglycan might be involved in neuronal functions, particularly in dopaminergic transmission, given its high expression in dopaminergic neurons of the substantia nigra (Nishiyama *et al*, 2004). Other neuronal-types also express ε-sarcoglycan, but the identity of these still remains to be identified (Chan *et al*, 2005). Overall, the broad expression of ε-sarcoglycan within the brain suggests that it may influence a large part of the brain.

Non-invasive studies have been carried out to study the neurophysiological profile in MDS patients, in order to begin to unravel the function of ε-sarcoglycan (Marelli *et al*, 2008). This methodology is known as transcranial magnetic stimulation (TMS). Studies using TMS have been able to show that MDS patients exhibit a reduction in the power of the $GABA_A$ receptor circuitry, because of primary dysregulation of the striato-pallido-thalamo-cortical loop (Marelli *et al*, 2008). Parallel studies on MDS patients further highlight that there exists a delayed event-related synchronization (ERS) of the motor cortex interneuronal function, which they suggest it may be due to a defective post-excitatory inhibition in the motor cortex at the end of the movement, which may reflect a lack of physiological synchronization of the GABAergic interneuron network (Cassim et al 2001; Marelli et al 2008). Given that ε-sarcoglycan is widely localized in various brain regions including the cortex and brainstem, Marelli *et al* (2008) suggested that neuronal dysfunction is likely to occur at multiple brain levels in MDS, rather than cortical impairment alone. What is more, the subcellular localization of ε-sarcoglycan in neuronal membranes suggests that it may play a role in synaptic functions, thus leading to an interneuronal system imbalance that sustains physiological inhibition in multiple brain regions (Marelli *et al*, 2008). No studies have yet been carried out to determine whether ε-sarcoglycan is localized

within GABAergic synapses, where classical full-length dystrophin-containing DPC complexes are exclusively localized (Brunig *et al*, 2002).

In non-neuronal tissues the role for ε-sarcoglycan is less apparent and it may be because mutation of ε-sarcoglycan may lead to subtle consequences (Xiao *et al*, 2003). Although wild-type ε-sarcoglycan is highly expressed in both embryonic and neonatal rodent striated muscle, MDS patients carrying a mutation in the SGCE gene never exhibit muscular dystrophy or myopathies (Xiao *et al*, 2003). It is being suggested that either ε-sarcoglycan is not critical for striated muscle embryogenesis, or closely related sarcoglycans may be capable of compensating ε-sarcoglycan deficiency and therefore no counter effects upon ε-sarcoglycan mutation can easily be identified. Substantially higher levels of the protein are expressed in smooth muscle when compared to skeletal muscle, it is therefore being suggested that ε-sarcoglycan is likely to play a more important role in smooth muscle when compared to skeletal muscle (Xiao *et al*, 2003). To date, it is not known what this function may be.

To begin to get a better understanding on the function of ε-sarcoglycan in neurons and MDS pathology, development studies on ε-sarcoglycan have been compared with other better-studied sarcoglycan family member proteins (Xiao *et al*, 2003). Unlike the other sarcoglycan family members, ε-sarcoglycan is more widely expressed among adult and embryonic tissue (Ettinger *et al*, 1997). What is more, ε-sarcoglycan expression is very early in development and precedes that of other sarcoglycans (Straub *et* al, 1999; Piras *et al*, 2000). According to these findings, it is being suggested that ε-sarcoglycan may therefore have a more widespread role in maintaining cell adhesion and tissue integrity, when compared with other sarcoglycan family members (Piras *et al*, 2000). In other words, it is being suggested that ε-sarcoglycan may participate in early development of brain, muscle, liver, kidney and heart tissue, as levels are higher in the fetal muscle compared to adult muscle of rats (Hjermind *et al*, 2008).

It is not known for the brain, but in muscle, ε-sarcoglycan is always associated with other sarcoglycan family members, that together form the sarcoglycan complex. There are two functions attributed to the sarcoglycan complex in the muscle,

the first is a mechanical function, and the second is a signaling function (Ozawa *et al*, 2005). In terms of mechanical function, studies carried out in the muscle have shown that in the absence of the sarcoglycan complex, binding of both β-dystroglycan to dystrophin as well as β-dystroglycan to α-dystroglycan are weakened. That is, the components of the dystrophin bolt are apt to disconnect (Ozawa *et al*, 2005). Therefore, in muscle, the sarcoglycan complex serves to strengthen the connection between the core components of the DPC complex. In terms of signaling function, α-dystrobrevin connects to the sarcoglycan complex at its N-terminus and to dystrophin at its C-terminus, which in turn binds to syntrophin. In turn syntrophin binds to nNOS and to voltage gated sodium channels, therefore involving the sarcoglycan complex in signaling functions. No evidence has yet been published to demonstrate whether ε-sarcoglycan is involved in such functions in the brain. However, given its known sarcoglycan complex formation in the muscle and its association with the DPC complex therein, it is plausible to suggest that a similar scenario may also be occurring in the brain.

According to biochemical analysis on sarcoglycan complex formation, results suggest that the loss-of function mutations in the SGCE gene, including the disruption of the sarcoglycan complex, does not produce detectable abnormalities in the peripheral nervous system (PNS) (Imamura *et al*, 2000), whereas it does induce vascular smooth muscle irregularities with consequences such as cardiomyopathy (Coral-Varquez *et al*, 1999). These results suggest that in sarcoglycan deficiency, differences exist between the pathophysiological mechanisms in smooth muscle and PNS (Nishiyama *et al*, 2004). It is therefore interesting and important to investigate the cellular associations and functions of ε-sarcoglycan within the brain as these may also differ to those observed in the muscle and other organs, and may reveal novel pathophysiological mechanisms that can be targeted with pharmacological treatments to cure patients with MDS. One major difference between the muscle and the brain is that the muscle undergoes mechanical stress whereas the brain does not. Therefore the functional requisites for ε-sarcoglycan in the muscle are likely to be different to those in the brain.

In 2002, Dickens et al discovered a cadherin-domain homologue within the extracellular portion of ε-sarcoglycan (figure 1.3.2). The function of this domain is not known for ε-sarcoglycan. However, cadherin-domain-containing proteins are typically adhesion molecules that modulate a wide variety of processes including cell polarization and migration (Tepass e*t al*, 2000; Dickens *et al*, 2002; Roemer *et al*, 1996). Multiple cadherin domains have been shown to form Ca^{++}-dependent rod-like structures with a conserved Ca^{++}-binding pocket at the domain-domain interface, that is utilised to form homotypic or heterotypic interactions with other proteins. Most of the calcium-binding residues found in the domain-domain interface in the cadherin domains of ε-sarcoglycan are conserved and therefore may be utilised for interactions with other proteins (Dickens *et al*, 2002). However, it remains to be established what proteins interact with the various binding sites found along the ε-sarcoglycan protein.

1.3.8 Summary

It is evident that mutations in the SGCE gene, in most cases, leads to MDS. Given the wide expression patterns exhibited by ε-sarcoglycan in and outside the brain, the mutated protein is likely to affect a variety of organs, and the consequences of such mutation will in part depend on the level of redundancy of that protein in a specific organ. Preliminary data suggest an extrasynaptic membrane-associated localization of ε-sarcoglycan, therefore indicating that the protein may not associate with DPC complexes localized at the PSD of inhibitory synapses. However, more detailed studies are required in order to determine the localization of ε-sarcoglycan within neurons of the brain and compare it to classical and delta dystrophin-containing DPC complexes, in order to determine whether it is part of these complexes or whether it associates with different protein complexes. This work has been researched in this thesis and is described in chapter 5.

Chapter 2:

2.0 *Materials and Methods*

2.1 Reagents and equipment

2.1.1 General Reagents.

General reagents, common to more than one protocol are listed in this section and under Appendix I, whereas those used only in specific procedures are mentioned throughout the method described and under Appendix II. All solutions and media were made using double deionised water (ddH_2O). Stock solutions were sterilised by autoclaving, or passing through a 0.22μm filter, and then stored at room temperature (RT), unless specified otherwise.

2.1.2 Chemicals

All molecular biology grade laboratory chemicals were purchased from Sigma-Aldrich and stored at room temperature, unless otherwise stated. Please see Appendix I, Box 1.

2.1.3 Biological kits and systems

Please see Appendix I, Box 2

2.1.4 Markers and enzymes

Please see Appendix I., Box 3

2.1.5 Media, buffers and solutions

Please see Appendix I, Box 4 (pH Buffers) and Box 5 (solutions used for specific protocols).

2.1.6 Equipment and suppliers

Please see Appendix 1, Box 6.

2.1.7 Reagents and Equipment for specific protocols

Please see Appendix II, Box 1.

2.1.8 Antibodies used in Western blotting and Immunocytochemistry detection analysis

Please see Appendix III, Table 1.

2.2 Isolation of subcellular fractions and protein detection

2.2.1 Protease inhibitors

All the samples obtained from homogenisations and cell fractionation procedures contained a combination of protease inhibitors. Previous colleagues in our lab have optimised the concentration of the protease inhibitors (PI) used (Susanne Flann *et al*, 1999). 1µl PI was added for every 1ml of sample suspension.

2.2.2 Preparation of subcellular fractions from rat forebrain or cerebellum

Subcellular fractions from Wistar rat forebrains were prepared by a method based on that of Cotman *et al*, (1971) as previously described (De Silva *et al*., 1979) and summarised in figure 2.2.2. Five adult rat forebrain or ten adult rat cerebellum brains were homogenised in homogenisation buffer (0.32M sucrose containing 1mM $MgCl_2$) using 12 strokes in a glass/Teflon homogeniser with 1mm clearance, at 500 rpm. The resultant homogenate was diluted to 10% (w/vol) in homogenisation buffer, and centrifuged 3,000 rpm (Sorval, SS34 rotor) for 10 minutes. The pellet was resuspended in homogenisation buffer and re-centrifuged as before. The supernatants of both centrifugations were combined and centrifuged at 12,700 rpm (Sorval, SS34 rotor) for 15 minutes, to form the P_2 pellet.

The P_2 pellet was washed twice in 0.32M sucrose and centrifuged at 17,000 rpm (Sorval, SS34 rotor) for 20 minutes after each wash, in order to remove any microsomal contamination. The supernatant obtained from the 20 minutes spin was spun at 42,000rpm (Beckman, 42.1 rotor) for 60 minutes, after which the microsomes (P3) and cell soluble (S3) was isolated (figure 2.2.2). Whereas the pellet obtained from the 20 minutes spin was resuspended and lysed in 125ml of 50 µM $CaCl_2$ pH 7.0, and allowed to stand on ice for 20 minutes. Subsequently, 25ml of 0.2M sodium phosphate buffer, pH 7.5, containing 0.05mM $CaCl_2$ and 5mM p-iodonitrotetrazolium violet (INT) and 0.4M sodium succinate was added and allowed to incubate for 25 minutes at 30 ºC. This step led to the formation of a formazan precipitate in

mitochondria, increasing the buoyant density. In this way, mitochondrial contamination of the synaptic membrane (SM) fraction, in particular, was reduced. The suspension was centrifuged at 10,000 rpm (Sorval, SS34 rotor) for 7 minutes. The resulting $P_{2\ INT}$ pellet was washed twice with 0.16 M sucrose containing 0.05mM $CaCl_2$, in order to remove any residual INT, and centrifuged at 20,000 rpm (Sorval, SS34 rotor) for 18 minutes after each wash.

The washed $P_{2\ INT}$ pellet was resuspended in 15ml of 0.32M sucrose-containing 0.05mM $CaCl_2$. This solution was underplayed with 0.8M, 1.0M and 1.2M sucrose, each containing 0.05mM $CaCl_2$.

The gradients were centrifuged for 120 minutes at 26,000 rpm (Beckman, SW28 rotor) and myelin, light membranes (LM) and synaptic membranes (SM) were harvested from the 0.32M / 0.8M, 0.8M / 1.0M and 1.0M / 1.2M interfaces respectively (figure 2.2.2). The mitochondrial fraction formed a pellet at the bottom of the tube. The harvested fractions were diluted in 0.05mM $CaCl_2$ and centrifuged at 42,000 rpm for 30min (Beckman, Ti60 rotor). The pellets were resuspended in 50µl of 0.32M sucrose containing PI (1µl/ml) and stored at -80 ºC.

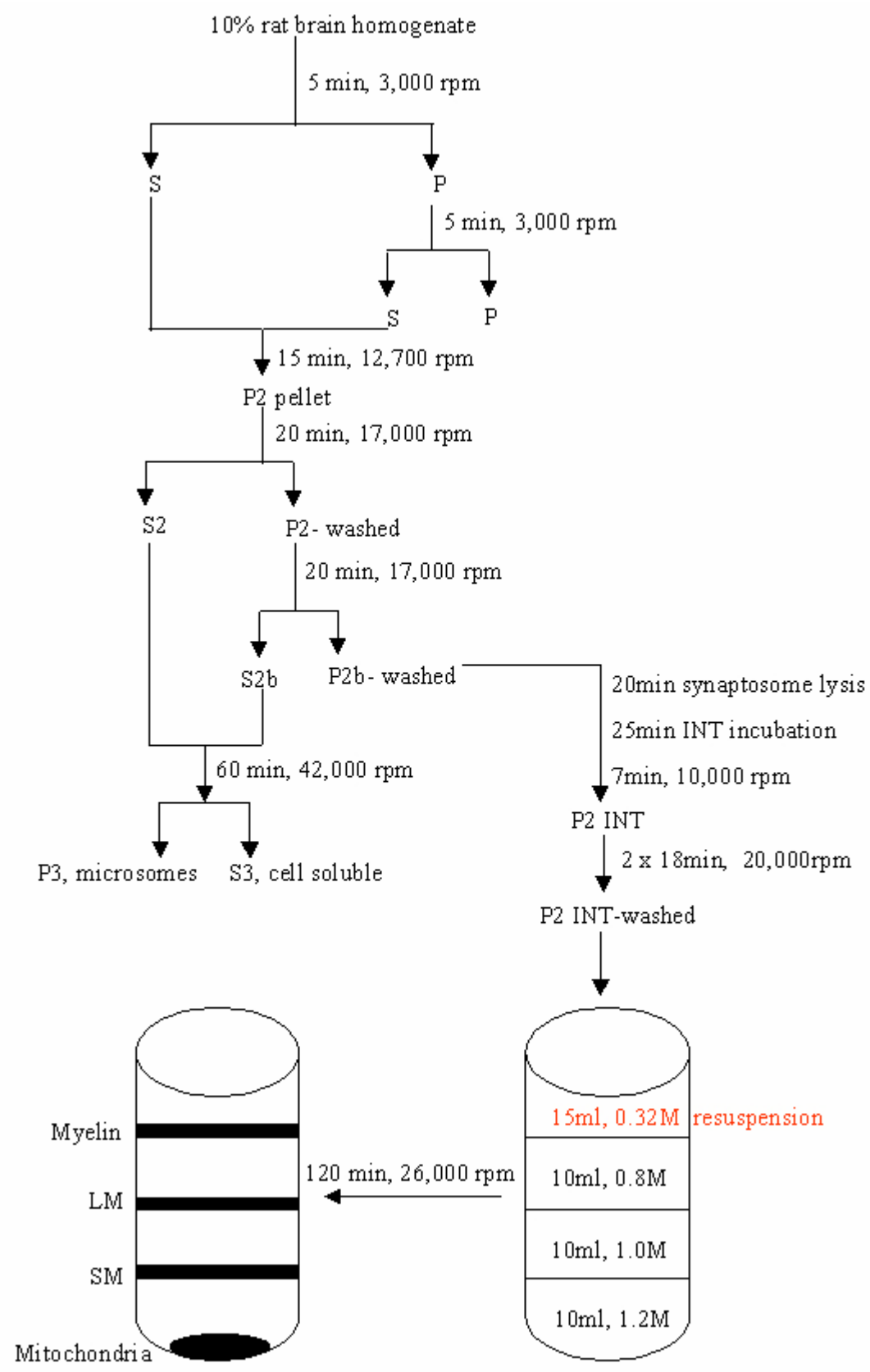

Figure 2.2.2: Subcellular fractions prepared by the Cotman *et al* (1971) method.

2.2.3 Preparation of PSD in rat Forebrain/Cerebellum by the Gurd *et al* (1982) method

A fresh SM fraction prepared by the Cotman *et al* (1971) method (refer to section 2.2.2) was used to isolate PSDs by a method based on Gurd *et al* (1982). The SM fraction was harvested and mixed with 30ml 0.05mM $CaCl_2$ and centrifuged at 42,000 rpm (Beckman, Ti60 rotor) for 30 min. The SM pellets were resuspended in 4ml of fresh deionised water and protease inhibitors (PI). To each of four new tubes, 1.25g 20% w/w PEG 6000, 1.25g (20% w/w Dextran T-500), 0.5ml (0.2M Sodium Carbonate Buffer pH.9.6), 200µl (25% w/v n-octyl glucopyranoside) and 1ml of the SM suspension was homogenised with 12 straight strokes with the Dounce homogeniser. All four tubes were centrifuged at 5,000 rpm for 15 minutes. The PSDs appeared at the interphase. The PSDs were harvested, mixed with deionised water and centrifuged at 12,000rpm for 2 minutes. This was repeated twice. The water was removed and the PSD pellet resuspended in 250µl of 0.32M sucrose. Protease inhibitors were added to the PSD and stored at $-80^{o}C$.

2.2.4 Preparation of PSD in Forebrain by the Carlin *et al* (1980) method

Subcellular fractions from Wistar rat forebrains were prepared by a method based on Cotman *et al* (1971), modified by Carlin *et al* (1980). Ten adult rat forebrain brains were homogenised in homogenisation buffer (0.32M sucrose containing 1mM MgCl2) using 12 strokes in a glass/Teflon homogeniser with 1mm clearance, at 500 rpm. The resultant homogenate was diluted to 10% (w/vol) in homogenisation buffer and centrifuged at 3,000 rpm (Sorval SS34 rotor) for 10 minutes. The pellet was resuspended in homogenisation buffer and re-centrifuged as before. The supernatants of both centrifugations were combined and centrifuged at 10,430 rpm (Sorval, SS34 rotor) for 15 min, to give a crude membrane P_2 fraction.

The brains in the P_2 pellet were resuspended and diluted to 10% (w/vol) in homogenisation buffer and centrifuged at 10,430 rpm (Sorval, SS34 rotor) for 10 minutes. The pellet obtained was resuspended in 15ml 0.32M Sucrose containing 0.05mM $CaCl_2$. This solution was underplayed with 0.8M sucrose, 1.0M and 1.2M

sucrose, each containing 0.05mM $CaCl_2$ (figure 2.2.2). The gradients were centrifuged at 26,000 rpm (Beckman, Sw28 rotor) for 120 minutes. The myelin, light membranes (LM) and synaptic membranes (SM) were harvested from the 0.32M / 0.8M, 0.8M / 1.0M and 1.0M / 1.2M sucrose interfaces respectively (figure 2.2.2), each containing 0.05mM $CaCl_2$. The mitochondrial fraction formed a pellet at the bottom of the tube. The myelin and LM fractions found at different sucrose interfaces were isolated and subsequently added to two separate tubes, diluted in 0.05mM $CaCl_2$, and centrifuged at 42,000 rpm (Beckman, Ti60 rotor) for 30 minutes. The pellets were resuspended in 500µl of 0.32M sucrose. PI was added to preserve the fractions. All fractions except the SM fraction, were stored at –80^{o}C.

PSDs were prepared by the Carlin *et al* (1980) method. The SM fractions (synaptosomes) harvested from the sucrose gradient were diluted with 60ml of 0.32M Sucrose 1mM $NaHCO_3$ (1g of initial weight of brain material/6ml sucrose solution). The diluted SM preparation was centrifuged at 42,000 rpm (Beckman, Ti60 rotor) for 30 minutes. The pellet obtained was resuspended in 6ml 0.32M Sucrose 1mM $NaHCO_3$ (10g initial weight of brain material/6ml sucrose solution) and 6ml Triton X-100 (1:1), mixed well, and centrifuged at 39,900 rpm (Beckman Ti60 rotor) for 20 minutes. The PSD pellet was resuspended in 0.32M Sucrose 1mM $NaHCO_3$. PI was added to preserve the fraction. The PSD was stored at –80^{o}C.

2.2.5 Protein determination by the Folin-Lowry method

An appropriate volume of sample or BSA standard (Bovine Serum Albumin) was added to 200µl of 1M NaOH, and the protein was allowed to solubilise for 10 min. The volume of each tube was adjusted to 500µl with distilled water, followed by the addition of a 2ml Lowry solution (49ml 2 % (w / v) Na_2CO_3, 0.5ml 2.12 % (w / v) Na_2 tartrate, 0.5ml 1 % CuSO4). The tubes were left to stand for 15 min at Room Temperature. 200µl aliquots of Folin Reagent (Lowry *et al*, 1951) diluted 1:1 with distilled water, were added to each tube and incubated 45 minutes at Room Temperature. The spectrophotometer was set to 750 nm. The instrument was zeroed with the blank containing the same preparation described above, replacing the volume of sample or BSA with the buffer containing the sample or BSA. The absorbance

measurements of the standards and unknown samples were measured. A BSA standard curve (0-200µg) was prepared by plotting the 750nm values (y-axis) versus their concentration in µg/ml (x-axis). The concentration of the unknown sample was determined using the standard curve. The final concentration of the sample was obtained by multiplying the concentration of the sample by the dilution factor, divided by the path length.

2.2.6 Sample preparation for SDS-gel analysis

Sample buffer x 2 (4% SDS, 20% Glycerol, 10% 2-mercaptoethanol, 0.004% Bromophenol Blue, 0.125M Tris-HCl) was diluted 1:1 with the sample. The sample preparation was heated at 95^{o}C for 5 minutes, followed by a 5 minute period on ice. The samples were then centrifuged in a microfuge at 12,000 g for 5 minutes, the supernatant was ready for loading on an SDS-polyacrylamide gel.

2.2.7 SDS-polyacrylamide gel electrophoresis

SDS-polyacrylamide gel electrophoresis was carried out as described by Laemmli (1970) using the Bio-Rad mini Protean II mini-gel apparatus. Typically, 10% (w / v) polyacrylamide gels were used, except where specified otherwise. 10 % gels were made up with 6.4ml distilled water, 3.75ml of 1.5 M Tris-HCl, pH 8.8, 150µl of 10 % (w / v) SDS, 5ml of 30 % (w / v) acrylamide containing 0.8 % (w / v) bis-acrylamide (Protogel, National Diagnostics) with 55µl of polymerisation. 12 % gels containing 5.5ml distilled water and 6ml Protogel, with all other constituents as described above. The stacking gel (5.5% w / v acrylamide) contained 2.9ml distilled water, 1.25ml of 0.5 M Tris-HCl, pH 6.8, 0.95ml Protogel, 50µl of 10 % (w / v) SDS with 31.5µl 10 % (w / v) AMPS and 7.5µl Temed.

Samples were prepared (refer to section 2.2.6) and gels run at 200 V until the dye-front reached the end of the gel. Pre-stained molecular weight markers were utilised (Appendix I, Box 3).

2.2.8 Coomassie Blue staining for protein-detection in polyacrylamide gels

The gel was placed in the Coomassie Blue stain (50 % (v / v) methanol, 10 % (v / v) acetic acid, 0.25 % (w / v) Coomassie Blue R250) for 45 min. The gel was removed and destained in 45 % (w / v) methanol and 5 % (w / v) acetic acid in water, until the gel background was no longer blue, and the protein bands could be clearly seen. The sensitivity of this stain is up to 0.2-0.5µg protein per band.

2.2.9 Western blotting

All protein samples were blotted onto nitrocellulose with a pore size of 0.45µm (Amersham, Hybond-ECL). A wet Western blotting procedure, modified from the method described by Towbin *et al* (1979) was developed using the Bio-Rad mini trans-blot cell blotting apparatus. The nitrocellulose was equilibrated in Blotting Buffer for 1 h prior to blotting. Electrophoretic transfer was carried out for 1 hour at 100 V constant voltage.

2.2.10 Ponceau S staining for protein-detection on Western blotted nitrocellulose

Ponceau S staining on Western blots was carried out as described by Harlow and Lane (1988). The blot was washed in Ponceau S solution (0.2 % (w/v) Ponceau S, 3% (w/v) TCA, 3 % (w/v) sulphosalicylic acid) for 5 min. This is a temporary stain, which can be washed off by rinsing in PBS before blocking and subsequent immunodevelopment. This is not a sensitive method for detection of proteins.

2.2.11 Development of Western blots: Enhanced chemiluminescence (ECL) detection system

Blocking was carried out in 5 % w / v Marvel dried milk in PBS. The Marvel was centrifuged for 5 minutes at 5,000 rpm before use. After allowing blocking for 30 minutes, the blot was washed in PBS, once for 15 minutes and then twice, for 5 minutes each. Incubation of primary antibody was carried out over night at 4 ºC. The dilution required of each batch of primary antibody was previously determined by testing the intensity of development of a standard blot. The blot was then washed in

PBS as before, once for 15 minutes and then twice for 5 minutes each time. Following this, incubation with a 1 in 2,000 dilution (in 5 % marvel in PBS) of secondary rabbit polyclonal antibody or mouse monoclonal antibody was carried out, for one hour at room temperature. The blot was washed for 15 minutes in PBS, followed by four additional 5-minute washes.

Equal volumes of solutions one and two from ECL detection kit or from supersignal WestDura ECL HRP substrate detection kit, were mixed to form the detection reagent. Surplus buffer was drained from the blot that was then incubated in the detection reagent for 1 minute. A piece of hyper-film ECL was placed over the wrapped blot and exposed for 15 seconds initially. Exposure time was varied dependent on the intensity of the reaction. After exposure, the film was developed for 4 min in developer and 2 min in fixer.

2.3 Isolation and detection of ε-sarcoglycan binding partners

2.3.1 Preparation of solubilised ε-sarcoglycan and binding partners from forebrain derived light membrane

Two rat forebrains were obtained and homogenised into 10mM Tris pH 7.0 Buffer and PI in a final volume of 20ml. The homogenate was centrifuged for 5 minutes at 3,000 rpm (SS34, Sorval), the supernatant was obtained and was centrifuged 42,000 rpm (Beckman, 42.1 rotor) for 1 hour at 4^{o}C. The pellets were resuspended in RIPA Buffer pH 7.5 in a final volume of 39ml, incubated for 30 minutes at 4^{o}C, stirring gently. The resuspension was centrifuged at 42,000 rpm for 1 hour at 4^{o}C (Beckman, 42.1 rotor). The pellet obtained represented the LM fraction containing ε-sarcoglycan isoforms solubilised from the membrane as part of any multi-protein complexes that exist within the membrane. The pellet was subsequently resuspended in 1ml of (50mM Tris-HCl pH 5.5 containing 1%SDS), ready for Immunoprecipitation

2.3.2 Cross-linking of anti-ε-sarcoglycan antibody to Dynabeads Protein G

100µl of Dynabeads Protein G (Invitrogen) were added to an eppendorf tube and placed on a magnet, to separate the beads from the solution. After removal of the solution, the dynabeads attracted to the magnet structure were released and washed three times with 0.5ml citrate-phosphate Buffer pH 5.0, and the solution was removed when the dynabeads were allowed to dissociate from the solution and bind to the magnet. 20µl of anti-ε-sarcoglycan antibody was mixed with the washed dynabeads Protein G, and incubated 40 minutes at Room Temperature in a test-tube rotator. Subsequently, the dynabeads are said to have captured the antibody, thus the eppendorf tube was placed near the magnet to isolate the dynabead-antibody complex, and the latter was washed a couple of times with 0.5ml citrate-phosphate Buffer 0.1% Tween 20 pH 5.0. Prior to cross-linking the dynabead-antibody complex, the latter was washed in 1ml 0.2M triethanolamine buffer pH 8.2.

The dynabead-antibody complex was resuspended in 20mM DMP in 0.2M triethanolamine pH 8.2, with gentle mixing for 30 min at 20^{o}C, to allow cross-linking. Using the magnet to isolate the dynabead-antibody complex, the supernatant was discarded and the cross-linking reaction was interrupted with 1ml 50mM Tris pH7.5, with a 15 minute gentle incubation at Room Temperature. Using the magnet, the cross-linked antibody-dynabead complex was washed a couple of times using 1ml PBS/T. Two additional washes of the cross-linked beads in 30µl 0.1M Citrate pH 2.0 were carried out and loaded on a gel to verify the efficiency of antibody binding and antibody cross-linking to the beads, respectively, during the procedure. The cross-linked beads were stored in PBS pH 7.4, containing 0.1% Tween-20 and 0.02% sodium azide, at 4^{o}C.

2.3.3 Immunoprecipitation of ε-sarcoglycan binding partners

The solubilised ε-sarcoglycan product (refer to section 2.3.1) was mixed with non-cross-linked Dynabead Protein G (Invitrogen) in a 1:40 ratio, incubated for 3 hours, with gentle rotation at Room Temperature. A magnet was subsequently used to separate the beads and unspecifically-bound proteins from the pre-cleared LM suspension. The pre-cleared LM suspension and Dynabeads Protein G cross-linked with the anti-ε-sarcoglycan antibody were mixed in a 1:40 ratio, respectively, incubated overnight with gentle rotation at 4^{o}C. The magnet was used to separate the beads containing the immunoprecipitated (IP) complex from the solution, such that the suspension could be removed, and the beads were washed twice in PBS. The IP complex was eluted from the Dynabead Protein G complex by addition of 30µl 0.1M Citrate pH 2.0, allowing to rotate for 2 minutes. A magnet was subsequently utilised to isolate the Dynabead Protein G from the suspension containing the IP complex, and the latter isolated. The elution step was repeated twice more.

2.4 Cell culture of cortical neurons

2.4.1 Preparing the coverslips

24 well tissue culture plates were prepared with coverslips coated with poly-D-lysine, under sterile conditions. Coverslips were autoclaved, washed with ethanol and allowed to dry prior to coating procedures. Each coverslip was added to a well and coated with 0.5ml of Coating material (100mg/l Poly-D-lysine in 0.15M Boric Acid, pH 8.4). The plates were incubated 2 hours at 37^{o}C in a sterile incubator. Post-incubation, each well was washed twice with Hanks' Balanced salt solution without Ca^{2+} and Mg^{2+}, and left in sterile PBS solution in a 37^{o}C sterile incubator, until needed.

2.4.2 Preparation of cortical neurons from E18 prenatal rats

Cortical neurons were prepared by a method based on Dresbach *et al* (2003). E18 pregnant rats were anaesthetised and its embryos removed. The heads were removed from the embryos, and the brain was dissected from the skull and transferred into a petridish with icecold Hanks' Balanced salt solution (HBSS) without Ca^{2+} and Mg^{2+}. The brains were cut along the midline and the forebrain was removed and immediately placed in another petridish with cold HBSS (without Ca^{2+} and Mg^{2+}). All the forebrains isolated were transferred to a 15ml tube, washed three times with 5ml HBSS (without Ca^{2+} and Mg^{2+}). Once all the HBSS media was removed, 1ml of pre-warmed Day 1 Media (refer to Appendix II) was added to the forebrain and very gently triturated with a thin glass until the solution was clear. The suspension was filtered through a 70μm cell strainer. To the filtered supsension, 1ml Day 1 Media was added for each brain isolated, and a further 2ml Day 1 Media was added to this mixture.

Cells were counted by adding 10μl of cortical neuron preparation to 10μl of Trypan Blue, and viewed under a microscope. 60,000 cells/cm^2 (high density) were plated on 24 well plates for transfection experiments, whereas 30,000 cells/cm^2 (low density) were plated on 24 well plates for immunocytochemistry. 24 hours after plating, the

Day 1 media was replaced with Day 2 Media (refer to Appendix II). Neurons were allowed to grow for two to three weeks in a sterile 37^{o}C incubator, and half the media in each well was replaced with fresh pre-warmed Day 2 Media every seventh day.

2.4.3 Preparation of DNA

pET32b vectors containing the 33kDa ε-sarcoglycan peptide, and pEGFP-N3 vectors containing Cexon78 or Dexon78 of classical and delta dystrophin isoforms respectively, were kind gifts by Derek DJ Blake and Christopher T Esapa of the Pharmacology Department, Oxford University.

2.4.4 Transfection of cortical neurons with pEGFP-N3Cexon78 and pEGFP-N3Dexon78 vectors

For tissue culture media and reagents, refer to Appendix II. Using 24 well tissue culture plates coated with poly-D-lysine (refer to section 2.4.1), each well was plated with 60,000 cells/cm^2 in 0.5ml of pre-warmed Neurobasal Media A, and incubated for 72 hours at 37^{o}C, with 5% CO_2 in 95% humified air. On day 3, half of the plating volume was removed and replaced with pre-warmed 250µl fresh Neurobasal Media B. Four days after plating, 1µg of DNA (refer to section 2.5.3) was prepared in a polypropylene tube and diluted into 50µl OPTI-MEM I. In a separate polypropylene tube, 4 µg of Lipofectamine 2000 (Invitrogen) was also diluted into 50µl OPTI-MEM I, and incubated for 5 minutes at Room Temperature. The diluted DNA/Lipofectamine 2000 (total of 100µl) were mixed together and incubated 20 minutes at Room Temperature. The supernatant from primary cultures was removed and replaced with 400µl/well of fresh Neurobasal Media B. 100µl of diluted DNA/Lipid complexes were added to each well, making a final volume of 500µl. The transfection was allowed to occur for 5 hours at 37^{o}C, 5% CO_2 with humified air. After 5 hours, the supernatant was removed and replaced with 0.5ml of Neurobasal Media B, and placed back in the incubator for 24 hours. The neurons were then fixed (refer to section 2.4.5 or 2.4.6) in order to visualise the protein of interest using a Nikon Eclipse TE300 microscope (refer to section 2.4.7).

2.4.5 PFA-Fixation (for cDp, dDp, ε-sg, MAP2, MANDAG, $GABA_AR$, GAD65, β3-tubulin and synaptophysin antibodies) of mature cortical neurons

For tissue culture media and reagents, refer to Appendix II. Coverslips were washed with pre-warmed PBS. Neurons were fixed by adding 0.5ml of 4%PFA (pH 7.4) in PBS for 20 minutes at Room Temperature. The coverslips were then washed twice with 25mM Glycine in PBS and blocked one hour at Room Temperature in Blocking Solution with Triton X-100. The coverslips were placed in a humified chamber onto Parafilm, and 50µl of primary antibody in Blocking Solution was left over night at 4^oC. The next day the cover slips were washed twice in PBS followed by incubation with 50µl secondary antibody in Blocking Solution without Triton X-100 for 1 hour at Room Temperature in the dark. The coverslips were then washed twice with PBS, followed by water washes, and then mounted with Vectashield Mounting Medium.

2.4.6 Methanol-Fixation (for dDp, PSD95 and NR1 antibodies) of mature cortical neurons

For tissue culture media and reagents, refer to Appendix II. Neurons were fixed with -20^oC cold Methanol for 5 min at -20^oC, followed by permealisation in 0.25% Triton X-100 for 5 min. Upon washing with PBS, unspecific binding was blocked for 1 hour at Room Temperature in 10%BSA in PBS. 50µl of primary antibody in Blocking Solution with Triton X-100 was added to each well and incubated over night in a humified chamber. The next day, the coverslips were washed twice in PBS, followed by 1 hour incubation with 50µl secondary antibody in Blocking Solution without Triton X-100 at Room Temperature, in the dark. After washes with PBS, and water, the coverslips were mounted with Vectashield Mounting Medium.

2.4.7 Viewing fixed neurons under the microscope

The stained cells were visualised using a Nikon Eclipse TE300 inverted microscope equipped with a Hamamatsu digital camera and images visualised using simple PCI (Digital Pixel) software.

2.5 Antibody production

2.5.1 Endofree Maxiprep Plasmid Kit for amplification of the epitope-containing DNA

For buffer solutions, refer to Appendix I, Box 4. For biological kits and systems, refer to Appendix I, Box 2. An Endofree Maxiprep Plasmid Kit (Qiagen) was utilised to amplify the DNA containing the epitope against which the antibody had to be raised against. Prior to starting, RNAse A was added to P1 buffer, and P3 buffer was chilled at 4^{o}C. A single colony was picked (refer to section 2.5.5) from a selective plate and used to inoculate a starter culture of 2-5ml LB medium containing the appropriate selective antibiotic. The colony in the LB medium was incubated for 8 hours at 37^{o}C with vigorous shaking (300 rpm). The starter culture was diluted to 1:500 into 150ml selective LB medium and incubated 16 hours at 37^{o}C with vigorous shaking (300 rpm). The bacterial cells were harvested by centrifugation at 6,000g for 15 minutes at 4^{o}C. The bacterial pellets were combined and resuspended in 10ml Buffer P1. 10ml Buffer P2 was subsequently added, mixed thoroughly by vigorously inverting the sealed tube 6 times, and incubated for 5 minutes at Room Temperature. 10ml of chilled Buffer P3 was added to the lysate and immediately mixed thoroughly by vigorously inverting the sealed tube 6 times or until the solution became neutralised. The lysate was poured into the barrel of the Qiafilter cartridge, incubated 10 minutes at Room Temperature. The cap from the Qiafilter Cartridge outlet nozzle was removed and the plunger was gently inserted into the Qiafilter maxi Cartridge and the cell lysate was filtered into a 50ml tube. 2.5ml of Buffer ER was added to the filtered lysate and mixed by inverting the tube approximately 10 times followed by a 30-minute incubation on ice. To equilibrate the QIAGEN-tip 500, 10ml of Buffer QBT were applied to the column, and the Buffer was allowed to exit the column by gravity flow. The filtered lysate was applied to the equilibrated QIAGEN-tip 500 and allowed to enter the resin by gravity flow. The QIAGEN-tip was washed twice with a 30ml Buffer QC. The DNA was eluted with 15ml Buffer QN. The DNA was then precipitated by adding 10.5ml (0.7 volumes) of isopropanol to the eluted DNA, mixed and centrifuged immediately at 15,000g (Beckman, SW28 rotor) for 30 minutes at 4^{o}C. The supernatant was carefully decanted. The DNA pellet was washed by

resuspending with 5ml of endotoxin-free Room Temperature 70% ethanol, and centrifuged at 15,000g (Beckman, SW28 rotor) for 10 minutes. The resulting supernatant was carefully decanted without disturbing the pellet. The pellet was allowed to air-dry for 10 minutes, and redissolved in a suitable volume of endotoxin-free Buffer TE (~300µl).

2.5.2 Analysis of DNA by sequencing

DNA sequencing by the dideoxy-mediated chain termination method was routinely automated and performed in Oswell Laboratories. 5µg of purified plasmid DNA to a 1.5ml microfuge tube were normally sent over for sequencing analysis after adjusting the volume to 50ml with ddH_2O (C = 100ng/µl). Sequencing data were analysed using ABI PRISMA software compatible with a Power Macintosh G3.

2.5.3 Spectrophotometric determination of DNA

The spectrophotometer was calibrated at 260nm by adding 1ml TE (Tris-EDTA buffer) in a cuvette. 10µl of each DNA sample was added to 900µl TE buffer and mixed well. The OD_{260} values were obtained from the spectrophotometer. The amount of DNA was quantified from the following formula:

$$\text{DNA concentration (µg/ml)} = \frac{OD_{260} \times 100 \text{ (dilution faction)} \times (50 \text{ µg/ml})^{*}}{1000}$$

* (conversion factor for ds DNA)

2.5.4 Preparation of Lysogeny broth (LB) agar ampicillin plates

The LB agar media was prepared in a 1L flask. The flask was covered with an aluminium foil and autoclaved for 20 minutes using the liquid cycle. 100µg/ml ampicillin was added to the autoclaved medium and mixed. A flame was passed on the beaker to remove any bubbles in the medium, and on the beaker mouth for sterilisation purposes. The LB agar was poured into sterile plates, and these were

allowed to stand at Room Temperature for a day. The plates were then stored upside down inside a bag to prevent drying out, at 4^{o}C.

2.5.5 Transformation protocol of *E. coli* with pET32b ε-sarcoglycan peptide

For cells, buffers, solutions and reagents, refer to Appendix I, box 5. BL21 (DE3) competent cells were thawn on ice. Separate 100μl aliquots of the competent cells were added to different 14ml BD Falcon polypropylene round-bottom tubes, whilst a 100μl aliquot of competent cells was obtained for use as a transformation control. To increase transformation efficiency, a 1:10 dilution of a 14.2M stock solution of β-mercaptoethanol (β-ME) was added to all cells, for a final concentration of 25mM β-ME, and gently swirled every 2 minutes. 25ng of pET32bε-sarcoglycan peptide was added to each transformation reaction and swirled gently. For the control transformation reaction, 1μl of pET32b plasmid lacking ligation was added to a separate 100μl aliquot of the competent cells and swirled gently. All transformation reactions were incubated on ice for 30 minutes. Each transformation reaction was heat-pulsed in a 42^{o}C water bath for 45 seconds, followed by a 2-minute incubation on ice. 0.9ml of a preheated (42^{o}C) SOC medium (2M filter-sterilised glucose solution) was added to each transformation reaction and subsequently incubated the reactions for 1hr, in a shaker (220rpm) and 37^{o}C. 100μl of the transformed cells containing the ligated pET32b vector were spread on to LB agar ampicillin plates using a sterile spreader. 200μl of the control transformants were plated onto an LB-ampicillin agar plate. The plates were incubated overnight at 37^{o}C. The single colonies of transformants were picked for either “Endofree Maxiprep Plasmid Kit” or for “Induction of target protein using IPTG on a large scale”.

2.5.6 Induction of target protein using IPTG on a large scale

For cells, buffers, solutions and reagents, refer to Appendix I, box 5. Single colonies of transformants were picked and inoculated each in a different 20ml aliquot of LB medium containing 100μg/ml ampicillin, left overnight in a shaker (220rpm) at 37^{o}C. A 1 liter culture (LB, 100μg/ml ampicillin) was inoculated 1:50 with the noninduced overnight culture under vigorous shaking (220rpm) at 37^{o}C, until an

OD_{600} of 0.5 was reached. A 1ml samples was taken just prior to induction, and the cells in the sample were pelleted using a microcentrifuge and resuspended in 50µl 5x SDS-PAGE sample buffer, for gel analysis. Overexpression of the peptide of interest was induced by addition of IPTG to a final concentration of 1mM. Once the OD_{600} of 0.5 was reached, a 1ml sample was collected and the cells were pelleted in a microcentrifuge and resuspended in 100µl 5x SDS PAGE sample buffer, for gel analysis. The induced cells in the 1 liter culture were then harvested by centrifugation at 4,000 g for 20 minutes, stored overnight at -20^{o}C.

2.5.7 Preparation of cleared BL21 (DE3) lysates under denaturing conditions for purification of the target protein

For buffer solutions, refer to Appendix I, box 4. The induced cell pellet was thawn for 15 min on ice and resuspended in Buffer B at 5ml per gram-wet weight. The cells were gently stirred for 30-60 minutes at Room Temperature. Once the solution became translucent, lysis was complete and the lysate was centrifuged at 10,000 g (Sorval, SS34 rotor) for 30 min at Room Temperature in order to pellet the cellular debris. The supernatant was ready to undergo protein purification under denaturing conditions. A 5µl aliquot of the supernatant was mixed with 5µl of 2x SDS-PAGE sample buffer and stored at -20^{o}C for SDS-PAGE analysis.

2.5.8 Batch purification of 6xHis-tagged proteins from BL21 (DE3) cells under denaturing conditions

For buffer solutions, refer to Appendix I, box 4. 1ml of the 50% Ni-NTA (Qiagen) slurry (binding capacity 5-10mg/ml) was equilibrated with Buffer B, and centrifuged at 2,000 rpm for 2 minutes. 1-2mg lysate was loaded onto an equilibrated column and mixed gently on a shaker (200rpm) for 60 min at Room Temperature. The lysate-resin mixture was carefully loaded into an empty column with the bottom cap still attached. Once the mixture settled in the column, the bottom cap was removed and the flow-through was collected and kept for gel analysis. The column was washed twice with 4ml Wash buffer pH 6.3, and the flow-through was collected for gel analysis. The recombinant 32.6kDa ε-sarcoglycan peptide was eluted 4 times with 0.5ml Elution buffer pH 5.9, followed by 4 times with 0.5ml Elution buffer pH

4.5. The fractions were collected and analysed by SDS-PAGE. The Ni-NTA Resin matrix was stored in Buffer B containing 30% ethanol, to inhibit microbial growth. It is recommended a maximum of 5 runs per column.

2.5.9 Selection and preparation of Dialysis Membrane

A 30 cm dialysis membrane with "molecular weight cut-off" (MWCO) 1000 was utilised. The membrane was boiled for several minutes in a large excess of 10mM sodium bicarbonate, followed by boiling for several minutes in 10mM Na_2EDTA. The boiling step in 10mM Na_2EDTA was repeated. The membrane was then washed several times in distilled water and stored at 4^{o}C in 20% to 50% ethanol, to prevent growth of cellulolytic microorganisms.

2.5.10 Dialysis of ε-sarcoglycan peptide

The MWCO 1000 dialysis membrane was removed from ethanol storage solution and rinsed with distilled water. A secure clamp was utilised to close one end of the membrane. The membrane was filled with ε-sarcoglycan peptide and the open end was also clamped avoiding any air above the sample. The sample was squeezed to check the integrity of the membrane and clamps. The dialysis membrane was immersed in a beaker containing 2 liter of cleavage buffer, allowing stirring gently overnight at 4^{o}C. The next day, the cleavage buffer was replaced with 1.5 liter of fresh cleavage buffer pH 7.4, allowing stirring gently for 2 hours at 4^{o}C. This last step was repeated. The dialysis membrane was removed from the buffer and the membrane was held vertically to remove excess buffer trapped near the clamp. The sample was removed with a Pasteur pipet.

2.5.11 Concentrating the purified ε-sarcoglycan peptide

Up to 2ml of the dialysed ε-sarcoglycan peptide was added to a Centricon YM-10 centrifugal filter device, and allowed to spin for 1 hour, at 25^{o}C, at 5,000 g (Sorvall, H1318 rotor). The dialysed ε-sarcoglycan peptide was concentrated to as little as a 25μl sample volume in cleavage buffer.

2.5.12 Recombinant Enterokinase (rEK) treatment on the 33kDa ε-sarcoglycan peptide

For buffer solutions, refer to Appendix I, box 4. The concentrated ε-sarcoglycan peptide containing the enterokinase (EK) tag was digested using Recombinant Enterokinase. Serial dilutions of 50U rEK in rEK Dilution/Storage Buffer were prepared to produce solutions containing 0.1, 0.2 and 0.5U enzyme per µl. These were assembled with the following components into 4 separate tubes, in order to estimate the appropriate range of enzyme**:**target protein ratio and incubation times. 5µl of 10x rEK Cleavage/Capture Buffer A, 10µg target protein, 1µl diluted rEK (the fourth tube received 1µl Dilution/Storage Buffer only), and x µl of deionised water to make a 50 µl total volume. The reactions were incubated at room temperature, taking 10 µl aliquots into 10µl of 2x SDS sample buffer after 2, 6 and 17 hours, such that the extent of cleavage of the samples could be determined by SDS-PAGE analysis. The optimum rEK**:**protein ratio for this study was 1**:**100, with a 17 hour incubation time. A total of 2mg ε-sarcoglycan peptide digested with rEK was obtained, and was concentrated in Centricon YM-10 centrifugal filter device. For details, refer to section 2.5.11.

2.5.13 Isolation of the ε-sarcoglycan peptide from the S-tag-containing peptide

For buffer solutions, refer to Appendix I, box 4. The 14kDa ε-sarcoglycan peptide and 18.6kDa tag, obtained by rEK digestion of the 32.6kDa ε-sarcoglycan peptide, were equilibrated in Wash/Bind buffer pH 7.5. The 4ml slurry S-tag Agarose Beads (Novus Biologicals), which can bind up to 1mg of S-tag, were also equilibrated in Wash/Bind buffer by gently mixing the beads with Wash/Bind buffer for 2 minutes, followed by a 2 minute centrifugation at 2,000 rpm. The supernatant was discarded and the 2ml settled Agarose beads were mixed with 2mg protein capacity (1mg of 14kDa ε-sarcoglycan peptide + 1mg of 18.6kDa tag), 2 hours at Room Temperature, with gentle rotation (14 rpm). The sample was added to 5ml spin-filter columns, and centrifuged 10 minutes at 500g. The supernatant contained the 14kDa ε-sarcoglycan peptide of interest. The beads were gently mixed on a rotator (14 rpm) for 5 minutes with 3M Magnesium Chloride, followed by a 2minute centrifugation at

2,000 rpm. The supernatant contained the 18.6kDa S-tag peptide. The beads were resuspended and gently mixed (14 rpm) in Wash/Bind buffer pH 7.5 for 5 minutes, followed by a 2 minute centrifugation, and stored in phosphate buffer, pH 7.3 containing 0.5M NaCl, 0.02% Thimerosal at 4^{o}C, for further use.

2.5.14 Bradford Protein Assay (for protein and antibody)

A BioRad protein assay kit was used to estimate the concentration of proteins. 20µl of different dilutions of the BSA (2mg/ml) protein standard were pipetted into separate 1ml cuvettes. 20µl of unknown samples were also pipetted into separate 1ml cuvettes. 1ml of 1x Dye reagent was added to each cuvette. All samples were incubated for 10 minutes at Room Temperature. The spectrophotometer was set to 280nm. The instrument was zeroed with the blank sample containing 1ml of 1x Dye reagent and 20µl of the same buffer found in the sample/BSA. The absorbance measurements of the standards and unknown samples were measured. A standard curve was prepared by plotting the 280nm values (y-axis) versus their concentration in µg/ml (x-axis). The concentration of the unknown sample was determined using the standard curve, and the final concentration was adjusted by multiplying by the dilution factor, and divided by 1cm (path length).

2.5.15 Lyophilisation

Prior to lyophilisation, the switches for both the vacuum and refrigeration were set to "auto"(switches are both down), the lights for vacuum and refrigeration were checked to make sure they were both on, the temperature was allowed to reach ~ 40^{o}C, and the pressure was allowed to reach ~100x10^{-3} M Bar. The sample was frozen in a –80^{o}C freezer until the sample was completely frozen. The open container containing the sample was covered with tin foil. A few small holes were punched in the tin foil in order to allow for more efficient pressure equalisation. The frozen sample was placed in a round bottom lyophiliser tube, and this in turn was placed into a rubber gasket attached to the lyophiliser. The valve attached to the rubber gasket was turned 180^{o}C clockwise to open the chamber to the pump. The vacuum reading should momentarily go down and then come back up as the vacuum pumps down the

tube. After a 2 hour to overnight incubation time, depending on the volume of each sample and the time it takes for each sample to completely dry-out, the valve was turned counter clockwise 180^{o}C and the lyophiliser tube containing the sample could be removed.

2.5.16 Antibody production

The lyophilised sample (refer to section 2.5.15) was sent to Sigma-Genosys for antibody production in rabbit hosts.

2.6 Isolation of anti-ε-sarcoglycan antibody from immunised Rabbit serum

2.6.1 Cross-linking of ε-sarcoglycan peptide to the AminoLink Column

Following the dialysis of the ε-sarcoglycan peptide in 1L PBS solution (refer to section 2.5.10), the peptide was concentrated (refer to section 2.5.11), prior to cross-linking to the AminoLink Column. The AminoLink Plus Resin was suspended by end-over-end mixing. Subsequently, top cap and then the bottom tab were sequentially removed, in order to avoid drawing air into the column. The column was centrifuged at 1,000g for 1 minute in order to remove the storage buffer. 2ml of Coupling Buffer pH 7.2 was added to the column, followed by centrifugation at 1,000g for 1 minute. This last step was repeated. The bottom cap was replaced and 2-3ml of ε-sarcoglycan peptide (1-2mg content) dissolved in pH 7.2 Coupling Buffer was added to the AminoLink Plus Column. 0.1ml of the prepared sample was saved for subsequent determination of coupling efficiency. In a fume hood, 40µl of 5M Sodium Cyanoborohydride Solution was added to the reaction slurry, and the top cap was replaced to allow the mixing of the column by end-over-end mixing at Room Temperature for 4 hours. The top and bottom cap were removed respectively, then the column was placed into a new tube where it could be centrifuged at 1,000g for 1 minute, and the non-bound protein was collected and saved, in order to determine the coupling efficiency by comparing the protein concentration of the non-bound fraction to the starting sample. The top cap was removed, followed by the removal of the bottom cap, and the column was placed into a new tube and centrifuged at 1,000g for 1 minute to remove Coupling Buffer. The column was washed with 2ml of Quenching Buffer and centrifuged. The washing step was repeated. The bottom cap was replaced, and in a fume hood, 2ml of Quenching Buffer were added to 40µl of Sodium Cyanoborohydride Solution, and the resulting solution was added to the column. The top cap was replaced to allow gentle mixing of the column for 30 minutes by end-over-end rocking. The top cap was carefully removed, as some gas pressure may have formed during the reaction. The bottom column cap was subsequently removed, and the column was placed into a new tube and centrifuged in

order to remove Quenching Buffer. The reactants and the non-coupled protein were washed away with 2ml of Wash Solution (1M NaCl, 0.05% NaN_3) and centrifuged at 1000g for 1 minute. This step was repeated four times. The column was equilibrated by adding 2ml of Storage Buffer B and centrifuged. This step was repeated two more times. The bottom cap was replaced and 2ml of Storage Buffer B were added to the top of the resin bed. The top cap was replaced and the equilibrated column was stored upright at 4^oC until further use.

2.6.2 Affinity purification of anti-ε-sarcoglycan antibody from immunised Rabbit serum

The AminoLink Column containing the 33kDa ε-sarcoglycan peptide covalently attached to the beaded agarose support by primary amine-containing proteins was equilibrated to Room Temperature. The top column cap, followed by the bottom cap, was removed and the column was centrifuged at 1,000g for 1 minute to remove any storage solution. The column was equilibrated with 6ml of Phosphate-Buffered saline (PBS) pH 7.4. The rabbit serum was diluted with PBS in a 1:1 ratio, and 2ml volumes of the diluted serum were added in succession to the column. 12ml of Coupling Buffer pH 7.2 was added to the column, the flow-through containing the non-bound serum antibody was collected and saved, in order to determine the coupling efficiency by comparing the antibody concentration of the non-bound fraction to the starting sample. The rabbit serum anti-ε-sarcoglycan antibody that bound to the affinity column was eluted with 8ml Elution Buffer (0.1M Glycine pH 2.5). The eluted samples were saved in separate 1ml fractions, each containing 50µl of Neutralization Buffer (1M Tris-HCl pH 9.0). pH strips were utilised to verify the elution containing the antibody was neutralised. The elution(s) containing the antibody was identified via spectrophotometric analysis at 280nm (refer to section 5.23). 100µl liquots of anti-ε-sarcoglycan antibody were added to separate eppindorff tubes and stored at $–80^oC$.

Chapter 3:

3.0 Classical and delta dystrophins are differently localized in brain and hence likely to form different DPC complexes.

3.1 Introduction

In brain, the molecular composition of the DPC complex at inhibitory synapses of hippocampal neurons is becoming well established and includes: classical full-length dystrophin, β-dystrobrevin, α and β-dystroglycan, syntrophins, and β-neurexin (Brunig, *et* al, 2002; Culligan *et al*, 2002) (see chapter 1, figure 1.1.7.1). A decade ago, Blake *et al* (1999) identified a novel alternatively spliced isoform of classical dystrophin, which I name delta dystrophin (see Chapter 1, figure 1.1.2.2B). Although the expression of delta dystrophin in the brain has already been demonstrated (Blake *et al*, 1999), no studies on the function or localization of delta dystrophin in the brain have been published to date, and very little information is known about its molecular interactions in brain (Blake *et al*, 1999). The amino acid sequence of classical and delta dystrophin differs by only one exon located at the C-terminal end of each protein (chapter 1, figure 1.1.2.2). Classical dystrophin contains classical exon 78 that can be replaced by a longer and unique sequence I name delta exon 78, to yield delta dystrophin. Classical dystrophin contains a number of different domains (chapter 1, figure 1.1.2.1) that allow the protein to associate with various DPC components and intracellular proteins. Classical exon 78 is not part of any of these domains in classical dystrophin. In fact, the significance of classical exon 78 still remains to be established. Given that classical exon 78 does not appear to participate in molecular interactions with the DPC complex, its replacement with delta exon 78 suggests delta dystrophin possesses all the requisites to serve a similar function to classical dystrophin. Hence it may replace classical dystrophin to form novel delta DPC-like complexes in the brain. If so, this raises a number of interesting questions. Do delta dystrophin DPC complexes

co-localize to the same subcellular compartments as classical dystrophin DPC complexes? Do they have the same protein composition and the same functions?

I present here a database search (BLAST database) on classical exon 78 and delta exon 78, in order to verify whether any recently identified conserved domain published on this database whose function is known, matches these two short amino acid sequences. I then use a biochemical approach to compare the subcellular distribution of classical and delta dystrophin in two different brain regions (forebrain and cerebellum), to determine if the two dystrophin isoforms have the same or different distributions in the brain, in order to begin to determine whether delta dystrophin may replace classical dystrophin in DPC formation and its functions. The distribution of classical and delta dystrophin presented is also compared with the subcellular distribution of other well-established DPC components in the brain. These experiments aim to determine the similarities and/or differences delta dystrophin complexes may have with the well-established classical dystrophin-containing DPC complexes in forebrain and cerebellum, and provide information on the ability of delta dystrophin to replace classical dystrophin in the formation of novel delta DPC-like complexes in the cerebellum as well as in the forebrain. The cerebellum was selected because of the abundance of inhibitory GABAergic neurons (Leto *et al*, 2008), given that classical dystrophin is associated with GABAergic nerve terminals (Brunig *et al*, 2002).

According to a number of publications, DPC complexes of neurons contain only classical full-length dystrophin and are highly enriched in PSD structures (Culligan *et al*, 2002; Blake *et al*, 1999; Waite *et al*, 2009; Pilgram *et al*, 2009). Its localization at PSD structures has been shown via a number of biochemical approaches (Blake *et al*, 1999) as well as by immunocytochemical studies of hippocampal cultures (Brunig *et al*, 2002). Classical dystrophin and associated DPC components are co-localized with PSD markers (Brunig *et al*, 2002), therefore, PSDs and a range of subcellular fractions from rat brain have been prepared in order to determine whether delta dystrophin is also enriched in PSDs. There are two common and widely used methods to isolate PSDs (see materials and methods) either using Triton X-100 extraction (Cohen *et al*, 1977; Carlin e*t al*, 1980) or phase partitioning using n-octyl glucopyranoside (Gurd *et al*, 1982). Given that the composition of PSDs extracted by the two methods may vary, and, given that the Triton X-100 preparation seems to

contain only tightly bound PSD components (Matus *et al*, 1978; Kraus and Beesley unpublished results), both methods have been utilized and compared with one another, to examine the distribution of delta and classical dystrophins in PSD structures in both the forebrain and cerebellum.

3.2 Results:

3.2.1 BLAST database search

To establish the significance of classical and delta exon 78, I examined these sequences by using the BLAST database (http://blast.ncbi.nml.nih.gov/Blast.cgi). I introduced the sequence of classical exon 78 (Table 3.2.1), and the database found homologies of the sequence in classical dystrophin proteins only, but did not match with any putative conserved domains present in other proteins, thus the significance of classical exon 78 remained unresolved. When I introduced the sequence of delta exon 78 (Table 3.2.1), the database found homologies with delta dystrophin proteins only, but again, it did not match with any putative conserved domains present in other proteins, thus the significance of delta exon 78 also remained unresolved. In order to establish whether there may exist distant sequence similarities between these exons and the protein sequence database, I carried out a different BLAST database search, named PSI-BLAST. Unlike the BLAST database, the PSI-BLAST has been demonstrated to be useful in detecting such similarities even after considerable modification of their sequence during evolution (Bergman *et al*, 2007). When I introduced these sequences in the PSI-BLAST database, the results obtained were identical to those described in Table 3.2.1. I therefore began to examine and compare the subcellular distribution of classical and delta dystrophin in forebrain, to establish whether the differences exhibited by classical and delta exon 78 may or may not affect the subcellular distribution of delta dystrophin, when compared to classical dystrophin. This in turn was important for determining whether delta dystrophin may be able to replace classical dystrophin in the formation of novel delta DPC-like complexes at these brain regions, or whether the substitution of exon 78 results in the production of different protein complexes with different subcellular localization and with different properties and functions.

Query	Protein sequence	Comparison with the cdd
Classical exon 78 (dystrophin)	RNAPGKPMREDTM	**No putative conserved domain has been detected other than in dystrophin isoforms.**
Delta exon 78 (dystrophin)	HNVGSLFHMADDLGRAMESLVSVMTD EEGAE	**No putative conserved domain has been detected other than in dystrophin isoforms.**

Table 3.2.1: classical and delta exon 78 contain no putative conserved domain.
A BLAST database was used to align exon 78 with sequences whose conserved domains are already established. The BLAST hit resulted negative. The significance of these exons to date remains unknown. Cdd, conserved domain database.

3.2.2 Isolation of brain subcellular fractions

Different subcellular fractions were obtained as described in M&M, chapter 2. These fractions were then probed with a number of antibodies to determine the distribution of the antigen proteins in the different subcellular fractions. The following subcellular fractions were obtained from forebrain and cerebellum of adult rat brains: brain homogenate (BH), P2 pellet, myelin (My), microsomes (Mc), light membrane (LM), synaptic membrane (SM) and mitochondria (Mt). The SM fraction was fractionated further to give the PSD fraction. The PSD fraction consists of a large number of proteins, including scaffolding proteins, receptors, signaling proteins and adhesion molecules. The BH obviously contains all the complete protein complement present in brain. The P2 pellet contains mainly nuclei or non-solubilised material of neurons and glia. Microsomes mostly consist of artifactual vesicles formed from the endoplasmic reticulum (ER), ribosomes, partially lysed cells, and occasional small nerve-ending particle contamination. Myelin mostly consists of myelin fragments together with fragments of axon membrane. LM mainly contains membrane fragments largely of non-synaptic origin; the SM contains mainly synaptic membrane material as well as some contaminants from other fractions, including membranes of non-synaptic origin. The mitochondria consists almost entirely of mitochondrial membrane and matrix material, as well as some DNA contamination.

Forebrain PSDs were isolated using either n-octyl glucopyranoside or Triton X-100. Fractions were assayed for protein concentration by the Folin-Lowry method, and then subjected to a number of tests to show they are not cross-contaminated. A Sodium Dodecyl Sulfate (SDS) polyacrylamide gel containing an even loading of the subcellular fractions isolated, was stained with Coomassie blue (figure 3.2.2.1) to reconfirm the protein loading is even throughout each lane. Figure 3.2.2.1 shows that the gels were evenly loaded, but as expected, the protein composition of each fraction was distinctly different and evenly loaded. Three separate markers (neuroplastin65, Gp50 and PSD-95) were used to test for cross-contamination between the subcellular fractions isolated.

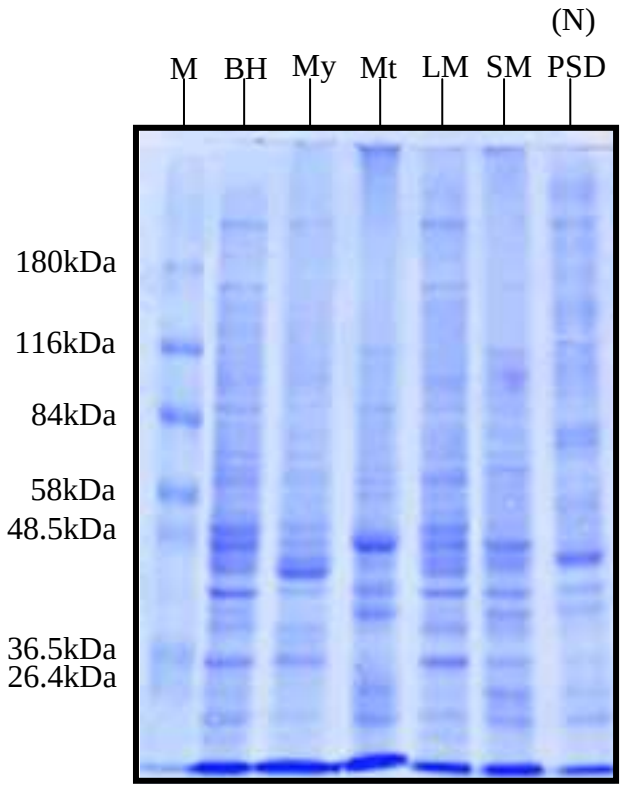

Figure 3.2.2.1: SDS PAGE separation of forebrain subcellular fractions.

Aliquots of subcellular fractions prepared from forebrain were separated on a 10% SDS PAGE gel. Proteins were visualised with Coomassie blue. Protein loading is 20μg/lane. Lane 1, Molecular Weight Markers; lane 2, Brain Homogenate (BH); lane 3, Myelin (My); lane 4, Mitochondria (Mt); lane 5, Light Membrane (LM); lane 6, Synaptic Membrane (SM); lane 7, Post Synaptic Density (PSD), isolated by the n-octyl glucopyranoside (N) method. Molecular weight standards are indicated.

I first examined the purity of forebrain subcellular fractions by determining the distribution of neuroplastins (np55 and np65, 55 and 65kDa respectively), using anti-neuroplastin antibody (Gp65) (figure 3.2.2.2). Previous work carried out in our lab has shown that both neuroplastins are enriched in the SM fraction, whereas only np65 is present in the PSD fraction (Hill *et al*, 1988). Np65/55 were therefore considered to be suitable markers for testing cross-contamination of the PSD fraction with membrane fractions. All subcellular fractions were loaded on to an SDS gel, followed by western blotting with anti-neuroplastin antibody (Gp65) (figure 3.2.2.2). The neuroplastin distribution was as expected. Neuroplastins 65 and 55 were visible in the Brain Homogenate, P2 pellet, LM fraction and appeared enriched in the SM lane. Only very low amounts of np65 and np55 were present in myelin and mitochondria fractions, suggesting there is very little cross-contamination with the fractions containing both neuroplastins.

Next I investigated the distribution of the neuroplastins within PSD fractions obtained by two different detergent methods, and compared it to the SM fractions (figure 3.2.2.3). Regardless of the method used for isolating the PSD fraction, np55 was consistently absent from the PSD fractions, and as expected, np65 was present in PSD fractions isolated by both methods. What is more, both neuroplastins were enriched in the SM fraction, as expected. The neuroplastin distribution showed that the subcellular fractions were successfully isolated. It is important to note that the level of np65 in the Triton X-100 extracted PSDs is much less than for the n-octylglucoside prepared PSDs. This is a novel result and important as it suggests that np65 may only be loosely bound to the PSD. In both preparations, the PSDs appear to be pure, as np55 did not contaminate the PSD fraction.

To further test cross-contamination of the PSD fraction with membrane fractions, the distribution of Gp50 (figure 3.2.2.4) was investigated. The Gp50 antibody detects the 50kDa β2-subunit of the ATPase subunit, known to be present in synaptic membranes (SM), but absent from the PSD and other fractions (Beesley *et al*, 1987). Upon western blotting of subcellular fractions and incubation with the anti-Gp50 antibody, I observed that only the LM and SM fractions contained the Gp50 protein, whereas the PSD fraction did not contain any Gp50 protein, in agreement with Beesley *et al* (1987). In fact, the 50kDa protein is highly enriched in the LM fraction, less

prominent in the SM fraction. In conclusion, the PSD fraction appears to be pure, as Gp50 did not contaminate the PSD fraction. No Gp50 was found in the remaining subcellular fractions, suggesting that there is no cross-contamination with the fractions containing Gp50.

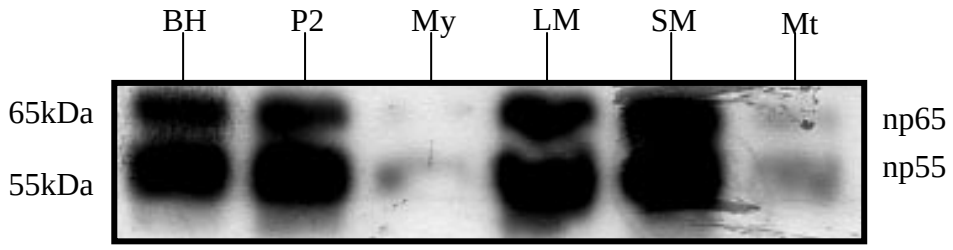

Figure 3.2.2.2: Western Blot of forebrain subcellular fractions immunodeveloped with anti-neuroplastin antibody (Gp65).

Neuroplastin 65 (np65) and neuroplastin 55 (np55) are abundant in the BH, P2 and LM fractions, and appear enriched in the SM fraction. Negligible quantities are found in the myelin and mitochondrial fractions. Protein loading is 20µg/lane. Lane 1, Brain Homogenate (BH); lane 2, Pellet 2 (P2); lane 3, Myelin (My); lane 4, Light Membrane (LM); lane 5, Synaptic Membrane (SM); lane 6, Mitochondria (Mt). Molecular weight standards are indicated.

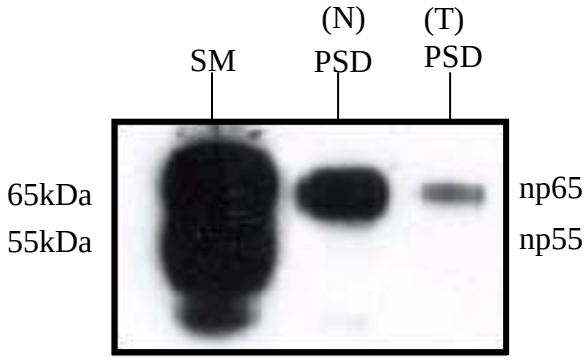

Figure 3.2.2.3: Western Blot of forebrain synaptic fractions immunodeveloped with anti-neuroplastin antibody (Gp65). PSDs were isolated by the Triton X-100 (T) or n-octyl glucopyranoside methods.

Neuroplastin 65 (np65) and neuroplastin 55 (np55) are enriched in the SM fraction. Only np65 is present in the PSD fractions. Triton X-100 extracted PSDs contain much less np65 than n-octyl glucopyranoside extracted PSDs. Protein loading is 20μg/lane. Lane 1, SM; lane 2, Post Synaptic Density (PSD), isolated by the n-octyl glucopyranoside (N) method; lane 3, Post Synaptic Density (PSD), isolated by the Triton X-100 (T) method. Molecular weight standards are indicated.

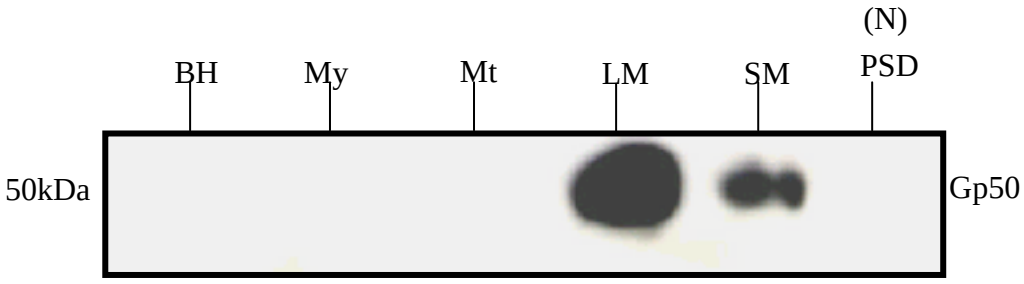

Figure 3.2.2.4: Western blot of forebrain subcellular fractions immunodeveloped with anti-Gp50 antibody. PSDs were prepared by the n-octyl glucopyranoside method. Gp50 is enriched in the LM and SM fractions only. Protein loading is 20µg/lane. Lane 1, Brain Homogenate (BH); lane 2, Myelin (My); lane 3, Mitochondria (Mt); lane 4, Light Membrane (LM); lane 5, Synaptic Membrane (SM); lane 6, Post Synaptic Density (PSD) isolated by the n-octyl glucopyranoside (N) method. Molecular weight standards are indicated.

For the third and final test for the purity of these subcellular fractions I determined the distribution of the PSD marker PSD-95 (figure 3.2.2.5). PSD-95 is a 95kDa scaffold protein that is very highly enriched in the PSD fraction of the forebrain (Kim *et al*, 1992; Hunt *et al*, 1996). Western blots including all subcellular fractions were incubated with anti-PSD-95 antibody. The 95kDa protein was successfully enriched in the PSD fraction and absent from all other fractions, suggesting there is no cross-contamination between the PSDs and the other subcellular fractions. In conclusion, my data show that the subcellular fractions do not show cross-contamination.

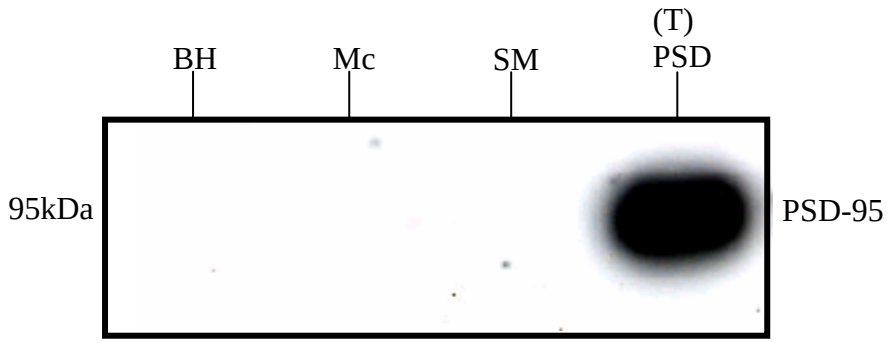

Figure 3.2.2.5: Western blot of forebrain subcellular fractions immunodeveloped with anti-PSD-95 antibody. The PSD fraction was prepared by the Triton X-100 (T) method.

As expected, PSD-95 is enriched in the PSD fraction only. Protein loading is 20μg/lane. Lane 1, Brain Homogenate (BH); lane 2, Microsomes (Mc); lane 3, Synaptic Membrane (SM); lane 4, Post Synaptic Density (PSD), isolated by the Triton X-100 (T) method. Molecular weight standards are indicated. T, Triton X-100.

3.2.3 Classical and delta dystrophin are differently distributed in the forebrain

Having established that the subcellular fractions were of comparable purity to that described in the literature (Beesley *et al*, 1987; Hill *et al*, 1988; Kim *et al*, 1992; Hunt *et al*, 1996), I then examined the subcellular distribution of delta dystrophin in the forebrain, and compared it to that of two crucial DPC components of the brain that are known to be enriched in the PSD: classical full-length dystrophin and β-dystrobrevin (Blake *et al*, 1999). Each forebrain subcellular fraction was loaded on an SDS gel for Coomassie Blue stain (figure 3.2.3.1) to ensure even loading of each subcellular fraction in every lane. After establishing even loading of forebrain subcellular fractions, the subcellular distribution of β-dystrobrevin, classical dystrophin and delta dystrophin was determined by immunoblotting a range of subcellular fractions, including SMs and PSDs prepared from rat forebrain. Immunoblots containing n-octyl glucopyranoside isolated PSDs were incubated with a panel of antibodies specific for β-dystrobrevin, classical dystrophin and delta dystrophin (figures 3.2.3.2, 3.2.3.3 & 3.2.3.4).

As expected, β-dystrobrevin was found to be enriched in the PSD fraction (figure 3.2.3.2) when compared with the LM, SM and BH fractions, as expected, in agreement with Blake *et al*, (1999). This result was reconfirmed using another set of freshly isolated subcellular fractions (data not shown). The enrichment of α-dystrobrevin 1 and 2 in the PSD fraction when compared to the LM, SM and BH fractions was also observed (figure 3.2.3.2), as expected (Blake *et al*, 1999). Higher molecular weight immunoreactive bands were present in all fractions (asterisks) except in myelin and mitochondria. Given that there are no known promoters in the dystrobrevin gene to account for these molecular weight bands, they could be non-dystrobrevin proteins that cross-react with the antibody.

In order to determine the subcellular distribution of classical dystrophin in the forebrain, a duplicate blot was prepared and incubated with anti-classical dystrophin antibody. The antibody recognized four separate classical dystrophin isoforms of different molecular weights (figure 3.2.3.3) in the PSD fraction, all of which are known to be expressed in the brain: cDp427, cDp140, cDp116 and cDp71

(Pilgram *et al*, 2009). As expected, classical full-length dystrophin (cDp427) was found to be highly enriched in the PSD fraction, when compared with the LM, SM and BH fractions (figure 3.2.3.3). By contrast, the shorter classical dystrophin isoforms cDp140, cDp116 and cDp71 were only moderately enriched in the PSD, when compared to the LM, SM fractions (figure 3.2.3.3). The myelin and mitochondrial fractions lacked all classical dystrophin isoforms, except for much reduced levels of cDp71, when compared to BH, LM, SM and PSD fractions. The cell soluble fraction contained much reduced levels of cDp427, cDp140, cDp116 and cDp71 when compared to the PSD, SM, LM and BH lane. The cell soluble fraction should not contain classical dystrophin isoforms, as these have been shown to be tightly associated with the cytoskeletal structures, predominantly the PSD, therefore they are highly insoluble (Blake *et al*, 1999). One possible explanation may be that during the fractionation procedure, some of the dystrophin isoforms become released from the membrane into the homogenization medium. Thus, the presence of classical dystrophin isoforms in the cytosol may represent small cross-contamination. A similar scenario was observed by Blake *et al* (1999) in the cell soluble fraction. It is important to note that immunoblots in this thesis were optimized for full-length dystrophin and thus are overexposed for some of the lower bands such as Dp71. These lower bands have saturated the film and thus are not giving a linear response in terms of comparing enrichments. There were two additional shorter isoforms with a molecular weight inferior to 71kDa present in most fractions (asterisks). Given there are no known promoters for these molecular weight bands, the latter may represent degradation products. In conclusion, figure 3.2.3.3 reconfirms that cDp427 is highly enriched in the PSD fraction, as expected (Blake *et al*, 1999).

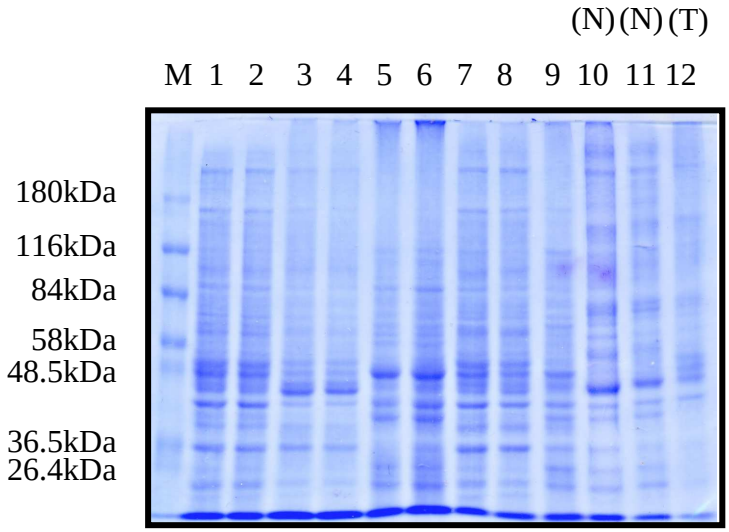

Figure 3.2.3.1: SDS PAGE separation of forebrain subcellular fractions, together with PSDs isolated by either the Triton X-100 detergent method or the n-octyl glucopyranoside method.

Aliquots of subcellular fractions prepared from forebrain were separated on a 10% SDS PAGE gel. Proteins were visualised with Coomassie blue. Lanes 1-9 show samples from duplicate experiments using subcellular fractions isolated using the n-octyl glucopyranoside method. Lanes 10 and 11 show PSDs isolated by the n-octyl glucopyranoside (N) method. Lane 12 shows the PSD fraction isolated by the Triton X-100 (T) method. Protein loading is 20µg/lane. Lanes 1-2, Brain Homogenate; lanes 3-4, Myelin; lanes 5-6, Mitochondria; lanes 7-8, Light Membrane; lane 9, Synaptic Membrane; lanes 10-11, Post Synaptic Density (PSD), isolated by the n-octyl glucopyranoside (N) method; lane 12, Post Synaptic Density (PSD), isolated by the Triton X-100 (T) method. Molecular weight standards are indicated. N, n-octyl glucopyranoside. T, Triton X-100. M, Molecular Weight Marker.

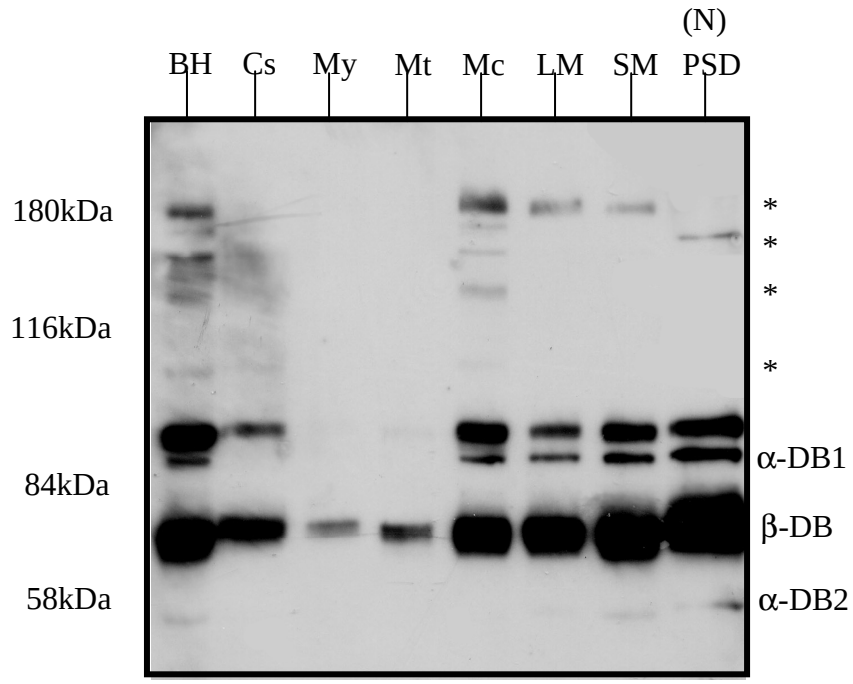

Figure 3.2.3.2: Western blot of forebrain subcellular fractions immunodeveloped with anti-β-dystrobrevin antibody.

As expected α1,α2, and particularly β-dystrobrevin are enriched in the PSD lane. Protein loading is 20μg/lane. Lane 1, Brain Homogenate (BH); lane 2, Cell soluble (Cs); lane 3, Myelin (My); lane 4, Mitochondria (Mt); lane 5, Microsomes (Mc); lane 6, Light Membrane (LM); Lane 7, Synaptic Membrane (SM); lane 8, Post-Synaptic Density (PSD), isolated by the n-octyl glucopyranoside (N) method. Molecular weight standards are indicated.

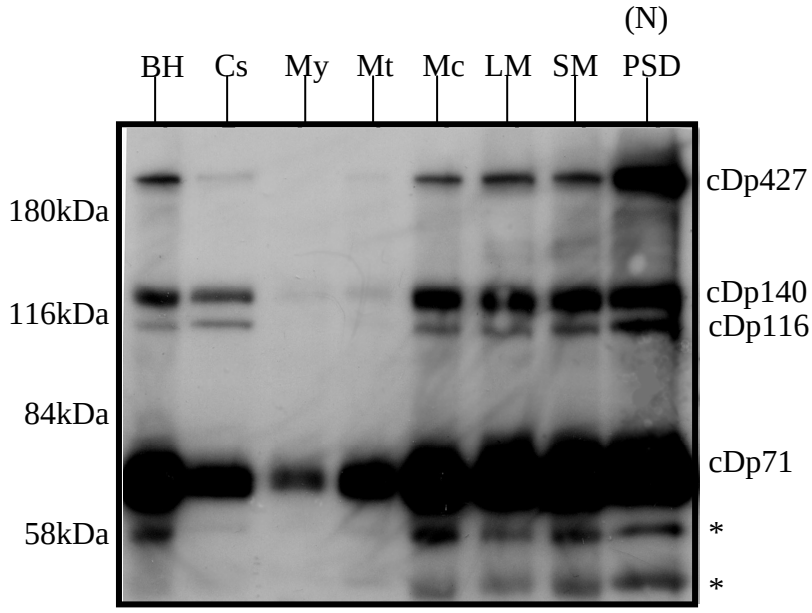

Figure 3.2.3.3: Western blot of forebrain subcellular fractions immunodeveloped with anti-classical dystrophin antibody.

Classical full-length dystrophin (cDp427) is enriched in the PSD fraction. cDp140, cDp116 and cDp71 are moderately enriched in the PSD fraction. Myelin and mitochondria lack all isoforms except for much reduced levels of cDp71, when compared to the BH and PSD fraction. The cell soluble fraction contains much reduced levels of all classical dystrophin isoforms, when compared to the BH and PSD fraction. Protein loading is 20μg/lane. Lane 1, Brain Homogenate (BH); lane 2, Cell Soluble (Cs); lane 3, Myelin (My); lane 4, Mitochondria (Mt); lane 5, Microsomes (Mc); lane 6, Light Membrane (LM); lane 7, Synaptic Membrane (SM); lane 8, Post Synaptic Density (PSD), isolated by the n-octyl glucopyranoside method (N). Molecular weight standards are indicated.

To determine whether delta dystrophin was enriched in the PSD, a duplicate blot was incubated with anti-delta dystrophin antibody (figure 3.2.3.4). In contrast to classical full-length dystrophin, delta full-length dystrophin was highly enriched in the microsomal fraction and only moderately enriched in the PSD fraction, when compared with the LM, SM and BH fractions. dDp140 was moderately enriched in the microsomal and PSD fraction, when compared to the membrane fractions (LM and SM), whereas dDp116 and dDp71 were found in most fractions, with dDp71 being generally more abundant than dDp116. Contrary to classical dystrophin in figure 3.2.3.3, the cell soluble fraction of figure 3.2.3.4 contains a moderate amount of dDp427, when compared to the BH, LM, SM and PSD fractions, followed by negligible amounts of dDp140, dDp116 and dDp71, when compared to the BH, LM, SM and PSD fractions. In addition to the four well-established delta dystrophin isoforms just described, the anti-delta dystrophin antibody recognized a number of additional bands (asterisks). A band in the PSD fraction that is slightly higher than dDp427 could represent an alternatively spliced isoform of dDp427. However, it remains to be tested whether such alternative delta dystrophin transcript exists or not. Given that there are no known promoters for the production of the remaining bands (asterisks) in the various subcellular fractions, they either represent degradation products of dystrophin proteins, or simply be immunoreactive bands of unrelated protein artifacts observed on the blot. Altogether, figures 3.2.3.3 and 3.2.3.4 suggest that delta full-length dystrophin (dDp427) has a different subcellular distribution to that of classical full-length dystrophin (cDp427) within the forebrain.

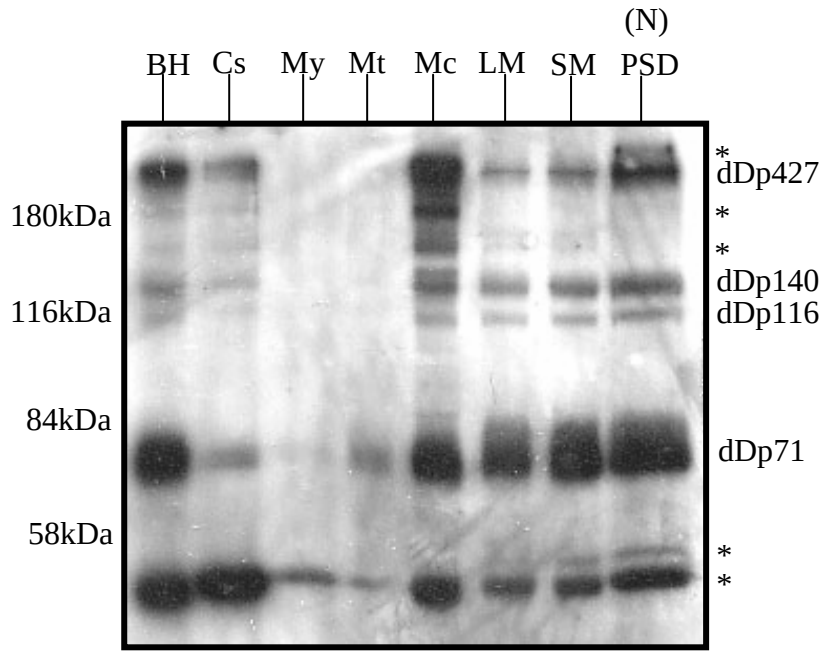

Figure 3.2.3.4: Western blot of forebrain subcellular fractions immunodeveloped with anti-delta dystrophin antibody.

Delta full-length dystrophin (dDp427) is highly enriched in the microsomes and only moderately enriched in the PSD fraction. dDp140 is moderately enriched in the microsomal and PSD fraction, whereas dDp116 and dDp71 are found in most fractions, with dDp71 being generally more abundant than dDp116. Protein loading is 20µg/lane. Lane 1, Brain Homogenate (BH); lane 2, Cell Soluble (Cs); lane 3, Myelin (My); lane 4, Mitochondria (Mt); lane 5, Microsomes (Mc); lane 6, Light Membrane (LM); lane 7, Synaptic Membrane (SM); lane 8, Post Synaptic Density (PSD), isolated by the n-octyl glucopyranoside (N) method. Molecular weight standards are indicated.

3.2.4 Classical and delta dystrophin are differently distributed in the cerebellum

The subcellular distribution of a protein in the forebrain may not always reflect the subcellular distribution found in the cerebellum. For example, PSD-95 is highly enriched in the PSD of the forebrain (Hunt *et al*, 1996, Kim *et al*, 1992), whereas it is less concentrated in the PSD fraction of the cerebellum. On the other hand, the cerebellum exhibits intense concentration of PSD-95 immunoreactivity in axon terminals, which is not observed in forebrain neurons (Hunt *et al*, 1996). Therefore, in order to establish whether delta dystrophin may replace classical dystrophin in the formation of novel delta DPC-like complexes at the PSD of the cerebellum, I determined and compared the subcellular distribution of classical dystrophin and delta dystrophin in the cerebellum, and also compared it to the forebrain.

I compared side by side the subcellular localization of classical dystrophin in the forebrain with the cerebellum because the concentration of this protein in the two brain regions has never been compared, although its localization at PSD structures of the forebrain and cerebellum has long been established (Kim *et al*, 1992). This is important as classical dystrophin is known to selectively localize at GABAergic synapses in the forebrain (Brunig *et al*, 2002), and given that approximately 50% of the cerebellar neuronal phenotypes are GABAergic interneurons (Leto *et al*, 2008), whilst only 20% of forebrain neurons are inhibitory (Xu *et al*, 2010), I decided to determine whether classical dystrophin was more enriched in the cerebellum PSDs when compared to forebrain PSDs, as this would allude to the possibility that in the cerebellum also, classical dystrophin may restrict to PSDs of inhibitory synapses, similar to what has been observed for the forebrain.

I immunoblotted a range of subcellular fractions prepared from rat cerebellum and compared these with forebrain subcellular fractions. The immunoblot was incubated with an antibody specific for classical dystrophin (figure 3.2.4.1). In figure 3.2.4.1, classical full-length dystrophin was found highly enriched in the PSD fraction of both brain regions, with cDp427 appearing more concentrated in the cerebellar PSDs when compared to forebrain PSDs. cDp140 was more concentrated in the cerebellar PSDs when compared to the forebrain PSDs, and was more concentrated

in the SM and cell soluble fractions of the cerebellum, when compared to the respective fractions of the forebrain (figure 3.2.4.1). Generally, there was more cDp140 in cerebellum than in forebrain throughout all the subcellular fractions. cDp116 and cDp71 were moderately enriched in the PSD fraction of the forebrain and cerebellum, when compared to the LM and SM fractions of the forebrain and cerebellum respectively (figure 3.2.4.1). Overall, all classical dystrophin isoforms were more concentrated in the cerebellum when compared to the forebrain, and they all enriched in the PSD fraction of either brain region. What is more, PSD enrichment in the cerebellum was greater than in the forebrain. It is important to note, however, that immunoblots were optimized for full-length dystrophin and thus are overexposed for some of the lower bands such as Dp71. These bands, unlike cDp427, are saturated and thus are not giving a linear response in terms of comparing enrichments. There were two additional shorter isoforms (asterisks) with a molecular weight inferior to 71kDa. Given there are no known promoters for these molecular weight bands, they may either represent degradation products, or non-classical dystrophin proteins that cross-react with the antibody.

To test whether delta dystrophin may replace classical dystrophin and form novel delta DPC-like complexes in PSD structures of the cerebellum, duplicate immunoblots were incubated with anti-delta dystrophin antibody (figure 3.2.4.2) such that these could also be compared with the subcellular distribution of classical dystrophin. Results showed low expression of dDp427 throughout the cerebellum, as opposed to the higher level of expression of dDp427 in the forebrain, although dDp427 was found to be enriched in the cerebellar PSD and microsomal fractions when compared to the cerebellar LM fraction. In contrast, forebrain dDp427 was highly enriched in the microsomal fraction of the forebrain and moderately enriched in the PSD of the forebrain, when compared to forebrain LM and SM fractions, in agreement with figure 3.2.3.4. dDp427 was more concentrated in the cell soluble fraction of forebrain when compared to the cell soluble fraction in the cerebellum. dDp140 and dDp116 were weakly distributed throughout forebrain and cerebellar fractions, and highly enriched only in the PSD fraction of the forebrain. dDp71 was found in most fractions of the forebrain and cerebellum (figure 3.2.4.2), but much depleted in the cell soluble and myelin fractions. The presence of delta dystrophin in the cell soluble fraction was reproduced in every experiment (figures 3.2.3.4 and 3.2.4.2), contrasting

with the knowledge that dystrophin is an insoluble protein (Blake *et al*, 1999). As will be shown in chapter 4 (figure 3.2.4.1), delta dystrophin specifically co-localizes with microtubules and therefore it may be that dissociation of microtubules during the fractionation procedure has resulted in solubilisation of a portion of the delta dystrophins into the cell soluble fraction. In forebrain and cerebellum there exist additional bands (asterisks) below the dDp427 point. These bands could either represent degradation products or they could also represent non-delta dystrophin proteins that cross-react with the antibody. Altogether, these results (figure 3.2.4.1 and 3.2.4.2) show two striking novel findings: firstly that the subcellular distribution of classical full-length and delta full-length dystrophins is markedly different; secondly, the regional distribution of these two molecules in brain is markedly different.

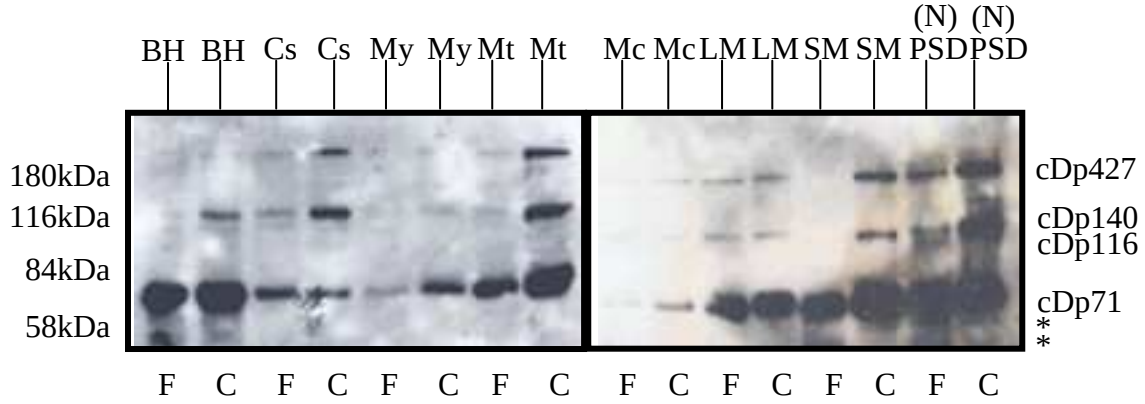

Figure 3.2.4.1: Western blot of forebrain and cerebellar subcellular fractions immunodeveloped with anti-classical dystrophin antibody.

cDp427 is highly enriched in the PSD fraction of the forebrain. cDp140, cDp116 and cDp71 are moderately enriched in forebrain PSDs. The same enrichment pattern is observed in the PSD of the cerebellum, with the latter exhibiting more classical dystrophin than the forebrain. The fractions are run in pairs with the left and right hand samples being forebrain and corresponding cerebellar fractions respectively. Protein loading is 20μg/lane. Lanes 1-2, Brain Homogenate (BH); lanes 3-4, Cell Soluble (Cs); lanes 5-6, Myelin (My); lanes 7-8, Mitochondria (Mt); lanes 9-10, Microsomes (Mc); lanes 11-12, Light Membrane (LM); lanes 13-14, Synaptic Membrane (SM); lanes 15-16, Post Synaptic Density (PSD), isolated by the n-octyl glucopyranoside (N) method. Molecular weight standards are indicated. F, forebrain. C, cerebellum.

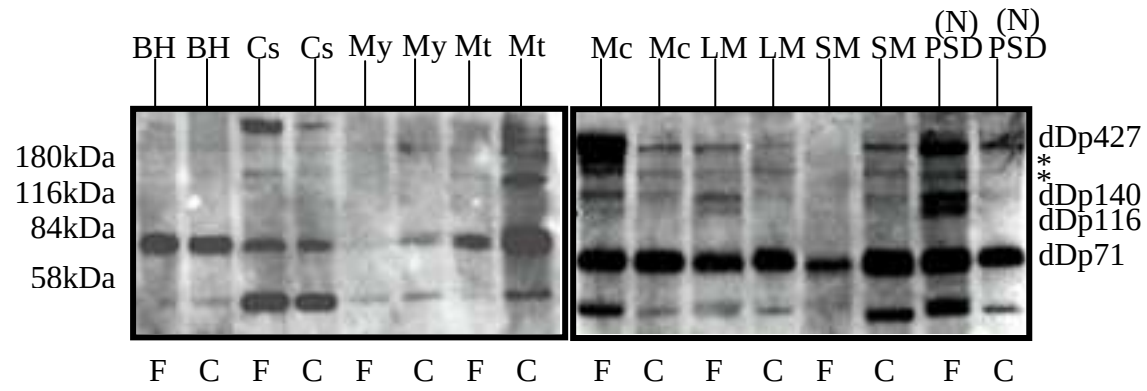

Figure 3.2.4.2: Western blot of forebrain and cerebellar subcellular fractions immunodeveloped with anti-delta dystrophin antibody.

Results show low expression of dDp427 throughout the cerebellum, as opposed to the higher level of expression of dDp427 in the forebrain. dDp427 is highly enriched in the microsomal fraction of the forebrain, exhibiting only moderate enrichment in the PSD fraction of the forebrain. In contrast, cerebellar dDp427 is generally weakly expressed when compared to the level of expression throughout the forebrain, although dDp427 is enriched in cerebellar microsomes and PSD. dDp140 and dDp116 are weakly distributed throughout forebrain and cerebellar fractions and are highly enriched only in the PSD fraction of the forebrain. dDp71 is ubiquitously expressed. The fractions are run in pairs with the left and right hand samples being forebrain and corresponding cerebellar fractions respectively. Protein loading is 20µg/lane. Lanes 1-2, Brain Homogenate (BH); lanes 3-4, Cell Soluble (Cs); lanes 5-6, Myelin (My); lanes 7-8, Mitochondria (Mt); lanes 9-10, Microsomes (Mc); lanes 11-12, Light Membrane (LM); lanes 13-14, Synaptic Membrane (SM); lanes 15-16, Post Synaptic Density (PSD), isolated by the n-octyl glucopyranoside (N) method. Molecular weight standards are indicated. F, forebrain. C, cerebellum.

3.2.5 Dystrophin is an integral PSD protein of the forebrain

Determining whether a protein is part of the PSD apparatus via a biochemical approach may sometimes yield an artefactual result compared to the in vivo scenario in the cell. For example, a number of biochemical studies have indicated that Bassoon is a PSD component (Dieck *et al*, 1998; Li et al, 2004). The true localization of Bassoon however is presynaptic, as revealed by double-fluorescence immunocytochemistry between Bassoon and various presynaptic markers (Dieck *et al*, 1998). Dieck *et al* (1998) then went on to assess the nature of Bassoon during the PSD extraction studies with two detergents, Triton X-100 and n-octyl glucopyranoside, and noted that neither detergent was able to solubilise significant amounts of Bassoon, but noticed that Triton X-100 was able to solubilise larger amounts of Bassoon compared to n-octyl glucopyranoside. I have also demonstrated in figure 3.2.2.3 that the Triton X-100 protocol (Carlin *et al*, 1980) may remove loosely bound PSD components that are not removed by the n-octyl glucopyranoside phase partitioning method (Gurd *et al*, 1982). The data in figure 3.2.2.3 shows that np65 is enriched in PSDs prepared by the phase partitioning method, whereas it is present only in low amounts in PSDs prepared using the Triton X-100 protocol (figure 3.2.2.3). This is consistent with previously published data (Smalla *et al*, 2000), which suggests that np65 can rapidly translocate out of the PSD and thus may be only loosely bound to the PSD. Thus, the following section established whether dystrophin is loosely bound to the PSD or whether it is an integral protein of the PSD of the forebrain (figure 3.2.5.1).

The subcellular distribution of dDp427 was determined by immunoblotting (figure 3.2.5.1) rat forebrain subcellular fractions, including PSDs prepared using the Triton X-100 and n-octyl glucopyranoside phase partitioning methods. The immunoblot was incubated with anti-delta dystrophin antibody. Delta full-length dystrophin was enriched in microsomes, in PSDs isolated by the Triton X-100 protocol, and in PSDs isolated by the n-octyl glucopyranoside method, when compared with the SM fraction (figure 3.2.5.1). In fact, the enrichment of dDp427 in PSDs isolated by the Triton X-100 method was similar to the enrichment of dDp427 in PSDs isolated by the n-octyl glucopyranoside method. In the microsomal and n-octyl

glucopyranoside PSD fractions only, dDp427 was detected as a doublet band (asterisk). The explanation for this is not clear. dDp140 and dDp116 were moderately enriched in PSDs isolated by the Triton X-100 method and in PSDs isolated by the n-octyl glucopyranoside method when compared with the SM fraction. dDp71 was found in all fractions tested. As a control, a duplicate blot was incubated with anti-classical dystrophin antibody (figure 3.2.5.2). As expected, cDp427 was highly enriched in PSD fractions isolated by either detergent method, when compared with the BH and SM fractions (figure 3.2.5.2). By contrast, only the n-octyl glucopyranoside PSD fraction contained moderate enrichment of cDp140 and cDp116 when compared to BH and SM fractions, whereas the Triton X-100 PSD fraction showed moderate enrichment of cDp116, but not cDp140. Dp71 was ubiquitously expressed. In conclusion, the type of detergent used to prepare the PSD fraction did not affect the enrichment patterns of classical and delta full-length proteins, as both were found equally enriched in the PSD of the forebrain isolated by either detergent method. The results suggest that both classical and delta full-length dystrophin are integral rather than loosely bound PSD proteins. Although this study suggests that classical and delta full-length dystrophin proteins appear to be integral PSD proteins, delta dystrophin is consistently highly enriched in microsomes and only moderately enriched in the PSD fractions (figure 3.2.5.1), hence the subcellular distribution of classical full-length and delta full-length dystrophins is markedly different and according to figures 3.2.4.1 and 3.2.4.2, the regional distribution of these two molecules is markedly different. The precise subcellular distribution of classical and delta dystrophin was further investigated immunocytochemically in chapter 4.

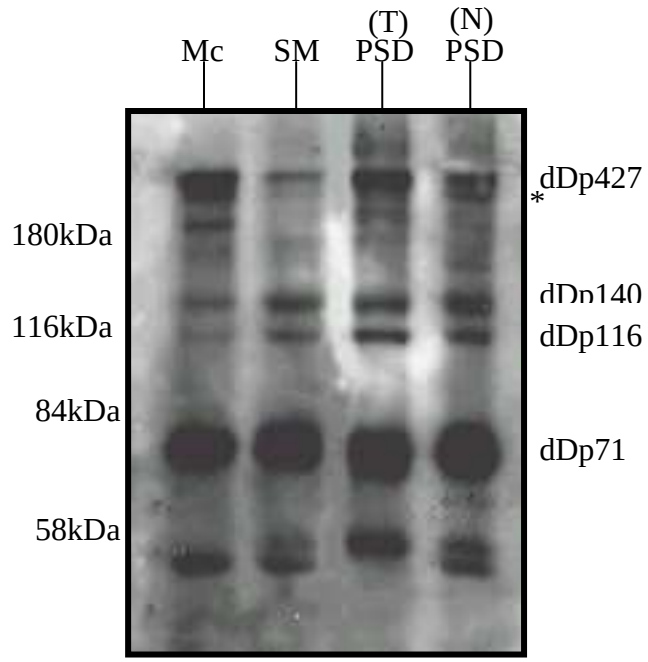

Figure 3.2.5.1: Western blot of forebrain subcellular fractions including PSDs prepared using the Triton X-100 or n-octyl glucopyranoside method and immunodeveloped with anti-delta dystrophin antibody.

Delta full-length dystrophin is more highly enriched in microsomes, compared to PSDs obtained by either the n-octyl glucopyranoside method or the Triton X-100 method. The similar level of enrichment in the PSD fractions prepared by both methods suggests that dDp427 is an integral PSD protein. The microsomal and n-octyl glucopyranoside PSD fraction show dDp427 as a doublet band (asterisk). dDp140 and dDp116 are moderately enriched in the PSDs obtained by either detergent method, and are found in lower concentrations in the remaining fractions tested. dDp71 is ubiquitously expressed. Protein loading is 20μg/lane. Lane 1, Microsomes (Mc); lane 2, Synaptic Membrane (SM); lane 3, Post Synaptic Density (PSD), isolated by the Triton X-100 (T) method; lane 4, Post Synaptic Density (PSD), isolated by the n-octyl glucopyranoside (N) method. Molecular weight standards are indicated. T, Triton X-100. N, n-octyl glucopyranoside.

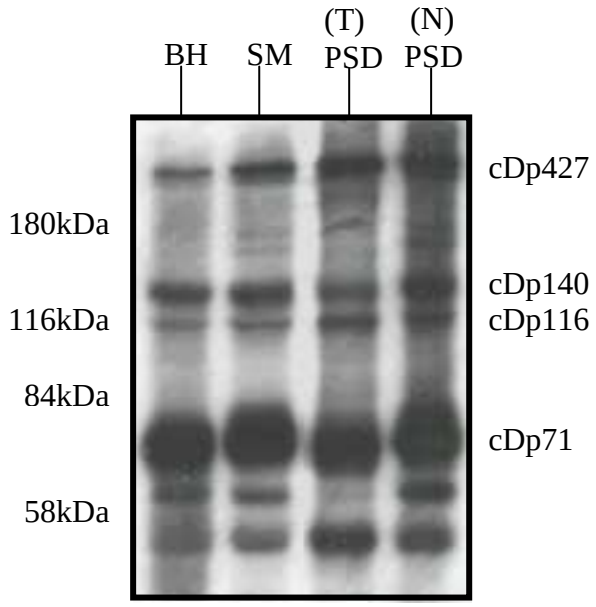

Figure 3.2.5.2: Western blot of forebrain subcellular fractions including PSDs prepared using the Triton X-100 or n-octyl glucopyranoside method and immunodeveloped with anti-classical dystrophin antibody.

Classical full-length dystrophin (cDp427) is enriched compared to SM in PSDs obtained by the n-octyl glucopyranoside method and the Triton X-100 method. cDp140 and cDp116 appear to be moderately enriched in PSDs obtained by the n-octyl glucopyranoside method, when compared to the SM and BH fractions, whereas the Triton X-100 PSD fraction shows moderate enrichment of cDp116, but not cDp140. cDp71 is ubiquitously expressed. Protein loading is 20µg/lane. Lane 1, Brain Homogente (BH); lane 2, Synaptic Membrane (SM); lane 3, Post Synaptic Density (PSD), isolated by the Triton X-100 (T) method; lane 4, Post Synaptic Density (PSD), isolated by the n-octyl glucopyranoside (N) method. Molecular weight standards are indicated. T, Triton X-100. N, n-octyl glucopyranoside.

3.3 Discussion:

3.3.1 Classical and delta dystrophin exhibit different regional and subcellular distribution in forebrain and cerebellum, hence they are likely to form different DPC complexes

A BLAST database search on classical exon 78 and delta exon 78 shows that other than classical and delta dystrophin isoforms, no other proteins contain these sequences. The functional significance of these exons remains unknown (Table 3.2.1), whereas the remaining domains of either classical and delta dystrophin are identical, and classical dystrophin is known to utilize these domains to form the DPC complex at PSDs of neurons (Culligan *et al*, 2002). I therefore compared the subcellular distribution of classical and delta dystrophin in forebrain and cerebellum, to establish whether their differences in exon 78 may or may not affect the subcellular distribution of delta dystrophin, when compared to classical dystrophin. This in turn was important for determining whether delta dystrophin was also a PSD protein and therefore able to replace classical dystrophin in the formation of novel delta DPC-like complexes in PSDs of forebrain and cerebellum, or, whether the substitution of exon 78 results in the production of different protein complexes with different subcellular localization and with different properties.

The data in this chapter show clear differences in the pattern of subcellular distribution of classical and delta full-length dystrophin proteins, the former being most highly enriched in PSD structures, the latter in the microsomal fractions. Furthermore, there is a striking difference in the level of expression of the two isoforms between the two brain regions, with delta full-length dystrophin being expressed at low levels in the cerebellum when compared to the forebrain, whilst classical full-length dystrophin is more concentrated in cerebellar fractions when compared to forebrain. These studies show that although the two proteins are highly homologous, they are likely to form protein complexes with different subcellular localization and with different properties and function. Given that classical and delta

exon 78 are the only sequences distinguishing classical dystrophin from delta dystrophin, they are likely to affect the subcellular distribution of classical and delta dystrophin within the forebrain and cerebellum. The details are described below.

I determined and compared the subcellular distribution of classical dystrophin in both forebrain and cerebellum subcellular fractions. Classical full-length dystrophin is highly enriched in the PSD fractions of the forebrain and cerebellum (figure 3.2.4.1), in agreement with publications (Kim *et al*, 1992; Culligan *et al*, 2002) and exhibits a subcellular distribution in the forebrain that is identical to that in the cerebellum (figure 3.2.4.1). Classical full-length dystrophin is strongly expressed in both brain regions, what is more, classical full-length dystrophin is more concentrated in cerebellar PSD, when compared to the corresponding forebrain PSD (figure 3.2.4.1). As classical dystrophin and DPC components selectively localize at GABAergic synapses in forebrain neurons (Brunig *et al*, 2002) and given that only 20% of the forebrain comprises of GABAergic neurons (Xu *et al*, 2010) whilst 50% of the cerebellum is composed of GABAergic neurons (Leto *et al*, 2008), the higher cDp427 band intensity in cerebellar compared to forebrain PSDs suggests that in the cerebellum also, cDp427 may be restricted to PSDs of inhibitory synapses. All in all, these results demonstrate that classical dystrophin is expressed in both brain regions, it is highly enriched in the PSD fraction of forebrain and cerebellum, and is likely to localize at PSDs of inhibitory synapses in the cerebellum, as well as the forebrain. What is more, in the cerebellum, classical full-length dystrophin is reported to form DPC complexes within the PSD (Kim *et al*, 1992). Therefore I suggest that in analogy to the forebrain, cerebellum DPC complexes containing cDp427 may also localize at GABAergic synapses. Immunocytochemical studies are required to confirm the biochemical data.

When the subcellular distribution of delta full-length dystrophin in forebrain and cerebellum subcellular fractions was examined, it revealed two very different scenarios, and these are again very different to those described for classical full-length dystrophin. In the forebrain, delta full-length dystrophin is highly enriched in the microsomal fraction whilst it is only moderately enriched in the PSD (figure 3.2.3.4). Whereas the expression of delta full-length dystrophin in the cerebellum is low when compared to the forebrain, although full-length delta dystrophin is enriched

in microsome and PSD fractions prepared from cerebellum. It is important to note that the cerebellum, although it comprises only 10% of the brain volume, it contains similar numbers of neurons when compared to the forebrain (Leto *et al*, 2008). Therefore, the low expression of delta full-length dystrophin throughout the subcellular fractions in the cerebellum is not due to a lower number of neurons in the cerebellum when compared to the forebrain, rather, it is probably due to a low level of delta dystrophin expression therein. Given that 20% of the forebrain is comprised of GABAergic neurons (Xu *et al*, 2010) whilst 50% of the cerebellum is comprised of GABAergic neurons (Leto et la 2008), the lower dDp427 band intensity in cerebellar PSDs when compared to forebrain PSDs suggests that dDp427 is not expressed specifically in GABAergic synapses. In conclusion, alternative splicing of the DMD gene product (classical and delta full-length dystrophin) is closely regulated in the two brain regions, with delta full-length dystrophin being expressed in forebrain as well as the cerebellum, albeit in lower amounts. What is more, these results also suggest that in the forebrain and in the cerebellum, delta full-length dystrophin may form novel delta DPC complexes outside the PSD (as suggested by the microsomal enrichment), as well as in PSD structures (as suggested by the PSD enrichment) of non-GABAergic synapses. This hypothesis is further verified in Chapter 4.

Based on the different regional and subcellular distributions exhibited by classical and delta full-length dystrophin isoforms, it is suggested that the molecular composition and function of delta full-length dystrophin-containing complexes that form within the forebrain and cerebellum, is likely to markedly differ from classical full-length dystrophin-containing complexes. Firstly, this is because my studies suggest delta full-length dystrophin may localize at PSDs of non-GABAergic synapses, whilst classical full-length dystrophin and its associated DPC proteins exclusively localize at PSDs of inhibitory synapses (Brunig *et al*, 2002). In turn this suggests that delta full-length dystrophin may bind to different protein partners and hence, has a different function and molecular composition when compared to classical dystrophin-containing DPC complexes. Secondly, the higher enrichment of delta full-length dystrophin in the microsomal fraction when compared to the moderate enrichment in the PSD fraction (figures 3.2.3.4 & 3.2.4.2) suggests delta full-length dystrophin also forms novel DPC complexes outside the PSD, and as a consequence, delta full-length dystrophin-containing complexes outside the PSD

may exhibit a different molecular composition compared to classical full-length dystrophin-containing proteins that exclusively localize at PSDs of inhibitory synapses. Thirdly, I show that β-dystrobrevin (figure 3.2.3.2), a component of classical full-length dystrophin-containing DPC complexes (Brunig *et al*, 2002; Culligan *et al*, 2002) also exhibits a different subcellular distribution to that exhibited by delta full-length dystrophin (figure 3.2.3.4). Therefore, all these studies demonstrate that the molecular composition of dDp427-containing DPC complexes is likely to be markedly different to the molecular composition of cDp427-containing DPC complexes, despite the fact that both classical and delta full-length dystrophins contain the same protein binding sequences. Therefore, regardless of the highly similar domain structure, classical and delta full-length dystrophin isoforms are likely to exert different functions in the different types of neuronal subcellular compartments in which they are found. These will include GABAergic and possibly non-GABAergic synapses, respectively. What is more, biochemical studies suggest delta full-length dystrophin appears to be more widely distributed in the brain when compared to classical-full-length dystrophin. This has been investigated further in the immunocytochemical studies described in chapter 4.

Classical and delta dystrophin both originate from the same gene, thus the low expression of delta full-length dystrophin in the cerebellum when compared to forebrain, as opposed to the higher expression of the classical full-length dystrophin in the cerebellum when compared to forebrain, is likely to occur by reducing alternative splicing mechanisms on the mRNA product derived from the DMD gene in the cerebellum, as this would ensure the continued production of classical dystrophin in the cerebellum whilst reducing the production of delta dystrophin therein. The differences in subcellular distributions exhibited by the classical and delta dystrophin isoforms, must be due to Cexon78 and Dexon78, as these are the only sequences that distinguish classical dystrophin from delta dystrophin respectively. In other words, a plausible hypothesis is that classical exon 78 may participate in directing classical full-length dystrophin exclusively to PSD structures, whereas delta exon 78 may participate in directing delta full-length protein to other PSD types and/or in microsomes. Thus, classical and delta exon 78 may encode a trafficking signal that participates in directing the proteins to different subcellular compartments. In fact, Sakamoto *et al* (2008) found that the binding site

to the PSD is located at the C-terminus end between the WW domain and the C-terminus of classical dystrophin, which is where classical and delta exon 78 are found (chapter 1, figure 1.1.2.2). What is more, Sakamoto *et al*, (2008) show that when this region is removed, the classical dystrophin isoforms are unable to associate with the PSD, instead, they localize in the cytoplasm, neurites and axons. Thus, Cexon78 and Dexon78 are clearly implicated in the trafficking of the classical and delta dystrophin proteins to or away from the PSD. In chapter 4 I investigate whether Cexon78 and Dexon78 alone, may encode different trafficking signals.

I have demonstrated in figure 3.2.2.3 that the Triton X-100 protocol is able to remove part of the loosely bound PSD components, as evidenced by np65 levels, whereas the n-octyl glucopyranoside protocol cannot. Thus I was able to determine whether delta full-length dystrophin is loosely bound to the PSD, or whether it is an integral PSD protein of the forebrain. I demonstrate that delta full-length dystrophin is enriched in the forebrain PSD fraction obtained by the Triton X-100 protocol, and was also consistently enriched in the forebrain PSD fraction obtained by the n-octyl glucopyranoside method. I also demonstrate that classical full-length dystrophin is consistently enriched in forebrain PSDs isolated by either detergent method. Given that neither detergent affects the enrichment of the full-length dystrophin isoforms in the PSD fractions, I suggest classical full-length dystrophin (Culligan *et al*, 2002) and delta full-length dystrophin are both integral proteins of the PSD apparatus of the forebrain. The negligible amount of classical full-length dystrophin in the cell soluble fraction of the forebrain (figure 3.2.3.3) is in agreement with this result. However, the relative enrichment of delta full-length dystrophin in the cell soluble fraction when compared to the PSD fraction (figure 3.2.3.4) does not support the suggestion that delta full-length dystrophin may be an integral PSD protein. What is more, dDp427 exhibits highest enrichment in the forebrain microsomal fraction, whilst it is only moderately enriched in the forebrain PSD fraction. In contrast, cDp427 exhibits highest enrichment in the PSD fraction. Thus, the results clearly suggest that classical full-length dystrophin is an integral PSD component, whereas this may not be the case for delta full-length dystrophin. In chapter 4 I have used intact neurons in order to determine the exact localization of delta dystrophin within the cell, and determined whether or not dDp427 is an integral protein of the PSD.

Mental impairment occurs in one third of DMD patients and is said to be due to a mutation of the DMD gene (Barbujani *et al*, 1990; Mehler *et al*, 2000; Blake *et al*, 2002; Anderson et al, 2002; Nowak *et al*, 2004) (chapter 1). Studies to date suggest that the CNS pathology in DMD patients is due to abnormal organization of the classical full-length dystrophin protein at selectively localized GABAergic inhibitory synapses, which in turn lead to faulty transmission with impaired cognitive impairments in young boys (Albrecht *et al*, 2002). The fact that delta full-length dystrophin is also a DMD derived protein and it is also expressed in neurons of the forebrain and cerebellum (figure 3.2.4.2), suggests a potentially alternative route by which a mutated DMD gene may contribute to the mild mental retardation observed in DMD boys. What is more, given that classical dystrophin-containing DPC complexes exclusively localize at GABAergic synapses (Brunig *et al*, 2002), whilst according to this chapter, delta dystrophin-containing DPC complexes are likely to localize more widely, and possibly including at non-GABAergic synapses, the CNS pathology may not only originate from GABAergic synapses, but non-GABAergic synapses and other parts of the neurone as well. The formation of novel delta dystrophin containing DPC complexes outside the PSD and within non-GABAergic synapses suggests that when the DMD gene is mutated it would alter the organization of delta dystrophin and associated proteins at these sites which, together with the mutated classical dystrophin isoform at GABAergic synapses, would altogether contribute to the CNS pathologies of DMD patients.

The shorter classical dystrophin isoforms identified, which include cDp140, cDp116 and cDp71, are only moderately enriched in the PSD of the forebrain (figure 3.2.3.3), and according to various publications, they are not considered PSD proteins, but have been shown to locate in perivascular astrocytes (Lidov *et al*, 1990, Lidov *et al*, 1995, Lidov *et al*, 1996), peripheral nerve (Lidov *et al*, 1995) and glial cells (Mehler *et al*, 2000), respectively. PSDs are known to absorb proteins of non-neuronal origin, examples of non-neuronal proteins absorbed in PSDs include α-dystrobrevin (Blake *et al*, 1999), and glial fibrillary acidic protein (Matus *et al*, 1980), which are clearly enriched in the PSD fraction of immunoblots, but in vivo they localize elsewhere. This may also be the case for cDp140, cDp116 and cDp71, as all three are known to locate outside neurons. However, it is also plausible that these classical dystrophin isoforms are genuine PSD components. Therefore, a

more detailed study is required in order to establish whether cDp140, cDp116 and cDp71 are part of another cellular compartment or cell. This is in part because the overexposure of the western blot caused the lower delta and classical dystrophin bands to be saturated and therefore not give a linear response in terms of comparing enrichments.

In conclusion, the expression of classical and delta dystrophin exhibit different regional and subcellular distribution in forebrain and cerebellum. What is more, classical full-length dystrophin exhibits highest enrichment in PSDs of the cerebellum compared to PSDs of the forebrain, and given the abundance of GABAergic synapses available in the cerebellum (Leto *et al*, 2008), is consistent with classical full-length dystrophin localizing at the PSD of inhibitory synapses. For delta full-length dystrophin, the situation is totally different, as dDp427 shows much lower expression in cerebellum compared to forebrain PSDs, suggesting it may be expressed by non-GABAergic synapses. Immunocytochemical studies (see chapter 4) are necessary to confirm this. Given that dDp427 appears to localize in non-GABAergic synapses (figure 3.2.4.2), whilst cDp427 and associated DPC components exclusively localize at GABAergic synapses (Brunig *et al*, 2002), it suggests that dDp427 forms novel DPC complexes plausibly at non-GABAergic synapses, but also more widely within neurons (see below). These complexes may well have a different molecular composition and function when compared to classical dystrophin-containing DPC complexes. Contrary to classical full-length dystrophin, I demonstrate that delta full-length dystrophin distribution in the forebrain is not only enriched in the PSD fraction, but exhibits highest enrichment in the microsomal fraction, suggesting delta full-length dystrophin is more widely distributed when compared to classical full-length dystrophin. Thus, delta full-length dystrophin may form complexes of different compositions outside the PSD, as well as in PSD structures, and indeed may have different functional roles in the CNS. In conclusion, I suggest that delta full-length dystrophin may not be able to replace classical dystrophin in the formation of novel delta DPC-like complexes at forebrain and cerebellum PSDs of inhibitory synapses, instead, it is likely to form different protein complexes with a different molecular composition, localization and function(s), when compared to classical full-length dystrophin-containing DPC complexes. Obviously it

would be expected that some components of classical and delta DPC complexes would be common to both.

The next chapter utilizes cortical neuronal cultures in order to investigate the subcellular distribution of delta dystrophin in relation to classical dystrophin and other well-established DPC components, in order to establish its function and precise localization in the cell.

Chapter 4:

4.0 Delta dystrophin does not replace classical dystrophin at GABAergic synapses to form novel delta dystrophin-containing DPC complexes.

4.1 Introduction

The biochemical studies carried out in chapter 3 show classical and delta full-length dystrophin exhibit distinct patterns of localization. This is because classical full-length dystrophin is exclusively enriched in the PSD fraction (Chapter 3, figure 3.2.3.3), whereas delta dystrophin is found to be more highly enriched in microsomes with only mild enrichment in the PSD fraction (Chapter 3, figure 3.2.3.4). It is this difference in subcellular localization coupled with the fact that they (classical and delta) both have the same protein binding motifs that suggest they form distinct sets of DPC complexes with different patterns of distribution. The difference in regional localization exhibited by classical and delta dystrophin in cerebellum versus forebrain (Chapter 3, figure 3.2.4.1 and 3.2.4.2) also supports this. In this chapter I therefore established immunocytochemically the cellular and subcellular localization of delta dystrophin and compared it with classical dystrophin and other DPC components that are known to localize at PSDs of GABAergic synapses. These studies were carried out to determine whether delta dystrophin may replace classical dystrophin in forming DPC complexes at PSDs of GABAergic synapses, or whether delta dystrophin indeed forms distinct sets of DPCs with different patterns of distribution, or both.

I used cortical neurons for the *in vivo* studies for two reasons. Firstly, various reports on cortical neurons of DMD brains have shown that these neurons exhibit disordered architecture, altered neuronal migration, abnormal neuronal orientation with attenuated terminal dendritic arbors (Mehler *et al*, 2000) and decreased cortical excitation. Hence cortical neurons are implicated in DMD brain disorders.

Secondly, the biochemical studies presented in chapter 3 revealed that delta dystrophin is more highly expressed in the forebrain, when compared to the cerebellum, hence the focus on cortical neurons. To confirm whether delta dystrophin is a PSD protein and whether it may replace classical dystrophin to form novel delta DPC complexes at the PSD of cortical inhibitory synapses, mature cortical neuronal cultures were used to co-label delta dystrophin with a number of synaptic markers including GAD65, $GABA_AR$, PSD-95 and NMDA receptors. This allowed me to determine whether delta dystrophin is synaptic and precisely which type of synapse it is found in, because molecularly specialized clusters of GAD65 and $GABA_AR$ are indicative of GABAergic terminals (Rao *et al*, 1998; Brunig *et al*, 2002), whereas NMDA receptors and PSD-95 are indicative of glutamatergic terminals (Craig *et al*, 1994; Hunt *et al*, 1996; Rao *et al*, 1998). Furthermore, I also co-labelled β-dystroglycan, the crucial core protein of the DPC complex at the PSDs of inhibitory synapses (Brunig *et al*, 2002; Pilgram *et al*, 2009; Waite *et al*, 2009), with delta dystrophin, in order to determine whether the two proteins co-localize, similarly to the well-established interaction and co-localization between classical dystrophin and β-dystroglycan (Ervasti *et al*, 1991; Grady *et al*, 2000; Brunig *et al*, 2002). I also co-labelled classical dystrophin with delta dystrophin, in order to directly compare the localization of the two isoforms and therefore establish the similiarities and/or differences in terms of localization exhibited by the two isoforms within these cultures. Concomitant with these studies, the significance of classical exon 78 and delta exon 78 (the only sequences that distinguish classical from delta dystrophin) was examined in more detail, as the data presented in this thesis suggests that there is a different subcellular localization of classical and delta dystrophin. It is plausible that delta exon 78 encodes a trafficking signal. I therefore transfected neurons using pEGFP-N3 vectors containing either classical or delta exon 78, in order to determine whether delta exon 78 alone may encode a trafficking signal that would explain the differences in subcellular distribution observed in the biochemical studies presented in chapter 3.

4.2 Results:

4.2.1 Comparison of delta dystrophin with PSD-95 in cortical neurons

In order to study the subcellular distribution of delta dystrophin within neurons of the forebrain, cortical neuronal cultures were prepared. These were grown for two weeks, because at this time point 92-95% of the neurons are reported to contain the highest density of spiny dendrites, a characteristic feature of in situ neurones (Papa *et al*, 1995; O'Brien *et al*, 1997; Rao *et al*, 1998). Once neurons have reached this state of maturity, cortical neurons were then fixed with PFA prior to immunolabeling. In order to determine whether delta dystrophin is present in the postsynaptic density (PSD), I began by testing whether delta dystrophin is present at PSDs of excitatory synapses. In figure 4.2.1, 14 div neurons were co-labelled for delta dystrophin and PSD-95 (postsynaptic density protein 95), a major component of PSDs of excitatory synapses (Hunt *et al*, 1996; Rao *et al*, 1998). Anti-delta dystrophin antibody is directed against delta exon 78, hence, recognising all four delta dystrophin isoforms (see chapter 1, figure 1.1.2.1). Figure 4.2.1 shows that neurons labelled with PSD-95 exhibited prominent punctate staining in dendritic spines (A1, 3), similar to that reported by Kornau *et al* (1995) and Rao *et al* (1998). Unlike PSD-95, delta dystrophin exhibited diffuse staining (A1, 2) throughout the dendrites of neurons containing PSD-95, but never co-localized with PSD-95 (white arrow, B1-3 and C1-3), hence suggesting delta dystrophin is not part of the postsynaptic density of excitatory synapses labelled with PSD-95. What is more, PSD-95 staining was often very close to the delta dystrophin stained processes (white arrow, C1-3), suggesting that these spines may originate from the delta dystrophin stained dendrites, but the delta dystrophin does not extend into the PSD. By comparing the pattern of PSD-95 staining with that of delta dystrophin (figure 4.2.1), I also observed that PSD-95 clusters did not stain all processes containing delta dystrophin (grey arrow, C1-3). In contrast, delta dystrophin stained all dendrites containing PSD-95 staining (A-C). In conclusion, delta dystrophin staining is more widely distributed than PSD-95 staining, and it does not localize at PSDs of excitatory glutamatergic synapses.

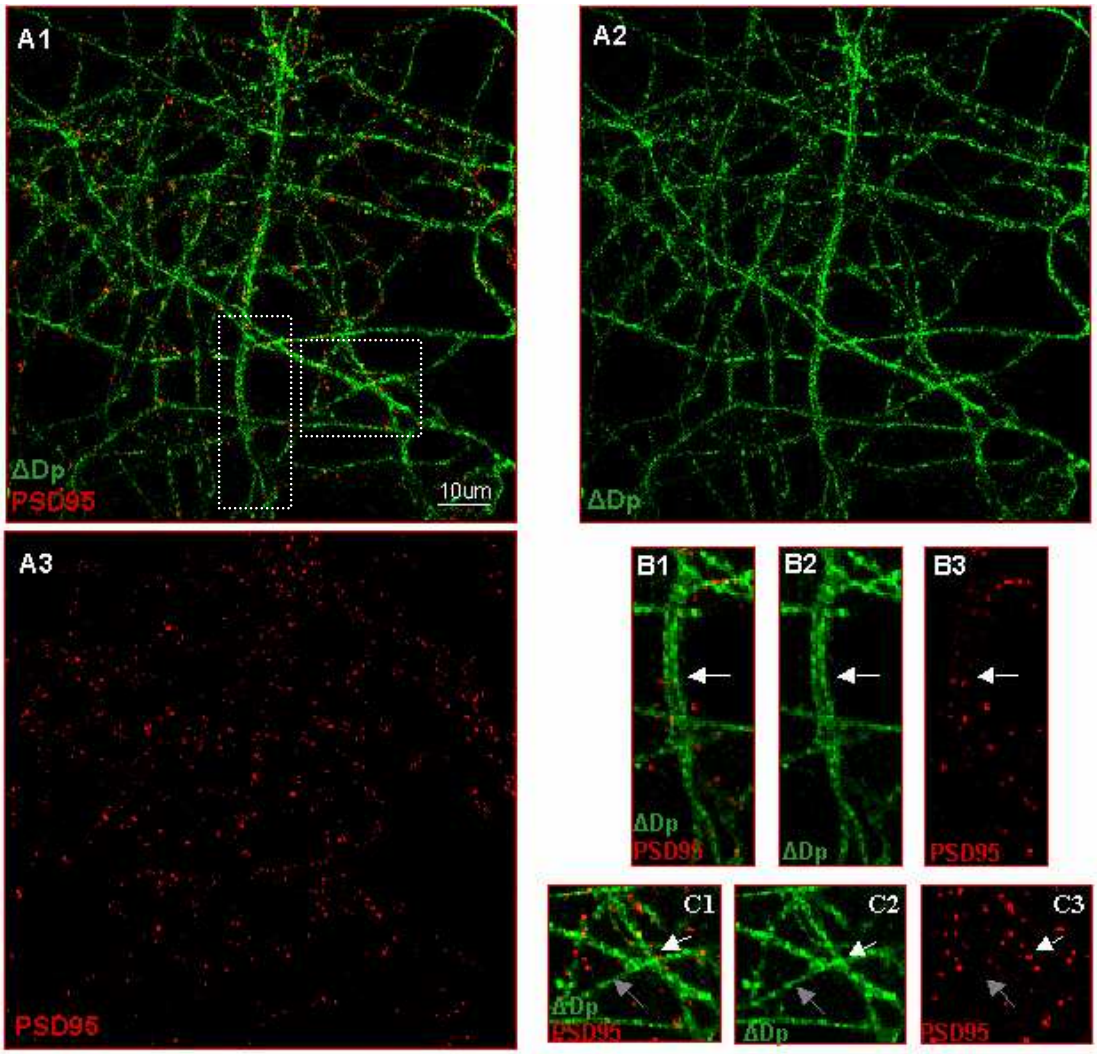

Figure 4.2.1: Comparison of delta dystrophin with PSD-95.

Rat cortical neurons were fixed at 2 weeks in culture and immunostained for delta dystrophin and PSD-95 (a marker for the PSD of excitatory synapses). Boxes show areas expanded in B and C. Neurons labelled with PSD-95 exhibited prominent punctate staining in dendritic spines (A3, B3, C3) whereas delta dystrophin exhibited diffuse staining throughout the dendrites labelled with PSD-95 (A1; white arrow, B1-3; white arrow, C1-3). The two proteins never co-localized (white arrow, B1; white arrow, C1). Delta dystrophin stained all dendrites labelled with PSD-95 (A1-3), hence it is present in neurons expressing this marker. In contrast, PSD-95 clusters did not stain all processes containing delta dystrophin (grey arrow, C1-3), hence delta dystrophin is also present in a wider set of neurons that do not express PSD-95. Given that delta dystrophin does not co-localize with PSD-95, delta dystrophin is likely absent from PSDs of glutamatergic synapses. Delta dystrophin (green), PSD-95 (red). Scale bar 10μm.

4.2.2 Comparison of delta dystrophin with the NMDA R in cortical neurons

In order to conclude with more confidence that delta dystrophin is absent from the PSD of excitatory synapses, a second marker for the postsynaptic density of glutamatergic synapses, namely the NMDA receptor (Rao *et al*, 1998), was utilised. Figure 4.2.2 shows 14 div cortical neurons co-labelled with delta dystrophin and NMDA receptor. The anti-NMDA receptor antibody recognised the NR1 subunit of the NMDA receptor. NR1 exhibited punctate staining, generally in a clustered form (arrowhead, D3), and restricted to the somadendritic domain and the distal tips of dendrites (A1-3). Contrary to NR1 staining, delta dystrophin exhibited diffuse staining throughout the cell body and along proximal dendrites where NR1 staining was also present (A1-3), but they never co-localized (arrowhead, B1-3; arrow, C1-3; arrowhead, D1-3;). What is more, all proximal dendrites labelled with NR1 contained delta dystrophin (arrow, C1-3), but not all processes containing delta dystrophin were stained with NR1 (arrows, D1-3), suggesting delta dystrophin is more widely distributed compared to NR1 staining. On rare occasions, digital overlap is observed and this is due to the density of cultures at this point of the coverslip. Taken together, figures 4.2.1 and 4.2.2 conclusively show that delta dystrophin is not found at the PSD of excitatory glutamatergic synapses. However, it is present along dendrites that express these markers. It is also present in a wider set of neurons, as it is present along the dendrites of neurons that do not express either of these (NR1 and PSD-95) markers.

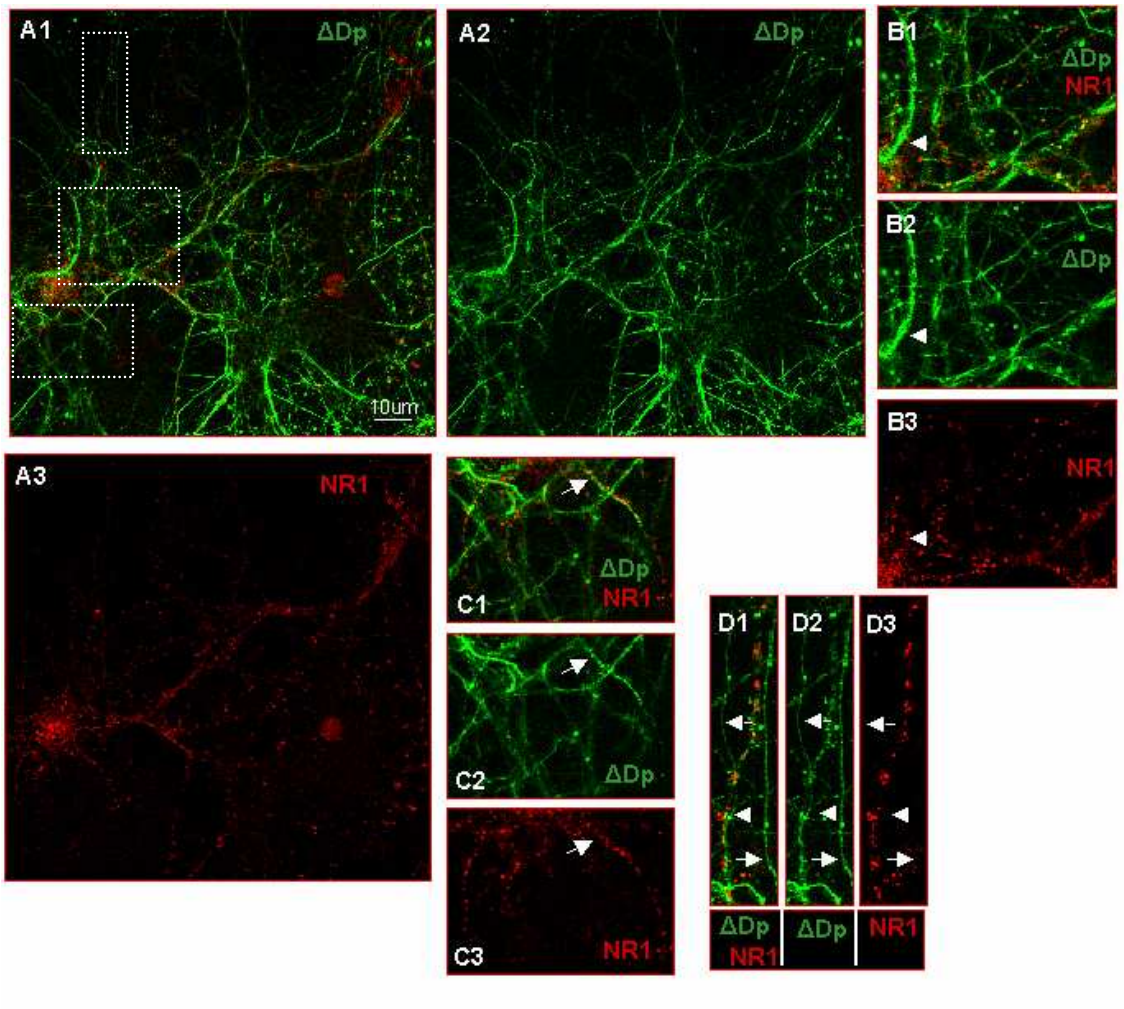

Figure 4.2.2: Comparison of delta dystrophin with the NMDA receptor.

Rat cortical neurons were fixed at 2 weeks in culture and immunostained for delta dystrophin and NMDA receptor NR1 subunit (a marker for the PSD of excitatory synapses). Boxes show areas expanded in B-D. NR1 exhibited punctate staining (A3), generally in a clustered form (arrowhead, D3), and restricted to the somadendritic domain and the distal tips of dendrites (A3). Contrary to NR1 staining, delta dystrophin exhibited diffuse staining throughout the cell body and along proximal dendrites (A2) where NR1 staining was also present (arrowhead, B1-3), but they never co-localized (arrowhead, B1-3; arrow, C1-3; arrowhead, D1-3). All proximal dendrites labelled with NR1 contained delta dystrophin (A1), suggesting delta dystrophin is expressed in neurons containing NR1. In contrast, not all processes containing delta dystrophin were stained with NR1 (arrows, D1-3), suggesting delta dystrophin is also present in a wider set of neurons that do not express NR1. Given that NR1 and delta dystrophin do not co-localize, delta dystrophin is not part of PSD structures of excitatory glutamatergic synapses. Delta dystrophin (green), NR1 (red). Scale bar 10μm.

4.2.3 Comparison of delta dystrophin with $GABA_A$ R in cortical neurons

Having established delta dystrophin is not a PSD component of excitatory synapses, I next investigated whether delta dystrophin is present at the PSD of inhibitory synapses. The $GABA_A$ receptor is a marker of the PSD of GABAergic synapses (Craig *et al*, 1994; Rao *et al*, 1998; Brunig *et al*, 2002) and is known to co-localize with classical dystrophin and other DPC components at the PSD of inhibitory synapses (Brunig *et al*, 2002; Vithlani *et al*, 2009). Therefore, fixed cortical neurons were co-labelled with antibodies specific for the essential α2 subunits of the $GABA_A$ receptor and for delta dystrophin (figure 4.2.3), to determine whether delta dystrophin localized at GABAergic PSDs. At 14 days in culture, staining for the $GABA_A$ R α2 subunit revealed a highly concentrated immunoreactivity distributed on the dendrites and a weaker staining on the soma at presumptive PSD structures of GABAergic synapses (A1, 3). On the contrary, delta dystrophin exhibited diffuse staining throughout the same soma and dendrites expressing $GABA_A$ R (A1, 2), but once again it does not co-localize with $GABA_A$ R (arrow, B1-3; arrow, C1-3). What is more, delta dystrophin is also present in processes where $GABA_A$ R staining is absent (arrow, A1-3), therefore suggesting delta dystrophin is more widely distributed and is present in neurons which do not express $GABA_A$R. An isolated process shows extensive $GABA_A$ R and delta dystrophin labelling (arrowhead, A1-3), these stretches are complementary and do not co-localize. In conclusion, delta dystrophin is not found in the PSD of GABAergic synapses although it is present in dendrites of neurons that express $GABA_A$ R. Furthermore, it is more widely distributed in neuronal subtypes that do not express $GABA_A$ R.

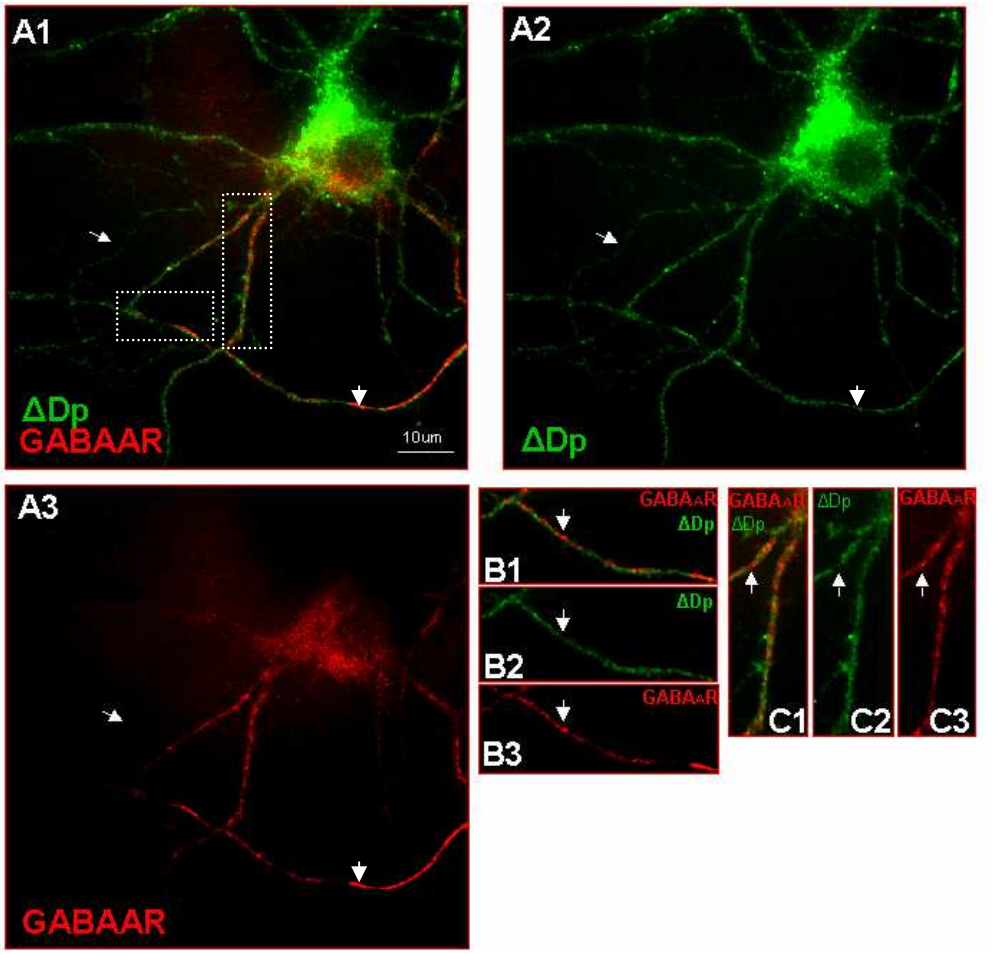

Figure 4.2.3: Comparison of delta dystrophin with $GABA_A$ R.

Rat cortical neurons were fixed at 2 weeks in culture and immunostained for delta dystrophin and $GABA_A$ receptor α2 subunit (a marker for the PSD of inhibitory synapses). Boxes show areas expanded in B and C. $GABA_A$ R α2 subunit revealed a highly concentrated immunoreactivity distributed on the dendrites (arrowhead, A1-3; arrow, B1-3; arrow, C1-3), and a weaker punctate staining on the soma at presumptive PSD structures of GABAergic synapses (A1, 3). On the contrary, delta dystrophin exhibited diffuse staining throughout the same soma and dendrites stained by $GABA_A$ R (A1-3), but the two proteins never co-localized (arrow, B1-3; arrow, C1-3), hence delta dystrophin is present in neurons expressing $GABA_A$ R, but is not a PSD component of these inhibitory synapses. What is more, delta dystrophin is present in all dendrites labelled with $GABA_A$ R (A-C), whereas $GABA_A$ R is not found in all processes containing delta dystrophin (arrow A1-3), suggesting delta dystrophin is more widely distributed in other neuronal subtypes that do not express $GABA_A$ R. Delta dystrophin (green), $GABA_A$ R (red). Scale bar 10μm.

4.2.4 Comparison of delta dystrophin with GAD 65 in cortical neurons

Given that delta dystrophin is not found at the postsynaptic apparatus of both GABAergic and glutamatergic synapses, I next determined whether delta dystrophin might be a component of the presynaptic apparatus in cortical neurons. In figure 4.2.4, 14 div neurons were fixed and co-labelled for delta dystrophin and GAD 65, a key enzyme for GABA synthesis and a presynaptic marker of GABAergic synapses (Rao *et al*, 1998; Brunig *et al*, 2002). GAD 65 exhibited punctate staining at the periphery of the soma and proximal dendrites (A1-3), suggesting a presynaptic localization within presumptive GABAergic terminals. On the other hand, delta dystrophin exhibited diffuse staining throughout the soma and neuronal processes (A1-2), as shown previously. Therefore, despite some digital overlap, the two proteins are differently distributed in the neuron (arrow, B1-3), suggesting delta dystrophin is not part of the presynaptic nerve terminals of GABAergic synapses. What is more, delta dystrophin always localized in dendrites innervated by GAD 65-containing terminals (A1-3), whereas the latter did not innervate all processes containing delta dystrophin (arrow, A1-3). In conclusion, delta dystrophin is not found in the presynapse of GABAergic synapses, although it is present in neurons that receive GABAergic innervation. Furthermore, delta dystrophin is present in a range of neuronal subtypes that do not receive GABAergic innervation. It is not uncommon to find random co-localization between two proteins that in fact do not co-localize. For instance, Rao *et al* (2000) also reported some co-localization between PSD-95 and GAD 65, although it is well established that the two proteins are part of two very distinct sets of synapses, excitatory and inhibitory synapses, respectively. Therefore, in the next study, the significance of random co-localization observed between delta dystrophin and the presynaptic marker was examined in more detail.

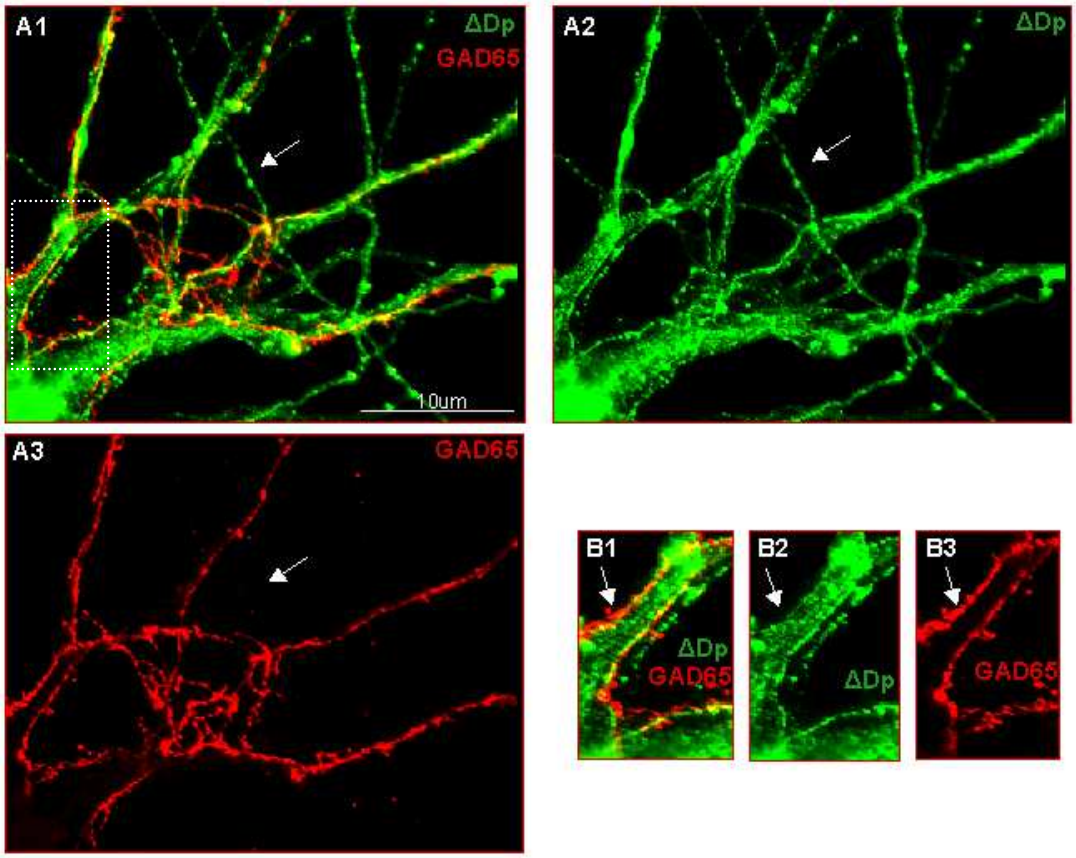

Figure 4.2.4: Comparison of delta dystrophin with GAD 65

Rat cortical neurons were fixed at 2 weeks in culture and immunostained for delta dystrophin and GAD 65 (a marker for the pre-synapse of inhibitory synapses). The box shows the area expanded in B. Delta dystrophin exhibited diffuse staining along the soma and various processes of the neuron (A1, 2). In contrast to a diffuse and internal staining exhibited by delta dystrophin, GAD 65 labelled the periphery (A1, 3) of the soma and processes labelled with delta dystrophin (A1-3). This suggests GAD 65 is at the presynapse of GABAergic terminals that innervate the soma and processes labelled with delta dystrophin, thus sending inhibitory signals to delta dystrophin-containing processes. Despite some digital overlap, the two proteins do not co-localize (arrow, B1-3), hence, delta dystrophin is not a presynaptic protein of inhibitory synapses. What is more, delta dystrophin is found in all dendrites innervated by GAD 65-labelled GABAergic nerve terminals (A1-3), whereas GAD 65-labelled GABAergic nerve terminals did not label the surface of all processes containing delta dystrophin (arrow, A1-3), suggesting delta dystrophin is present in a range of neuronal subtypes when compared to neurons receiving GAD 65-labelled innervation. Delta dystrophin (green), GAD 65 (red). Scale bar 10μm.

4.2.5 Comparison of delta dystrophin with synaptophysin in cortical neurons

To determine whether delta dystrophin is absent from excitatory and inhibitory presynaptic terminals, fixed neurons were co-labelled for delta dystrophin and synaptophysin (figure 4.2.5), a synaptic vesicle protein and a marker of all presynaptic terminals found in the brain (Leimer *et al*, 1996; Evans *et al*, 2005). In figure 4.2.5, synaptophysin exhibited a punctate staining located along the periphery of the neuron, suggesting a presynaptic localization at presumptive excitatory and inhibitory terminals (A1, 3). In contrast to this staining pattern, delta dystrophin exhibited a diffuse staining pattern throughout the soma and neuronal processes (A1, 2) which did not co-localize with the presynaptic staining pattern exhibited by synaptophysin (arrow, B1-3; arrow, C1-3), suggesting delta dystrophin is absent from the presynapse of excitatory and inhibitory terminals, in agreement with figures 4.2.3 and 4.2.4. What is more, excitatory and inhibitory axon terminals containing synaptophysin always innervated dendrites containing delta dystrophin (A1-3), whereas not all processes containing delta dystrophin were innervated by nerve terminals labelled with synaptophysin (arrow, A1-3). Thus, delta dystrophin is localized in dendrites innervated by excitatory and inhibitory terminals. What is more, excitatory and inhibitory innervation does not occur along the axon, therefore, the distribution of delta dystrophin along processes that do not receive innervation by nerve terminals labelled with synaptophysin suggests delta dystrophin may localize in axons. This was further examined in subsequent experiments. Altogether, figures 4.2.1-4.2.5 show that delta dystrophin is widely distributed within a neuron, but is absent from pre and postsynapses of inhibitory and excitatory neurons, suggesting delta dystrophin is not part of the synaptic structure. What is more, the western blot data in chapter 3, in agreement with this immunocytochemical data, also highlighted delta full-length dystrophin as exhibiting a different subcellular distribution when compared to the highly PSD enriched classical full-length dystrophin protein. Given that DPC complexes in neurons localize at inhibitory postsynaptic terminals only (Brunig *et al*, 2002), and given that the data up to this point in this thesis suggests delta dystrophin is not a synaptic protein, I next determined whether or not DPC complexes existed in these cultures, and I determined the exact localization of delta dystrophin within these

cortical neuronal cultures and in relation to other well established DPC components, notably β-dystroglycan.

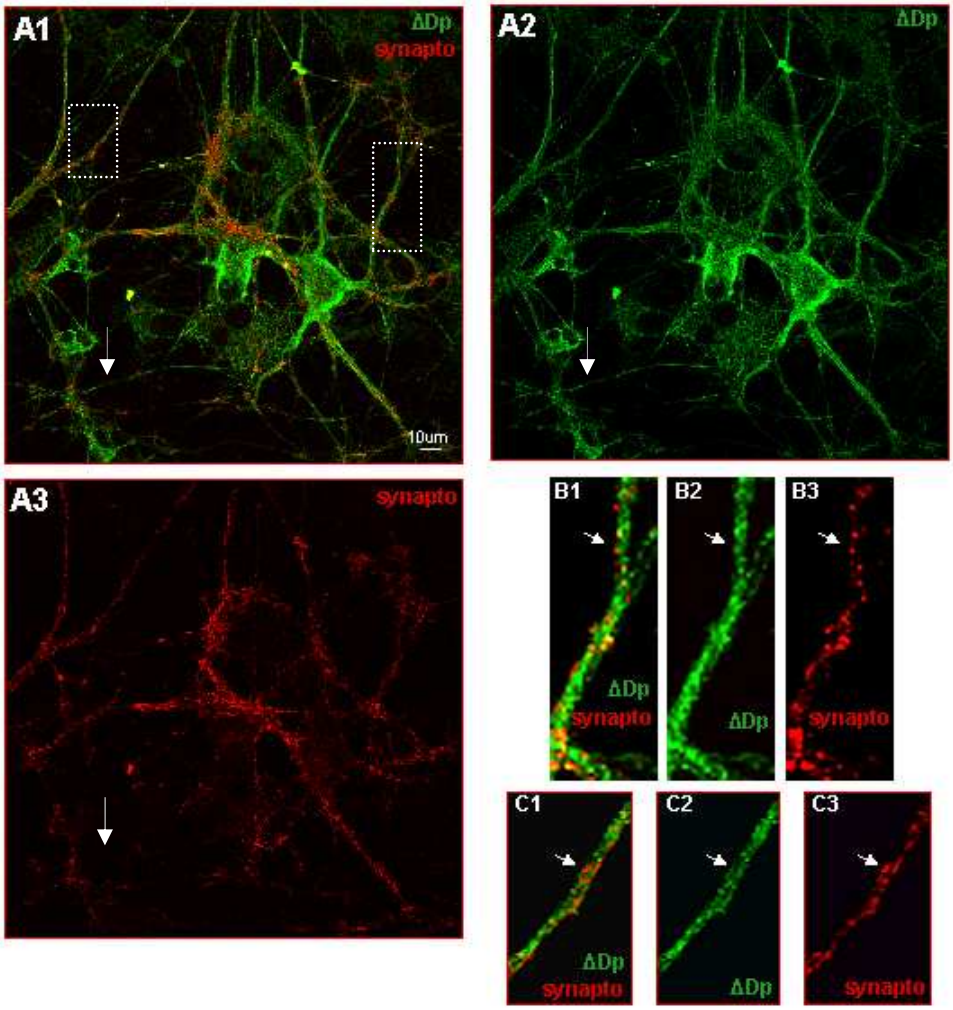

Figure 4.2.5: Comparison of delta dystrophin with synaptophysin.

Rat cortical neurons were fixed at 2 weeks in culture and immunostained for delta dystrophin and synaptophysin (a vesicle protein and marker of either excitatory or inhibitory presynapses). Boxes show the areas expanded in B and C. Delta dystrophin exhibited diffuse staining along the soma and various processes of the neuron (A1, 2). In contrast, synaptophysin exhibited punctate staining along the periphery of the neurons (A1, 3), suggesting a presynaptic localization at presumptive excitatory and inhibitory terminals. Although delta dystrophin labelled dendrites innervated by synaptophysin, the two proteins did not co-localize (arrow, B1-3; arrow, C1-3), suggesting delta dystrophin is absent from the presynapse of excitatory and inhibitory terminals. What is more, delta dystrophin labelled all dendrites innervated by synaptophysin-containing nerve terminals, but not all synaptophysin-containing nerve terminals synapsed onto processes labelled with delta dystrophin, suggesting delta dystrophin is more widely distributed within a neuron. Delta dystrophin (green), synaptophysin (red). Scale bar 10μm.

4.2.6 Comparison of delta dystrophin with β-dystroglycan in cortical neurons

In order to confirm classical dystrophin-containing DPC complexes existed in these cultures, and demonstrate delta dystrophin may not be part of these DPC complexes, fixed neurons were co-labelled for delta dystrophin and β-dystroglycan (figure 4.2.6), a crucial core component of the classical dystrophin-containing DPC complex at PSDs in brain neurons (Brunig *et al*, 2002; Pilgram *et al*, 2009; Waite *et al*, 2009). In figure 4.2.6, β-dystroglycan was found as brightly labelled puncta arranged in lines running over cell bodies and dendrites only (A1, 3), in agreement with the published data (Brunig *et al*, 2002). In contrast, delta dystrophin exhibited diffuse staining along the soma and proximal dendrites stained by β-dystroglycan (A1, 2), but they never co-localized (white arrow, B1-3; white arrow, C1-3). What is more, delta dystrophin was found in all dendrites labelled with β-dystroglycan (A1-3), whereas β-dystroglycan did not label all processes containing delta dystrophin (grey arrow, B1-3; grey arrow, D1-3). Thus, in agreement with our previous studies (figures 4.2.1-4.2.5), delta dystrophin is widely distributed within a neuron, but also between different neuronal subtypes. Furthermore, it does not co-localize with the postsynaptic DPC component β-dystroglycan, and this is supported by earlier results (figures 4.2.1-4.2.5) demonstrating delta dystrophin is an extra-synaptic protein. The lack of co-localization between delta dystrophin and β-dystroglycan, a classical dystrophin-containing DPC component, suggests that delta dystrophin is likely to form novel DPC complexes whose molecular composition, as well as subcellular distribution, differs to classical dystrophin-containing complexes. Therefore in the next study, I tested whether classical dystrophin was also differently distributed when compared to delta dystrophin (figure 4.2.7), similarly to what has been observed with delta dystrophin and the classical dystrophin-binding protein, namely β-dystroglycan (figure 4.2.6).

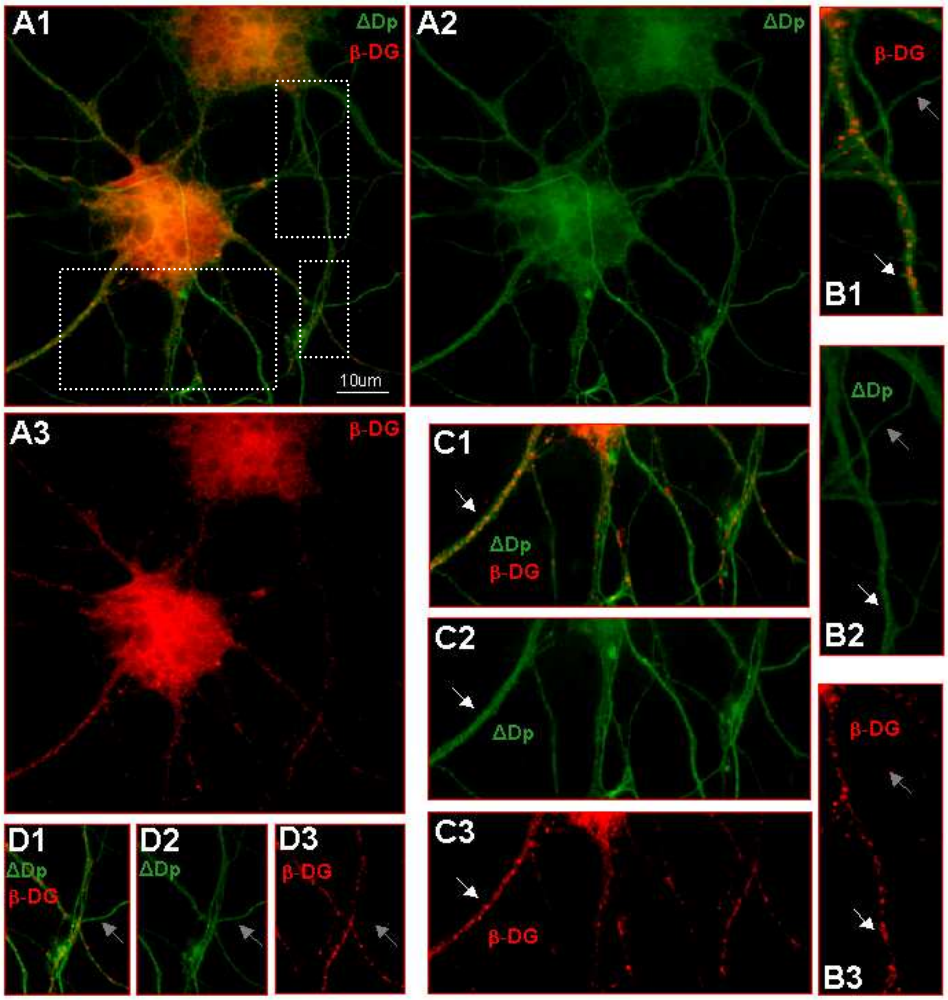

Figure 4.2.6: Comparison of delta dystrophin with β-dystroglycan

Rat cortical neurons were fixed at 2 weeks in culture and immunostained for delta dystrophin and β-dystroglycaṇ (a DPC component at the PSD of inhibitory synapses). Boxes show the areas expanded in B-D. β-dystroglycan was found as brightly labelled puncta arranged in lines running over cell bodies and dendrites (A3). In contrast, although delta dystrophin was also localized within the same soma and proximal dendrites labelled by β-dystroglycan (A1-3), the staining was diffuse and the two proteins did not co-localize (white arrow, B1-3; white arrow, C1-3). This suggests delta dystrophin may not associate with β-dystroglycan to form novel delta DPC-like complexes at inhibitory postsynaptic structures containing β-dystroglycan. What is more, delta dystrophin was found in all dendrites expressing β-dystroglycan (A1), whereas β-dystroglycan was not expressed in all processes containing delta dystrophin (grey arrow, B1-3; grey arrow, D1-3) suggesting delta dystrophin is widely distributed within a neuron, but also between different neuronal subtypes. Delta dystrophin (green), β-dystroglycan (red). Scale bar 10μm.

4.2.7 Comparison of delta dystrophin with classical dystrophin in cortical neurons

14 div neurons were fixed and co-labelled for delta dystrophin and classical dystrophin (figure 4.2.7), a component of the classical dystrophin-containing DPC complexes found exclusively at inhibitory postsynapses (Knuesel *et al*, 1999; Knuesel *et al*, 2001; Brunig *et al*, 2002). Similarly to β-dystroglycan (figure 4.2.6), classical dystrophin was found as brightly labelled puncta arranged in lines running over cell bodies and dendrites (A1, 3), which was expected as the two proteins are known to associate and participate in the formation of classical dystrophin-containing DPC complexes exclusively localized at PSD structures of GABAergic synapses in the brain (Brunig *et al*, 2002; Pilgram *et al*, 2009; Waite *et al*, 2009; Vithlani *et al*, 2009). The profile of immunostaining of classical dystrophin is identical to that reported by Brunig *et al* (2002). The punctate labelling of classical dystrophin (A3; white arrow, B3; white arrow, C3) was different from the diffuse staining exhibited by delta dystrophin throughout the soma and neural processes (A1, 2). Similarly with β-dystroglycan, classical dystrophin did not co-localize with delta dystrophin (white arrow, B1-3; white arrow, C1-3). What is more, delta dystrophin was always found in dendrites labelled with classical dystrophin (A1-3), whereas classical dystrophin did not always label processes stained by delta dystrophin (grey arrow, C1-3). In conclusion, these results suggest delta dystrophin is widely distributed within neurons expressing classical dystrophin, but also between different neuronal subtypes that do not express classical dystrophin. Furthermore, these results also suggest that delta and classical dystrophin exhibit different subcellular distributions in neurons, in agreement with the western blots presented in the preceding chapter (Chapter 3, figure 3.2.3.3, 3.2.3.4, 3.2.4.1, 3.2.4.2). Therefore, given that delta dystrophin does not co-localize with classical dystrophin (figure 4.2.7) and β-dystroglycan (figure 4.2.6) and the inhibitory PSD marker (figure 4.2.3), the results re-confirm delta dystrophin does not replace classical dystrophin to form novel DPC-like complexes at PSDs of inhibitory synapses. Instead, delta dystrophin is likely to form novel DPC-like complexes outside the PSD (figures 4.2.1-4.2.5) that have a different molecular composition (figure 4.2.6) and a different distribution (figure 4.2.6 and 4.2.7) to classical dystrophin-containing DPC complexes.

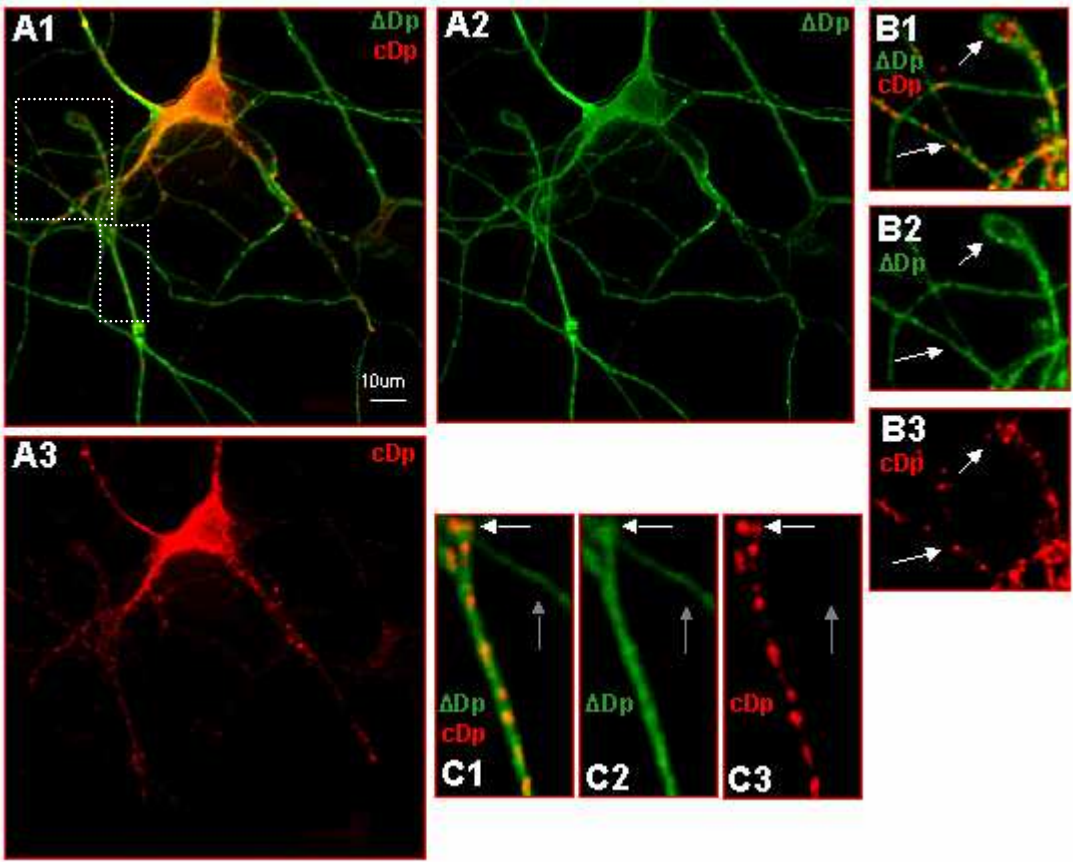

Figure 4.2.7: Comparison of delta dystrophin with classical dystrophin

Rat cortical neurons were fixed at 2 weeks in culture and immunostained for delta dystrophin and classical dystrophin (a marker for the DPC complex at the PSD of inhibitory synapses). Boxes show the areas expanded in B-C. Classical dystrophin was found as brightly labelled puncta arranged in lines running over the cell body and dendrites (A3; white arrow, B3; white arrow, C3). In contrast, although delta dystrophin was also localized within the same soma and dendrites labelled by classical dystrophin (A1-3), the staining of delta dystrophin was diffuse (white arrow, C1-2) and the two proteins did not co-localize (white arrow, B1-3; white arrow, C1-3). This suggests delta dystrophin is absent from the PSD of inhibitory synapses containing classical dystrophin and therefore may not replace classical dystrophin to form novel delta DPC-like complexes therein. What is more, classical dystrophin did not stain all processes containing delta dystrophin (grey arrow, C1-3), whereas delta dystrophin stained all dendrites labelled with classical dystrophin (A1-3). This suggests delta dystrophin is widely distributed within neurons expressing classical dystrophin, but also between different neuronal subtypes that do not express classical dystrophin. Delta dystrophin (green), classical dystrophin (red). Scale bar 10μm.

4.2.8 Comparison of delta dystrophin with rhodamine-phalloidin in cortical neurons

Our studies clearly indicate that delta dystrophin is involved in extra-synaptic functions. In order to determine a more precise localization of delta dystrophin within the cells, neurons were fixed and co-labelled for delta dystrophin and rhodamine-phalloidin (figure 4.2.8), a marker that labels filamentous actin (F-actin). F-actin underlies all of the neuron plasma membrane (Capani *et al*, 2001; Dickinson *et al*, 2004; Farah *et al*, 2008). This study was carried out because delta dystrophin, like classical dystrophin, contains an actin-binding domain. Classical dystrophin has been shown to utilise the C-terminal actin-binding domain in order to directly interact with F-actin (Hemmings I *et al*, 1992). I therefore determined whether delta dystrophin might also interact with F-actin via its C-terminal actin-binding domain, and therefore localize delta dystrophin to the submembrane domain. In figure 4.2.8, F-actin staining localized adjacent to the plasma membrane (A1, 3) and dendritic spines (arrows, B1, 3) of the entire neurone, as expected (Dickinson *et al*, 2004). Delta dystrophin exhibited a diffuse staining pattern throughout the neuronal processes stained by F-actin (A1-3), but never co-localized with F-actin (arrows, B1-3; arrow, C1-3). In fact, delta dystrophin staining was always distant from the filamentous marker underlying all of the neuron plasma membrane, and was restricted to the more central parts of these neuronal processes (A1; arrow, C1-3). What is more, delta dystrophin labelled all processes containing F-actin. Given that F-actin is localized adjacent to the peripheral membrane of the entire cell (Dickinson *et al*, 2004) and is present in all neurons, the results suggest that delta dystrophin is a widely distributed protein present in most, if not all, neuronal processes. This is in agreement with the wide distribution of delta dystrophin suggested by the previous results (figures 4.2.1-4.2.7). In conclusion, delta dystrophin does not co-localize with F-actin, and given that the localization of delta dystrophin appears to be more internal when compared to F-actin, it suggested delta dystrophin might co-localize with the microtubule-based cytoskeleton. I therefore determined whether delta dystrophin may co-localize with the microtubule-based cytoskeleton and whether such co-localization is restricted to axons, or dendrites, or to both these types of processes.

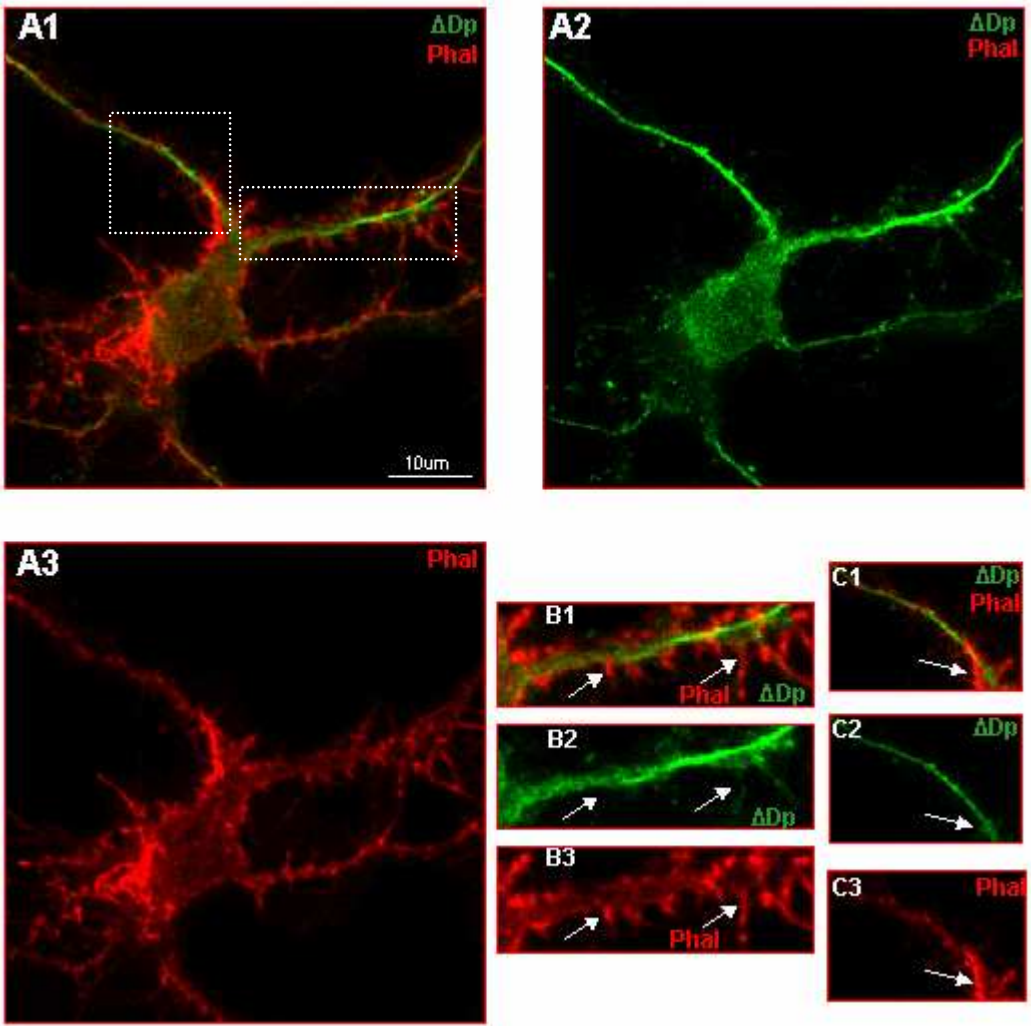

Figure 4.2.8: comparison of delta dystrophin with rhodamine-phalloidin

Rat cortical neurons were fixed at 2 weeks in culture and immunostained for delta dystrophin and rhodamine-phalloidin (a marker that labels F-actin found adjacent to the plasma membrane of neurons). Boxes show the areas expanded in B and C. F-actin stained dendritic spines (arrows, B1, 3) and stained beneath the plasma membrane (arrow, C1, 3) throughout the neurone (A3). Delta dystrophin also stained all the neuronal processes stained by F-actin (A1), but never co-localized with F-actin (arrows, B1-3; arrow, C1-3). This study suggests delta dystrophin is distant from the membrane of the neuron and is therefore localized at the more central part of neuronal processes. Delta dystrophin (green), rhodamine-phalloidin (red). Scale bar 10μm.

4.2.9 Delta dystrophin and MAP2 exhibit substantial co-localization in cortical neurons

In order to begin to establish a potential delta dystrophin-binding partner within the central part of neuronal processes, 14 div neurons were fixed and co-labelled for delta dystrophin and MAP2 (microtubule associated protein 2) (figure 4.2.9). This is because MAP2 is associated with the tubulin cytoskeleton and similarly to delta dystrophin, is found in the soma and in the central parts of dendrites. More precisely, MAP2 is a marker for neurons and is restricted to a sub population of dendrites and it is absent from the axon (Matus *et al*, 1981; Bloom *et al*, 1983; Rao *et al*, 1998; Farah *et al*, 2008). In figure 4.2.9, MAP2 was localized along the central part of a subpopulation of dendrites (white arrow, B1, 3) and was also found in the soma of the isolated neuron (A1, 3). Delta dystrophin exhibited diffuse staining within the soma (A1, 2) and along the central part of a subpopulation of dendrites (white arrow, B1, 2) where MAP2 was found. Strikingly the two proteins exhibited substantial co-localization (white arrow, B1-3). Given that MAP2 is a neuronal marker, the coexpression of delta dystrophin and MAP2 within the same cell confirms that delta dystrophin is a neuronally expressed protein. What is more, delta dystrophin also exhibited diffuse staining in processes where no MAP2 staining was found (grey arrow, B1-3), suggesting delta dystrophin is more widely distributed than MAP2. In the processes where no MAP2 staining was observed, delta dystrophin again exhibited diffuse staining along the central part of the processes (grey arrow, B1-3). Given that MAP2 is absent from axons and some dendrites, this result does not exclude the possibility that delta dystrophin might also be found in the central parts of the axons of neurons, in addition to the central parts of dendrites where no MAP2 staining is found. Immunocytochemical studies using axonal markers are required in order to verify this hypothesis. In conclusion, delta dystrophin is more widely distributed within a single neuron when compared to MAP2, in agreement with earlier results (figure 4.2.1-4.2.8). Furthermore, its substantial co-localization with MAP2 further suggested that delta dystrophin may co-localize with the microtubule-based cytoskeleton.

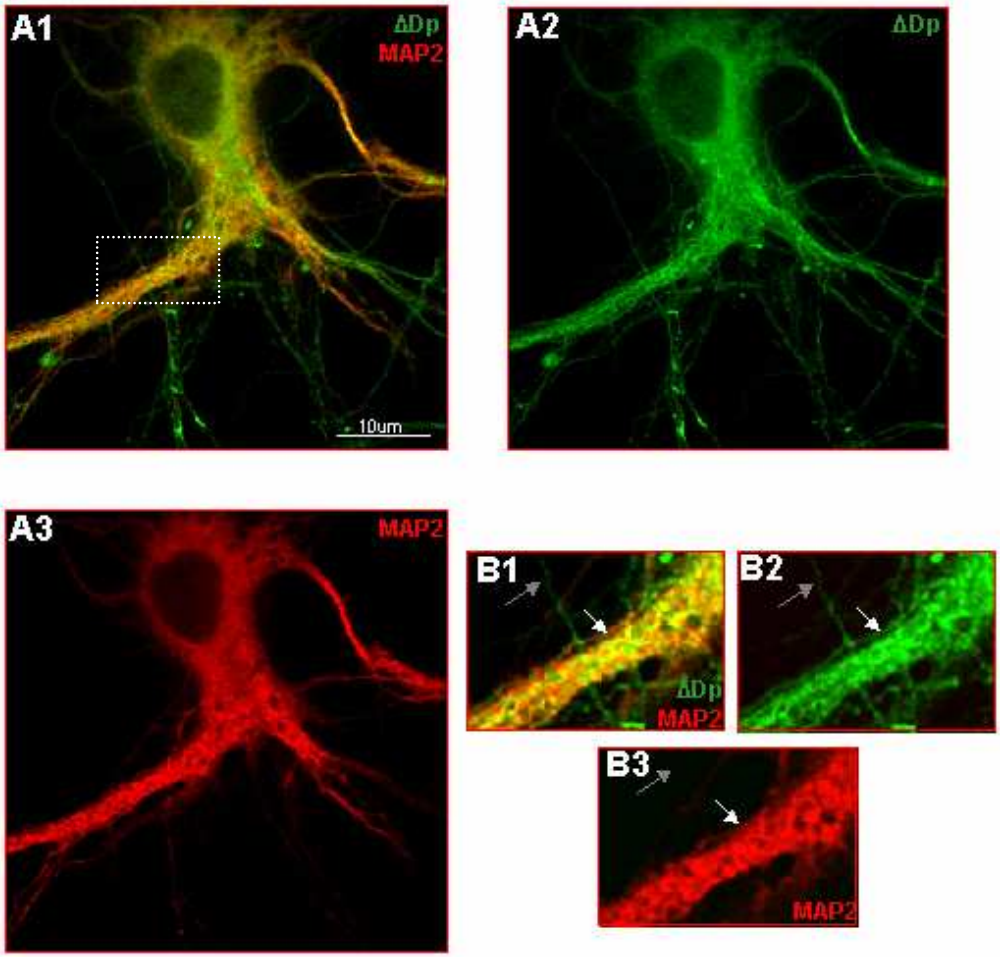

Figure 4.2.9: delta dystrophin exhibits substantial co-localization with MAP2

Rat cortical neurons were fixed at 2 weeks in culture and immunostained for delta dystrophin and MAP2 (a late dendritic marker, not found in axon). The box shows the area expanded in B. Delta dystrophin was found in the same subpopulation of dendrites labelled with MAP2 and there is evidence of substantial co-localization (white arrow, B1-3). What is more, although delta dystrophin stained and substantially co-localized with all dendritic structures containing MAP2 staining (white arrow, B1-3), not all processes stained with delta dystrophin were labelled with MAP2 (grey arrow, B1-3). Given that MAP2 is known to stain only a subpopulation of dendrites and it is absent from the axon, this result suggests delta dystrophin is more widely distributed, but always expressed, within the central parts of neuronal processes, when compared to MAP2. Given that MAP2 is a neuronal marker, this study also confirms delta dystrophin is expressed in neurons. Delta dystrophin (green), MAP2 (red). Scale bar 10μm.

4.2.10 Delta dystrophin co-localizes with β3-tubulin in cortical neurons

The distribution of delta dystrophin in processes where MAP2 was absent, in addition to the substantial co-localization exhibited between delta dystrophin and MAP2 in a sub population of dendrites, suggested delta dystrophin may co-localize with the microtubule (MT) cytoskeleton. This is because the MT cytoskeleton is the 'highway' along which MAP2 proteins travel to various destinations of the cell (Drewes *et al*, 1998; Dehmelt *et al*, 2004; Fletcher *et al*, 2010), and unlike MAP2, the MT cytoskeleton is found along the central parts of process throughout the entire neurone, including the axon (Mandell *et al*, 1995; Jaglin *et al*, 2009). To determine whether delta dystrophin is associated with the MT network, 14 div neurons were fixed and co-labelled for delta dystrophin and β3-tubulin (figure 4.2.10). β3-tubulin is a molecular subunit of the MT cytoskeleton found along the central part of the soma, axon and all the dendrites (Mandell *et al*, 1995; Jaglin *et al*, 2009). Figure 4.2.10 shows delta dystrophin and β3-tubulin fully co-localized (white arrow, B1-3), with both proteins exhibiting diffuse staining throughout the central parts of the entire neuron, including the cell body, dendrites, and presumably the axon (A1-3). This study suggests that delta dystrophin is distributed in axons, soma and dendrites, in agreement with figures 4.2.1-4.2.9. The co-localization between delta dystrophin and β3-tubulin also suggests delta dystrophin is directly or indirectly associated with the microtubule cytoskeleton found in all neuronal processes, including axons. Given that β3-tubulin is a protein known to be nearly completely devoid from spines (Calabrese *et al*, 2006), the full co-localization between delta dystrophin and β3-tubulin clearly indicates that delta dystrophin is also absent from spines. This finding is in agreement with figure 4.2.1, whereby PSD-95, a protein found exclusively in spines of excitatory synapses (Hunt *et al*, 1996), does not co-localize with delta dystrophin. The full co-localization between delta dystrophin and β3-tubulin (figure 4.2.10) is also consistent with the lack of co-localization between delta dystrophin and postsynaptic markers ($GABA_A$ R and NMDA receptors) as well as with presynaptic markers (GAD65 and synaptophysin), because β3-tubulin is nearly devoid in the synapse (Calabrese *et al*, 2006). Taken together, the results (figures 4.2.1-4.2.10) clearly demonstrate delta dystrophin is an extra-synaptic protein, expressed within the central parts of neurons, directly or indirectly associated with β3-tubulin, and

therefore may not replace classical dystrophin to form novel delta DPC-like complexes at the PSD of GABAergic synapses. Lastly, the co-localization between delta dystrophin and β3-tubulin throughout most, if not all, neurons, suggests delta dystrophin is present in a range of neuronal subtypes, in agreement with figures 4.2.1-4.2.9.

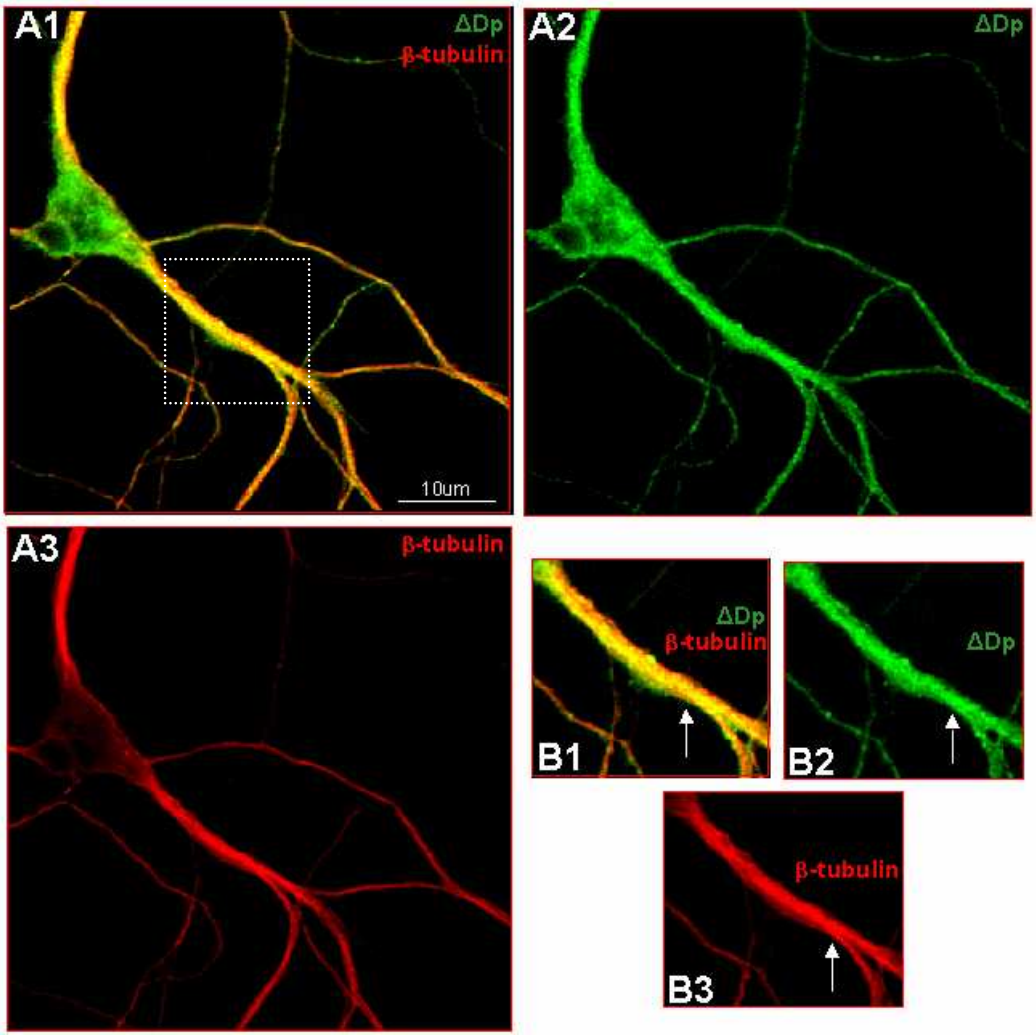

Figure 4.2.10: delta dystrophin co-localizes with β3-tubulin

Rat cortical neurons were fixed at 2 weeks in culture and immunostained for delta dystrophin and β3-tubulin (a neuronal marker and molecular subunit of the MT cytoskeleton found in dendrites, soma and axon of all neurons). The box shows the area expanded in B. Delta dystrophin exhibited diffuse staining within the central parts of all neuronal processes labelled with β3-tubulin and the diffuse staining exhibited by delta dystrophin was identical to the diffuse staining exhibited by β3-tubulin (A1-3). The two proteins fully co-localized (arrow, B1-3), delta dystrophin labelled all processes containing β3-tubulin, and β3-tubulin labelled all processes containing delta dystrophin. Given that β3-tubulin is found within the central parts of the cell body, dendrites and the axon of all neurons, the full co-localization with β3-tubulin suggests delta dystrophin also localizes within the central parts of the cell body, dendrites and axon (A1-3) present in a range of neuronal subtypes. This suggests that delta dystrophin is associated, directly or indirectly, with the microtubule cytoskeleton, and is absent from the synapse. Delta dystrophin (green), β3-tubulin (red). Scale bar 10μm.

4.2.11 Recombinant Cexon78 EGFP and Dexon78 EGFP sequences are unable to traffick differently in the cell

Studies up to this point (chapter 3 and 4) clearly demonstrate that classical and delta full-length dystrophin proteins exhibit different subcellular distributions in neurons of the brain. Classical full-length dystrophins containing classical exon 78 (Cexon78) at their C-terminus are segregated to the PSD (Beesley *et al*, 1999; Brunig *et al*, 2002; Pilgram *et al*, 2009; Waite *et al*, 2009), whereas delta dystrophin proteins containing delta exon 78 (Dexon78) at their C-terminus are segregated to the MT network (figures 4.2.1-4.2.10). Given that Cexon78 and Dexon78 are the only sequences that distinguish classical from delta dystrophin respectively, I therefore transfected (figure 4.2.11.2) cortical neuronal cultures with C-terminally EGFP-tagged Cexon78 (figure 4.2.11.1B) and Dexon78 (figure 4.2.11.1C), in order to determine whether Cexon78 and Dexon78 alone may encode a trafficking signal to the PSD and MT network, respectively. Our collaborators Derek Blake and Chris Esapa kindly provided these vectors already containing the classical or delta exon 78 fused to EGFP. As a control, expression of the EGFP tag only (figure 4.2.11.1A) was investigated in 14 div neuronal cultures (figure 4.2.11.2A). The EGFP tag was successfully transfected into the neurons, as highlighted by the green fluorescence observed within the neurons (figure 4.2.11.2A). Similarly to publications (Bryen *et al*, 2004), the EGFP protein was diffusely distributed throughout the neuron (A; white arrow, A1), and was also localized in spine-like structures (A1, grey arrow). Expression of the EGFP tagged Cexon78 (figure 4.2.11.2B) exhibited diffuse staining throughout the central parts of the neurone (white arrow, B1), and punctate staining in what appears to be spine-like structures (grey arrow, B1) was also observed. This staining pattern did not resemble the exclusively punctate staining exhibited by classical dystrophin in neuronal cultures (figure 4.2.7) and in those published by Brunig *et al* (2002). Similarly to Cexon78, the EGFP tagged Dexon78 (figure 4.2.11.2C) exhibited diffuse staining throughout the central parts of the neuron (white arrow, C1), and punctate staining in what appears to be spine-like structures (grey arrow, C1). The staining patterns of Dexon78 also did not resemble the exclusively diffuse staining pattern exhibited by delta dystrophin (figures 4.2.1-4.2.10) in neuronal cultures presented in this thesis. In fact, both Cexon78 and Dexon78 staining patterns showed a closer resemblance to

EGFP staining, although the latter did not exhibit this relative enrichment in spines (grey arrow, A1). Thus, these studies suggest that classical and delta exon 78 sequences alone are unable to traffick differently in the cell. It is highly likely that Cexon78 and Dexon78 interact with other structural elements within the dystrophin sequence in order to direct trafficking of the classical and delta dystrophin proteins to different parts of the neuron.

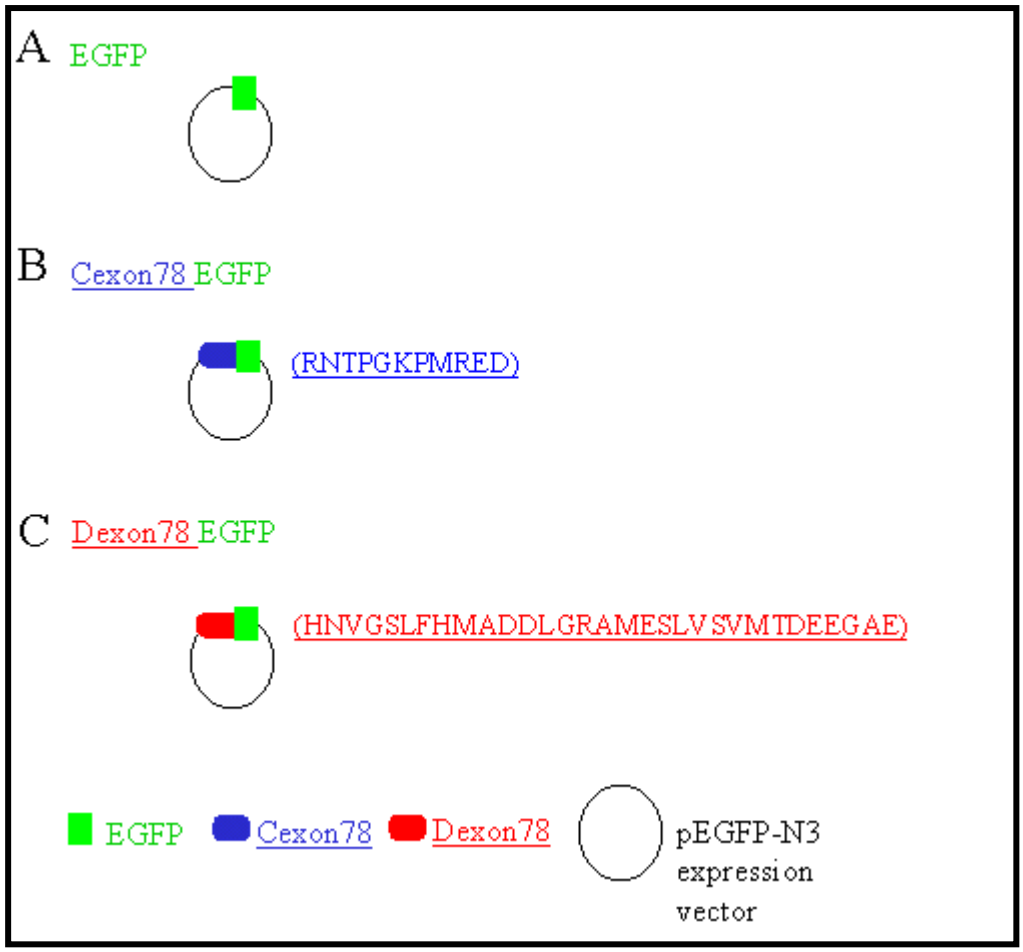

Figure 4.2.11.1: pEGFP-N3 vectors containing cDNAs of classical or delta exon 78 fused with enhanced green fluorescent protein (EGFP).

In order to study the function of classical exon 78 (Cexon78) and delta exon 78 (Dexon78) found in the C-terminus of dystrophin isoforms, recombinant vectors containing the exon78 sequence of either classical or delta dystrophin were prepared. A. As a control, pEGFP-N3 vector containing only the EGFP tag (green) was used. B. pEGFP-N3 vector containing an EGFP tag (green) fused to Cexon78 (blue). Brackets contain the sequence of Cexon78 (blue). C. pEGFP-N3 vector containing an EGFP tag (green) fused to Dexon78 (red). Brackets contain the sequence of Dexon78 (red). EGFP, enhanced green fluorescent protein.

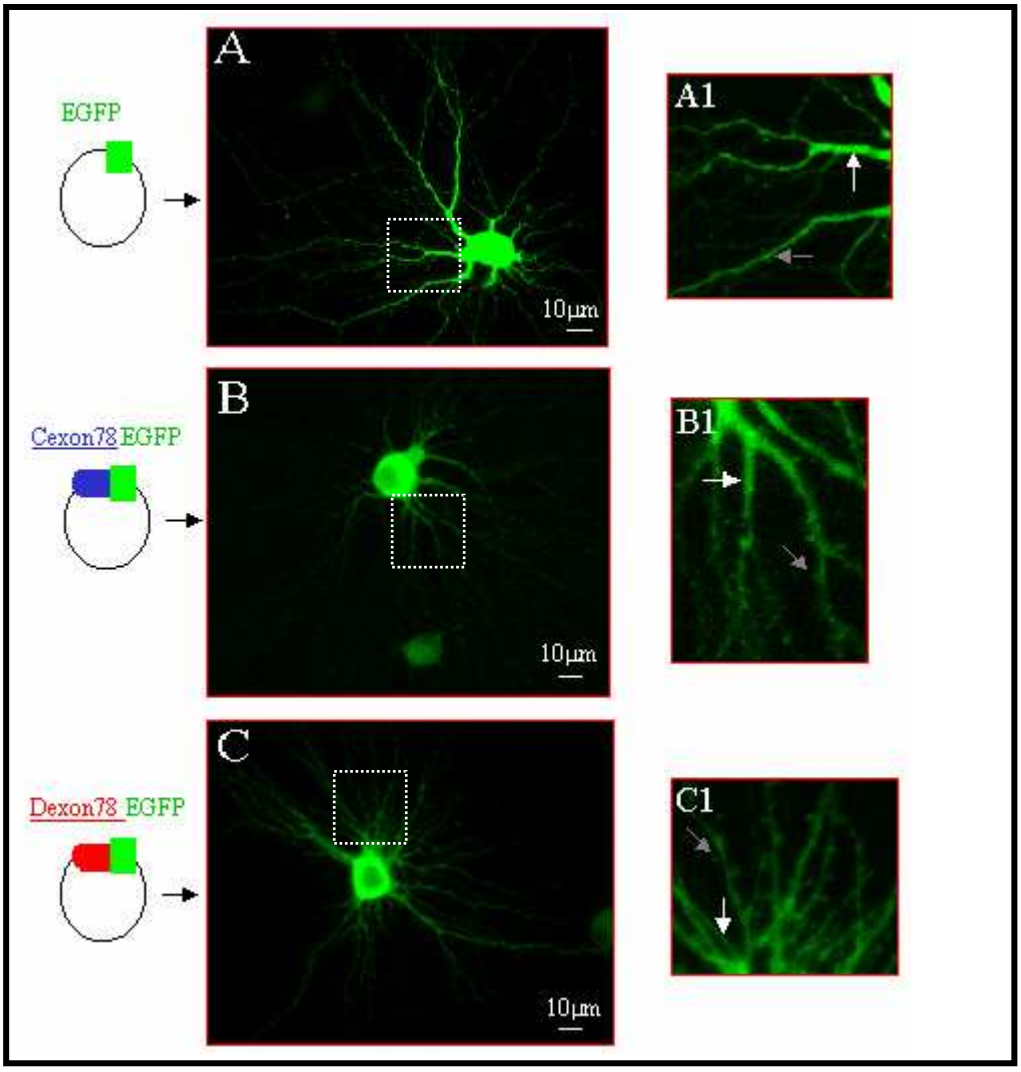

Figure 4.2.11.2: Dexon78 and Cexon78 exhibit a similar subcellular distribution in neurons.

In order to study the function of classical exon 78 (Cexon78) and delta exon 78 (Dexon78) found in the C-terminus of dystrophin isoforms, recombinant vectors containing the exon78 sequence of either classical or delta dystrophin were transfected into 14 div neurons. Boxes show areas expanded in A1-C1. A: expression of the EGFP tag only. B: expression of the EGFP tagged Cexon78. C: expression of the EGFP tagged Dexon78. Both Cexon78 and Dexon78 exhibited diffuse staining (white arrow, B1; white arrow, C1) throughout neuronal processes, as well as punctate staining (grey arrow, B1; grey arrow, C1) in what appears to be spine-like structures. Thus, classical and delta exon 78 sequences alone, do not encode the entire trafficking signal for the dystrophin isoforms, but are likely to encode only part of the trafficking signal sequence. EGFP, enhanced green fluorescent protein. Scale bar 10µm.

4.3 Discussion

4.3.1 Delta dystrophin does not replace classical dystrophin at GABAergic synapses to form novel delta dystrophin-containing DPC complexes.

To date, DPC complexes containing classical dystrophin in neurons have been exclusively localized at the PSD of inhibitory synapses (Brunig *et al*, 2002). More precisely, the DPC complex in neurons contains the classical full-length dystrophin isoform, whereas the shorter classical dystrophin isoforms are reported to form different DPC-like complexes that are only observed outside of neurons (see chapter 1). In this chapter, I have utilised an immunocytochemical approach to determine whether delta dystrophin may replace classical dystrophin to form novel delta DPC-like complexes at the PSD of inhibitory synapses of cortical neuronal cultures. According to this work, I show that delta dystrophin is expressed in cortical neurons (figures 4.2.9, 4.2.10) and that a subpopulation of these neurons also co-express classical dystrophin (figure 4.2.7). However, the two proteins are distributed differently within the cell and therefore do not co-localize (figure 4.2.7). Furthermore, I show that contrary to classical dystrophin, delta dystrophin is not a synaptic protein (figure 4.2.1-4.2.10), as it did not co-localize with any of the synaptic markers tested (figure 4.2.1-4.2.5). In fact, our studies show that delta dystrophin fully co-localizes with the microtubule cytoskeleton throughout the soma, dendrites and possibly axons (figure 4.2.10). My studies therefore suggest that delta dystrophin is directly or indirectly associated with the microtubule cytoskeleton network and therefore may not replace classical dystrophin in the formation of novel delta DPC-like complexes at the PSD of inhibitory synapses. Given that classical full-length dystrophin-containing DPC complexes in neurons have, to date, only been localized at PSD structures of inhibitory synapses, the data presented in this thesis also suggests that in neurons, delta dystrophin can never replace classical dystrophin in DPC formation. Instead, I suggest delta dystrophin is likely to form novel, yet unidentified, delta-

DPC-like complexes within the central parts of the neuron rather than at PSD structures, where classical full-length dystrophin is absent.

After researching the literature and comparing it to our results, it is becoming increasingly clearer that in neurons, delta dystrophin forms DPC-like complexes that are likely to exhibit a different molecular composition to DPC complexes containing classical dystrophin. This point is emphasised by the fact that delta dystrophin and β-dystroglycan, a core component of classical dystrophin-containing DPC complexes, are differently distributed within our cortical neuronal cultures (figure 4.2.6), therefore β-dystroglycan may not be a component of delta dystrophin-binding DPC complexes in neurons of the forebrain. Brunig *et al* (2002) reinforces this result because they demonstrate β-dystroglycan is exclusively localized at PSD structures of inhibitory synapses of the forebrain, whilst I demonstrate that delta dystrophin is an extrasynaptic protein (figures 4.2.1-4.2.5) that co-localizes with the microtubule cytoskeleton (figure 4.2.10). Hence the two proteins are differentially distributed in neurons and therefore β-dystroglycan may not be a component of delta dystrophin-binding DPC complexes therein. What is more, Blake *et al* (1999) shows that delta dystrophin may not associate with a second classical dystrophin-binding DPC component, namely β-dystrobrevin, as delta dystrophin is not immunoprecipitated by β-dystrobrevin in the brain. This is in agreement with my result in chapter 3 (figure 4.2.7), whereby I demonstrate that delta dystrophin and β-dystrobrevin exhibit a different subcellular distribution in the forebrain. Therefore β-dystrobrevin may not be a component of delta dystrophin-binding DPC complexes. Given that β-dystroglycan and β-dystrobrevin are both components of classical dystrophin-containing DPC complexes that may not associate with delta dystrophin, these results strongly suggest that in neurons, delta dystrophin is likely to form DPC complexes whose molecular composition, as well as localization, differs to classical dystrophin-containing DPC complexes localized at the PSD of inhibitory synapses. This is further supported by the striking difference in the level of expression of the two dystrophin isoforms between the two brain regions studied, namely forebrain and cerebellum (Chapter 3, figures 3.2.4.1 & 3.2.4.2), with delta full-length dystrophin being expressed at low levels in the cerebellum when compared to the forebrain,

whilst classical full-length dystrophin is more concentrated in cerebellar fractions when compared to forebrain.

Although the sequence homology between classical and delta dystrophin is very high (they only differ by a single exon), the different molecular associations and localization within the cell, together with the difference in the level of expression exhibited by the two dystrophin isoforms in the forebrain when compared to the cerebellum (chapter 3, figures 3.2.4.1 & 3.2.4.2) suggests different roles for the two proteins. A co-localization between delta dystrophin and β3-tubulin suggests that delta dystrophin is directly or indirectly associated with the microtubule cytoskeleton. Prins *et al* (2009) show that classical dystrophin, the isoform of delta dystrophin, contains an MT-binding domain within the last spectrin domain through to the first third of the WW domain, and demonstrate via an (cosedimentation) immunoprecipitation approach, that classical dystrophin and the MT network can directly associate to one another. Given that delta dystrophin also contains this MT-binding site unaltered by Dexon78 (as Dexon78 is not found within the MT-binding domain), and if we take into consideration the full co-localization between delta dystrophin and β3-tubulin, it is possible to suggest that delta dystrophin may also directly associate with β3-tubulin by utilising the MT-binding domain at the C-terminal end of delta dystrophin. It is likely that classical dystrophin and delta dystrophin both associate with MTs, but if so they must associate with MTs found in two distinct parts of the neuron, as classical and delta dystrophin are never seen to co-localize (figure 4.2.7) and exhibit different subcellular distributions (chapter 3, figures 3.2.3.3 and 3.2.3.4). It is possible that classical dystrophin associates with the few MTs present only at PSDs structures, whereas delta dystrophin, due to its restricted localization at the central parts of neuronal processes, may only associate with MTs found at the central parts of neuronal processes. Thus, although the two dystrophin proteins are almost identical in the amino acid sequence, this is a good example of how alternative splicing can control the subcellular localization of a protein and hence alter its functions within a cell. A key question is what are the signals that direct classical and delta dystrophin to such widely differing subcellular locations.

In addition to its MT-binding domains, classical dystrophin also contains a domain that enables its association with actin, and another domain that enables its association with intermediate filaments (Stone *et al*, 2005; Prins *et al*, 2009). Given that spines are strikingly enriched in actin and nearly completely devoid of intermediate filaments and MTs (Calabrese *et al*, 2006), and given that MTs and intermediate filaments are highly concentrated in the dedritic shaft (Calabrese *et al*, 2006) and extensively meshed together along the central parts of axons and dendrites, my studies and studies by Prins *et al* (2009) lead to the suggestion that most of the binding to the MT network may be carried out primarily by delta dystrophin, and not classical dystrophin. In contrast, classical dystrophin may be important for associating with actin underlying the PSD of inhibitory neurons, as actin is the major cytoskeletal protein found therein. Taken together, these studies show that classical dystrophin and delta dystrophin may, together, function to stabilise the cell as a whole, by associating with actin and microtubules found throughout the neuron. Any interaction with intermediate filaments has not yet been investigated.

Prins *et al* 2009 has already demonstrated that classical dystrophin is capable of stabilising MTs from cold-induced depolymerisation. I suggest that delta dystrophin, in analogy to classical dystrophin, may also function to stabilise the MT cytoskeleton by utilising the same binding domain used by classical dystrophin. No studies have yet investigated whether delta dystrophin may indeed stabilise the MT network, however, studies have shown that the MT cytoskeleton becomes deranged when the DMD gene is mutated (Prins *et al*, 2009; Percival *et al*, 2007), and given that both classical and delta dystrophin originate from the DMD gene, this suggests that both the classical and the delta dystrophin isoform are likely involved in maintaining the stability of the MT cytoskeleton. The possible involvement of delta dystrophin in maintaining the stability of the MT cytoskeleton is further supported by the full co-localization exhibited between delta dystrophin and the MT cytoskeleton throughout the neuron (figure 4.2.10). Furthermore, delta dystrophin, in contrast to classical dystrophin, localizes in regions of the neuron where most of the MT network is found. Therefore, given that delta dystrophin contains an MT-binding domain and fully co-localizes with most of the MT network found in the neuron, it strongly suggests delta dystrophin may have a potential role in stabilising the MT cytoskeleton in neurons. Maintaining the stability of the MT cytoskeleton is vital for the cell,

because the MT cytoskeleton is considered to be the motorway on which vesicles and proteins are transported and targeted to their appropriate destination (Drewes *et al*, 1998; Dehmelt *et al*, 2004; Fletcher *et al*, 2010). When the stability of the MT cytoskeleton is lost as a consequence of DMD mutation, the trafficking of proteins and a wide range of cellular functions may also be affected, leading to the cognitive impairments established in DMD patients. Therefore, the potential function for delta dystrophin in providing stability for the MT network deserves great attention and needs further investigation, as it could unravel novel pathways underlying the aberrant cognitions in DMD brains.

To date there is no knowledge on the function and binding abilities for Cexon78 and Dexon78 (see chapter 3). However, we show that as a consequence of these exons, classical and delta dystrophin distribute differently (chapter 3, figures 3.2.3.3-3.2.3.4, 3.2.4.1-3.2.4.2; Chapter 4, figures 4.2.1-4.2.10). I therefore used a lipofectamine transfection approach on cortical neuronal cells to determine whether Cexon78 and Dexon78 alone may encode a trafficking signal that targets the two proteins to different parts of the cell: PSD and MT cytoskeleton, respectively (figure 4.2.11.2). According to our study (figure 4.2.11.2), both Cexon78 (figure 4.2.11.2B) and Dexon78 (figure 4.2.11.2C) exhibited a mixture of diffuse staining throughout the neuron and punctate staining in spine-like structures, that is very different to the exclusively punctate staining exhibited by the classical dystrophin protein (figure 4.2.7) and the exclusively diffuse staining exhibited by the delta dystrophin protein (figures 4.2.1-4.2.10), respectively. My results therefore show that Cexon78 and Dexon78 alone, are unable to traffick to the PSD and MT cytoskeleton respectively. Given that they are the only sequences that distinguish classical from delta dystrophin, and the two dystrophin isoforms are known to distribute differently in neurons, I suggest Cexon78 and Dexon78 are likely to interact with one or more sequences along the dystrophin protein to differentially target the dystrophin isoforms within the neuron.

Sakamoto *et al* (2008) have carried out a lipofectamine experiment using classical minidystrophins containing the C-terminus, as well as classical minidystrophins that lack the C-terminus and suggest that classical dystrophin contains a region extending from the WW domain to the C-terminal domain of

dystrophin that is important for the trafficking and binding to the membrane of the PSD. Sakamoto *et al* (2008) have not examined whether the entire domain, or only a part of this domain is important for the trafficking and binding to the membrane of the PSD. Cexon78 is found within this domain, and our lipofectamine study (figure 4.2.11.2) demonstrates that Cexon78 alone is unable to encode a trafficking signal to the PSD, therefore a wider proportion of the WW domain to the C-terminal domain of the protein, in collaboration with Cexon78, is required in order to traffick to and associate with the PSD. What is more, whilst classical minidystrophins containing the C-terminus localize to the PSD, classical minidystrophins that lack the C-terminus reside in the cytoplasm, neurites and axons (Sakamoto *et al*, et al 2008), similar to the subcellular distribution observed for delta dystrophin throughout our immunostudies (figures 4.2.1-4.2.10) presented in this chapter. Therefore, the study by Sakamoto *et al*, (2008), combined with our immunocytochemistry and lipofectamine study reveals a very important potential function for Cexon78 and Dexon78. It is likely that Cexon78, found in the C-terminal domain of classical dystrophin, in cooperative interaction with the region extending from the WW domain to the C-terminal domain acts to localize classical dystrophin to the PSD in neurons. Furthermore, it is highly plausible that Dexon78 may function to disrupt the PSD-binding domain extending from the WW domain to the C-terminus, leading to delta dystrophin being distributed throughout the neurites and axons of the neurons (figures 4.2.1-4.2.10), similar to classical minidystrophins lacking the C-terminus domain. This may explain why delta dystrophin is localized within the central parts of neurites and axons, where it associates with β3-tubulin via its MT-binding domain.

In conclusion, delta dystrophin is an extrasynaptic protein, therefore it does not replace classical dystrophin at GABAergic synapses to form novel delta dystrophin-containing DPC-like complexes therein. I suggest delta dystrophin is likely to form novel delta dystrophin-containing DPC-like complexes within the central parts of the neuron rather than at PSD structures. I also suggest that the molecular composition of DPC complexes containing delta dystrophin will differ to DPC complexes containing classical dystrophin. This point is emphasised by the fact that delta dystrophin and β-dystroglycan, a core component of classical dystrophin-containing DPC complexes, do not co-localize (figure 4.2.6). In support of this, the

difference in distribution of the two dystrophin isoforms in the forebrain and cerebellum (chapter 3, figure 3.2.4.2) suggest the two isoforms may carry out different functions in the neuron. I have demonstrated that delta dystrophin fully co-localizes with β3-tubulin, a component of the MT cytoskeleton. I suggest Cexon78 and Dexon78 collaborate with the region extending from the WW domain to the C-terminus to traffick the two dystrophin isoforms to different cellular compartments. I suggest that in analogy to classical dystrophin, delta dystrophin may also directly interact with the MT cytoskeleton via its MT-binding domain. I also suggest that in analogy to classical dystrophin, delta dystrophin may participate in maintaining stability of the MT cytoskeleton, and hence may contribute together with classical dystrophin to the cognitive pathology in DMD patients by generating a deranged MT cytoskeleton, as a consequence of a mutated DMD gene. Lastly, from the immunocytochemical studies of the cortical neurons described in this chapter, all neurons viewed under the light microscope expressed delta dystrophin. Given that 80% of forebrain neurons are excitatory, whilst only 20% of forebrain neurons are inhibitory (Xu *et al*, 2010), I confidently suggest that delta dystrophin is expressed in excitatory neurons of cortical neuronal cultures.

5.0 *Part 2*

Chapter 5:

5.1 ε-sarcoglycan is likely to form novel complexes in the brain that are not related to dystrophin protein complexes

5.2 Introduction

Having established that delta dystrophin does not replace classical dystrophin to form novel delta dystrophin-containing DPC complexes in GABAergic synapses of the brain (Chapter 4), my next goal was to determine whether ε-sarcoglycan, recently discovered to be present in the brain, may be part of the classical or delta dystrophin-containing DPC complexes in the brain. The second goal was to generate an antibody against ε-sarcoglycan, in order to be able to carry out immunopurification studies for the identification of ε-sarcoglycan binding partners in the brain. The presence of ε-sarcoglycan in DPC complexes outside the brain has already been described (Ervasti *et al*, 1990; Yoshida *et al*, 1990; Ozawa *et al*, 1998; Liu *et al*, 1999; Durbeej *et al*, 1999; Straub *et al*, 1999; Imamura *et al*, 2000; Fort *et al*, 2005; Chen *et al*, 2006; Cai *et al*, 2007). To date, studies have suggested ε-sarcoglycan is not directly associated with the DPC complex, in fact, there are other sarcoglycan components that associate with ε-sarcoglycan as well as the DPC complex, therefore creating an indirect link between the ε-sarcoglycan protein and the DPC complex (Ervasti *et al*, 1990; Yoshida *et al*, 1990; Ozawa *et al*, 1998; Durbeej *et al*, 1999; Fort *et al*, 2005). In smooth muscle for example, ε-sarcoglycan associates with three other sarcoglycan proteins (β, γ, δ-sarcoglycans) that together make up the sarcoglycan complex (Ervasti *et al*, 1990), it is the β/δ-sarcoglycan core that links ε-sarcoglycan to the DPC complex (Chen *et al*, 2006). In the outermost membrane of Schwann cells, ε-sarcoglycan forms a different sarcoglycan complex composed of ε, β, δ and ζ sarcoglycans, that is associated with the DPC complex via the β/δ-sarcoglycan core (Imamura *et al*, 2000; Cai *et al*, 2007; Chen *et al*, 2006) (See chapter 1 introduction, part two).

To date, there is no knowledge as to whether ε-sarcoglycan is part of DPC complexes in the brain. What is more, the formation of a sarcoglycan complex in the

brain, which appears to be important for linking ε-sarcoglycan to the DPC complex, has yet to be established in brain. Preliminary studies by western blot analysis suggest γ and δ sarcoglycans are absent from brain at the protein level (Hack *et al*, 2000), although δ-sarcoglycan, but not γ-sarcoglycan, has been detected at the mRNA level (Lim *et al*, 1995; Bönnemann *et al*, 1995; Nigro *et al*, 1996; Nishiyama *et al*, 2004). ζ-sarcoglycan has, to date, been detected only at the mRNA level in the brain (Wheeler *et al*, 2002; Shiga *et al*, 2006), whilst β-sarcoglycan and ε-sarcoglycan isoforms have both been identified at the protein level in the brain (Ettinger *et al*, 1997; McNally *et al*, 1998; Wheeler *et al*, 2002; Xiao *et al*, 2003; Nishiyama *et al*, 2004; Chan *et al*, 2005; Shiga *et al*, 2006). It is clear from the publication data mentioned above that if a sarcoglycan complex exists in neurons, its molecular composition would significantly differ from the sarcoglycan complex found in smooth muscle, and is more likely to resemble the sarcoglycan complex found in Schwann cells. Therefore, given that the brain expresses ε, β, δ and ζ sarcoglycans at the mRNA level, and given that all four sarcoglycans are known to complex together in the Schwann cells and link ε-sarcoglycan to the DPC complex therein, this chapter presents a number of studies to determine whether ε-sarcoglycan, in analogy to Schwann cells, may be a component of the DPC complex in neurons of the brain.

The chapter initially describes a biochemical study that determines the subcellular distribution of ε-sarcoglycan in the two different brain regions (forebrain and cerebellum). This data was then used to compare the subcellular distribution of ε-sarcoglycan with the subcellular distribution of other well-established DPC components in forebrain and cerebellum, presented in Chapter 3 (figure 3.2.3.2, 3.2.3.3, 3.2.3.4, 3.2.4.1, 3.2.4.2). The aim was to determine whether or not ε-sarcoglycan exhibits the same subcellular distribution as delta dystrophin and/or other components of the classical dystrophin-containing DPC complexes, which would suggest whether ε-sarcoglycan may or may not be a component of classical and/or delta dystrophin-containing DPC complexes in forebrain and cerebellum. Mature cortical neuronal cultures were then used for immunocytochemical co-labelling for ε-sarcoglycan and classical dystrophin, a core component of the classical dystrophin-containing DPC complexes exclusively localized at PSD structures of GABAergic synapses (Blake *et al*, 1999; Brunig *et al*, 2002), in

order to determine whether there exists a co-localization between ε-sarcoglycan and classical dystrophin. Co-localization would suggest ε-sarcoglycan is part of the classical dystrophin-containing DPC complexes at GABAergic synapses. Thirdly, immunoprecipitation experiments were carried out to determine the potential for association between ε-sarcoglycan, classical and delta dystrophin, by establishing the ability of ε-sarcoglycan to pull-down classical and delta dystrophin isoforms from whole forebrain extracts. Lastly, I generated an anti-ε-sarcoglycan antibody for immunopurification and identification studies for ε-sarcoglycan-binding partners.

5.3 Results:

5.3.1 Isolation of forebrain and cerebellum subcellular fractions

Different subcellular fractions were obtained from forebrain and cerebellum of adult rat brains, as described in M&M (chapter 2). The following subcellular fractions were obtained: brain homogenate (BH), P2 pellet, myelin (My), microsomes (Mc), light membrane (LM), synaptic membrane (SM) and mitochondria (Mt). The SM fraction was fractionated further to give the PSD fraction. These forebrain and cerebellum subcellular fractions, isolated and described in Chapter 3, were utilised in this chapter to study and compare the subcellular localization of ε-sarcoglycan in the brain, therefore cross-contamination tests and Coomassie Blue testing of these fractions can be verified in Chapter 3, figures 3.2.2.1-3.2.3.1. The subcellular distribution of ε-sarcoglycan in forebrain and cerebellum was determined by immunoblotting the range of subcellular fractions described above, including SMs and PSDs prepared from rat forebrain and cerebellum. PSDs of forebrain and cerebellum were isolated by the n-octyl-glucopyranoside method.

5.3.2 ε-sarcoglycan is a membrane-associated protein of the forebrain, and only present in low levels in PSDs

An immunoblot containing forebrain subcellular fractions was incubated with anti-ε-sarcoglycan antibody (figure 5.3.2), in order to determine the subcellular distribution of ε-sarcoglycan within the forebrain. As expected, the brain homogenate fraction contained two ε-sarcoglycan isoforms close to the 50kDa molecular weight (figure 5.3.2), with similar intensities to one another, suggesting the two isoforms exhibit similar levels of expression within the forebrain. Since ε-sarcoglycans are glycosylated proteins (McNally *et al*, 1998), the precise molecular weight of the two isoforms cannot be calculated and therefore their molecular weights can only be estimated by SDS analysis. According to previous immunoblot analysis of mouse wholebrain homogenates by Nishiyama *et al* (2004), the two ε-sarcoglycan isoforms had a molecular weight of 47kDa and 49kDa. The two isoforms identified in figure 5.3.2 shared very similar molecular weights to those published by Nishiyama *et al* (2004) and therefore to avoid confusion, these were also labeled as 47kDa and 49kDa isoforms. Both isoforms enriched in the membrane fractions (microsomes, LM and SM), when compared to the brain homogenate fraction. What is more, ε-sarcoglycan isoforms did not enrich in the PSD fraction, although a weak doublet band was visible within the PSD lane. In conclusion, these results suggest that in the forebrain, the two ε-sarcoglycan isoforms are membrane-associated proteins present in fractions of non-synaptic (LM and microsomes) and primarily synaptic (SM) origin.

Within the LM fraction, the two isoforms of 47 and 49kDa were expressed at similar band intensities. What is more, in the SM and microsome fractions, the two isoforms were expressed at similar band intensities when compared to the LM fraction, suggesting both isoforms were equally expressed within each particular subcellular fraction. Both isoforms were absent from the cytosol, suggesting that the two isoforms are membrane bound rather than freely distributed in the cytosol. The mitochondrial fraction showed only weak expression of the two isoforms, suggesting neither isoform is enriched within the mitochondrial fraction. In contrast to all these fractions, the myelin lane expressed the 47kDa isoform as a thick band whilst the band of the 49kDa isoform was only weakly expressed. This result suggests that the two isoforms do not always

exhibit the same subcellular distribution in forebrain subcellular fractions and thus their distribution may undergo differential control mechanisms within the forebrain.

All subcellular fractions, with the exception of the cytosolic and mitochondrial fractions, contained bands of higher molecular weight proteins (figure 5.3.2). According to the literature, there are to date no ε-sarcoglycan isoforms of such molecular weights in the brain or in any other organ studied. Therefore they are likely to represent cross-reactive bands or non-ε-sarcoglycan proteins reacting with the antibody. However, asterisks (figure 5.3.2) may represent potential dimeric or trimeric formation of ε-sarcoglycan isoforms that may form during the separation of the proteins in the SDS gel. Such bands would appear as high molecular weight bands of approximately 100kDa (dimer) and 150kDa (trimer) bands, respectively. However these higher molecular weight bands may be due to other cross-reacting proteins. It is not uncommon to find formation of dimeric and trimeric mammalian sarcoglycans in the presence of SDS, as previously reported by Shi *et al* (2004) and Hashimoto *et al* (2006). Furthermore, according to the western blot, there is some discrepancy in the mobility of the two isoforms when the subcellular fractions are compared to one another. This is likely to be due to some post-translational modification, such as glycosylation (McNally *et al*, 1998) and phosphorylation (Ettinger *et al*, 1997; Nishiyama *et al*, 2004) exerted on the mammalian ε-sarcoglycan isoforms, similar to what has already been reported for other sarcoglycan family members (Shi *et al*, 2004; Hashimoto *et al*, 2006) and which slightly alters the mobility of the isoforms in the gel. Based on these findings, the band observed between the 84kDa and 116kDa markers in the myelin lane may represent the dimeric form of 47kDa isoform that has been glycosylated, rather than the dimeric form of the 49kDa isoform, given that the latter was only weakly expressed whereas the 47kDa isoform was strongly expressed in the myelin fraction.

In conclusion, the studies show ε-sarcoglycan isoforms are membrane-associated proteins (figure 5.3.2) that are only present in low levels in the PSD fraction. Given that classical full-length dystrophin-containing DPC complexes are highly enriched in PSD structures (Chapter 3, figure 3.2.3.2, 3.2.3.3, 3.2.4.1), and classical dystrophin and associated DPC components are exclusively localized at GABAergic synapses (Blake *et al*, 1999; Brunig *et* al, 2002; Culligan *et al*, 2002), these studies

suggest that in the forebrain, both ε-sarcoglycan isoforms are unlikely to be components of classical dystrophin-containing DPC complexes due to the different compartmentalization of ε-sarcoglycan and classical dystrophin-containing DPC complexes. Secondly, given that delta dystrophin co-localizes with the MT cytoskeleton (Chapter 4, figure 4.2.10), these studies also suggest that in forebrain, both ε-sarcoglycan isoforms are unlikely to be components of delta dystrophin-containing DPC complexes.

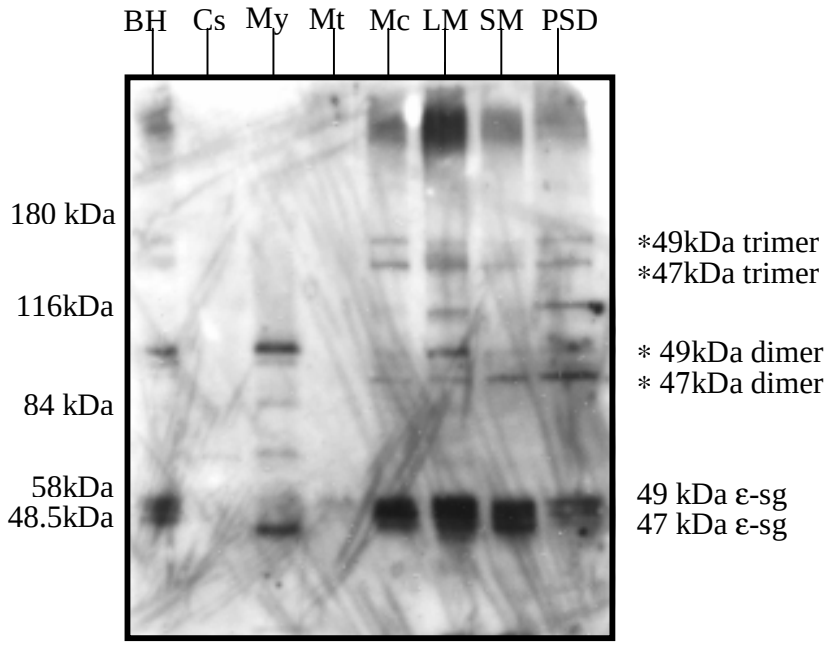

Figure 5.3.2: Western Blot of forebrain subcellular fractions immunodeveloped with anti-ε-sarcoglycan antibody.

Two ε-sarcoglycan isoforms of 47kDa and 49kDa are expressed in the forebrain, and are found to enrich in the LM, SM and microsomal fractions, but not in the PSD fraction. These results suggest ε-sarcoglycan isoforms are membrane-associated proteins. Protein loading is 20μg/lane. Lane 1, Brain Homogenate (BH); lane 2, Cell soluble (Cs); lane 3, Myelin (My); lane 4, Mitochondria (Mt); lane 5, Microsomes (Mc); lane 6, Light Membrane (LM); lane 7, Synaptic Membrane (SM); lane 8, Post-Synaptic Density (PSD). Molecular weight standards are indicated. *, potential dimeric and trimeric formation of ε-sarcoglycan isoforms.

5.3.3 ε-sarcoglycan is a membrane-associated protein of the cerebellum, and only present in low levels in PSDs

The subcellular distribution and/or level of expression of a protein in the forebrain does not always reflect that of the cerebellum, as in the case of PSD95 (Hunt *et al*, 1996, Kim *et al*, 1992) and delta full-length dystrophin (Chapter 3, figure 3.2.4.2), respectively. Therefore, the subcellular distribution of ε-sarcoglycan isoforms in the forebrain and cerebellum was determined, in order to compare the subcellular localizations and level of expression of the two isoforms in the two different brain regions. This study was also carried out in order to determine whether ε-sarcoglycan may enrich in cerebellar PSDs and therefore be a potential component of classical dystrophin-containing DPC complexes in PSDs of the cerebellum. Secondly, I was able to determine whether ε-sarcoglycan may have a similar subcellular distribution to delta dystrophin in the cerebellum, and hence, whether it may be part of delta dystrophin-containing DPC complexes, which according to results presented in Chapter 4, are localized at microtubule structures within neurons. Thirdly, these results were also important to suggest whether ε-sarcoglycan may or may not be part of novel protein complexes at membrane structures within the cerebellum.

An immunoblot containing a range of rat forebrain and cerebellar subcellular fractions was incubated with anti-ε-sarcoglycan antibody (figure 5.3.3). In figure 5.3.3, ε-sarcoglycan was found as a 47kDa and 49kDa duplet band in both the forebrain and cerebellar brain homogenates. Within the brain homogenate of the forebrain, the 47kDa and 49kDa ε-sarcoglycan isoforms were expressed with similar intensity to one another (figure 5.3.3), suggesting that the two isoforms are expressed in similar quantities within the forebrain, in agreement with figure 5.3.2. In contrast, within the brain homogenate fraction of rat cerebellum, there was less of the 49kDa isoform when compared to the 47kDa band, as previously observed by Nishiyama *et al* (2004). What is more, the intensity of the 47kDa isoform in the total homogenate of the rat cerebellum was similar to the respective fraction in the forebrain, whereas the band intensity of the 49kDa isoform in the cerebellum was lower compared to the forebrain, as observed by Nishiyama *et al* 2004. In other words, these results suggest that the 47kDa isoform is

expressed in similar levels in both brain regions, whereas the level of expression of the 49kDa isoform in the two brain regions appears to be regionally controlled.

In the forebrain, the 47kDa and the 49kDa isoforms (figure 5.3.3) both enriched in microsomes, LM and SM fractions, in agreement with figure 5.3.2. Within the microsome fraction of the forebrain (figure 5.3.3), the 47kDa isoform exhibited the same band intensity as the 49kDa isoform, and these levels of expression were also observed within the LM and SM fractions of forebrain. In other words, all three fractions contained very similar levels of enrichment of both isoforms, in agreement with figure 5.3.2. The cerebellum also exhibited a synaptic membrane enrichment pattern of both ε-sarcoglycan isoforms, and similarly to the forebrain, neither isoform enriched in the PSD fraction (figure 5.3.3). Given that to date, classical dystrophin-containing DPC complexes in neurons of the cerebellum have been localized exclusively in PSD structures (chapter 3, figures 3.2.3.2, 3.2.3.3 and 3.2.4.1; Moukhles *et al*, 2001), figure 5.3.3 suggests that the two ε-sarcoglycan isoforms are unlikely components of the classical dystrophin-containing DPC complex at the PSD of the cerebellum, as well as the forebrain, because neither isoform is enriched in the PSD of forebrain and cerebellum. It is important to note however, that the PSD fraction is not completely devoid of the isoforms, in fact there exists a low level of ε-sarcoglycan isoforms in the PSD of the forebrain, followed by a more intense doublet band of the isoforms in the PSD of the cerebellum, suggesting the two isoforms certainly are present in the PSD fraction. In view of the high enrichment of classical dystrophin in the PSD fraction (Chapter 3, figure 3.2.3.3), and the low level of ε-sarcoglycan isoforms in this fraction, it is unlikely that ε-sarcoglycan is a component of the classical dystrophin-containing DPC complex at forebrain and cerebellar PSDs. Furthermore, with regard to delta dystrophin, the biochemical studies (Chapter 3, figure 3.2.4.2; this chapter, figure 5.3.3) show that although both ε-sarcoglycan isoforms and delta full-length dystrophin enrich in the microsomal fraction, ε-sarcoglycan isoforms also enrich in the LM and SM fractions, whereas delta dystrophin does not. This is true in both forebrain and cerebellar subcellular fractions. The immunocytochemical study (Chapter 4, figure 4.2.10) confirm these differences, in fact delta dystrophin in neurons fully co-localizes with the MT cytoskeleton, away from the membrane (Chapter 4, figure 4.2.8), whereas ε-sarcoglycan isoforms are exclusively membrane-enriched (this chapter, figures 5.3.2, 5.3.3). These studies therefore suggest that ε-sarcoglycan isoforms are

unlikely to be components of delta dystrophin-containing DPC complexes of the forebrain and cerebellum, due to different compartmentalization restrictions.

Although both ε-sarcoglycan isoforms are clearly membrane-associated proteins in both the forebrain and cerebellum, ε-sarcoglycan isoforms within the membrane fractions of the cerebellum are differently distributed when compared to the respective membrane fractions in the forebrain. In fact, only the SM fraction of the cerebellum contained both ε-sarcoglycan isoforms enriched therein, similar to the SM fraction found in the forebrain. In contrast, the microsomes and LM fractions of the cerebellum contained low levels of 49kDa isoform and enriched levels of the 47kDa isoform, whilst the forebrain microsomes and LM fractions contained both isoforms enriched therein. What is more, both isoforms are expressed at lower levels in membrane fractions of the cerebellum, when compared to the respective fractions in the forebrain. Therefore, the results clearly indicate that the 47kDa isoform exhibits the same membrane distribution in both brain regions, although at slightly lower levels in cerebellum, whilst the level of expression of the 49kDa isoform in the membrane fractions of the forebrain is by far greater when compared to the membrane fractions of the cerebellum. In other words, the level of expression of the 47kDa and 49kDa isoforms in the membrane fractions are regionally controlled, but unlike the 47kDa isoform, the 49kDa isoform is differentially expressed in the membrane fractions of the forebrain when compared to the membrane fractions of the cerebellum. Furthermore, the myelin fraction of both forebrain and cerebellum only contained the 47kDa isoform, whilst negligible to null levels of the 49kDa band was observed. Thus, based on the myelin result, the 47kDa and 49kDa isoforms also appear to exhibit differential localization within the forebrain, as well as within the cerebellum. Lastly, the higher intensity of the doublet band within the membrane fractions of the forebrain when compared to the membrane fractions of the cerebellum, and the lower intensity of the 47kDa isoform in the myelin fraction of the forebrain when compared to the corresponding fraction in the cerebellum altogether suggest that the level of expression and distribution of the two isoforms in the two brain regions is highly regulated.

In conclusion, both ε-sarcoglycan isoforms occur predominantly in membrane fractions, both of synaptic (SM) and non-synaptic origin (LM and microsomes). There

appears to be lower expression of the 49kDa isoform in cerebellum compared to forebrain. Significantly only the 47kDa isoform is present in myelin. Neither isoform is enriched in the PSD fractions, unlike classical full-length dystrophin and associated DPC proteins (Chapter 3, figure 3.2.3.2, 3.2.3.3, 3.2.4.1), therefore it is most unlikely that ε-sarcoglycan is a component of classical DPC complexes present in the PSD of either brain compartment. Given that to date, classical dystrophin-containing DPC complexes are said to exclusively localize at GABAergic synapses (Brunig *et al*, 2002), these studies suggest that ε-sarcoglycan may not associate with these classical dystrophin-containing complexes at GABAergic synapses. Lastly, given that the immunocytochemical data demonstrates delta dystrophin co-localizes with the MT cytoskeleton (Chapter 4, figure 4.2.10), away from the membrane (Chapter 4, figure 4.2.8), whereas ε-sarcoglycan isoforms exclusively localize at the membrane, these studies also suggest that due to compartmentalization restrictions, neither ε-sarcoglycan isoform may associate with the delta dystrophin-containing DPC complexes in the forebrain and cerebellum. Hence, it seems likely that ε-sarcoglycan isoforms are likely to form novel, as yet unidentified protein complexes in brain.

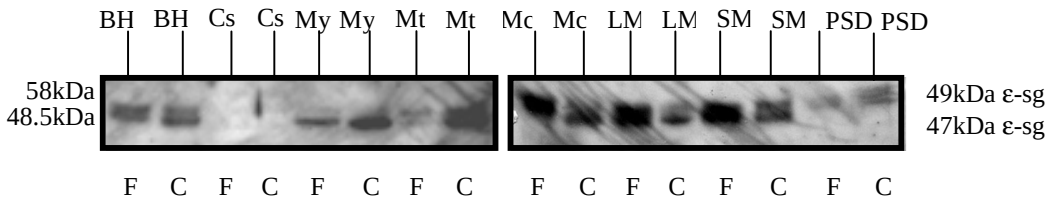

Figure 5.3.3: Western Blot of forebrain and cerebellar subcellular fractions immunodeveloped with anti ε-sarcoglycan antibody.

Two ε-sarcoglycan isoforms (47kDa and 49kDa) are expressed in forebrain and cerebellar compartments. The brain homogenate of forebrain expresses similar levels of these isoforms, whereas the cerebellum brain homogenate expresses lower levels of the 49kDa isoform when compared to the 47kDa isoform in the cerebellum brain homogenate and with respect to the two isoforms in the brain homogenate of the forebrain, in agreement with Nishiyama *et al* 2004. Both 47kDa and 49kDa isoforms enrich in the SM fraction of the forebrain and cerebellum. No enrichment is observed in the PSD fraction of either brain compartment. In the forebrain, both isoforms are equally expressed in microsomes, LM and SM fractions. Contrary to the forebrain, the microsomes and LM fractions of the cerebellum express lower levels of the 49kDa isoform when compared to the 47kDa isoforms, whereas the SM fraction of the cerebellum expresses similar levels of both isoforms. Furthermore, the myelin fractions of the forebrain and cerebellum only express the 47kDa isoform, with the cerebellum expressing more of this isoform than the forebrain. Therefore, the two ε-sarcoglycan isoforms are membrane-associated proteins that exhibit differential localization within and between the two brain compartments. The fractions are run in pairs with the left and right hand samples being forebrain and corresponding cerebellar fractions respectively. Protein loading is 20μg/lane. Lanes 1 & 2, Brain Homogenate (BH); lanes 3 & 4, Cell Soluble (Cs); lanes 5 & 6, Myelin (My); lanes 7 & 8, Mitochondria (Mt); lanes 9 & 10, Microsomes (Mc); lanes 11 & 12, Light Membrane (LM); lanes 13 & 14, Synaptic Membrane (SM); lanes 15 & 16, Post Synaptic Density (PSD). Molecular weight standards are indicated. F, forebrain. C, cerebellum.

5.3.4 ε-sarcoglycan, classical and delta dystrophin are differently distributed in cortical neurons, suggesting ε-sarcoglycan is unlikely to be a component of classical and delta dystrophin-containing DPC complexes in cortical neurons.

The biochemical studies (figures 5.3.2-5.3.3) presented in this chapter highlight that ε-sarcoglycan isoforms are membrane-associated proteins that are unlikely to associate with classical and delta dystrophin-containing DPC complexes in brain. The next goal was to demonstrate, via an immunocytochemical approach, the differences in subcellular distribution exhibited by ε-sarcoglycan and classical dystrophin (the core component of classical dystrophin-containing DPC complexes in PSD structures of neurons) and delta dystrophin (the core component of delta dystrophin-containing DPC complexes at MT structures of neurons), which would exclude the possibility of an interaction between them.

In order to study the distribution of ε-sarcoglycan and classical dystrophin within neurons of the forebrain, cortical neuronal cultures were grown for two weeks prior to immunolabeling. The cultures were grown for this long because at this time-point neurons reach a state of maturity, with 92-95% of the neurons containing the highest density of spiny dendrites, a characteristic feature of in situ neurones (Papa *et al*, 1995; O'Brien *et al*, 1997, Rao *et al*, 1998). 14 div neurons were fixed and then co-labelled for ε-sarcoglycan and classical dystrophin. Anti-ε-sarcoglycan antibody was directed against the last 98 amino acids of mouse ε-sarcoglycan, thus capable of recognising both 47kDa and 49kDa ε-sarcoglycan isoforms. Anti-classical dystrophin antibody was directed against classical exon 78 of the C-terminus, thus capable of recognising all four classical dystrophin isoforms expressed in the brain. Cortical neurons labelled with anti-classical dystrophin antibody (figure 5.3.4) exhibited brightly labelled puncta (arrowhead, B1, 3) arranged in lines running over cell bodies (A3) and proximal dendrites (arrowhead, B1, 3) similar to that reported by Brunig *et al* (2002) in hippocampal neurons. Neurons labelled with anti-ε-sarcoglycan antibody stained the same soma (A2) and proximal dendrites (arrowhead, B1, 2) containing classical dystrophin, similar to that reported by Esapa *et al* 2007, however they never co-localized (arrowhead, B1). What is more, within

the same dendrites containing classical dystrophin, ε-sarcoglycan also stained the more distal parts of the dendrites (arrow, B1-3), whereas classical dystrophin staining was not found there (arrow, B1-3), rather, classical dystrophin immunoreactivity was restricted to proximal dendrites only (arrowhead, B1-3). Given that classical full-length dystrophin is the only classical dystrophin isoform expressed in neurons (Blake *et al*, 1999), it is a core component of DPC complexes exclusively localized at GABAergic synapses (Brunig *et al*, 2002) and does not co-localize with ε-sarcoglycan (figure 5.3.4), figure 5.3.4 suggests ε-sarcoglycan is unlikely a component of classical full-length dystrophin-containing DPC complexes at GABAergic synapses of cortical neurons of the forebrain, in agreement with figures 5.3.2 and 5.3.3.

The next goal was to demonstrate, via an immunocytochemical approach, the differences in distribution exhibited by ε-sarcoglycan and delta dystrophin. Unfortunately, both antibodies are rabbit antibodies and therefore would be recognised by the same rabbit secondary antibody, hence, merging the two images would not allow a clear distinction of ε-sarcoglycan staining from delta dystrophin staining. Furthermore, given that the distributions of the two proteins are clearly very different, and the antibody stocks were very limited, I decided to avoid fixing 14 div cortical neurons to directly compare the distribution of ε-sarcoglycan with delta dystrophin. Instead, I decided to compare the immunolocalization of ε-sarcoglycan exhibited in this chapter (figure 5.3.4) with the immunolocalization of delta dystrophin exhibited in Chapter 4 (figures 4.2.1-4.2.10). The results clearly show that ε-sarcoglycan isoforms are exclusively distributed along the membrane of neurons (this chapter, figures 5.3.2-5.3.4; Esapa *et al*, 2007), whereas delta dystrophin isoforms are exclusively localized at the MT-cytoskeleton (Chapter 4, figure 4.2.10), away from the membrane (Chapter 4, figure 4.2.8). Hence, the different compartmentalizations suggest that ε-sarcoglycan is unlikely to be a component of delta dystrophin-containing complexes in cortical neurons.

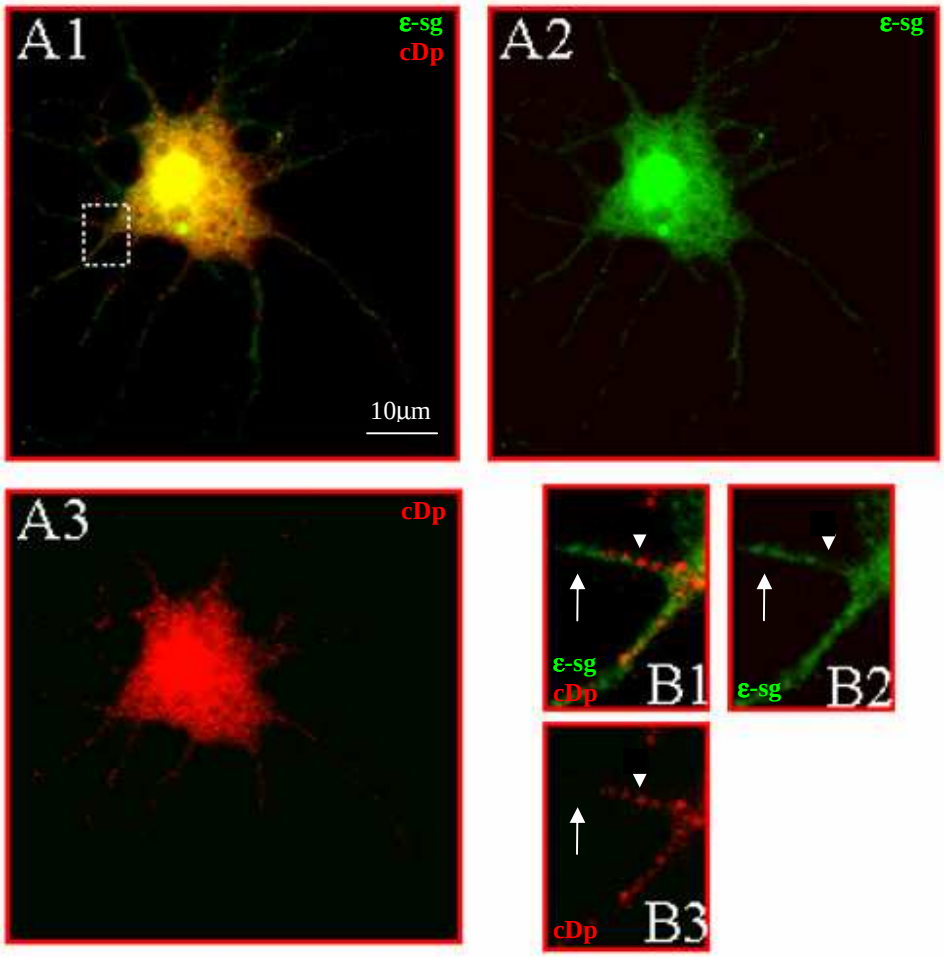
A1
ε-sg
cDp
10μm
A2
ε-sg
A3
cDp
ε-sg
cDp
B1
ε-sg
B2
cDp
B3

Figure 5.3.4: ε-sarcoglycan does not co-localize with classical dystrophin.

Rat cortical neurons were fixed at 2 weeks in culture and immunostained for classical dystrophin (a marker for the classical dystrophin-containing DPC complex at the PSD of inhibitory synapses) and ε-sarcoglycan (a membrane-associated protein). The box shows the area expanded in B. Classical dystrophin was found as brightly labelled puncta arranged in lines running over cell bodies (A3) and dendrites (arrowhead, B1, 3), in agreement with Brunig *et al* 2002. ε-sarcoglycan was also distributed along the same soma (A1, 2) and proximal dendrites (arrowhead, B1-3), in agreement with Esapa *et al* 2007. The abundance of classical dystrophin in the soma was similar to that reported by Brunig *et al* 2002, but its significance remains to be investigated, whereas the abundance of ε-sarcoglycan in the cell body was due to its localization in some intracellular structures including the Golgi apparatus and post-Golgi vesicles (Esapa *et al*, *2007*). Despite their abundance in the cell body, this figure highlights ε-sarcoglycan and classical dystrophin never co-localized (arrowhead, B1). ε-sarcoglycan was also distributed in more distal parts of the dendrites, where classical dystrophin was absent (arrow, B1-3). This suggests that ε-sarcoglycan is unlikely to be a component of classical dystrophin-containing DPC complexes at GABAergic synapses of cortical neurons of the forebrain. ε-sarcoglycan (green), classical dystrophin (red). Scale bar 10μm.

5.3.5 The low levels of classical dystrophin isoforms imunoprecipitated by ε-sarcoglycan suggest ε-sarcoglycan is unlikely to associate with classical dystrophin-containing DPC complexes in the forebrain

Biochemical analysis (figures 5.3.2 and 5.3.3) and cortical neuronal (figure 5.3.4) immunocytochemical studies all suggest that ε-sarcoglycan is unlikely to be a component of DPC complexes in brain, due to different compartmentalization restrictions. The next goal was to carry out an immunoprecipitation (IP) study using an immunoaffinity column cross-linked to the anti-ε-sarcoglycan antibody, in order to re-investigate whether there is any binding interaction between ε-sarcoglycan and delta dystrophin, as well as with the neuron-specific classical full-length dystrophin isoform (cDp427) (Blake *et al*, 1999) in the forebrain. In order to carry out such experiment, forebrain homogenates were treated with RIPA buffer (see M & M), such that ε-sarcoglycan isoforms could be solubilised from the membrane as part of any multi-protein complexes that exist within the membrane and made available to interact with the anti-ε-sarcoglycan antibody during the immunoprecipitation experiment. Protein complexes are said to be more soluble in RIPA buffer when compared to other lysis buffers (Lambert *et al*, 2008), hence the choice of this buffer for these experiments, however, limitations of the RIPA buffer include lower solubility of membrane proteins, as well as of cytoskeleton and extracellular region proteins (Lambert *et al*, 2008). Therefore, a control experiment was carried out to ensure that the membrane-associated ε-sarcoglycan proteins were successfully solubilized by RIPA buffer, by using an anti-ε-sarcoglycan antibody cross-linked to a column in order to allow immunoprecipitation (IP) of proteins from a BH preparation prior to RIPA buffer treatment, followed by an IP from a solubilized RIPA buffer BH preparation. Results showed that the RIPA buffer treated homogenate immunoprecipitated far more ε-sarcoglycan than in the control IP lane (data not shown), suggesting the solubilization with RIPA buffer was successful.

Beads cross-linked to anti-ε-sarcoglycan antibody, kindly provided by our collaborators (Derek J Blake and Christopher T Esapa, University of Oxford), were mixed with the solubilized brain homogenate material in order to allow binding of the

anti-ε-sarcoglycan antibody with ε-sarcoglycan and any ε-sarcoglycan-binding proteins. An immunoblot containing brain homogenate (solubilized with RIPA buffer), immunoprecipitated protein (IP) material, and a control, was incubated with anti-ε-sarcoglycan antibody (figure 5.3.5.1). The control lane contained eluates from beads that were not cross-linked with anti-ε-sarcoglycan antibody (figure 5.3.5.1), in order to measure the level of non-specific binding that may occur between the uncross-linked beads and the solubilized brain homogenate material. In the brain homogenate lane, two ε-sarcoglycan isoforms of 47kDa and 49kDa were present, as expected. In the IP lane, ε-sarcoglycan was successfully immunoprecipitated as one thick band of about 50 kDa. Our control lane demonstrated that beads that had not been cross-linked with the anti-ε-sarcoglycan antibody did not immunoprecipitate any ε-sarcoglycan protein. Asterisks refer to bands in the brain homogenate that may represent cross-reactive bands of non-ε-sarcoglycan proteins, otherwise the same bands would also have been observed in the IP lane.

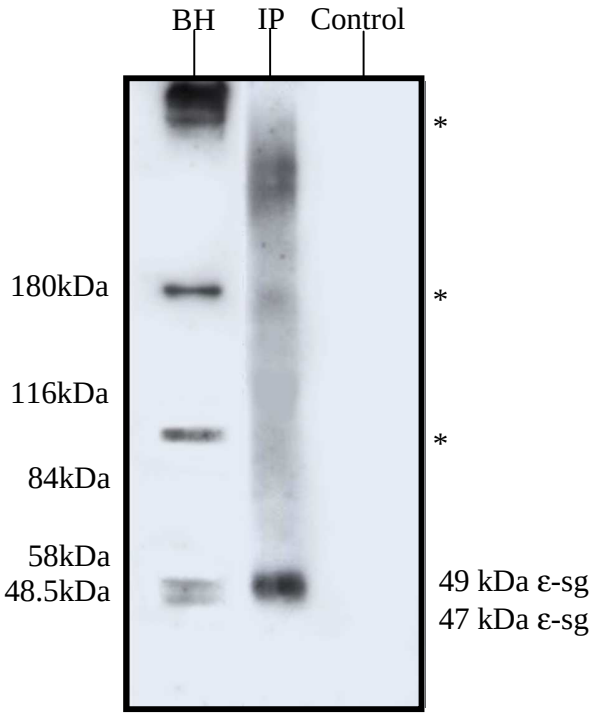

Figure 5.3.5.1: Western Blot containing anti-ε-sarcoglycan immunoprecipitated proteins of the forebrain, immunodeveloped with anti-ε-sarcoglycan antibody.

The brain homogenate fraction contains two ε-sarcoglycan isoforms, 47kDa and 49kDa respectively. ε-sarcoglycan isoforms were successfully immunoprecipitated by the beads cross-linked to the anti-ε-sarcoglycan antibody, resulting into a thick band of around 50kDa in the IP lane. The control lane, containing beads that were not cross-linked to the anti-ε-sarcoglycan antibody, contains no ε-sarcoglycan protein, suggesting that the beads alone were unable to immunoprecipitate the ε-sarcoglycan protein. Protein loading is 20μg/lane. Lane 1, Brain Homogenate (BH); lane 2, immunoprecipitated material (IP); lane 3, Control. Molecular weight standards are indicated. *, may represent cross-reactive bands of non-ε-sarcoglycan proteins.

Given that the IP lane contained a single thick band as opposed to a doublet band, I have demonstrated that the 50kDa band in the immunoprecipitate (IP) lane indeed represented the two ε-sarcoglycan isoforms (47kDa, 49kDa isoforms) rather than the cross-linked anti-ε-sarcoglycan antibody 50kDa IgG heavy chain protein that may have detatched from the beads during elution of the IP complex. Therefore, the immunoblot used in figure 5.3.5.1 was stripped using Glycine pH 2.5, a mild stripping procedure that reduces the amount of protein loss from the membrane when compared to other harsher SDS stripping treatments (http://www.piercenet.com/files/TR0023-Strip-&-reprobe-blots.pdf), and subsequently incubated with the secondary antibody alone. The aim was to detect the presence of any primary antibody that may have detached from the column during the elution procedure. The stripped immunoblot was incubated using double the amount of secondary antibody that would normally be used, and results show that the antibody did not pick up any 50kDa antibody heavy chain band in the IP lane (figure 5.3.5.2), demonstrating that the anti-ε-sarcoglycan antibody cross-linked to the beads was not removed from the column during elution of the IP material, but remained successfully cross-linked to the beads in the column. To verify that the stripping procedure with Glycine pH 2.5 did not remove all the protein on the blot, this western blot was re-incubated with anti-ε-sarcoglycan antibody followed by a secondary antibody incubation procedure. The result obtained (data not shown) was weaker but identical to figure 5.3.5.1, suggesting that most of the protein was not removed during the stripping procedure. Therefore, the thick 50kDa band (figure 5.3.5.1) represents the two ε-sarcoglycan isoforms merged together, rather than the 50kDa antibody heavy chain. For example, in figure 5.3.3, the SM lane of the forebrain contains saturated levels of the two isoforms that, similar to the IP lane in figure 5.3.5.1, also appear as one thick band.

Figure 5.3.5.2: Western Blot from figure 5.3.5.1 stripped with Glycine pH 2.5, and subsequently immunodeveloped with anti-rabbit secondary antibody.

The 47kDa and 49kDa ε-sarcoglycan isoforms are absent from the brain homogenate lane, suggesting that the stripping procedure was successful. The IP lane also contains no bands, suggesting that the primary anti-ε-sarcoglycan antibody was not removed from the column during the elution step of the immunoprecipitated complex. Protein loading is 20μg/lane. Lane 1, Brain Homogenate (BH); lane 2, immunoprecipitated material (IP); lane 3, Control. Molecular weight standards are indicated.

In order to test whether classical full-length dystrophin was also immunoprecipitated by the ε-sarcoglycan antibody and protein bound to the column, a duplicate immunoblot containing brain homogenate (solubilised with RIPA buffer), immunoprecipitated protein (IP) material, and a control, was incubated with anti-classical dystrophin antibody (figure 5.3.5.3). In the solubilised brain homogenate lane, the anti-classical dystrophin antibody picked up all 4 classical dystrophin isoforms. In the IP lane, none of the immunoprecipitated dystrophin proteins were enriched in this lane when compared to the brain homogenate fraction, with the most abundant isoform being cDp71, followed by 2 equally weaker cDp140 and cDp116 protein bands. Possibly negligible amounts of cDp427 were also present. In the control lane, only negligible amounts of unspecific binding were observed, representing the cDp140, cDp116 and cDp71 bands, therefore suggesting that classical dystrophin isoforms in the IP lane were specifically immunoprecipitated by the ε-sarcoglycan antibody cross-linked to the beads rather than by the beads themselves. In conclusion, the level of cDp427 in the IP lane is negligible, and given that cDp427 is the only dystrophin isoform expressed in neurons (Blake *et al*, 1999) where it forms classical dystrophin-containing DPC complexes exclusively at GABAergic PSD structures, this study, in agreement with figures 5.3.2-5.3.4, suggests that ε-sarcoglycan isoforms are not part of classical full-length dystrophin-containing complexes in neurons of the forebrain. Furthermore, given the low but existing levels of shorter classical dystrophin isoforms (cDp140, cDp116 and cDp71) in the IP lane, this result also suggests that outside neurons, where the shorter classical dystrophin isoforms reside (Blake *et al*, 1999), low amounts of ε-sarcoglycan may be part of non-neuronal classical dystrophin-containing complexes in the forebrain. However, given that the level of the short classical dystrophin isoforms that were immunoprecipitated by ε-sarcoglycan is low compared to that in the starting material, and that there is no enrichment compared to the brain homogenate level, it seems unlikely that ε-sarcoglycan complexes with these shorter dystrophin isoforms in the brain. However, it does seem likely that there may be other as yet unidentified binding partners in the brain.

Unfortunately, the anti-delta dystrophin antibody required to test whether delta dystrophin isoforms were immunoprecipitated by the anti-ε-sarcoglycan antibody was depleted. In order to overcome this problem, I decided to carry out a mass

spectrometry analysis study on ε-sarcoglycan interacting proteins, to investigate whether delta dystrophin would be identified in the list of ε-sarcoglycan associated proteins, and concominantly identify potential novel binding partners of ε-sarcoglycan. To achieve this, a large amount of anti-ε-sarcoglycan antibody was required and therefore it was necessary to raise an anti-ε-sarcoglycan antibody. The next section describes all the procedures for anti-ε-sarcoglycan antibody production.

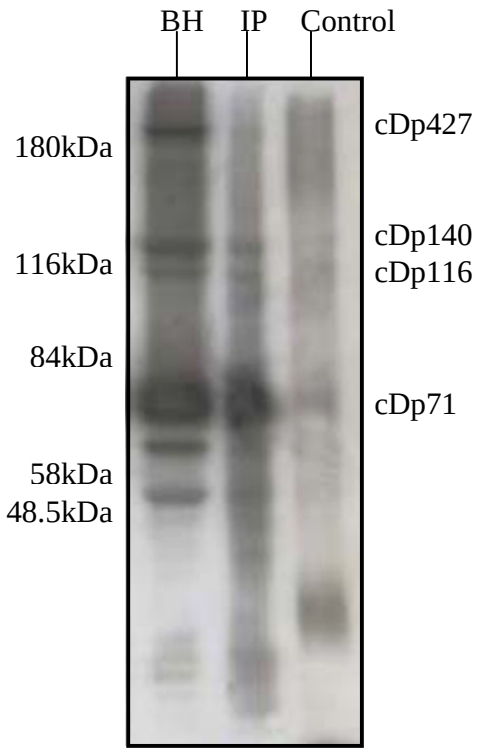

Figure 5.3.5.3: Western Blot containing immunoprecipitated classical dystrophin isoforms of the forebrain, immunodeveloped with anti-classical dystrophin antibody.

All four classical dystrophin isoforms, cDp427, cDp140, cDp116 and cDp71 are identified in the brain homogenate fraction. Only low levels of classical dystrophin isoforms are immunoprecipitated (IP lane). The highest level of immunoprecipitated protein is the cDp71 isoform, followed by cDp140 and cDp116 isoforms. The cDp427 isoform is possibly immunoprecipitated at negligible levels. The control lane depicts only negligible levels of unspecific binding between the non-cross-linked beads and the classical dystrophin isoforms (cDp140, cDp116 and cDp71), suggesting the proteins in lane 2 are pulled-down by the ε-sarcoglycan antibody rather than the beads. Given the low yield of immunoprecipiated material, it suggests that ε-sarcoglycan isoforms are likely to associate with other novel-binding partners. Protein loading is 20µg/lane. Lane 1, Brain Homogenate (BH); lane 2, immunoprecipitated material (IP); lane 3, Control. Molecular weight standards are indicated.

5.3.6 Anti-ε-sarcoglycan antibody production for the characterization of ε-sarcoglycan binding partners

There are no anti-ε-sarcoglycan antibodies currently available commercially that have been raised against the same epitope as the antibody used in this chapter, and our collaborators Derek DJ and Esapa CT had depleted their in-house ε-sarcoglycan antibody stock, which I had been supplied with. The next section therefore describes the various steps carried out in order to obtain an anti-ε-sarcoglycan antibody that recognized the same epitope as the anti-ε-sarcoglycan antibody used up to this point of the chapter. The aim was to use the antibody to further investigate the potential association between ε-sarcoglycan and classical and/or delta dystrophin-containing DPC components, as well as to investigate novel interacting partners of ε-sarcoglycan.

In order to begin the antibody production, collaborators Blake DJ and Esapa CT provided me with a pET32b vector containing a peptide (figure 5.3.6.1A) that they had previously utilised to raise their in-house anti-ε-sarcoglycan antibody. The pET32b vector was used to transform BL21 (DE3) competent cells, a type of *E.coli* cells that are compatible with the pET32b vector. The ε-sarcoglycan peptide inserted in the vector had been previously fused to a series of tags at its N-terminus, and a His tag at its C-terminus (figure 5.3.6.1B), such that it could be easily traced and isolated without the need of an anti-ε-sarcoglycan antibody. An SDS gel containing five samples of BL21 (DE3) cells that had each been transformed with the pET32b vector containing the ε-sarcoglycan peptide was stained with Coomassie Blue gel stain (figure 5.3.6.2). Each lane represents BL21 (DE3) cells grown in a different 1 L flask, and given the need to produce large (8mg) quantities of the ε-sarcoglycan epitope, a total of 5 L culture was grown. All BL21 (DE3) cells, except in lane 1, were treated with isopropyl β-D-1-thiogalactopyranoside (IPTG). As highlighted in figure 5.3.6.2, the IPTG treatment successfully induced the pET32b vector to express a large amount of the 33kDa ε-sarcoglycan peptide (lanes 2-5), when compared to BL21 (DE3) cells that did not receive IPTG treatment (lane 1). In order to reconfirm that the overexpressed protein was represented by the ε-sarcoglycan peptide, a duplicate SDS gel was western blotted (figure 5.3.6.3) and incubated with an anti-His antibody, recognizing the His-tag of the ε-sarcoglycan peptide fused at the N-

and C-terminal end of the peptide (figure 5.3.6.1). Figure 5.3.6.3 confirmed that the overexpressed 33kDa protein was indeed the ε-sarcoglycan peptide in all flasks treated with IPTG (lanes 2-5), whereas only low levels of expression of the ε-sarcoglycan peptide were present where no IPTG was added (lane 1). This suggested that cells were successfully transformed and IPTG clearly induced the transformed BL21 (DE3) cells to produce large quantities of the desired peptide.

A.

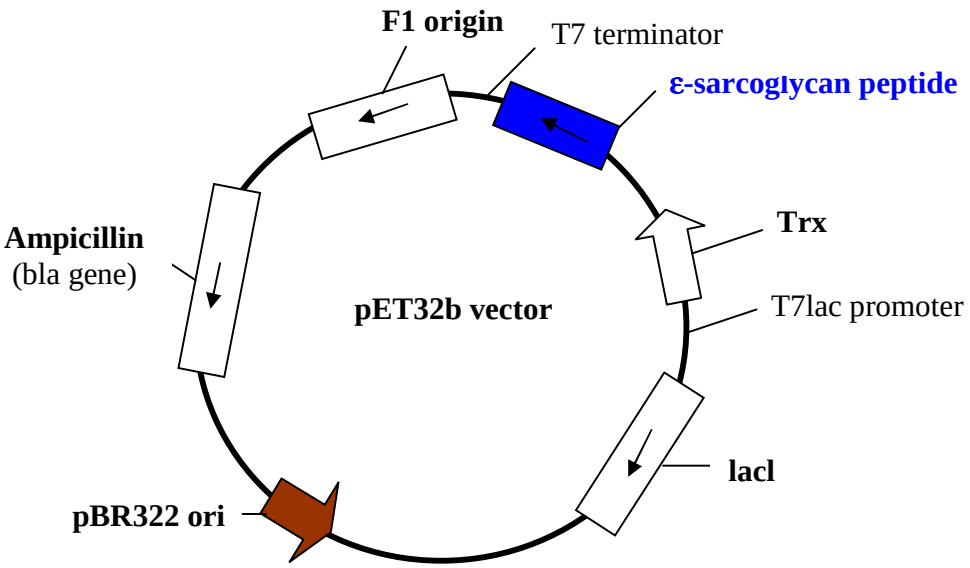

B.

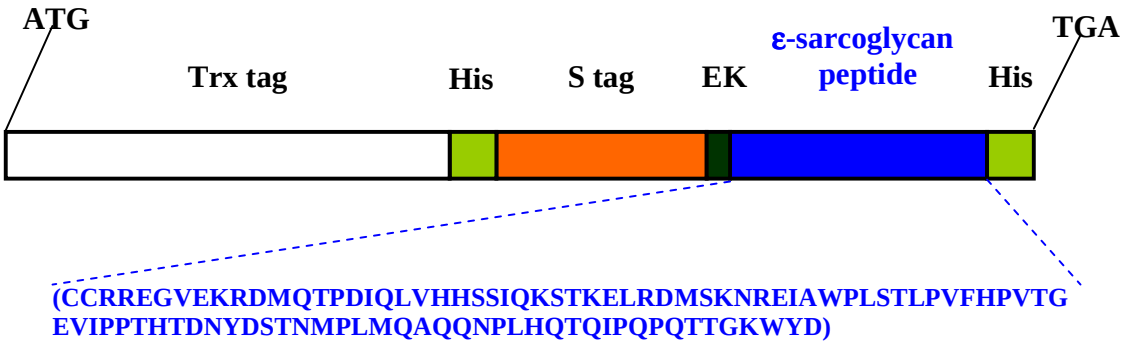

Figure 5.3.6.1: A pET32b vector designed for cloning and high-level expression of peptide sequences. ε-sarcoglycan peptide has been inserted in the Multiple Cloning Site (MCS).

A. The pET32b vector contains a T7lac promoter, T7 transcription terminator, *lac1* gene (lac repressor), pBR322 origins of replication, f1 for single-stranded plasmid production, and bla gene for ampicillin resistance. B. The ε-sarcoglycan peptide (accession number AAH12665) represents the last 98 amino acids (residues 316-413) of a 413 amino acid full-length ε-sarcoglycan protein. In the construct, the peptide contains a series of tags at its N-terminal end, and a His tag at its C-terminal end. The tags at the N-terminus of the peptide include thioredoxin (Trx), His tag, S-tag and an enterokinase (EK) tag. In brackets is the amino acid sequence of ε-sarcoglycan peptide (blue).

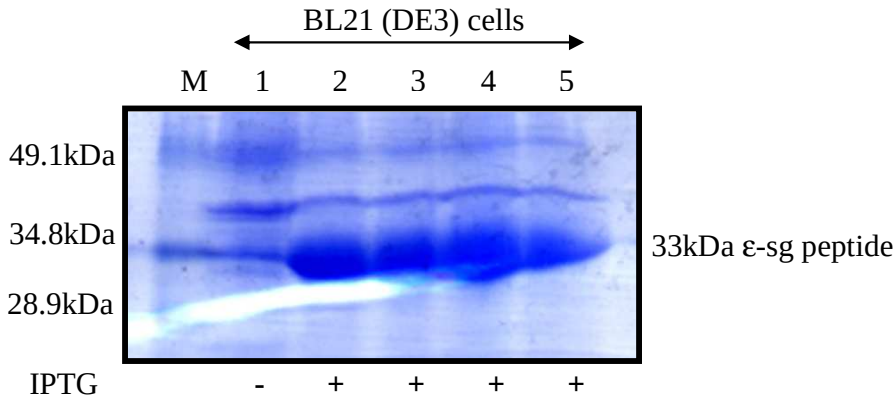

Figure 5.3.6.2: SDS PAGE separation of BL21 (DE3) cells transformed with the pET32b ε-sarcoglycan peptide and treated with IPTG.

Aliquots of BL21 (DE3) cells were separated on a 12% gel. Proteins were visualized with Coomassie blue. As a control, BL21 (DE3) cells were not treated with IPTG, to demonstrate BL21 (DE3) cells alone are not able to overexpress the peptide (lane 1). Lanes 2-5 represent BL21 (DE3) cells treated with IPTG, resulting in overexpression of the 33kDa ε-sarcoglycan band. Sample loading is 10μl/lane, from a total fraction of 1L. Lanes 1-5, BL21 (DE3) cells transformed with the pET32b vector containing the desired peptide. Molecular weight standards are indicated. IPTG, isopropyl β-D-1-thiogalactopyranoside.

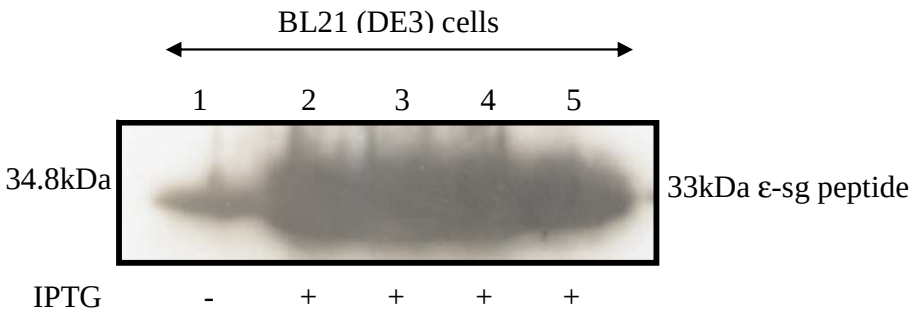

Figure 5.3.6.3: Western Blot of IPTG induced BL21 (DE3) cells immunodeveloped with anti-His antibody.

This study confirms that the overexpressed 33kDa band observed in figure 5.3.6.2 (lanes 2-5) corresponds to the ε-sarcoglycan peptide, given that the anti-His antibody was able to pick up the His tag found exclusively in the N and C-terminus of the overexpressed 33kDa ε-sarcoglycan peptide (lanes 2-5). The 33kDa ε-sarcoglycan peptide was the only immunoreactive band on the blot. Sample loading is 10μl/lane. Lanes 1-5, BL21 (DE3) cells transformed with the pET32b vector containing the desired peptide. Molecular weight standards are indicated. IPTG, isopropyl β-D-1-thiogalactopyranoside.

BL21 (DE3) competent cells containing the overexpressed ε-sarcoglycan peptide were lysed and their protein content was run through a Nickel column in order to isolate the ε-sarcoglycan peptide from the protein mixture found in BL21 (DE3) competent cells. Given that the Nickel column binds specifically to the His tag, which was only present in the ε-sarcoglycan peptide, the latter was able to specifically bind to the Nickel column, therefore allowing specific isolation of the peptide from the protein mixture found in BL21 (DE3) cells. An SDS gel containing the various steps of ε-sarcoglycan peptide purification was stained with Coomassie Blue gel stain (figure 5.3.6.4). Lanes 1 and 2 depict the ε-sarcoglycan peptide obtained from lysed BL21 (DE3) competent cells before and after binding to the Nickel column, respectively. Lanes 3 and 4 represent successful binding of the ε-sarcoglycan peptide to the Nickel column during the two washes through the Nickel column, as only negligible amounts of the ε-sarcoglycan peptide were eluted off from the column (lanes 3 and 4). Lanes 5-7 and 8-10 contained the ε-sarcoglycan peptide (33kDa) successfully eluted off the Nickel column with Elution Buffer (100mM NaH_2PO_4, 10mM Tris-HCl, 8M Urea) pH4.5 and pH5.9, respectively. High molecular weight doublet bands (asterisks) were visible in the eluted fractions, which may represent dimeric and trimeric forms of the ε-sarcoglycan peptide. However, these dimers and trimers were observed in the form of doublets. Given there is no glycosylation in BL21 (DE3) cells, the doublets may not represent different glycosylated dimeric and trimeric forms of the single 33kDa ε-sarcoglycan peptide eluted from the column. When a duplicate SDS gel was western blotted and incubated with anti-His antibody (figure 5.3.6.5), it demonstrated that the 33kDa eluted protein from the Nickel column was indeed the ε-sarcoglycan peptide (lanes 2-6), that the peptide was completely eluted from the column (lane 7), and that only a single band from the dimer (asterisk) and from the trimer (asterisk) was identified by the His antibody, indicating that only these are indeed ε-sarcoglycan dimeric and trimeric aggregations, respectively. Therefore, the remaining bands next to the ε-sarcoglycan dimer and trimer (figure 5.3.6.4, lanes 6-10) could represent endogenous proteins that lack Histidine residues but associated non-specifically with the ε-sarcoglycan tagged protein, and consequently eluted with the ε-sarcoglycan peptide (figure 5.3.6.4, lanes 6-10).

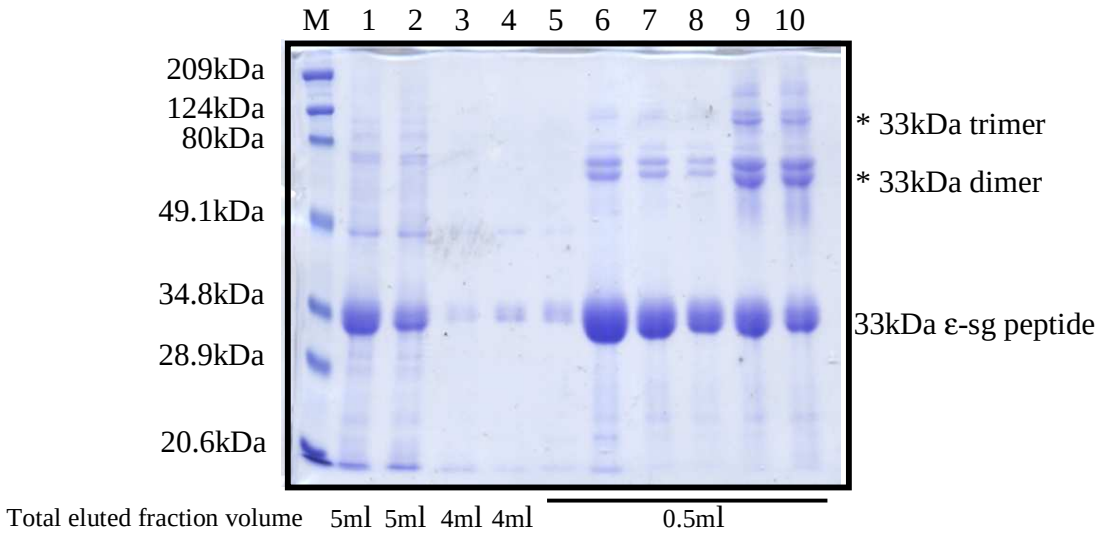

Figure 5.3.6.4: SDS PAGE separation of ε-sarcoglycan peptides isolated using a Nickel Column.

Cleared lysates of IPTG-induced BL21 (DE3) cells containing the overexpressed ε-sarcoglycan peptides were separated on a 12% SDS gel. Proteins were visualized with Coomassie blue. Lanes 1 and 2 originate from the same batch of total volume of lysed IPTG-induced BL21 (DE3) cells, before (lane 1) and after (lane 2) the addition to the Nickel column, respectively. Only half of the peptide introduced (lane 1) exited the column (lane 2), suggesting enough peptide had successfully bound to the column until the column became saturated thus allowing the surplus peptide to exit the column. Lanes 3 and 4 confirmed that almost none of the bound ε-sarcoglycan peptide detatched from the Nickel column during the washing procedure. Lanes 5-7 and 8-10 depict the peptide was successfully eluted from the column with Elution Buffer pH4.5 and pH5.9, respectively, eliminating contaminating proteins normally found in BL21 (DE3) cells. Sample loading is 10µl/lane. Due to variations in the total eluted fraction volumes from which lanes 1-10 were obtained, appropriate dilutions on the sample for loading were carried out, such that each sample loaded was as if it originated from the same total eluted volume. Lane 1, ε-sarcoglycan before its addition to the nickel column; lane 2, surplus ε-sarcoglycan that did not bind to the Nickel column; lane 3-4, washes of the nickel column bound to ε-sarcoglycan peptides; lane 5-10, elution of the ε-sarcoglycan peptide. Molecular weight standards are indicated. *, potential dimeric and trimeric forms of the ε-sarcoglycan peptide. IPTG, isopropyl β-D-1-thiogalactopyranoside.

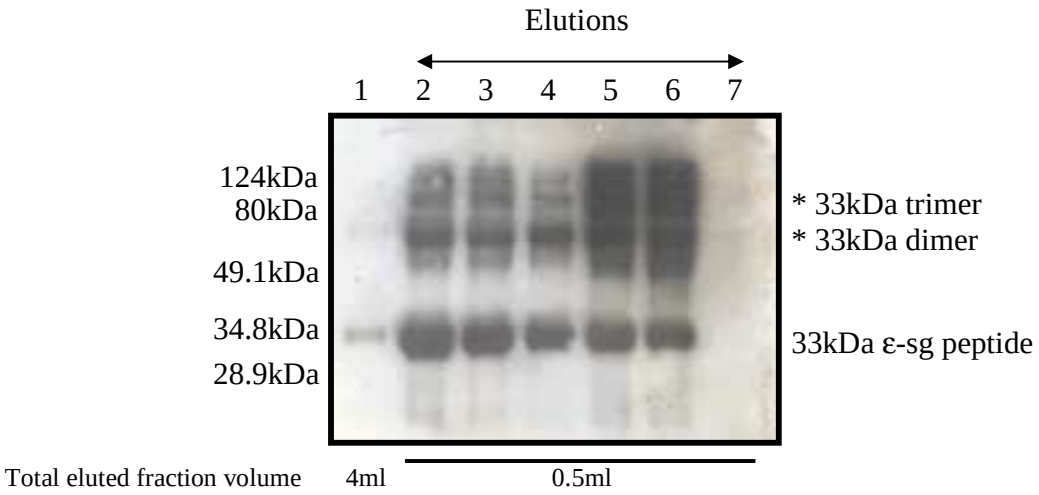

Figure 5.3.6.5: Western Blot of purified 33kDa ε-sarcoglycan peptides immunodeveloped with anti-His antibody.

In lanes 2-6, the anti-His antibody was able to recognize the His tag of a 33kDa protein, confirming it is the ε-sarcoglycan peptide. Lane 7 confirms that all the peptides bound to the column were successfully eluted within lanes 2-6, as no ulterior peptide is eluted in lane 7. Lane 1 demonstrates that most of the ε-sarcoglycan peptide remains bound to the column during the wash procedure, as only negligible levels elute during the wash procedure (lane 1). Sample loading is 10µl/lane. Due to variations in the total eluted fraction volumes from which lanes 1-7 were obtained, appropriate dilutions on the sample for loading were carried out, such that each sample loaded was as if it originated from the same total eluted volume. Lane 1, wash; lanes 2-7, elution of the ε-sarcoglycan peptide. Molecular weight standards are indicated. *, confirmed dimeric and trimeric formation of ε-sarcoglycan peptide.

As shown in figure 5.3.6.1, the N-terminus of the ε-sarcoglycan peptide contained a variety of tags that may induce an unwanted immunogenic response, which could generate an antibody against the tag or part of the tag, rather than the peptide of interest. Therefore all four tags found at the N-terminus of the ε-sarcoglycan peptide were removed by recombinant enterokinase (rEK) treatment, an enzyme that cuts the enterokinase (EK) tag found adjacent to ε-sarcoglycan (figure 5.3.6.1), leading to the immediate removal of all tags found at the N-terminus of the ε-sarcoglycan peptide. An SDS gel containing the overexpressed ε-sarcoglycan peptide before and after rEK treatment was stained with Coomassie Blue gel stain (figure 5.3.6.6). Lane 1 contained the ε-sarcoglycan peptide (33kDa) prior to enzyme cutting and detachment of the N-terminal tag sequence from the ε-sarcoglycan peptide. Lanes 2-7 show the tag (18kDa) was successfully removed from the 33kDa peptide at different enzyme incubation time-points. The 14kDa band represents the ε-sarcoglycan peptide without the tags. S-tag Agarose beads already cross-linked to an anti-S-tag-antibody were utilised to promote the association between the S-tag found in the 18kDa peptide and the anti-S-tag antibody cross-linked to the beads, such that the 14kDa ε-sarcoglycan peptide remaining in solution contained almost no contamination by the 18kDa tag. An SDS gel (figure 5.3.6.7) demonstrating the successful isolation of a purified ε-sarcoglycan peptide (lane 1, 2) from the tag (lane 3, 4) was stained with Coomassie Blue gel stain. Lanes 1 and 2 only contained the ε-sarcoglycan peptide, therefore the peptide does not appear contaminated by the 18kDa tag. Lanes 3 and 4 only contained the 18kDa tag, suggesting no visible contamination with the ε-sarcoglycan peptide. Figure 5.3.6.7 demonstrates that the two enzyme digest products were successfully separated from one another. A Folin-Lowry protein assay was carried out in order to measure a total of 3mg of the 14kDa ε-sarcoglycan peptide, which was subsequently lyophilized before being sent to Sigma-Genosys, where the immunization for rabbit polyclonal antibody production took place in two rabbits.

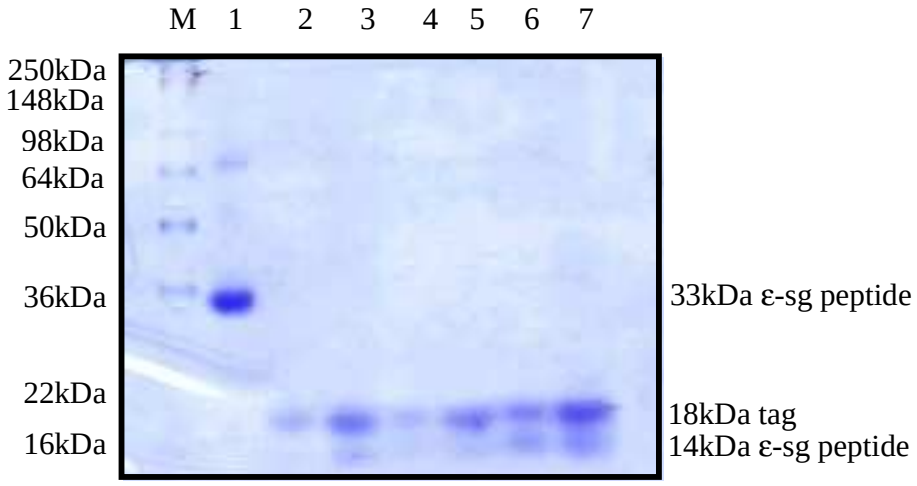

Figure 5.3.6.6: SDS PAGE separation of 18kDa tag and a 14kDa ε-sarcoglycan peptide obtained by recombinant Enterokinase (rEK) digestion of the 33kDa ε-sarcoglycan peptide.

The experiment was carried out according to Materials and Methods (section 5.22). Aliquots of the 33kDa ε-sarcoglycan peptide mixed with the 97kDa rEK enzyme were separated on a 10% gel. Proteins were visualized with Coomassie blue. Lane 1 contains the 33kDa ε-sarcoglycan peptide prior to digestion with rEK. Lanes 2-7 show the 33kDa peptide is successfully digested into a 14kDa ε-sarcoglycan peptide and 18kDa tag at different incubation time-points. The optimal incubation time is 16hours (lane 7), where the digestion gives the highest level of digested peptide. Sample loading is 10µl/lane from a total volume of 50µl. Lane 1, undigested ε-sarcoglycan peptide; lane 2, 1:50 (enzyme: protein concentration) two hours rEK incubation; lane 3, 1:100 two hours rEK incubation; lane 4, 1:50 four hours rEK incubation; lane 5, 1:100 four hours rEK incubation; lane 6, 1:50 sixteen hours rEK incubation; lane 7, 1:100 sixteen hours rEK incubation. Molecular weight standards are indicated.

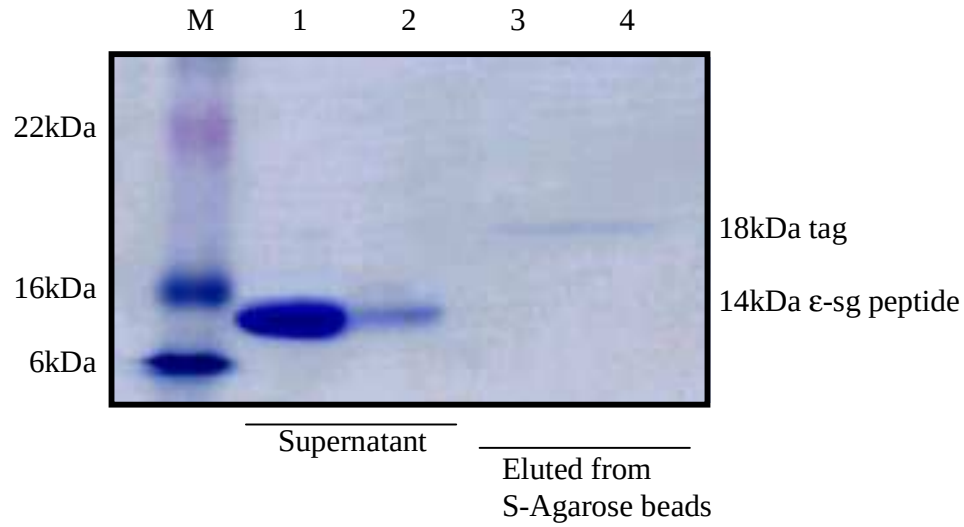

Figure 5.3.6.7: SDS PAGE separation of the purified 14kDa ε-sarcoglycan peptide.
The experiment was carried out according to Materials and Methods (section 5.23). Separate aliquots of the purified 18kDa tag and 14kDa ε-sarcoglycan peptide were separated on a 12% gel. Proteins were visualized with Coomassie blue. After a 16 hour digestion of the 8mg ε-sarcoglycan peptide by the rEK enzyme, equal amounts of the 18kDa tag and 14kDa ε-sarcoglycan peptide were generated. S-Agarose beads, capable of binding to the S-tag found in the 18kDa tag, were added to the digest and allowed to bind to the S-tag. Subsequently, the solution was centrifuged, generating a pellet containing the 18kDa tag bound to the S-Agarose beads, and a supernatant with an uncontaminated 14kDa ε-sarcoglycan peptide preparation. Lanes 1-2 demonstrate the 14kDa ε-sarcoglycan peptide found in the supernatant is not contaminated by the presence of the 18kDa tag. Lanes 3-4 demonstrate that the 18kDa tag eluted from the S-Agarose beads does not contain residual amounts of 14kDa ε-sarcoglycan peptides. Protein loading is 10µl/lane. Lanes 1-2, 14kDa ε-sarcoglycan peptide; lanes 3-4, 18kDa tag. Molecular weight standards are indicated.

Prior to the arrival of the antibody, dynabeads were cross-linked with the 33kDa ε-sarcoglycan peptide. Upon the arrival of the immunized serum, the latter was run through a column containing dynabeads cross-linked to the 33kDa ε-sarcoglycan peptide, to affinity purify the antiserum such that only the antibody raised against the ε-sarcoglycan peptide was present in the eluate. The bound antibody was then eluted from the column. Table 5.3.6 represents the spectrophotometer readings denoting which elution contained the anti-ε-sarcoglycan antibody eluted from the column. In order to test the ability of the antibody to recognize the native ε-sarcoglycan protein, as well as the ε-sarcoglycan peptide, western blots containing forebrain homogenates and the purified 33kDa ε-sarcoglycan peptide were incubated with the newly purified anti-ε-sarcoglycan antibody (figure 5.3.6.8). The newly purified anti-ε-sarcoglycan antibody was only able to recognize the 33kDa ε-sarcoglycan peptide whereas it was unable to pick-up the native ε-sarcoglycan protein. A duplicate western blot was prepared (figure 5.3.6.9) and incubated with the last aliquot of anti-ε-sarcoglycan antibody provided by our Oxford collaborators, in order to determine whether the inability to detect the native ε-sarcoglycan protein was due to our in-house antibody or whether it was due to the brain homogenate preparation. According to this study (figure 5.3.6.9), the antibody clearly detected both the 33kDa ε-sarcoglycan peptide and the native 47kDa and 49kDa ε-sarcoglycan isoforms, confirming that the newly purified anti-ε-sarcoglycan antibody is not able to recognize ε-sarcoglycan isoforms in the brain homogenate, and cannot be used further to purify ε-sarcoglycan binding proteins for identification by Mass Spectrometry.

Column elutions* *0.1M Glycine pH 2.5	**Spectrophotometer Reading for protein determination (280nm)**
Fraction 1, 1ml	0.00
Fraction 2, 1 ml	0.02
Fraction 3, 1ml	**0.41**
Fraction 4, 1ml	**0.90**
Fraction 5, 1ml	**0.60**
Fraction 6, 1ml	0.13
Fraction 7, 1ml	0.06
Fraction 8, 1ml	0.03

Table 5.3.6: Spectrophotometer reading used to identify the elution containing the new anti-ε-sarcoglycan antibody.

A column cross-linked to the 33kDa ε-sarcoglycan peptide as described in materials and methods (section 6.12) was used to affinity purify the new anti-ε-sarcoglycan antibody present in the rabbit antiserum. The antibody eluted in the third, fourth and fifth eluted fractions, where the spectrophotometer reading is the highest (red). The reading of the remaining eppendorf tubes is negligible suggesting that the new anti-ε-sarcoglycan is concentrated in eppendorfs 3, 4, 5 only.

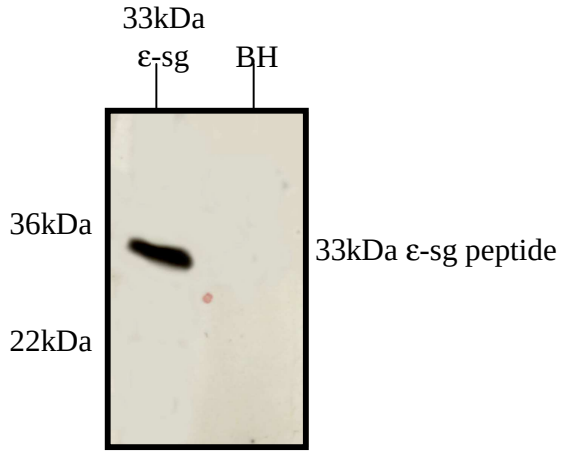

Figure 5.3.6.8: Western Blot containing a forebrain homogenate preparation, and an aliquot of pure 33kDa ε-sarcoglycan peptide, immunodeveloped with the new anti-ε-sarcoglycan antibody.

In the lane containing a preparation of pure 33kDa ε-sarcoglycan peptide, the new anti-ε-sarcoglycan antibody is capable of recognizing the 33kDa peptide. However it is unable to recognize the native 47kDa and 49kDa ε-sarcoglycan isoforms that are known to be expressed in the brain homogenate (BH lane). These results demonstrate that although the antibody production was successful it was not able to recognize native ε-sarcoglycan in brain homogenate. Protein loading is 20μg/lane. Lane 1, pure aliquot of 33kDa ε-sarcoglycan peptide. Lane 2, Brain Homogenate (BH). Molecular weight standards are indicated.

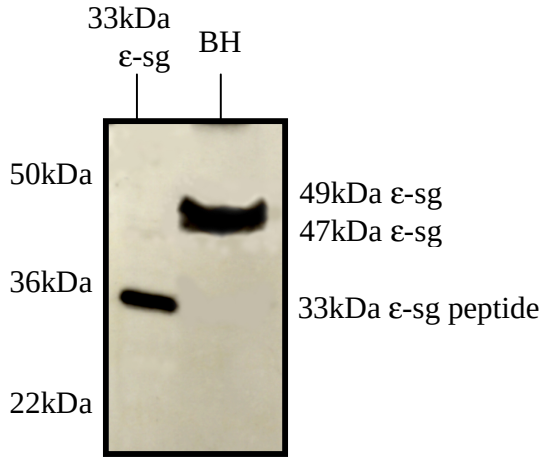

Figure 5.3.6.9: Western Blot containing a forebrain homogenate preparation, and an aliquot of pure 33kDa ε-sarcoglycan peptide, immunodeveloped with the last aliquot of anti-ε-sarcoglycan antibody provided by our Oxford collaborators.

In contrast with the new anti-ε-sarcoglycan antibody, the original anti-ε-sarcoglycan antibody provided by the Oxford collaborators is able to recognize the 33kDa peptide in the lane containing a preparation of pure 33kDa ε-sarcoglycan peptide, and it is also able to recognize the native 47kDa and 49kDa isoforms in the brain homogenate fraction. Protein loading is 20μg/lane. Lane 1, pure aliquot of 33kDa ε-sarcoglycan peptide. Lane 2, Brain Homogenate (BH). Molecular weight standards are indicated.

5.4 Discussion:

5.4.1 ε-sarcoglycan is likely to form novel complexes in the brain that are not related to dystrophin protein complexes

The data in this chapter highlights clear differences in the patterns of subcellular distribution of ε-sarcoglycan isoforms (figure 5.3.3) when compared to classical full-length dystrophin (Chapter 3, figure 3.2.4.1) in forebrain and cerebellar subcellular fractions. In fact, classical full-length dystrophin and associated DPC components enrich in PSDs of both forebrain and cerebellum (Chapter 3; figure 3.2.3.2, 3.2.3.3 and 3.2.4.1), more precisely, in neurons of the brain they have been shown to localize exclusively at PSD structures of GABAergic synapses (Blake *et al*, 1999; Brunig *et al*, 2002; Culligan *et al*, 2002). Contrary to classical full-length dystrophin and associated DPC components, neither 47kDa nor 49kDa ε-sarcoglycan isoforms enrich in the PSD fraction of the forebrain or cerebellum (figure 5.3.2 and 5.3.3). Instead, both isoforms predominantly occur in membrane fractions of non-synaptic (LM and microsomes) and primarily synaptic origin (SM) of the forebrain and cerebellum (figure 5.3.2, 5.3.3). What is more, the immunocolocalization study presented in this chapter is in agreement with the biochemical data, as it highlights that ε-sarcoglycan isoforms are not part of PSD structures of GABAergic synapses containing classical dystrophin, as ε-sarcoglycan isoforms do not co-localize with classical dystrophin (figure 5.3.4) therein. Lastly, the staining pattern of ε-sarcoglycan isoforms presumably along the membrane of the neurone (figure 5.3.4) does not resemble the typical punctate staining pattern of classical dystrophin and associated DPC components found at the soma and along proximal dendrites (Chapter 4, figure 4.2.6, 4.2.7). In conclusion, the results presented in this chapter strongly suggest that although ε-sarcoglycan and delta dystrophin are expressed in the same neurons, ε-sarcoglycan isoforms may not be part of classical full-length dystrophin-containing DPC complexes at GABAergic synapses in neurons, rather, they are likely to form novel and yet unidentified protein complexes at the membrane of neurons.

The data in this chapter also highlights clear differences in the patterns of subcellular distribution of ε-sarcoglycan isoforms (figure 5.3.3) when compared to delta full-length dystrophin (Chapter 4, figure 4.2.11.1) in forebrain and cerebellar subcellular fractions. In fact, delta full-length dystrophin is highly enriched in the microsomal fraction, to a lesser extent in other membrane fractions, and only moderately enriched in the PSD fraction of the forebrain and cerebellum (Chapter 3, figure 3.2.4.2). In contrast, the 47kDa and 49kDa ε-sarcoglycan isoforms predominantly occur in membrane fractions of non-synaptic (LM and microsomes) and primarily synaptic origin (SM) of the forebrain and cerebellum (figure 5.3.2, 5.3.3). The immunocolocalization study presented in Chapter 4 (figure 4.2.10) confirms the differences in subcellular distribution between delta dystrophin and ε-sarcoglycan isoforms, as it clearly demonstrates that delta dystrophin exclusively co-localizes with the microtubule (MT) cytoskeleton found throughout the central parts of the entire neuron, away from the membrane (Chapter 4, figure 4.2.8). This is a very different subcellular distribution when compared to the exclusive neuronal membrane enrichment and localization of both ε-sarcoglycan isoforms (figure 5.3.2, 5.3.3; Esapa *et al*, 2007). Therefore, these results suggest that due to the different compartmentalization restrictions, ε-sarcoglycan isoforms are unlikely to associate with delta dystrophin-containing DPC complexes at MT structures within forebrain and cerebellar neurons. Instead, ε-sarcoglycan isoforms are likely to form novel, yet unidentified proteins complexes at the membrane of neurons. Furthermore, ε-sarcoglycan staining was only identified in a subpopulation of neurons viewed under the microscope, whereas delta dystrophin was found in most if not all neurons, including neurons expressing ε-sarcoglycan. This result further reinforces the conclusion that ε-sarcoglycan isoforms and delta dystrophins are not part of the same protein complex in neurons.

According to the results presented in figure 5.3.3, in membrane fractions of the forebrain and cerebellum, the level of expression and distribution exhibited by the two ε-sarcoglycan isoforms is not identical. In fact, figure 5.3.3 highlights that in the forebrain, both 47kDa and 49kDa ε-sarcoglycan isoforms are expressed at higher levels when compared to the respective membrane fractions of the cerebellum, suggesting that the level of expression of the isoforms in the membrane fractions are regionally controlled. What is more, unlike the 47kDa isoform, the 49kDa isoform is differentially

expressed within the membrane fractions of the forebrain when compared to the membrane fractions in the cerebellum. Lastly, significantly only the 47kDa isoform is present in the myelin fraction of the forebrain and cerebellum, suggesting that the 47kDa and 49kDa isoforms not only exhibit differential localization within the cerebellum, but also within the forebrain. Altogether these results suggest that the level of expression and distribution of the two isoforms in the two brain regions is highly regulated. On the other hand, the different subcellular distributions of ε-sarcoglycan isoforms in the two brain regions may reflect the differences in glycosylation of the isoforms, as opposed to true differences in their expression patterns. It is important to add that the patterns of level of expression of these sarcoglycan isoforms in the two regions is also very different from that of classical and delta dystrophin isoforms, further reinforcing the hypothesis that ε-sarcoglycan isoforms form novel protein complexes independent of classical and delta dystrophin.

The immunoprecipitation study used to re-investigate the association potentials between ε-sarcoglycan and classical dystrophin isoforms within the forebrain highlights a very faint, almost undetectable, cDp427 band being immunoprecipitated by ε-sarcoglycan antiserum (figure 5.3.5.3). Classical full-length dystrophin (cDp427) is a neuron-specific isoform that exclusively localizes at PSDs of GABAergic synapses (Brunig *et al*, 2002). Given that the biochemical studies presented in this chapter (figure 5.3.2, 5.3.3) highlight a weak doublet ε-sarcoglycan band in the PSD fraction of forebrain and cerebellum (figure 5.3.2, 5.3.3), the results cannot exclude the possibility that such a very small amount of ε-sarcoglycan may indeed reside in PSDs and interact with the cDp427 isoform localized therein. However, most if not all of cDp427 remained unbound in the starting brain homogenate material (figure 5.3.5.3, lane 1) used for the immunoprecipitation study, therefore suggesting that most if not all of the cDp427 is unlikely to associate with the ε-sarcoglycan isoforms, in agreement with the immunocytochemical study (figure 5.3.4), therefore suggesting ε-sarcoglycan isoforms are likely to associate with other novel, yet unidentified binding partners. Kinugawa *et al* (2009) describes that in MDS patients containing mutated ε-sarcoglycan proteins, the GABAergic inhibitory system is functionally intact. This statement further reinforces the conclusions from our studies that in neurons, ε-sarcoglycan isoforms are unlikely

components of DPC complexes in GABAergic synapses, otherwise the functions of the GABAergic system in MDS patients would have been altered.

The immunoprecipitation study highlights that higher levels of cDp140 and cDp71 isoforms were also immunoprecipitated by ε-sarcoglycan isoforms (figure 5.3.5.3, lane 3). cDp140 and cDp71 isoforms are reported to locate exclusively in astrocytic cells (Blake *et al*, 1999; Culligan *et al*, 2002), and given that only the 47kDa (not the 49kDa isoform) ε-sarcoglycan isoform is known to be expressed in astrocytes (Nishiyama *et al*, 2004), the results suggest that in vivo, the 47kDa ε-sarcoglycan isoform may interact with the cDp140 and cDp71 isoforms in astrocytes and therefore be a component of classical dystrophin-containing DPC complexes therein. However, given that the band intensity of each of the immunoprecipitated short classical dystrophin isoforms (figure 5.3.5.3, lane 3) was much less concentrated when compared to the classical dystrophin isoforms band intensity found in the starting material (figure 5.3.5.3, lane 1), it is likely that in forebrain, at least most of the classical dystrophin isoforms are not associated with ε-sarcoglycan. This again raises the possibility that ε-sarcoglycan isoforms associate with other as yet unidentified partners to form novel complexes. It is often hypothesized in the literature that brain ε-sarcoglycan may possibly associate with other kinds of membrane proteins and/or cytoskeletal proteins rather than the DPC complex (Nishiyama *et al*, 2004; Esapa *et al*, 2007), in agreement with the data presented in this chapter. To date, the proteins interacting with ε-sarcoglycan in the brain have yet to be identified.

The brain is not the only organ whose ε-sarcoglycan protein may function independently from the DPC complex. The kidney and retina also contain ε-sarcoglycan proteins that do not associate with DPC complexes (Fort *et al*, 2005; Durbeej *et al*, 1999). In the kidney, both ε-sarcoglycan and DPC components are expressed within the same cell, but similarly to that observed in our cortical cultures (figure 5.3.4), they are differentially distributed and therefore do not interact (Durbeej *et al*, 1999). Also in neurons of the retina, ε-sarcoglycan is not part of the DPC complex (Fort *et al*, 2005), whereas in photoreceptor terminals of the retina, ε-sarcoglycan does associate with DPC components (Fort *et al*, 2005). Therefore, there are specific cells in the retina where ε-sarcoglycan does associate with DPC components and other cell-types where ε-sarcoglycan is independent of DPC complexes (Fort *et al*, 2005). In the lung also,

depending on the cell-type, ε-sarcoglycan is either associated with the DPC complex or due to compartmentalization restrictions, may be found independently from the DPC complex (Durbeej *et al*, 1999). These studies therefore strongly indicate that the function of ε-sarcoglycan can also work independently of the DPC complex, and that the brain may well contain ε-sarcoglycan proteins that function independently of DPC complexes.

The anti-ε-sarcoglycan antibody used in this chapter was unable to distinguish the 47kDa isoform from the 49kDa isoform, as the antibody recognised an epitope found in both isoforms, therefore from the immunoprecipitation study in figure 5.3.5.3, it was impossible to decipher which of the two ε-sarcoglycan isoforms was associated with which of the immunoprecipitated classical dystrophin isoforms. Similarly in our cortical neuronal study (figure 5.3.4), it was impossible to determine whether both ε-sarcoglycan isoforms were co-expressed in the same cells or same parts of the cells, or whether each isoform was expressed in a cell-type specific manner or in different membrane compartments of the same cell. It would therefore be interesting to generate an antibody against exon 8 or exon 11b, the two epitopes that distinguish the 47kDa ε-sarcoglycan isoform from the 49kDa ε-sarcoglycan isoform (chapter 1; figure 1.1.2.1) respectively. These could be used in immunocytochemical studies to establish their cellular localizations throughout the entire brain. Secondly, each ε-sarcoglycan antibody could be cross-linked to a separate column, in order to search for proteins that may specifically interact with their unique cytoplasmic tails, for subsequent analysis by Mass Spectrometry and ultimately the functions of any such proteins identified. These antibodies, in concomitance with other antibodies against the DPC components, would also allow to determine by immunocytochemical techniques, whether in analogy to the retina (Durbeej *et al*, 1999; Fort *et al*, 2005), the brain 47kDa and 49kDa ε-sarcoglycan isoforms may or may not be part of DPC complexes in some cells and be independent of DPC complexes in other cell-types.

In this thesis I have also attempted to produce a new anti-ε-sarcoglycan antibody such that a number of immunopurification studies could be carried out, and Mass Spectrometry could be used to investigate the nature of the immunopurified components of the complexes interacting with the 47kDa and 49kDa ε-sarcoglycan isoforms. Unfortunately the new antibody was only able to recognize the ε-sarcoglycan

peptide but not the native ε-sarcoglycan protein on western blots. I confirmed that the ε-sarcoglycan peptide used for the immunization of the rabbit was not defective, as a small aliquot of anti-ε-sarcoglycan antibody gift remaining from our previous experiments was able to recognize the peptide, as well as the native protein, suggesting that the peptide contained an unmutated epitope against which an antibody could be successfully raised. One possible explanation as to why the new in-house antibody did not pick up the native ε-sarcoglycan protein may be that the new in-house antibody may recognize part, if not all, of the His tag left at the C-terminus of the 14kDa ε-sarcoglycan peptide used for the immunization. As a consequence, the new antibody would be unable to pick-up the native protein lacking the His tag, whereas it consistently recognized the ε-sarcoglycan peptide containing the His-tag. Another possibility is that the antibody was of low affinity and hence only recognized high concentrations of the peptide, but was not sufficiently sensitive to detect the lower concentrations of ε-sarcoglycan present in tissue samples. A third possibility is that the epitope recognized on the peptide is blocked in the full-length proteins, for example, as a result of glycosylation. For the future, in addition to the generation of antibodies specific for either the 47kDa isoform, or the 49kDa isoform, it would be interesting to also generate a new anti-ε-sarcoglycan antibody recognizing both isoforms, cross-link this antibody to a column, isolate the proteins that interact with ε-sarcoglycan isoforms, and subsequently identify these associated proteins by Mass Spectrometry. These antibody productions will provide an important step forward towards the understanding of the function of ε-sarcoglycan isoforms in the brain.

The function of ε-sarcoglycan remains largely unknown (Tai *et al*, 2009), although it is well accepted that mutation of ε-sarcoglycan causes Myoclonus Dystonia (MDS; Chapter 1, part two). MDS patients with ε-sarcoglycan mutations do not show any signs of muscle disease, SGCE mutations appear to induce only neurological disorders (Hjermind *et al*, 2008). Further elucidations of the cellular localization of ε-sarcoglycan in mammalian brain will be important in the identification of candidate neuronal groups and circuits through which ε-sarcoglycan mutations lead to the specific psychiatric symptom complex associated with MDS (Chan *et al*, 2005). The membrane localization of ε-sarcoglycan isoforms (figures 5.3.2 & 5.3.3) and their expression in the mouse brain monoaminergic neurons (Chan *et al*, 2005) suggests that the symptom complex of MDS

may be related to the effects of decreased ε-sarcoglycan activity on the development or function of these neurons (Chan *et al*, 2005). Other neuronal-types have been found to express ε-sarcoglycan although the nature of these neurons remains to be identified, suggesting that ε-sarcoglycan may also influence neurotransmission by these neurons (Chan *et al*, 2005). The expression of the 47kDa ε-sarcoglycan isoform in astrocytes of the brain (Nishiyama *et al*, 2004) suggests that decreased ε-sarcoglycan activity in glial functions may also be a contributing factor to MDS, although this remains to be verified. Esapa *et al* (2007) suggested one possible mechanism by which a mutation of the ε-sarcoglycan protein may lead to MDS. According to their studies, ε-sarcoglycan proteins containing mutations in the extracellular region are retained intracellularly and degraded by the proteosome. In other words, the ε-sarcoglycan mutant is no longer allowed to reach the plasma membrane where its functions are carried out. Therefore Esapa *et al* (2007) suggest MDS is probably caused by a loss of ε-sarcoglycan function at the plasma membrane. Esapa *et al* (2007) also suggest that ε-sarcoglycan, a membrane-associated protein (figure 5.3.2 & 5.3.3), is expressed in neurons of the basal ganglia and cerebellum (Esapa *et al,* 2007) and may therefore co-operate with other membrane proteins to modulate the activity of these neurons (Esapa *et al*, 2007). Hjermind *et al*, 2008 hypothesised that the major cause of MDS might be related to the existence of a brain-specific isoform, which may have brain-specific intracellular interactions that play a role in neuronal differentiation and synaptic transmission, as suggested in mice (Hjermind *et al*, 2008). When mutated, such a brain specific isoform gives rise to neurological disorders without affecting the muscle. It is clear from these studies that a lot of further work needs to be carried out before the mechanisms underlying MDS are understood.

The 47kDa and 49kDa isoforms exhibit structural differences at their cytoplasmic tails (Nishiyama *et al*, 2004), but the significance of these differences remains unresolved. No studies have yet investigated whether these structural differences may influence the trafficking of the protein. The results in this chapter, in agreement with Nishyama *et al* (2004), suggest differential localization of the two isoforms in forebrain and cerebellum subcellular fractions, which I suggest it may be due to their different cytoplasmic domains, although this hypothesis remains to be verified. Nishiyama *et al* (2004) suggest that the structural differences at their C-terminus may cause ε-sarcoglycan isoforms to play different roles at synapses within neurons of the forebrain and

cerebellum. However this hypothesis also remains to be verified. The extracellular domain of either ε-sarcoglycan isoform contains putative cadherin-like domains and a calcium-binding pocket which is typically found in proteins involved in homotypic or heterotypic interactions with other glycoproteins (Dickens *et al*, 2002; Ozawa *et al*, 2005), it is therefore possible that ε-sarcoglycan may also be implicated in similar interactions, although this hypothesis remains to be verified. Proteins containing a cadherin domain have also been shown to modulate a wide variety of processes, such as cell polarization (Tepass *et al*, 2000), migration (Tepass *et al*, 2000) as well as cell adhesion (Dickens *et al*, 2002). Developmental studies on ε-sarcoglycan have suggested its participation in the early development of brain, muscle, liver, kidney and heart tissue, due to its high levels of expression in fetal life of rats when compared to adult life (Hjermind *et al*, 2008). The cadherin-like domains in the ε-sarcoglycan protein may be involved in modulating polarization and/or migration and /or adhesion during development, although again this hypothesis remains to be verified. It is clear that a large number of studies need to be carried out before the function of ε-sarcoglycan in the brain is understood.

In conclusion, based on the results presented in this chapter, ε-sarcoglycan is unlikely to be a component of classical and delta dystrophin-containing DPC complexes, rather, it is a membrane protein that is part of novel, yet unidentified, complexes in the brain.

Chapter 6

6.1 Conclusions

The work carried out in this thesis has led to the following novel conclusions:

6.1.1 Part 1

- Biochemical studies presented in this thesis suggest classical and delta dystrophin exhibit different regional and subcellular distribution in forebrain and cerebellum. The level of expression of classical dystrophin is higher in the cerebellum when compared to the forebrain, whereas the level of expression of delta dystrophin is lower in the cerebellum when compared to the forebrain.

- Biochemical studies confirm the published data showing that classical full-length dystrophin is exclusively enriched in PSDs of the forebrain and cerebellum (chapter 3, figure 10).

- Biochemical studies show that in the forebrain and cerebellum, contrary to classical dystrophin, delta dystrophin is most highly enriched in microsomes and only moderately enriched in the PSD fraction.

- Immunocytochemical data shows delta dystrophin is in fact an extra-synaptic protein that fully co-localizes with β3-tubulin (chapter 4, figure 10), a component of the microtubule (MT) cytoskeleton. Therefore, delta dystrophin may not replace classical dystrophin at GABAergic synapses to form novel delta dystrophin-containing DPC-like complexes therein. Instead, I suggest delta dystrophin is likely to form novel delta dystrophin-containing DPC-like complexes within the central parts of the neuron.

- I also suggest that the molecular composition of DPC complexes containing delta dystrophin differ from DPC complexes containing classical dystrophin. This point is emphasized by the fact that delta dystrophin and β-dystroglycan, a

core component of classical dystrophin-containing DPC complexes, do not colocalize (chapter 4, figure 6). Indeed the difference in distribution in the forebrain and cerebellum (chapter 3, figure 11) exhibited by the two isoforms also suggests the two isoforms may carry out different functions in the neuron. Obviously it would be expected that some components of classical and delta DPC complexes would be common to both.

- The data showing the different localization of full-length classical and delta dystrophin suggest Cexon78 and Dexon78 may interact with the region extending from the WW domain to the C-terminus to traffick the two dystrophin isoforms to different cellular compartments, PSD and microtubule cytoskeleton respectively.

- I suggest that delta dystrophin may utilize the MT-binding domain to directly associate with the MT network it is found to colocalize with.

- I also suggest that delta dystrophin may also participate in maintaining stability of the MT cytoskeleton, and hence, as a consequence of a mutated DMD gene, both delta dystrophin and classical dystrophin may contribute to the cognitive pathology in DMD patients by altering the MT cytoskeleton.

- I suggest delta dystrophin is likely to be expressed in different neuronal sub-types of excitatory neurons of the forebrain, since all forebrain neurons viewed under the light microscope expressed delta dystrophin, and 80% of these neurons are said to be excitatory (Xu *et al*, 2010), whilst only 20% are inhibitory (Xu *et al*, 2010).

6.1.2 Part 2

- Both 47kDa and 49kDa ε-sarcoglycan isoforms occur predominantly in membrane fractions, both of synaptic (SM) and non-syanptic origin (LM and microsomes).

- There appears to be lower expression of the 49kDa isoform in cerebellum compared to forebrain.

- Significantly only the 47kDa isoform is present in a myelin enriched fraction. The myelin fraction also contains fragments of axon membrane attached to the myelin.

- Neither isoform is enriched in the PSD fractions, unlike classical full-length dystrophin and associated DPC proteins (Chapter 3, figure 7, 8, 10). Therefore it is most unlikely that ε-sarcoglycan is a component of classical DPC complexes present in the PSD. Given that to date, classical dystrophin-containing DPC complexes are said to exclusively localize at GABAergic synapses (Brunig *et al*, 2002), these studies suggest that ε-sarcoglycan may not associate with these classical dystrophin-containing complexes at GABAergic synapses.

- Delta dystrophin localizes with the MT cytoskeleton (Chapter 4, figure 10), away from the membrane (Chapter 4, figure 8), whereas ε-sarcoglycan isoforms exclusively localize at the membrane. Therefore due to compartmentalization restrictions, neither ε-sarcoglycan isoform may associate with the delta dystrophin-containing DPC complexes in the forebrain and cerebellum.

- Therefore ε-sarcoglycan isoforms are likely to form novel, yet unidentified complexes in brain.

6.2 Future Work

6.2.1 Part 1

- For future work, I suggest to generate an anti-mouse classical dystrophin antibody and an anti-rabbit delta dystrophin antibody to immunoprecipitate and isolate the proteins that interact with these isoforms, and subsequently identify these interacting proteins via Mass Spectrometry Analysis. Concominant with these studies, I suggest to carry out co-localization studies in various cell-types of the brain, to directly compare the distribution of these isoforms in various brain regions and with respect to the distribution observed in cortical neurons described in this Thesis.

- For the future, I suggest studying the molecular composition of classical and delta dystrophin-containing DPC complexes in glial and neuronal cells. This is because evidence implicating glial and neuronal DPC complexes in DMD is continuously growing. For example, the abnormal cytoarchitecture of the cerebral cortex is due to the loss of a DPC component in glial cells (Satz *et al*, 2010). Furthermore, deletion of some DPC components in neurons blunts hippocampal LTP, indicating the DPC is involved in synaptic activity (Satz *et al*, 2010). Hence, the structural and functional brain abnormalities in DMD may be a consequence of a combination of DPC-like complexes in astrocyte cells in addition to the DPC complex found at the PSD of neuronal synapses. To date, no studies have yet determined whether delta dystrophin is expressed in glial cells.

- The co-localization between delta dystrophin and β3-tubulin presented in Chapter 4 suggests that delta dystrophin is directly or indirectly associated with the microtubule cytoskeleton. For future work, I suggest to investigate whether such association occurs in a direct or indirect manner. Prins *et al* (2009) have already demonstrated that classical dystrophin does contain an MT-binding domain, with which it directly associates with the MT network. I have established that the MT-binding domain in delta dystrophin exists and is unaltered by Dexon78. I suggest establishing, via a (cosedimentation)

immunoprecipitation approach, whether the delta dystrophin MT-binding domain is utilized to directly associate delta dystrophin with the MT network.

- The literature reveals that classical dystrophin contains actin and intermediate filament binding domains (Stone *et al*, 2005; Prins *et al*, 2009), and I have established that these domains in delta dystrophin exist and are unaltered by Dexon78. For future work, I suggest to investigate whether delta dystrophin utilizes these domains to directly associate with actin and intermediate filaments.

- It has already been demonstrated that classical dystrophin is capable of stabilising MTs from cold-induced depolymerization (Prins *et al*, 2009). For future work, I suggest to investigate whether delta dystrophin may also function to stabilize the MT cytoskeleton, as no studies have yet investigated this. The MT cytoskeleton becomes deranged when the DMD gene is mutated (Prins *et al*, 2009; Percival *et al*, 2007), and given that both classical and delta dystrophin originate from the DMD gene, this suggests that both the classical and the delta dystrophin isoform are likely involved in maintaining the stability of the MT cytoskeleton, and require further investigation. It would also be interesting to compare the stability of the MT network in wild-type and dystrophin-deficient mice, by utilizing cortical cultures obtained from wild, mdx mice, and if possible, other mdx models.

- For the future, it would be interesting to investigate in more detail the function and binding abilities of Cexon78 and Dexon78 (see chapter 3). The studies presented in this thesis show that as a consequence of these exons, classical and delta dystrophin distribute differently (chapter 3, figures 8-9, 10-11; Chapter 4, figures 1-10). A key question is what are the signals that direct classical and delta dystrophin to such widely differing subcellular locations. My results show that Cexon78 and Dexon78 alone, are unable to traffick to the PSD and MT cytoskeleton respectively. Separate studies carried out by Sakamoto *et al* (2008) found that the region extending from the WW domain to the C-terminal domain is necessary to localize classical dystrophin to the PSD in neurons; mislocalisation to neurites and axons of neurons occurs when this region is

removed. I suggest that Dexon78, localized within the WW domain and C-terminus region, may function to disrupt the PSD-binding domain found within this crucial C-terminal region, leading to delta dystrophin being distributed throughout the neurites and axons of the neurons (figures 1-10), similar to classical minidystrophins lacking the C-terminus domain (Sakamoto *et al*, 2008). This may explain why delta dystrophin observed in chapter 4 is localized within the central parts of neurites and axons, where it co-localizes with β3-tubulin. For the future, it would therefore be interesting to determine the fragments between the WW domain and the C-terminus domain, involved in trafficking the classical dystrophin isoforms to the PSD. The disruption of this trafficking signal by Dexon78 is a good indicator of a crucial region within the C-terminus containing the trafficking signal that directs classical dystrophin to the PSD.

- There is to date no knowledge as to whether delta dystrophin is expressed in the muscle, the tissue whereby the disease is most drastically manifested. Hence I suggest investigating and comparing the cellular and subcellular distribution of classical and delta dystrophin therein, via the use of biochemical, immunohistochemical and immunocytochemical analyses. The identification of delta dystrophin in muscle tissue would provide a novel potential therapeutic target to treat patients with DMD. Ofcourse, the expression of delta dystrophin in other organs is important as well and will also need to be investigated. To date, with the exception of the liver (Blake *et al*, 1999) and the brain (this Thesis; Blake *et a*, 1999), there is no knowledge of any other organ expressing delta dystrophin. These studies will also be necessary, as they will reveal novel and potentially alternative routes underlying DMD.

6.2.2 Part 2

- For the future, it would be interesting to generate a new anti-ε-sarcoglycan antibody able to recognize both the 47kDa and 49kDa isoform, cross-link this antibody to a column, immunoprecipitate and isolate the proteins that interact with the isoforms, and subsequently identify the associated proteins by Mass Spectrometry. It is often hypothesized in the literature that brain ε-sarcoglycan may possibly associate with other kinds of membrane proteins and/or cytoskeletal proteins rather than the DPC complex (Nishiyama *et al*, 2004; Esapa *et al*, 2007), in agreement with the data presented in this thesis. To date, the proteins interacting with ε-sarcoglycan in the brain have yet to be identified. This antibody production will provide an important step forward towards the understanding of the function of ε-sarcoglycan isoforms in the brain and in MDS pathology.

- It would also be interesting to generate an antibody against exon 8 or exon 11b, the two epitopes that distinguish the 47kDa ε-sarcoglycan isoform from the 49kDa ε-sarcoglycan isoform (chapter 1; figure 1) respectively. These could be used in immunocytochemical studies to establish and distinguish their cellular localizations throughout the entire brain. Secondly, each ε-sarcoglycan antibody could be cross-linked to a separate column in order to immunoprecipitate and isolate proteins that may specifically interact with their unique cytoplasmic tails. Mass Spectrometry could then be used to analyze and identify the isolated proteins. These antibodies, in concomitance with other antibodies against the DPC components, would allow to determine by immunocytochemical and immunohistochemistry techniques whether, the brain 47kDa and 49kDa ε-sarcoglycan isoforms, in analogy to the retina (Durbeej *et al*, 1999; Fort *et al*, 2005), may or may not be part of DPC complexes in some cells and be independent of DPC complexes in other cell-types.

- For future work, it would be interesting to establish the significance of the structural differences exhibited at the cytoplasmic tails of the 47kDa and 49kDa ε-sarcoglycan isoforms (Nishiyama *et al*, 2004). The results in Chapter 5, in

agreement with Nishyama *et al* (2004), show differential localization of the two isoforms in forebrain and cerebellum subcellular fractions, which I suggest it may be due to their different cytoplasmic domains, although this hypothesis remains to be verified. Nishiyama *et al* (2004) suggest that the structural differences at their C-terminus may cause ε-sarcoglycan isoforms to play different roles at synapses within neurons of the forebrain and cerebellum. For the future, it would be interesting to verify both of these hypotheses.

- For future work, I suggest to identify the proteins interacting with the extracellular domain of the 47kDa and 49kDa ε-sarcoglycan isoform. This is because the extracellular domain of either ε-sarcoglycan isoform contains putative cadherin-like domains and a calcium-binding pocket, which is typically found in proteins involved in homotypic or heterotypic interactions with other glycoproteins (Dickens *et al*, 2002; Ozawa *et al*, 2005). These interactions would normally lead to the modulation of a variety of processes, such as cell polarization (Tepass *et al*, 2000), migration (Tepass *et al*, 2000) as well as cell adhesion (Dickens *et al*, 2002). For future work, I suggest to immunoprecipitate the proteins that associate with ε-sarcoglycan's extracellular domain, in order to determine whether ε-sarcoglycan may be involved in any of these processes.

References

Albrecht D.C., Froehner, S.C. (2002) Syntrophins and dystrobrevins: defining the dystrophin scaffold at synapses. *Neurosignals*, **11**, 123-129.

Allamand, V., and Campbell, K. P. (2000). Animal models for muscular dystrophy: Valuable tools for the development of therapies. *Human Molecular Genetics*, **9**, 2459-2467.

Allen, J.E., Rodgin, D.W. (1960) Mental retardation in association with progressive dystrophy. *Amer J Dis Child.*, **100**, 208-211.

Amalfitano, A., Rafael, J.A., Chamberlain, J.S. (1997) Structure and mutation of the dystrophin gene. *Dystrophin: Gene, Prot. and Cell Biol.*, 1-26.

Anderson, J.L., Head, S.I., Rae, C., and Morley, J.W. (2002) Brain function in Duchenne muscular dystrophy. *Brain*, **125,** 4-13.

Asmus, K.D., Hug, G.L., Bobrowski, K., Mulazzani, Q.G., Marciniak, B. (2006) Transients in the oxidative and H-atom-induced degradation of 1,3,5-trithiane. Time-resolved studies in aqueous solution. *J. Phys. Chem. A.,* **110**, 9292-9300.

Asmus, F., Salih, F., Hjermind, L.E. (2005) Myoclonus-dystonia due to genomic deletions in the epsilon-sarcoglycan gene. *Ann. Neurol*., **58**, 792–797.

Asmus, F., Zimprich, A., Tezenas Du Montcel, S. (2002) Myoclonus dystonia syndrome: epsilon-sarcoglycan mutations and phenotype. *Ann. Neurol*., **52**, 489-492.

Austin, R.C., Howard, P.L., D'Souza, V.N., Klamut, H.J., Ray, P.N. (1995) Cloning and characterization of alternatively spliced isoforms of Dp71. *Hum. Mol. Genet.*, 4, 1475-1483.

Barbujani, G., Russo, A., Danieli, G.A., Spiegler, A.W., Borkowska, J., Petrusewicz, I.H. (1990) Segregation analysis of 1885 DMD families: significant departure from the expected proportion of sporadic cases. *Hum. Genet*., **84**, 522-6.

Barresi, R., Moore, S.A., Stolle, C.A., Mendell, J.R., Campbell, K.P. (2000) Expression of gamma-sarcoglycan in smooth muscle and its interaction with the smooth muscle sarcoglycan-sarcospan complex. *J. Biol. Chem.*, **275**, 38554–38560.

Beesley, P.W., Paladino, T., Gravel, C., Hawkes, R.A., Gurd, J.W. (1987) Characterization of gp50, a major glycoprotein present in rat brain synaptic membranes, with a monoclonal antibody. *Brain Res.*, **408**, 65-78.

Benson, D.L., Cohen, P.A. (1996) Activity-independent segregation of excitatory and inhibitory synaptic terminals in cultured hippocampal neurons. *J. Neurosci*., **16**, 6424-6432.

Blake, D.J. (2002) Dystrobrevin dynamics in muscle-cell signalling: a possible target for therapeutic intervention in Duchenne muscular dystrophy? *Neuromusc. Dis.*, **12**, 110-117.

Blake, D.J., Hawkes, R., Benson, M.A., and Beesley, P.W. (1999) Different dystrophin-like complexes are expressed in neurons and glia. *J.Cell Biol.*, **147**, 645-658.

Blake, D.J., Kroger, S. (2000) The neurobiology of Duchenne muscular dystrophy: learning lessons from muscle?. *Trends Neurosci.*, **23**, 92-99.

Blake, D.J., Weir, A., Newey, S.E., and Davies, K.E. (2002) Function and genetics of dystrophin and dystrophin-related proteins in muscle. *Physiol Rev.*, **82**, 291-329.

Bloom, G.S., Vallee, R.B. (1983) Association of microtubule-associated protein 2 (MAP 2) with microtubules and intermediate filaments in cultured brain cells. *J. Cell Biol*., **96**, 1523-1531.

Bönnemann, C.G., Modi, R., Noguchi, S., Mizuno, Y., Yoshida, M., Gussoni, E., McNally, E.M., Duggan, D.J., Angelini, C., Hoffman, E.P., Ozawa, E., Kunkel, L.M. (1995) β-sarcoglycan (A3b) mutations cause autosomal recessive muscular dystrophy with loss of the sarcoglycan complex. *Nat. Genet*., **11**, 266–273.

Bonuccelli, G., Sotgia, F., Capozza, F., Gazzerro, E., Minetti, C., Lisanti, M.P. (2007) Localized treatment with a novel FDA-approved proteasome inhibitor blocks the degradation of dystrophin and dystrophin-associated proteins in mdx mice. *Cell Cycle*, **6**, 1242-1248.

Brenman, J.E., Chao, D.S., Gee, S.H., McGee, A.W., Craven, S.E., Santillano, D.R. (1996) Interaction of nitric oxide synthase with the postsynaptic density protein PSD-95 and alpha1-syntrophin mediated by PDZ domains. *Cell*, **84**, 757-767.

Brenman, J.E., Chao, D.S., Xia, H., Aldape, K., Bredt, D.S. (1995) Nitric oxide synthase complexed with dystrophin and absent from skeletal muscle sarcolemma in Duchenne muscular dystrophy. *Cell*, **82**, 743–752.

Brunig, I., Suter, A., Knuesel, I., Luscher, B., and Fritschy J.M. (2002) GABAergic terminals are required for postsynaptic clustering of dystrophin but not of $GABA_A$ Receptors and gephyrin. *J. Neurosci*., **22**, 4805-4813.

Burdi, R., Rolland, J.F., Fraysse, B., Litvinova, K., Cozzoli, A., Giannuzzi, V., Liantonio, A., Camerino, G.M., Sblendorio, V., Capogrosso, R.F., Palmieri, B., Andreetta, F., Confalonieri, P., De Benedictis, L., Montagnani, M., De Luca, A. (2009) Multiple pathological events in exercised dystrophic mdx mice are targeted by pentoxifylline: outcome of a large array of in vivo and ex vivo tests. *J. Appl. Physiol.*, **106**, 1311-1324.

Cai, H., Erdman, R.A., Zweier, L., Chen, J., Shaw, J.H., Baylor, K.A., Stecker, M.M., Carey, D.J., Chan, Y.M. (2007) The sarcoglycan complex in Schwann cells and its role in myelin stability. *Exp. Neurol*., **205**, 257-269.

Calabrese, B., Wilson, M.S., Halpain, S. (2006) Development and regulation of dendritic spine synapses. *Physiology (Bethesda)*, **21**, 38-47.

Capani, F., Deerinck, T.J., Ellisman, M.H., Bushong, E., Bobik, M., Martone, M.E. (2001) Phalloidin-eosin followed by photo-oxidation: a novel method for localizing

F-actin at the light and electron microscopic levels. *J. Histochem. Cytochem.,* **49**, 1351-1361.

Capani, F., Ellisman, M.H., Martone, M.E. (2001) Filamentous actin is concentrated in specific subpopulations of neuronal and glial structures in rat central nervous system. *Brain Res.*, **923**, 1-11.

Capani, F., Martone, M.E., Deerinck, T.J., Ellisman, M.H. (2001) Selective localization of high concentrations of F-actin in subpopulations of dendritic spines in rat central nervous system: a three-dimensional electron microscopic study. *J. Comp. Neurol.*, **435**, 156-170.

Carlin, R.K., Grab, D.J., Cohen, R.S., and Siekevitz, P. (1980) Isolation and characterization of postsynaptic densities from various brain regions: enrichment of different types of postsynaptic densities. *J. Cell. Biol.*, **86**, 831-843.

Carretta, D., Santarelli, M., Sbriccoli, A., Pinto, F., Catini, C., Minciacchi, D. (2004) Spatial analysis reveals alterations of parvalbumin- and calbindin-positive local circuit neurons in the cerebral cortex of mutant mdx mice. *Brain Res.*, **1**, 1-11.

Carretta, D., Santarelli, M., Vanni, D., Carrai, R., Sbriccoli, A., Pinto, F., Minciacchi, D. (2001) The organisation of spinal projecting brainstem neurons in an animal model of muscular dystrophy. A retrograde tracing study on mdx mutant mice. *Brain Res.*, **895**, 213-22.

Carretta, D., Santarelli, M., Vanni, D., Ciabatti, S., Sbriccoli, A., Pinto, F., Minciacchi, D. (2003) Cortical and brainstem neurons containing calciumbinding proteins in a murine model of Duchenne muscular dystrophy: selective changes in the sensorimotor cortex. *J. Comp. Neurol.*, **456**, 48-59.

Cassim, F., Monaca, C., Szurhaj, W., Bourriez, J.L., Defebvre, L., Derambure, P., Guieu, J.D. (2001) Does post-movement beta synchronization reflect an idling motor cortex? *Neuroreport*, **12**, 3859–3863.

Cavaldesi, M., Macchia, G., Barca, S., Defilippi, P., Tarone, G., Petrucci, T.C. (1999). Association of the dystroglycan complex isolated from bovine brain synaptosomes with proteins involved in signal transduction. *J. Neurochem*., **72**, 1648–1655.

Ceccarini, M., Torreri, P., Lombardi, D.G., Macchia, G., Macioce, P., Petrucci, T.C. (2005) Molecular basis of dystrobrevin interaction with kinesin heavy chain: structural determinants of their binding. *J. Mol. Biol.*, **354**, 872-82.

Chamberlain, J.S., Metzger, J., Reyes, M., Townsend, D., Faulkner, J.A. (2007) Dystrophin-deficient mdx mice display a reduced life span and are susceptible to spontaneous rhabdomyosarcoma *FASEB J*., **21**, 2195-2204.

Chan, P., Gonzalez-Maeso, J., Ruf, F., Bishop, D.F., Hof, P.R., and Sealfon, S.C. (2005) Epsilon-sarcoglycan immunoreactivity and mRNA expression in mouse brain. *J.Comp Neurol.*, **482**, 50-73.

Chang, W.J., Iannaccone, S.T., Lau, K.S., Masters, B.S., McCabe, T.J., McMillan, K., Padre, R.C., Spencer, M.J., Tidball, J.G., Stull, J.T. (1996) Neuronal nitric oxide synthase and dystrophin-deficient muscular dystrophy. *Proc. Nat. Acad. Sci. USA*, **93**, 9142–9147.

Chen, J., Shi,W., Zhang,Y., Sokol,R., Cai,H., Lun,M., Moore,B.F., Farber,M.J., Stepanchick,J.S., Bonnemann,C.G., and Chan,Y.M. (2006) Identification of functional domains in sarcoglycans essential for their interaction and plasma membrane targeting. *Exp.Cell Res.*, **312**, 1610-1625.

Cheng, A.,Wang, S., Cai, J., Rao, M.S. and Mattson, M.P. (2003) Nitric oxide acts in a positive feedback loop with BDNF to regulate neural progenitor cell proliferation and differentiation in the mammalian brain. *Dev. Biol.*, **258**, 319-333.

Cif, L., Valente, E.M., Hemm, S., Coubes, C., Vayssiere, N., Serrat, S. (2004) Deep brain stimulation in myoclonus-dystonia syndrome. *Mov. Disord*., **19**, 724–727.

Clarris, H.J., McKeown, S., Key, B. (2002) Expression of neurexin ligands, the neuroligins and the neurexophilins, in the developing and adult rodent olfactory bulb. *Int. J. Dev. Biol*., **46**, 649-652.

Cohen, R.S., Blomberg, F., Berzins, K. and Siekevitz, P. (1977) Structure of postsynaptic densities isolated from dogcerebral cortex. Overall morphology and protein composition. *J. Cell Biol*., **74**, 696-711.

Collins, C. A., and Morgan, J. E. (2003) Duchenne's muscular dystrophy: animal models used to investigate pathogenesis and develop therapeutic strategies. I*nternational Journal of Experimental Pathology*, **84**, 165–172.

Coral-Varquez, R., Cohn, R.D., Moore, S.A., Hill, J.A., Weiss, R,M., Davisson, R.L, Straub, V., Barresi, R., Bansal, D., Hrstka, R.F., Williamson, R., Campbell, K.P. (1999) Disruption of the sarcoglycan-sarcospan complex in vascular smooth muscle: a novel mechanism for cardiomyopathy and muscular dystrophy. *Cell*, **98**, 465-474.

Craig, A.M., Blackstone, C.D., Huganir, R.L., Banker, G. (1994) Selective clustering of glutamate and gamma-aminobutyric acid receptors opposite terminals releasing the corresponding neurotransmitters. *Proc. Natl. Acad. Sci. USA*, **91**, 12373–12377.

Culligan, K., Ohlendieck, K. (2002) Diversity of the Brain Dystrophin-Glycoprotein Complex. *J.Biomed.Biotechnol.* , **2**, 31-36.

Daniel A. Fletcher 1,2 & R. Dyche Mullins3 (2010) Cell mechanics and the cytoskeleton. *Nature*, **463**, 485-492.

Danko, I., Chapman, V. and Wolff, J. A. (1992) The frequency of revertants in *mdx* mouse genetic models for Duchenne muscular dystrophy. *Pediatr. Res.*, **32**, 128-131.

Dehmelt, L., Halpain, S. (2004) The MAP2/Tau family of microtubule-associated proteins. *Gen. Biol.*, **6**, 1-10.

Deng, B., Glanzman, D., Tidball, J.G. (2009) Nitric oxide generated by muscle corrects defects in hippocampal neurogenesis and neural differentiation caused by muscular dystrophy. *J. Physiol*., **587**, 1769-1778 .

Dickens, N.J., Beatson, S., and Ponting, C.P. (2002) Cadherin-like domains in alpha-dystroglycan, alpha/epsilon-sarcoglycan and yeast and bacterial proteins. *Curr.Biol.*, **12**, R197-R199.

Dickinson, R.B., Caro, L., Purichz, D.L. (2004) Force generation by cytoskeletal filament end-tracking proteins. *Biophys. J*., **87**, 2838–2854.

Dieck, S.T., Sanmarti-Vila, L., Langnaese, K., Richter, K., Kindler, S., Soyke, A., Wex, H., Smalla, K.H., Kampf, U., Franzer, J.T., Stumm, M., Garner, C.C., Gundelfinger, E.D. (1998) Bassoon, a novel zinc-finger CAG/glutamine-repeat protein selectively localized at the active zone of presynaptic nerve terminals. *J. Cell Biol*., **142**, 499-509.

Drewes, G., Mandelkow, E.A. (1998) EMMAPs, MARKs and microtubule dynamics. *Trends Biochem. Sci.,* **23**, 307-311.

Duchenne, G.B.A. (1868). Recherches sur la paralysie musculaire pseudohypertrophique, ou paralysie myo-sclerosique. *Arch. Gen. Med.,* **11**, 5–25.

Durbeej, M., Campbell, K.P. (1999) Biochemical Characterization of the Epithelial Dystroglycan Complex. *J. Biol. Chem*., **274**, 26609–26616.

Durbeej, M., Campbell, K. P. (2002) Muscular dystrophies involving the dystrophin-glycoprotein complex: an overview of current mouse models. *Curr. Opin. Gen. & Dev.*, **12**, 349–361.

Durbeej, M., Cohn, R.D., Hrstka, R.F., Moore, S.A., Allamand, V., Davidson, B.L. (2000) Disruption of the beta-sarcoglycan gene reveals pathogenetic complexity of limb-girdle muscular dystrophy type 2E. *Mol. Cell*., **5**, 141-151.

Einbond, A., Sudol, M. (1996) Towards prediction of cognate complexes between the WW domain and proline-rich ligands. *FEBS Lett*., **384**, 1-8.

Emery, A.E.H. (1993) *Duchenne Muscular Dystrophy*. Oxford University Press.

England, S.B., Nicholson, L.V., Johnson, M.A., Forrest, S.M., Love, D.R., Zubrzycka-Gaarn, E.E., Bulman, D.E., Harris, J.B., Davies, K.E. (1990) Very mild muscular dystrophy associated with the deletion of 46% of dystrophin. *Nature*, **343**, 180-182.

Ervasti, J.M., Campbell, K.P. (1993) A role for the dystrophin-glycoprotein complex as a transmembrane linker between laminin and actin. *J. Cell. Biol*., **122**, 809-823.

Ervasti, J.M., Campbell, K.P. (1991) Membrane organization of the dystrophin-glycoprotein complex. *Cell*, 66, 1121-1131.

Ervasti, J.M., Ohlendieck,K., Kahl, S.D., Gaver, M.G., Campbell, K.P. (1990) Deficiency of a glycoprotein component of the dystrophin complex in dystrophic muscle. *Nature*, **345**, 315–319.

Esapa, C.T., Waite, A., Locke, M., Benson, M.A., Kraus, M., McIlhinney, R.A.J., Sillitoe, R.V., Beesley, P.W., and Blake, D.J. (2007) SGCE missense mutations that cause myoclonus-dystonia syndrome impair eps-sarcoglycan trafficking to the plasma membrane: modulation by ubiquination and torsinA. *Hum. Mol. Gen.*, **16**, 327-342.

Estrada, F.J., Mornet, D., Rosas-Vargas, H., Angulo, A., Hernández, M., Becker, V., Rendón, A., Ramos-Kuri, M., Coral-Vázquez, R.M. (2006) A novel isoform of delta-sarcoglycan is localized at the sarcoplasmic eticulum of mouse skeletal muscle. *Biochem. Biophys. Res. Commun.*, **340**, 865-871.

Ettinger, A.J., Feng, G., and Sanes, J.R. (1997) ε-Sarcoglycan, a broadly expressed homologue of the gene mutated in limb-girdle muscular dystrophy 2D. *J. Biol. Chem.*, **272**, 32534–32538.

Ettinger, A.J., Feng, G. and Sanes, J.R. (1998) Additions and corrections to epsilon-Sarcoglycan, a broadly expressed homologue of the gene mutated in limb-girdle muscular dystrophy 2D. *J. Biol. Chem.*, **273**, 19922.

Evans, G.J.O., Cousin, M.A. (2005) Tyrosine phosphorylation of synaptophysin in synaptic vesicle recycling. *Biochem. Soc. Trans*., **33**,1350–1353.

Fanin, M., Duggan, D.J., Mostacciuolo, M.L., Martinello, F., Freda, M.P., Soraru, G., Trevisan, C.P., Hoffman, E.P., Angelini, C. (1997) Genetic epidemiology of muscular dystrophies resulting from sarcoglycan gene mutations. *J. Med. Genet*., 34, 973–977.

Farah, C.A., Leclerc, N. (2008) HMWMAP2: new perspectives on a pathway to dendritic identity. *Cell Mot. Cytosk*., **65**, 515–527.

Feener, C.A., Koenig, M., Kunkel, L.M. (1989) Alternative splicing of human dystrophin mRNA generates isoforms at the carboxy terminus. *Nature*, 338, 509-511.

Ferletta, M., Kikkawa, Y., Yu, H., Talts, J.F., Durbeej, M., Sonnenberg, A., Timpl, R., Campbell, K.P., Ekblom, P., Genersch, E. (2003) Opposing roles of integrin α6Aβ1 and dystroglycan in laminin-mediated extracellular signal-regulated kinase activation. *Mol. Biol. Cell*., **14**, 2088–20103.

Fort, P., Estrada, F.J., Bordais, A., Mornet, D., Sahel, J.A., Picaud, S., Vargas, H.R., Coral-Vázquez, R.M., and Rendon, A. (2005) The sarcoglycan-sarcospan complex localization in mouse retina is independent from dystrophins. *Neurosci Res*., **53**, 25–33.

Fritchy, J.M., Schweizer, C., Brunig, I., Luscher, B. (2003) Pre- and post-synaptic mechanisms regulating the clustering of type A γ-aminobutyric acid receptors ($GABA_A$ receptors). *Biochem. Soc. Trans*., **31**, 889-892.

Gerrits, M.C., Foncke, E.M., Koelman, J.H., Tijssen, M.A. (2009) Pediatric writer's cramp in myoclonus-dystonia: maternal imprinting hides positive family history. *Eur. J. Paediatr. Neurol.* **13**, 178-80.

Gorecki, D., Geng, Y., Thomas, K., Hunt, S.P., Barnard, E.A., and Barnard, P. J. (1992) Expression of the dystrophin gene in mouse and rat brain. *Neuroreport,* **12,** 713-776.

Grabowski, M., Zimprich, A., Lorenz-Depiereux, B., Kalscheuer, V., Asmus, F., Gasser, T., Meitinger, T., Strom, T.M.. (2003). The epsilon-sarcoglycan gene SGCE), mutated in myoclonus-dystonia syndrome, is maternally imprinted. *Eur. J. Hum. Genet.*, **11**, 138–144.

Grady, R.M., Zhou, H., Cunningham, J.M., Henry, M.D., Campbell, K.P., Sanes, J.R. (2000) Maturation and maintenance of the neuromuscular synapse: genetic evidence for roles of the dystrophin--glycoprotein complex. *Neuron.* 25, 279-293.

Graf, E.R., Zhang, X.Z., Jin, S.X., Linhoff, M.W., Craig, A.M. (2004) Neurexins induce differentiation of GABA and Glutamate post-synaptic specializations via neurologins. *Cell*, **119**, 1013-1026.

Griffin, J.L., Williams, H.J., Sang, E., Clarke, K., Rae, C., Nicholson, J.K. (2001) Metabolic profiling of genetic disorders: a multitissue 1H nuclear magnetic resonance spectroscopic and pattern recognition study into dystrophic tissue. *Anal. Biochem*., **293**, 16–21.

Grimes, D.A., Han, F., Lang, A.E., St George-Hyssop, P., Racacho, L., Bulman, D.E. (2002) A novel locus for inherited myoclonus-dystonia on 18p11. *Neurology*, **59**, 1183–1186.

Gundelfinger, E.D., Dieck, T.S. (2000) Molecular organization of excitatory chemical synapses in the mammalian brain. *Naturwissenschaften,* 87,513-523.

Gurd, J.W., Gordon-Weeks, P., Evans, W.H. (1982) Biochemical and morphological comparison of postsynaptic densities prepared from rat, hamster, and monkey brains by phase partitioning. *J. Neurochem*., **39**, 1117-1124.

Hack, A.A., Groh, M.E. and McNally, E.M. (2000) Sarcoglycans in muscular dystrophy. *Microsc. Res. Technol*., **48**, 167–180.

Han, F., Lang, A.E., Racacho, L., Bulman, D.E., Grimes, D.A. (2003) Mutations in the epsilon-sarcoglycan gene found to be uncommon in seven myoclonus-dystonia families. *Neurology*, **61**, 244–246.

Hashimoto, R., Yamaguchi, M. (2006) Dynamic changes in the subcellular localization of Drosophila β-sarcoglycan during the cell cycle. *Cell Struct. Funct.*, **31**, 173-180.

Hedrich, K., Meyer, E.M., Schule, B. (2004) Myoclonus-dystonia: detection of novel, recurrent, and de novo SGCE mutations. *Neurology*, **62**, 1229–1231.

Hemmings, L., Kuhlman, P.A., Critchley, D.R. (1992) Analysis of the actin-binding domain of α-actinin by mutagenesis and demonstration that dystrophin contains a functionally homologous domain. *J. Cell Biol*., **116**, 1369-1380.

Hill, I.E., Selkirk, C.P., Hawkes, R.B., Beesley, P.W. (1988) Characterization of novel glycoprotein components of synaptic membranes and postsynaptic densities, gp65 and gp55, with a monoclonal antibody. *Brain Res*., **461**, 27-43.

Hindley, S., Jurlink, B.H., Gysbers, J.W., Middlemiss, P.J., Herman, M.A. and Rathbone, M.P. (1997) Nitric oxide donors enhance neurotrophin-induced neurite outgrowth through a cGMP-dependent mechanism. *J. Neurosci. Res.*, **47**, 427-439.

Hinton, V.J., De Vivo, D.C., Nereo, N.E., Goldstein, E., Stern, Y. (2000) Poor verbal working memory across intellectual level in boys with Duchenne dystrophy. *Neurology*, **54**, 2127–2132.

Hjermind, L.E., Vissing, J., Asmus, F. (2008) No muscle involvement in myoclonus-dystonia caused by epsilon-sarcoglycan gene mutations. *Eur. J. Neurol.*, **15**, 525–529.

Hnia, K., Zouiten, D., Cantel, S., Chazalette, D., Hugon, G., Fehrentz, J.A., Masmoudi, A., Diment, A., Bramham, J., Mornet, D., Winder, S.J. (2007) ZZ domain of dystrophin and utrophin: topology and mapping of a beta-dystroglycan interaction site. *Biochem. J*., **401**, 667-677

Hoffman, E., Brown, R., Kunkel, L. (1987) Dystrophin: the protein product of the Duchenne muscular dystrophy locus. *Cell*, **51,** 919–28.

Holt, K.H., Campbell, K.P. (1998) Assembly of the sarcoglycan complex-Insights for muscular dystrophy. *J. Biol. Chem*., **273**, 34667–34670.

Hopf, F.W., Steinhardt, R.A. (1992) Regulation of intracellular free calcium in normal and dystrophic mouse cerebellar neurons. *Brain Res.*, (578), 49-54.

Huang, X., Poy, F., Zhang, R., Joachimiak, A., Sudol, M., Eck, M.J. (2000) Structure of aWW domain containing fragment of dystrophin in complex with β-dystroglycan. *Nat. Struct. Biol*. **7**, 634–638.

Hunt, C.A., Schenker, L.J., Kennedy, M.B. (1996) PSD-95 is associated with the postsynaptic density and not with the presynaptic membrane at forebrain synapses. *J. Neurosci*., **16**, 1380-1388.

Im, W.B., Phelps, S.F., Copen, E.H., Adams, E.G., Slightom, J.L., Chamberlain, J.S. (1996) Differential expression of dystrophin isoforms in strains of mdx mice with different mutations. *Hum. Mol. Genet*., **8**, 1149-1153.

Imamura, M., Araishi, K., Noguchi, S., and Ozawa, E. (2000) A sarcoglycan-dystroglycan complex anchors Dp116 and utrophin in the peripheral nervous system. *Hum. Mol. Genet.*, **9**, 3091-3100.

Imamura, M., Mochizuki, Y., Engvall, E., Takeda, S. (2005) Epsilon-sarcoglycan compensates for lack of alpha-sarcoglycan in a mouse model of limb-girdle muscular dystrophy. *Hum. Mo.l Genet.*., **14**, 775-783.

Jaglin, X.H., Chelly, J. (2009) Tubulin-related cortical dysgeneses: microtubule dysfunction underlying neuronal migration defects. *Trends Gen*., **25**, 555-566.

Jordan, B.A., Fernholz, B.D., Boussac, M., Xu, C., Grigorean, G., Ziff, E.B., Neubert, T.A. (2004) Identification and verification of novel rodent postsynaptic density proteins. *Mol. Cell. Prot*., **3**, 857–871.

Karagan, N.J. (1979) Intellectual functioning in Duchenne muscular dystrophy: a review. *Psychol. Bull.*, 86, 250–259.

Kim, T.W., Wu, K., Xu, J.L., Black, I.B. (1992) Detection of dystrophin in the post-synaptic density of rat brain and deficiency in a mouse model of Duchenne muscular dystrophy. *Proc. Natl. Acad. Sci. USA*, **89**, 11642-11644.

Kinugawa, K., Vidailhet, M., Clot, F., Apartis, E., Grabli, D., and Roze, E. (2009) Myoclonus-Dystonia: An Update. *Mov. Dis.*, **24**, 479–489.

Klein, C., Liu, L., Doheny, D., Kock, N., Muller, B., de Carvalho Aguiar, P., Leung, J., de Leon, D., Bressman, S.B., Silverman, J. (2002) Epsilon-sarcoglycan mutations found in combination with other dystonia gene mutations. *Ann. Neurol*., **52**, 675–679.

Knuesel, I., Mastrocola, M., Zuellig, R.A., Bornhauser, B., Schaub, M.C., Fritschy, J.M. (1999) Altered synaptic clustering of $GABA_A$ receptors in mice lacking dystrophin (mdx mice). *Eur. J. Neurosci*., **11**, 4457-4467.

Knuesel, I., Zuellig, R.A., Schaub, M.C., Fritschy, J.M. (2001) Alterations in dystrophin and utrophin expression parallel the reorganization of GABAergic synapses in a mouse model of temporal lobe epilepsy. *Eur. J. Neurosci.*, 13, 1113-1124.

Kobayashi, Y.M., Kanagawa, M., Faulkner, J.A., Sigmund, C., Campbell, K.P. (2003) Increased epsilon-sarcoglycan expression preventsmuscular dystrophy in alpha-sarcoglycan deficient mice. *Mol. Biol. Cell*, **14**, 48-53.

Kock, N., Kasten, M., Schule, B. (2004). Clinical and genetic features of myoclonus-dystonia in 3 cases: a video presentation. *Mov. Disord*., **19**, 231-234.

Koenig, M., Hoffman, E.P., Bertelson, C.J., Monaco, A.P., Feener, C., Kunkel, L.M. (1987) Complete cloning of the Duchenne muscular dystrophy (DMD) cDNA and preliminary genomic organization of the DMD gene in normal and affected individuals. *Cell*, **50**, 509-517.

Koenig, M., Monaco, A.P., Kunkel, L.M (1988) The complete sequence of dystrophin predicts a rod-shaped cytoskeletal protein. *Cell*, **53**, 219-28.

Kornau, H.C., Schenker, L.T., Kennedy, M.B., Seeburg, P.H. (1995) Domain interaction between NMDA receptor subunits and the postsynaptic density protein PSD-95. *Science*, **269**, 1737-1740.

Kudoh, H., Ikeda, H., Kakitani, M., Ueda, A., Hayasaka, M., Tomizuka, K., Hanaoka, K. (2005) A new model mouse for Duchenne muscular dystrophy produced by 2.4 Mb deletion of dystrophin gene using Cre-loxP recombination system. *Biochem. Biophys. Res. Commun.*, **328**, 507-516.

Kueh, S.L.L, Head, S.I., Morley, J.W. (2008) $GABA_A$ receptor expression and inhibitory post-synaptic currents in cerebellar purkinje cells in dystrophin-deficient mdx mice. *Clinic. Exp. Pharm. Phys.*, **35**, 207–210

Kurtis, M.M, Luciano, M.S, Yu, Q., Goodman, R.R, Ford, B., Raymond, D., Pullman, S.L., Pullman, R.S. (2010) Clinical and neurophysiological improvement of SGCE myoclonus dystonia with GPi deep brain stimulation. *Clin. Neurol. Neurosurg*., **112**, 149-152.

Lai, Y., Thomas, G.D., Yue, Y., Yang, H.T., Li, D., Long, C., Judge, L., Bostick, B., Chamberlain, J.S., Terjung, R.L., Duan, D. (2009) Dystrophins carrying spectrin-like

repeats 16 and 17 anchor nNOS to the sarcolemma and enhance exercise performance in a mouse model of muscular dystrophy. *J. Clin. Invest.*, **119**, 624-635.

Lambert, C.M.N. (2008) Sample prep for proteomics of breast cancer: proteomics and gene ontology reveal dramatic differences in protein solubilization preferences in radioimmunoprecipitation assay and urea lysis buffers. *Prot. Sci.*, **6**, 1-24.

Lapidos, K.A., Kakkar, R., McNally, E.M. (2004) The dystrophin glycoprotein complex: signaling strength and integrity for the sarcolemma. *Circ. Res*., **94**, 1023-1031.

Lederfein, D., Levy, Z., Augier, N., Mornet, D., Morris, G., Fuchs, O., Yaffe, D., Nudel, U. (1992) A 71-kilodalton protein is a major product of the Duchenne muscular dystrophy gene in brain and other nonmuscle tissues. *Proc. Natl. Acad. Sci. USA*, **89**, 5346-5350.

Legardinier, S., Legrand, B., Raguénès-Nicol, C., Bondon, A., Hardy, S., Tascon, C., Le Rumeur, E., Hubert, J.F. (2009) A two-amino acid mutation encountered in duchenne muscular dystrophy decreases stability of the rod domain 23 (R23) spectrin-like repeat of dystrophin. *J. Biol. Chem*., **284**, 8822-8832.

Legardinier, S., Raguénès-Nicol, C., Tascon, C., Rocher, C., Hardy, S., Hubert, J.F., Le Rumeur, E. (2009) Mapping of the lipid-binding and stability properties of the central rod domain of human dystrophin. *J. Mol. Biol.* , **389**, 546-558.

Leimer, U., Franke, W.W., Leube, R.F. (1996) Synthesis of the mammalian synaptic vesicle protein synaptophysin in insect cells: a model for vesicle biogenesis. *Exp. Cell Res*., **224,** 88–95

Leto, K., Bartolini, A., Rossi, F. (2008) Development of cerebellar GABAergic interneuorons: origin and shaping of the “minibrain” local connections. *Cerebellum*, **7**, 523-529.

Li, D.P., Chen, S.R., Finnegan, T.F., and Pan, H.L. (2004) Signalling pathway of nitric oxide in synaptic GABA release in the rat paraventricular nucleus. *J. Physiol.*, **554**, 100-110.

Li, K.W., Hornshaw, M.P., Van Der Schors, R.C., Watson, R., Tate, S., Casetta, B., Jimenez, C.R., Gouwenberg, Y., Gundelfinger, E.D., Smalla, K.H., and Smit, A.B. (2004) Proteomics analysis of rat brain postsynaptic density. Implications of the diverse protein functional groups for the integration of synaptic physiology. *J.Biol.Chem.*, **279**, 987-1002.

Lidov, H.G. (1996) Dystrophin in the nervous system. *Brain Pathol*., **6**, 63-77.

Lidov, H.G.W., Beers, T.J., Watkins, S.C. and Kunkel, L.M. (1990) Localization of dystrophin to postsynaptic regions of central nervous system cortical neurons. *Nature*, **348**, 720-728.

Lidov, H.G.W., Byers, T.J., and Kunkel, L.M. (1993) The distribution of dystrophin in the murine central nervous system. *Neuroscience,* **54**, 167-187.

Lidov, H.G., Selig, S., Kunkel, L.M. (1995) Dp140: a novel 140 kDa CNS transcript from the dystrophin locus. *Hum. Mol. Genet.*, **4**, 329-335.

Lim, L.E., Duclos, F., Broux, O., Bourg, N., Sunada, Y., Allamand, V., Meyer, J., Richard, I., Moomaw, C., Slaughter, C., Tomé, F. M. S., Fardeau, M., Jackson, C.E., Beckmann, J.S., Campbell, K.P. (1995) β-Sarcoglycan: characterization and role in limb-girdle muscular dystrophy linked to 4q12. *Nat. Genet*., **11**, 257–265.

Liu, L.A, Engvall, E. (1999) Sarcoglycan isoform in skeletal muscle. *J. Biol. Chem*., **274**, 38171–38176.

Lüscher, B., Keller, C.A. (2004) Regulation of GABAA receptor trafficking, channel activity, and functional plasticity of inhibitory synapses. *Pharmacol. Ther.*, **102**, 195-221.

Macioce, P., Gambara, G., Bernassola, M., Gaddini, L., Torreri, P., Macchia, G., Ramoni, C., Ceccarini, M., and Petrucci, T.C. (2003) Beta-dystrobrevin interacts directly with kinesin heavy chain in brain. *J. Cell Sci.*, **116**, 4847-4856.

Mahloudji, M., Pikielny, R.T. (1967) Hereditary essential myoclonus. *Brain*, **90**, 669–674.

Mandell, J.W., Banker, G.A. (1995) The microtubule cytoskeleton and the development of neuronal polarity. *Neurobiol. Aging*, **16**, 229-238.

Marelli, C., Canafoglia, L., Zibordi, F., Ciano, C., Visani, E., Zorzi, G. (2008) A neurophysiological study of myoclonus in patients with DYT11 myoclonus-dystonia syndrome. *Mov. Dis.*, 2008; 23: 2041–8.

Marsh, G.G., Munsat, T.L. (1974) Evidence for early impairment of verbal intelligence in Duchenne muscular dystrophy. *Arch. Dis. Child.*, **49**, 118–122.

Matus, A., Bernhardt, R., and Jones, T.H. (1981) High molecular weight microtubules-associated proteins are preferentially associated with dendritic microtubules in brain. *Proc. Natl. Acad. Sci. USA*, **78**, 3010-3014.

Matus, A., Pehling, G., Ackermann, M., Maeder, J. (1980) Brain postsynaptic densities: the relationship to glial and neuronal filaments. *J. Cell. Biol.*, **87**, 346-359.

Matus, A.I., Taff-Jones, D.H. (1978) Morphological and molecular composition of isolated postsynaptic junctional structures. *Proc. R. Soc. Lond. B. Biol. Sci.*, **203**, 135-151.

McNally, E.M., Ly, C.T., and Kunkel, L.M. (1998) Human epsilon-sarcoglycan is highly related to alpha-sarcoglycan (adhalin), the limb girdle muscular dystrophy 2D gene. *FEBS Lett.*, **422**, 27-32.

Mehler, M.F. (2000) Brain dystrophin, neurogenetics and mental retardation. *Brain Res. Rev*., **32**, 277– 307.

Mehler, K.F., Haas, K.Z., Kessler, J.A., Stanton, P.K. (1992) Enhanced sensitivity of hippocampal pyramidal neurons from mdx mice to hypoxia-induced loss of synaptic transmission. *Proc. Nat. Acad. Sci. USA*, **89**, 2461-2465.

Moizard, M.P., Billard, C., Toutain, A., Berret, F., Marmin, N., Moraine, C. (1998) Are Dp71 and Dp140 brain dystrophin isoforms related to cognitive impairment in Duchenne muscular dystrophy? *Am. J. Med. Genet.*, **80**, 32-41.

Moore, C.J., Hewitt, J.E. (2009) Dystroglycan glycosylation and muscular dystrophy. *Glycoconj J*., **26**, 349-357.

Moore, S.A., Saito, F., Chen, J., Michele, D.E., Henry, M.D., Messing, A., Cohn, R.D., Ross-Barta, S.E., Westra, S, Williamson, R,A,, Hoshi, T., Campbell, K.P. (2002) Deletion of brain dystroglycan recapitulates aspects of congenital muscular dystrophy. *Nature*, **418**, 422-425.

Moore, C.J., Winder, S.J. (2010) Dystroglycan versatility in cell adhesion: a tale of multiple motifs. *Cell. Commun. Signal.*, **8**, 1-12.

Moreno-Lopez, B., Romero-Grimaldi, C., Noval, J.A., Murillo-Carretero, M., Matarredona, E.R. and Estrada, C. (2004) Nitric oxide is a physiological inhibitor of neurogenesis in the adult mouse subventricular zone and olfactory bulb. *J. Neurosci.*, **24**, 85-95.

Morris, R.G., Garrud, P., Rawlins, J.N., O'Keefe, J. (1982) Place navigation impaired in rats with hippocampal lesions. *Nature*, 297, 681-683.

Moukhles, H., Carbonetto, S. (2001) Dystroglycan contributes to the formation of multiple dystrophin-like complexes in brain. *J. Neurochem.*, **78**, 824-834.

Muir, J.K., Lobner, D., Monyer, H., Choi, D.W. (1996) $GABA_A$ receptor activation attenuates excitotoxicity but exacerbates oxygen-glucose deprivation-induced neuronal injury in vitro. *J. Cereb. Blood Flow Metab.*, **16**, 1211-1218.

Muller, B., Hedrich, K., Kock, N. (2002) Evidence that paternal expression of the epsilon-sarcoglycan gene accounts for reduced penetrance in myoclonus-dystonia. *Am. J. Hum. Genet.*, **71**, 1303–1311.

Muntoni, F., Mateddu, A., Serra, G. (1991) Passive avoidance behaviour deficit in the mdx mouse. *Neuromuscul. Disord.*, **1**, 121-3.

Muntoni, F., Torelli, S., Ferlini, A. (2003) Dystrophin and mutations: one gene, several proteins, multiple phenotypes. *Lancet Neuro.*, **2**, 731-740.

Newey, S.E., Benson, M.A., Ponting, C.P., Davies, K.E., Blake, D.J. (2000) Alternative splicing of dystrobrevin regulated the stoichiometry of syntrophin binding to the dystrophin protein complex. *Curr. Biol.*, **10**, 1295–1298.

Nigro, V., Moreira, D.S.E., Piluso, G., Vainzof, M., Belsito, A., Politano, L., Puca, A.A., Passos-Bueno, M.R., Zatz, M. (1996) Autosomal recessive limb-girdle muscular dystrophy, LGMD2F, is caused by a mutation in the δ-sarcoglycan gene. *Nat. Genet.*, **14**, 195–198.

Nishiyama, A., Endo, T., Takeda, S., Imamura, M. (2004) Identification and characterization of ε-sarcoglycans in the central nervous system. *Brain Res. Mol. Brain Res.*, **125**,1–12.

Noguchi, S., McNally, E.M., Othmane, B.K., Hagiwara, Y., Mizuno, Y., Yoshida, M., Yamamoto, H., Bonnemann, C.G., Gussoni, E., Denton, P.H., Kyriakides, T., Middleton, L., Hentati, F., Hamida, B.M., Nonaka, I., Vance, J.M., Kunkel, L.M.,

Ozawa, E. (1995) Mutations in the dystrophin-associated protein gamma-sarcoglycan in chromosome 13 muscular dystrophy. *Science*, **270**, 819–822.

Noguchi, S.E. Wakabayashi, M., Imamura, M., Yoshida, M., Ozawa, E. (2000) Formation of sarcoglycan complex with differentiation in cultured myocytes. *Eur. J. Biochem.*, **267**, 640–648.

Norwood, F.L., Sutherland-Smith, A.J., Keep, A.J., Kendrick-Jones, J. (2000) The structures of the N-terminal actin-binding domain of human dystrophin and how mutations in this domain may cause Duchenne or Becker Muscular Dystrophy. *Structure*, **8**, 481-491.

Nowak, K.J., Davies, K.E. (2004) Duchenne muscular dystrophy and dystrophin: pathogenesis and opportunities for treatment. *EMBO Reports*, **5**, 872-876.

Nudel, U., Zuk, D., Einat, P., Zeelon, E., Levy, Z., Neuman, S., Yaffe, D. (1989) Duchenne muscular dystrophy gene product is not identical in muscle and brain. *Nature*, **337**, 76-78.

O'Brien, R.J., Mammen, A.L., Blackshaw, S., Ehlers, M.D., Rothstein, J.D., Huganir, R.L. (1997) The development of excitatory synapses in cultured spinal neurons. *J. Neurosci*., **17**, 7339–7350.

Ozawa, E., Mizuno, Y., Hagiwara, Y., Saoka, T.S., and Shida, M.Y. (2005) Molecular and cell biology of the sarcoglycan complex. *Muscle Nerve*, **32,** 563–576.

Ozawa, E., Noguchi, S., Mizuno, Y., Hagiwara, Y., Yoshida, M. (1998) From dystrophinopathy to sarcoglycanopathy: evolution of a concept of muscular dystrophy. *Muscle Nerve*, **21**, 421– 438.

Papa, M., Bundman, M.C., Greenberger, V., Segal, M. (1995) Morphological analysis of dendritic spine development in primary cultures of hippocampal neurons. *J. Neurosci*., **15**, 1-11.

Parker, M.A., Stasiv, Y., Benraiss, A., Chmielnicki, E., Grinberg, A., Westphal, H., Goldman, S.A. and Enikolopov, G. (2003) Nitric oxide negatively regulates mammalian adult neurogenesis. *Proc. Natl. Acad. Sci. USA*, **100**, 9566–9571.

Percival, J.M., Gregorevic, P., Odom, G.L., Banks, G.B., Chamberlain, J.S., Froehner, S.C. (2007) rAAV6-microdystrophin rescues aberrant golgi complex organization in mdx skeletal muscles. *Traffick*, **8**: 1424–1439.

Peters, M.F., O'Brien, K.F., Puccio, H.M.S, Kunkel, L.M., Adams, M.E., Froehner, S,C. (1997) β-dystrobrevin, a new member of the dystrophin family. *JBC*, **272**, 31561-31569.

Pilgram, G.S.K., Potikanond, S., Baines, R.A., Fradkin, L.G., Noordermeer, J.N. (2009) The roles of the dystrophin-associated glycoprotein complex at the synapse. *Mol. Neurobiol*., **41**, 1-21.

Piluso, G., Mirabella, M., Ricci, E., Belsito, A., Abbondanza, C., Servidei, S., Puca, A.A., Tonali, P., Puca, G.A., Nigro, V. (2000) Gamma1- and gamma2-syntrophins, two novel dystrophin-binding proteins localized in neuronal cells. *J. Biol. Chem.*, **275**, 15851-15860.

Piras, G., El Kharroubi, A., Kozlov, S., Escalante-Alcalde, D., Hernandez, L., Copeland, N.G., Gilbert, D.J., Jenkins, N.A., Stewart, C.L. (2000) Zac1 (Lot1), a potential tumor suppressor gene, and the gene for epsilon-sarcoglycan are maternally imprinted genes: identification by a subtractive screen of novel uniparental fibroblast lines. *Mol. Cell. Biol*., **20**, 3308–3315.

Prins, K.W., Humston, J.L. Mehta, A., Tate, V., Ralston, E., Ervasti, J.M. (2009) Dystrophin is a microtubule-associated protein. *J. Cell Biol.*, 186, 363–369.

Rao, A., Cha, E.M., Craig, A.M. (2000) Mismatched Appositions of Presynaptic and postsynaptic Components in Isolated Hippocampal Neurons. *J. Neurosci*., **20**, 8344–8353

Rao, A., Craig, A.M. (2000) Signaling between the actin cytoskeleton and the postsynaptic density of dendritic spines. *Hippocampus*, **10**, 527-541.

Rao, A., Kim, E., Sheng, M., Craig, A.M. (1998) Heterogeneity in the molecular composition of excitatory postsynaptic sites during development of hippocampal neurons in culture. *J. Neurosci*., **18**, 1217–1229.

Roberds, S.L., Leturcq, F., Allamand, V., Piccolo, F., Jeanpierre, M., Anderson, R.D., Lim, L.E., Lee, J.C., Tome, F.M., Romero, N.B., Fardeau, M., Beckmann, J.C., Kaplan, J., Campbell, K.P. (1994) Missense mutations in the adhalin gene linked to autosomal recessive muscular dystrophy. *Cell*, **78**, 625–633.

Roberts, R.G., Borrow, M., Bentley, D.R. (1992) Point mutations in the dystrophin gene. *Proc. Natl. Acad. Sci. USA*, **89**, 2331-2335.

Roemer, T., Madden, K., Chang, J. and Snyder, M. (1996) Selection of axial growth sites in yeast requires Axl2p, a novel plasma membrane glycoprotein. *Genes Dev*., **10**, 777–793.

Russo, K., Di Stasio, E., Macchia, G., Rosa, G., Brancaccio, A., Petrucci, T.C. (2000). Characterization of the β-dystroglycan-growth factor receptor 2 (Grb2) interaction. *Biochem. Biophys. Res. Commun*., **274**, 93–98.

Sadoulet-Puccio, H.M., Kunkel, L.M. (1996) Dystrophin and its isoforms. *Brain Pathol.*, 6, 25-35.

Sakamoto, T., Arima, T., Ishizaki, M., Kawano, R., Koide, T., Uchida, Y., Yamashita, S., Kimura, N., Hirano, T., Maeda, Y., Uchino, M. (2008) Regions downstream from the WW domain of dystrophin are important for binding to postsynaptic densities in the brain. *Neuromusc. Disord*., **18**, 382-388.

Sander, M., Chavoshan, B., Harris, S.A., Iannaccone, S.T., Stull, J.T., Thomas, G.D., Victor, R.G. (2000) Functional muscle ischemia in neuronal nitric oxide synthase-

deficient skeletal muscle of children with Duchenne muscular dystrophy. *Proc. Natl. Acad. Sci. USA*, **97**, 13818-13823.

Satz, J.S., Ostendorf, A.P., Hou, S., Turner, A., Kusano, H., Lee, J.C., Turk, R., Nguyen, H., Ross-Barta, S.E., Westra, S., Hoshi, T., Moore, S.A., Campbell, K.P. (2010) Distinct functions of glial and neuronal dystroglycan in the developing and adult mouse brain. *J Neurosci*., **30**, 14560-14572.

Sbriccoli, A., Santarelli, M., Carretta, D. (1995) Architectural changes of the cortico-spinal system in the dystrophin defective *mdx* mouse. *Neurosci. Lett*., **200**, 53-56

Schüle, B., Kock, N., Svetel, M., Dragasevic, N., Hedrich, K., De Carvalho Aguiar, P., Liu, L., Kabakci, K., Garrels, J., Meyer, E.M., Berisavac, I., Schwinger, E., Kramer, P.L., Ozelius, L.J., Klein, C., Kostic,V. (2004) Genetic heterogeneity in ten families with myoclonus-dystonia. *J. Neurol. Neurosurg. Psychiatry*, **75**, 1181-1185.

Sciandra, F., Schneider, M., Giardina, B., Baumgartner, S., Petrucci, T.C., Brancaccio, A. (2001) Identification of the beta-dystroglycan binding epitope within the C-terminal region of alpha-dystroglycan. *Eur. J. Biochem*., **268**, 4590-4597.

Scoville, W.B., Milner, B. (1957) Loss of recent memory after bilateral hippocampal lesions. *J. Neurol. Neurosurg. Psych.*, **21**, 11–21.

Sesay, A.K., Errington, M.L., Levita, L., Bliss, T.V. (1996) Spatial learning and hippocampal long-term potentiation are not impaired in mdx mice. *Neurosci. Lett.*, **211**, 207–210.

Shi, W., Chen, Z., Schottenfeld, J., Stahl, R.C., Kunkel, L.M., Chan, Y.M. (2004) Specific assembly pathway of sarcoglycans is dependent on beta- and delta-sarcoglycan. *Muscle Nerve*, **29**, 409-419.

Shiga, K., Yoshioka, H., Matsumiya, T., Kimura, I., Takeda, S., and Imamura, M. (2006) Zeta-sarcoglycan is a functional homologue of gamma-sarcoglycan in the formation of the sarcoglycan complex. *Exp. Cell Res.*, **312**, 2083-2092.

Sicinski, P., Geng, Y., Ryder-Cook, A.S., Barnard, E.A., Darlison, M.G. and Bamard, P.J. (1989) The molecular basis of muscular dystrophy in the mdx mouse: a point mutation. *Science*, **244**, 1578-1580.

Singer, S.J. (1990) The structure and insertion of integral proteins in membranes. *Annu. Re. Cell Biol.*, **6**, 247-296.

Singh, S.M., Kongari, N., Cabello-Villegas, J., Malella, K.M. (2010) Missense mutations in dystrophin that trigger muscular dystrophy decrease protein stability and lead to cross-β aggregates. *Proc. Natl. Acad. Sci. USA*, **107**, 15069-15074.

Sitnik, R. (1997) Novel point mutations in the dystrophin gene. *Hum. Mutat.*, **10**, 217-222.

Sjoblom, B., Ylanne, J., Djinovic-Carugo, K. (2008) Novel structural insights into F-actin-binding and novel functions of calponin homology domains. *Curr. Opin.Struct. Biol.*, **18**, 702-708.

Slep, K. J., Vale R.D. (2007) Structural basis of microtubule plus end tracking by XMAP215, CLIP-170, and EB1. *Mol. Cell.*, **27**, 976-991.

Smalla, K.H., Matthies, H., Langnäse, K., Shabir, S., Böckers, T.M., Wyneken, U., Staak, S., Krug, M., Beesley, P.W., Gundelfinger, E.D. (2000) The synaptic glycoprotein neuroplastin is involved in long-term potentiation at hippocampal CA1 synapses. *Proc. Natl. Acad. Sci. USA*, **97**, 4327-4332.

Southan, G.J., Szabó, C. (1996) Selective pharmacological inhibition of distinct nitric oxide synthase isoforms. *Biochem. Pharmacol*., **51**, 383–394

Spence, H.J., Dhillon, A.S., James, M., Winder, S.J. (2004) Dystroglycan, a scaffold for the ERK-MAP kinase cascade. *EMBO reports*, **5**, 484-489.

Stone, M.R., O'Neill, A., Catino, D., Bloch, R.J. (2005) Specific interaction of the actin-binding domain of dystrophin with intermediate filaments containing keratin. *Mol. Biol. Cell*, **16**, 4280–4293.

Straub, V., Ettinger, A.J., Durbeej, M., Venzke, D.P., Cutshall, S., Sanes, J.R., and Campbell, K.P. (1999) epsilon-sarcoglycan replaces alpha-sarcoglycan in smooth muscle to form a unique dystrophin-glycoprotein complex. *J. Biol. Chem.*, **274**, 27989-27996.

Tai, C.H, Yen, R.F., Lin, C.H., Yen, K. Y., Yip, P.K, Wu, R.M., Lee, M.J. (2009) Focal brain glucose hypermetabolism in myoclonus-dystonia syndrome caused by an epsilon-sarcoglycan gene mutation. *Parkinsonism Relat. Disord*., **8**, 614-616.

Tepass, U., Truong, K., Godt, D., Ikura, M. and Peifer, M. (2000). Cadherins in embryonic and neuralmorphogenesis. *Nat. Rev. Mol. Cell Biol*., **1**, 91–100.

Tezenas du Montcel, S., Clot, F., Vidailhet, M., Roze, E., Damier, P., Jedynak, C.P., Camuzat, A., Lagueny, A., Vercueil, L., Doummar, D., Guyant-Maréchal, L., Houeto, J.L., Ponsot, G., Thobois, S., Cournelle, M.A., Durr, A., Durif, F., Echenne, B., Hannequin, D., Tranchant, C., Brice, A. (2005) Epsilon sarcoglycan mutations and phenotype in French patients with myoclonic syndromes. *J. Med. Genet.*, **43**, 394-400.

Thomas, G.D., Sander, M., Lau, K.S., Huang, P.L., Stull, J.T., Victor, R.G. (1998) Impaired metabolic modulation of alpha-adrenergic vasoconstriction in dystrophin-deficient skeletal muscle. *Proc. Natl. Acad. Sci. USA*, **95**, 15090-15095.

Torelli, S., Ferlini, A., Obici, L., Sewry, C., Muntoni, F. (1999) Expression, regulation and localization of dystrophin isoforms in human foetal skeletal and cardiac muscle. *Neuro. Dis*., **9**, 541-551.

Tretter, V., Moss, S.J. (2008) GABA(A) receptor dynamics and constructing GABAergic synapses. *Front. Mol. Neurosci*., **1**, 1-13.

Vaillend, C., Billard, J.M. (2002) Facilitated CA1 hippocampal synaptic plasticity in dystrophin-deficient mice: role for GABAA receptors? *Hippocampus*, **12**, 713–717.

Vaillend, C., Billard, J.M., Claudepierre, T., Rendon, A., Dutar, P., Ungerer, A. (1998) Spatial discrimination learning and CA1 hippocampal synaptic plasticity in mdx and mdx3cv mice lacking dystrophin gene products. *Neuroscience*, **86**, 53-66.

Vaillend, C., Billard, J. M., Laroche, S. (2004) Impaired long-term spatial and recognition memory and enhanced CA1 hippocampal LTP in the dystrophin-deficient DMD^{mdx} mouse. *Neurobiol. Disease*, **17**, 10-20.

Vaillend, C., Rendon, A., Misslin, R., Ungerer, A. (1995) Influence of dystrophin-gene mutation on mdx mouse behavior. I. Retention deficits at long delays in spontaneous alternation and bar-pressing tasks. *Behav. Genet.*, **25**, 569–579.

Vaillend, C., Ungerer, A., Billard, J.M. (1999) Facilitated NMDA receptormediated synaptic plasticity in the hippocampal CA1 area of dystrophin-deficient mice. *Synapse*, 33, 59–70.

Vainzof, M., Ayub-Guerrieri, D., Onofre, P.C., Martins, P.C., Lopes, V.F., Zilberztajn, D., Maia, L.S., Sell, K., Yamamoto, L.U. (2008) Animal models for genetic neuromuscular diseases. *J. Mol. Neurosci.*, **34**, 241-248.

Valente, E.M., Misbahuddin, A., Brancati, F. (2003) Analysis of the epsilon-sarcoglycan gene in familial and sporadic myoclonusdystonia: evidence for genetic heterogeneity. *Mov. Disord.*, **18**, 1047–1051.

Venoux, M., Delmouly, K., Milhavet, O., Vidal-Eychenié, S., Giorgi, D., Rouquier, S. (2008) Gene organization, evolution and expression of the microtubule-associated protein ASAP (MAP9). *BMC Genomics*, **9**, 406-412.

Vithlani, M,. Moss, S.J. (2009) The role of GABAAR phosphorylation in the construction of inhibitory synapses and the efficacy of neuronal inhibition. *Biochem. Soc. Trans.*, **37**, 1355-1358.

Waite, A., Tinsley, C.L., Locke, M., and Blake, D.J. (2009) The neurobiology of the dystrophin-associated glycoprotein complex. *Annals. of Medicine*, **41**, 344-359.

Wehling-Henricks, M., Oltmann, M., Rinaldi, C., Myung, K.H., Tidball, J.G. (2009) Loss of positive allosteric interactions between neuronal nitric oxide synthase and phosphofructokinase contributes to defects in glycolysis and increased fatigability in muscular dystrophy. *Hum. Mol. Genet*., **18**, 3439-3451.

Wheeler, M.T., Zarnegar, S. and McNally, E.M. (2002) Zeta-sarcoglycan, a novel component of the sarcoglycan complex, is reduced in muscular dystrophy. *Hum. Mol. Genet.*, **11**, 2147–2154.

Wilton, S.D., Fletcher, S. (2008) Exon skipping and Duchenne muscular dystrophy: hope, hype and how feasible? *Neurol. India*, **56**, 254-262.

Xiao, J. and LeDoux, M.S. (2003) Cloning, developmental regulation and neural localization of rat epsilon-sarcoglycan. *Brain Res. Mol. Brain Res*., **119**, 132–143.

Winder, S.J., Knight, A.E., Kendrick-Jones, J. (1997) Protein structure. In *Dystrophin, Gene, Protein and Cell Biology*, pp. 27-55, Cambridge University Press, UK.

Xu, X., Roby, K.D., Callaway, E.M. (2010) Immunochemical characterization of inhibitory mouse cortical neurons: three chemically distinct classes of inhibitory cells. *J. Comp. Neurol.*, **518**, 389-404.

Yokoi, F., Dang, M.T., Mitsui, S., Li., Y. (2005) Exclusive paternal expression and novel alternatively spliced variants of e-sarcoglycan mRNA in mouse brain. *FEBS Letters*, **579**, 4822–4828.

Yoshida, M., Hama, H., Ishikawa-Sakurai, M., Imamura, M., Mizuno, Y., Araishi, K., Wakabayashi-Takai, E., Noguchi, S., Sasaoka, T., Ozawa, E. (2000) Biochemical evidence for association of dystrobrevin with the sarcoglycan-sarcospan complex as a basis for understanding sarcoglycanopathy. *Hum. Mol. Genet*., **9**, 1033–1040.

Yoshida, M., Ozawa, E. (1990) Glycoprotein complex anchoring dystrophin to sarcolemma. *J. Biochem.*, **108**, 748– 752.

Yoshida, M., Suzuki, A., Yamamoto, H., Noguchi, S., Mizuno, Y., Ozawa, E. (1994) Dissociation of the complex of dystrophin and its associated proteins into several unique groups by n-octyl beta-D-glucoside. *Eur. J. Biochem.*, **222**, 1055-1061.

Zaccaria, M.I., Tommaso, F.D., Brancaccio, A., Paggi, P., Petrucci, T.C. (2001) Dystroglycan distribution in adult mouse brain: a light and electron microscopy study. *Neuroscience*, **2**, 311-324.

Zimprich, A., Grabowski, M., Asmus, F., Naumann, M., Berg, D., Bertram, M., Scheidtmann, K., Kern, P., Winkelmann, J., Muller-Myhsok, B., Riedel, L., Bauer, M., Muller, T., Castro, M., Meitinger, T., Strom, T.M., Gasser, T. (2001) Mutations in the gene encoding ε-sarcoglycan cause myoclonus-dystonia syndrome. *Nat. Genet.*, **29**, 66– 69.

List of Appendices

Appendix I: General Molecular Biology Reagents

Box 1- Chemicals (SIGMA)

All molecular biology grade laboratory chemicals were purchased from Sigma-Aldrich and stored at room temperature unless stated otherwise. Where necessary, solutions were sterilized by autoclaving, or filtering through a 0.22μm filter.

3 (N-morpholino) propanesulfonic acid (MOPS); Invitrogen.
Acetic acid
Acrylamide Solution (40% w/v); BioRad
Agar, Noble
Ampicillin. Stock solution 205mg/mL in
autoclaved purite H_2O, stored at –20°C
β-mercaptoethanol (β-ME)
β-(N-morpholino) propanesulfonic acid (MOPS); Invitrogen
Boric Acid
Brilliant Blue R250 (Coomassie)
Bromophenol Blue
Calcium Chloride
Citric Acid
Copper Sulphate
Dextran T-500; Pharmacosmos
Dibasic Sodium Phosphate Dehydrate
Dimethoxypropane (DMP)
Disodium hydrogen phosphate heptahydrate (Na_2HPO_4)
Deoxycholate (DOC)
Ethanol
Folin reagent
Glycerol
Glycine
HCl
isopropanol
L-Glutamine
Glutamic Acid (glutamate)
Magnesium Chloride
Marvel dried milk powder
Methanol
NaOH
n-octyl glucopyranoside. Store at 4°C.
Polyethylene glycol 6000 (PEG 6000); Sciencelab
p-iodonitrotetrazolium violet (INT). Store at 4°C.
Polyethylene glycol
Ponceau S
Potassium Acetate
Potassium Chloride
Protogel; National Diagnostics
Sodium Azide
Sodium Bicarbonate
Sodium Carbonate
Sodium Chloride
Sodium dihydrogen phosphate
Sodium dodecyl sulphate (SDS)
Sodium hydroxide
Sodium succinate
Sodium tartrate
Sucrose
Sulphosalicylic acid
Thimerosal;

Trichloroethane (TCA)
Triethanolamine; Fisher Scientific.
Tretrametiletilendiammina (Temed); Pierce
Thiethanolamine; Fisher Scientific
Thimerosal
Triton X-100
Tryptone; Neogen Corporation.
Tween-20 (Polyoxyethylenesorbitan monolaurate)
Urea
Yeast extract; Difco Labs

Box 2: Biological Kits and Systems

AminoLink Column; Pierce.
Bradford Method for protein Detection; Biorad
ECL detection kit; Pierce
Endofree-Maxiprep kit; Qiagen tip-500.
Protease Inhibitors; Boehringer Manheim.
Supersignal WestDura ECL HRP substrate detection kit; Pierce.

Box 3: Markers and enzymes

Prestained SDS-PAGE broad range standards; Biorad.
SeeBlue Plus2 Pre-stained Standard; Invitrogen.
Recombinant Enterokinase; Novagen.

Box 4: Buffers

0.2M Triethanolamine Buffer pH 8.2: 2.98g triethanolamine, make pH 8.2, adjust volume with ddH_2O to 100mL. Sterilize using a filter. Store at RT.
1M Tris Buffer pH 7.5: 12.4g Tris, make pH 7.5, adjust volume with ddH_2O to 100mL. Sterilize using a filter. Store at RT.
10mM Tris Buffer pH 7.0: 0.121g Tris, make pH 7.0, adjust volume with ddH_2O to 100mL. Sterilize using a filter. Store at RT
50mM Tris pH 5.5 with SDS: 0.5mL of 1M Tris Buffer pH 5.5 + 1mL SDS, adjust volume with ddH_2O to 10mL. Sterilize using a filter. Store at RT.
Blotting Buffer pH 8.3: 25mM Tris, 192mM glycine, 1% (w/v) SDS, 20% (v/v) methanol. Store at 4^oC.
Buffer B (lysis buffer) pH 8.0: 100mM NaH_2PO_4, 10mM Tris-HCl, 8M Urea. Adjusted to pH 8.0 and sterilized by Filter. Store at RT.
Buffer QBT (equilibration buffer): 750mM NaCl, 50mM MOPS pH 7.0, 15% isopropanol (v/v), 0.15% Triton X-100 (v/v). Sterilize using a filter. Store at RT.
Buffer QC (wash buffer): 1.0 M NaCl, 50mM MOPS pH 7.0, 15% isopropanol (v/v). Sterilize using a filter. Store at RT.
Buffer QN (elution buffer): 1.6M NaCl, 50mM MOPS pH 7.0, 15% isopropanol (v/v). Sterilize using a filter. Store at RT.
Citrate-phosphate Buffer pH 5.0 (washing buffer): 4.7g Citric Acid + 9.2g Dibasic Sodium Phosphate. Adjust the pH to 5.0 ad adjust the volume to 1L with ddH_2O. Sterilize busing a Filter. Store at RT.
Citrate-phosphate Buffer pH 5.0 with 0.1% Tween 20: 99.9mL Citrate-phosphate Buffer pH 5.0 + 0.1mL Tween 20. Store at RT.
Cleavage Buffer pH 7.4: 20mM Tris-HCl, 50mM NaCl, 2mM $CaCl_2$. Adjusted to pH 7.4 and sterilized using a Filter. Stored at 4^oC.
Cleavage/Capture Buffer A: 200mM Tris-HCl, 500mM NaCl, 20mM $CaCl_2$. Adjusted to pH 7.4 and sterilize using a Filter. Stored at 4^oC.
Coupling Buffer pH 7.2: 0.1M phosphate, 0.15M Sodium Chloride. Adjust the pH to 7.2 and adjust the volume to 500mL with ddH_2O. Sterilize using a Filter. Store at 4^oC.
Dilution/Storage Buffer pH 7.4: 20mM Tris-HCl, 200mM NaCl, 2mM $CaCl_2$, 50% glycerol. Adjusted to pH7.4 and sterilize using a Filter. Stored at -20^oC.
Elution buffer pH2.5: 0.1M Glycine adjusted to pH 2.5. Sterilize using a Filter. Store at 4^oC.
Elution buffer pH 4.5: 100mM NaH_2PO_4, 10mM Tris-HCl, 8M Urea. Adjusted to pH 4.5 and sterilize using a Filter. Store at RT.
Elution buffer pH 5.9: 100mM NaH_2PO_4, 10mM Tris-HCl, 8M Urea. Adjusted to pH 5.9 and sterilize using a Filter. Store at RT.
Endotoxin-free Buffer TE: 10mM Tris-HCl pH 8.0, 1mM EDTA. Sterilize by autoclave/Filter. Store at RT.
Neutralization buffer: 1M Tris-HCl in ddH_2O. Adjust to pH 9.0. Sterilize using a Filter. Store at RT.
P1 Buffer (resuspension buffer): 59mM Tris-HCl pH8.0, 10mM EDTA, 100µg/mL RNaseA. Sterilize by autoclave/Filter. Store at 4^oC.
P2 Buffer (lysis buffer): 200mM NaOH, 1% SDS (w/v). Sterilize by autoclave/Filter. Store at RT.
P3 Buffer (neutralization buffer): 3.0 M potassium acetate pH 5.5. Sterilize by autoclave/Filter. Store at 4^oC.
Phosphate Buffered Saline (PBS): 8g NaCl + 0.2g KCl, $1.44Na_2HPO_4$ in 800mL of ddH_2O. Adjust the pH to 7.4 with HCl and adjust the volume to 1L with ddH_2O. Sterilize by autoclave/Filter. Store at RT.
Quenching Buffer pH 7.4: 1M TrisHCl, 0.05% Sodium Azide. Adjust the pH to 7.4 and sterilize using a Filter. Store at 4^oC.
RIPA Buffer pH 7.5: 0.5mL 1M Tris Buffer pH 7.5 + 0.1mL Triton X-100 + 0.05g DOC + 1mL of 1M NaCl. Adjust final volume to 10mL. Sterilize using a Filter. Store at 4^oC.
Storage Buffer pH 7.4: PBS pH7.4, 0.5M NaCl, 0.02% Thimerosal. Sterilize using a Filter. Store at 4^oC.
Storage Buffer B pH 7.4: PBS containing 0.05% sodium azide. Sterilize by Filter. Store at RT.
TE buffer: 10mM Tris (pH 8.0), 1mM EDTA (pH 8.0). Filter sterilize.

Tris-buffered Saline (TBS): Make 0.1% v/v polyoxythylenesorbitan monolaurate (Tween 20) in PBS. Sterilize using a Filter. Store at RT.
Tris-HCl buffer pH 8.0: dissolve 121.1g of Tris base in 800mL of ddH_2O. Adjusted the pH to 8.0 by adding concentrated HCl, make final volume to 1L and sterilize by autoclaving.
Wash/Bind Buffer pH 7.5: 20mM Tris, 0.15M NaCl, 0.1% Triton X-100. Adjusted the pH to 7.5. Sterilize using a Filter. Store at RT.
Wash Buffer pH 6.3: 100mM NaH_2PO_4, 10mM Tris-HCl, 8M Urea. Adjusted to pH 6.3 and sterilized by Filter. Store at RT.

Box 5: Cells, Buffers, Solutions and reagents used for bacterial growth and IPTG induction

Bacterial cell line:
BL21 (DE3) competent cells; Stratagene.

Reagents:
Ampicillin; Stock solution 205mg/mL in autoclaved purite H_2O. Stored at -20^oC.
Isopropyl β-D-1-thiogalactopyranoside (IPTG); Sigma, store at 4^oC.
β-mercaptoethanol (β-ME); Sigma, store at 4^oC.

Solutions:
Lysogeny Broth (LB) media: 1L = 10g NaCl + 10g Tryptone + 5g Yeast extract. Adjusted to pH 7.0 and autoclaved.
Lysogeny Broth (LB) agar media: LB media + 2% Agar. Autoclaved and then cooled to 55^oC before addition of ampicillin to 100μg/mL and pouring plates.
SOC medium: 2M filter-sterilised glucose solution.

Box 6: Equipment

Glass/Teflon homogeniser with 1mm clearance.
15 cm tissue culture plates; Sigma-Aldrich.
24 well tissue culture plates; Sigma-Aldrich.
50mL high-speed polypropylene centrifuge tubes; Thermo Scientific.
37^{o}C and 42^{o}C water bath.
Beckman (Beckman GS 6R, Beckman GS 15 R, Allegra 21R).
Beckman Ti60 rotor (angle), Beckmane 42.1 rotor, in a Beckman ultracentrifuge L8/L8M.
Cell strainer, 70μm; BD Biosciences. .Store at RT.
Centricon YM-10; Millipore.
Dialysis membrane, MWCO 1,000; Spectra.
Electroporation cuvettes; Invitrogen.
Electroporator II; Invitrogen (*E. coli* pulse/charge electroporation; 1800V).
Filters; 0.22μm acrodiscs, Gelman Sciences.
Glass coverslips 24mm, Thermo Scientific.
Haemocytometer; Weber.
High-speed centrifuge and SS-34 rotor (Sorvall), H1318 rotor (Sorvall)
Hyper-film ECL; Amersham
Incubator/shaker Model G-25; New Brunswick Scientific Co. Inc., NJ, USA.
Inverted microscope: Nikon Eclipse TE300 microscope.
Microscope slides; BDH.
Nitrocellulose membrane, pore size 0.45μm; Amersham.
Qiafilter Maxi Cartridge; Qiagen
Beckman Rotors: 42.1, Sw28, Beckman
Semi-micro cuvettes with 1cm path length; FisherBrand.
Sonicator with a 3-mm-diameter probe.
Spectrophotometer, Heλios γ, Unicam.
Spin-filter columns; Novagen.
Tissue culture plastic; Nunc from life Technologies
Transmission electron microscope; Hitachi H600.
Ultra-free Centrifugal filter device; Millipore
Vacuum for lyophilization.
Zeiss Axioplan light microscope.

Appendix II: Media, solutions and reagents for cell culture

Box 1. Tissue culture media and reagents

Reagents

B27 supplement; Gibco. Store at –20°C.
Bovine serum albumin (BSA); Sigma. Stored at 4°C.
DMEM; Dulbecco's Modified Eagles Media, Sigma. Stored at 4°C.
Foetal calf serum (FCS); Seralabs. Stored at –20°C.
Hanks' Balanced Salt Solution (HBSS) without Ca^{2+} and Mg^{2+}; Sigma. Stored at 4°C.
Horse Serum; Gibco. Heat inactivated at 60°C for 30 minutes. Stored at –20°C.
L-Glutamine; Sigma. 200mM stock. Stored at –20°C.
Lipofectamine 2000; Invitrogen. Stored at 4°C.
Methanol; Sigma. Stored at RT.
Neurobasal Medium; Invitrogen. Store at 4°C.
OPTI-MEM I; Invitrogen. Stored at 4°C.
Paraformaldehyde (PFA); Sigma. Stored at –20°C.
Penicillin; Gibco. Stored at –20°C.
Poly-D-lysine; Sigma. Stored at –20°C.
Streptomycin; Gibco. Stored at –20°C.
Triton X-100; Sigma. Stored at RT.
Trypan Blue; Sigma. Stored at 4°C.
Trypsin; 2.5% stock solution; Gibco. Stored at –20°C.
Vectashield Mounting Medium; Vector Lab. Stored at 4°C.

Media:

Day 1 Media: DMEM containing 10% FCS, 2mM Glutamine, 100U/mL penicillin/100µg/mL streptomycin. Stored at 4°C.
Day 2 Media: Neurobasal Medium containing 2mM L-Glutamine, 1mL B27 supplement, 100U/mL penicillin/100µg/mL streptomycin. Stored at 4°C.
Neurobasal Media A: Neurobasal medium containing 0.5mM L-Glutamine, B27 supplement and 25µm glutamate. Stored at 4°C.
Neurobasal Media B: Neurobasal medium containing 0.5mM L-Glutamine, B27 supplement, no glutamate. Store at 4°C.

Solutions:

4%PFA in PBS: 4mL PFA in a total volume of 100mL PBS. Store at – 20°C.
25mM Glycine in PBS: 1.87g Glycine in a total volume of 1L PBS. Store at 4°C.
Blocking Solution with Triton X-100: 10% Horse Serum, 5% sucrose, 3% BSA, 82% PBS, 0.2% Triton X-100. Store at -20°C.
Blocking Solution without Triton X-100: 10% Horse Serum,. 5% sucrose, 3% BSA, 82% PBS. Store at -20°C.

Appendix III: Antibodies

Table 1: List of antibodies used for Immunocytochemistry (IHC) and/or Western blots (WB).

Antibody	Company	Protein recognised	MW	Species Reactivity	IHC and WB dilutions
Anti-classical dystrophin antibody	Gift from Oxford Dr.Blake lab	Classical Dystrophin cDp427,cDp140, cDp116, cDp71	427, 140, 116, 71kDa	Rabbit	IHC 1:10 WB 1:100
Anti-delta dystrophin antibody	Gift from Oxford Dr.Blake lab	Delta Dystrophin dDp427,dDp140, dDp116, dDp71	427, 140, 116, 71kDa	Rabbit	IHC 1:20 WB 1:200
Anti-dystrobrevin antibody	Gift from Oxford Dr.Blake lab	α1,α2, β-dystrobrevin	78, 59, 55kDa	Rabbit	WB 1:1000
Anti-ε-Sarcoglycan antibody	Gift from Oxford Dr.Blake lab	ε-sarcoglycan	45kDa	Rabbit	IHC 1:50 WB 1:500
Anti-PSD95 antibody	Affinity BioReagents	PSD-95	95kDa	Mouse	IHC 1:1000 WB 1:100
Anti-Gp65 (anti-neuroplastin) antibody	In-house antibody	np55, np65	55, 65kDa	Mouse	WB 1:50
Anti-Gp50 antibody	In-house antibody	Gp50	50kDa	Mouse	WB 1:1
Anti-MAP2 antibody	Sigma	MAP2a, MAP2b, MAP2c	280, 270, 75, 70kDa	Mouse	IHC 1:750 WB 1:1000
Anti-MANDAG antibody	Gift from Oxford Dr.Blake lab	β-dystroglycan	43kDa	Mouse	IHC 1:50
Anti-$GABA_AR$ antibody	Chemicon	$GABA_A$ Receptor	55kDa	Mouse	IHC 1:50

Anti-NMDAR antibody	Millipore	NMDA Receptor	130kDa	Mouse	IHC 1:100
Anti-synaptophysin antibody	Sigma	synaptophysin	38kDa	Mouse	IHC 1:750 WB 1:2000
Anti-GAD-65 antibody	Chemicon	GAD65	65kDa	Mouse	IHC 1:500
Anti-β3-tubulin antibody	Sigma	β3-tubulin	46kDa	Mouse	IHC 1:400 WB 1:1000
Rat polyclonal antibody	Invitrogen	Secondary Rat Antibody	-	Anti-rat	WB 1:2000
Mouse monoclonal antibody	Invitrogen	Secondary mouse Antibody	-	Anti-mouse	WB 1:2000
Alexa Fluor 568	Molecular Probes	Secondary Mouse Antibody	-	Anti-Mouse	IHC 1:1000
Alexa Fluor 488	Molecular Probes	Secondary Rabbit Antibody	-	Anti-Rabbit	IHC 1:1000